Norne Field Development Plan

School of Mining and Geosciences

Capstone Design Project

Prof. Masoud Riazi

Team C

Arlan Tokpayev

Sultan Konkabayev

Zhandos Dauletov

Zhanulan Syrymov

Raiymbek Muratbekov

Arsen Kenzhebekov

May 2024

Table of Content

List of Tables

List of Figures

Overview

Team Members

Zhanulan Syrymov - Team Leader:

- **Role**: Director of Geology and Petrophysics Department

Arsen Kenzhebekov - Vice Team Leader:

- **Role**: Co-Director of Reservoir Simulation Department | Static Modeller

Arlan Tokpayev:

- **Role**: Director of Reservoir Engineering Department

Raiymbek Muratbekov:

- **Role**: Co-Director of Reservoir Simulation Department | Dynamic Modeller

Sultan Konkabayev:

- **Role**: Director of Drilling & Completion Engineering Department | Surface facilities

Zhandos Dauletov:

- **Role**: Director of Production Engineering Department | Economist & HSE

Introduction to the Norne Field

The Field Development Plan is important for the Norne Field because of its complex geological features, operations challenges and it requires strategic resource allocation. It is an offshore field that is located in the Norwegian Sea. The Norne Field has varying reservoir rock and fluid properties. The FDP allows us to consider the field characteristics through detailed reservoir modeling and simulation, thus enabling the engineers to tailor their extraction methods for maximal recovery with minimal risks.

The economic prospect of the FDP is particularly valuable to the Norne Field, which is a mature field with production dating back to 1991. As the production of oil moves on, it becomes challenging to ensure production efficiency, thus presenting new challenges for increasingly advanced recovery techniques, such as water and gas injection, to sustain production levels. The FDP assesses EOR methods to delay decline in field production and make the continued production plan economically sustainable.

An FDP with strict views about the environment obeys the demand of developing itself within these confines and satisfies the requirement for the development to be implemented under offshore operations by aligning various regulatory and environmental standards in Norway. Such operations include waste management, control of emissions, and minimization of the adverse effect of operations on the immediate marine environment. Moreover, the FDP for Norne incorporates risk assessment and contingency planning, which is especially critical for offshore fields that suffer uncertain operational conditions posed by weather, their remote location, and high intervening costs.

Virtually all aspects of the FDP lend themselves to the orientation of the optimal allocation of resources, scheduling, and maintenance plans, as well as producing cost-effective production operations. It is paramount for the phased development enabling alignment to leverage the licensing terms dictated by Norway and meet stakeholder expectations. In the end, through the creation of FDP, the Norne Field operators are in a condition to responsibly manage the reservoir and its production: allowing continuous enhanced oil recovery, compliance with regulatory environments, and assurance of ongoing support from stakeholders and investors to sustain and prolong field economic relevance.

Objectives

1. **Data Collection and Initial Analysis**: Search and analyze all available geological, geophysical, petrophysical and engineering data which includes seismic data, log data, core samples, reservoir properties, and production histories to assess field attributes properly. Inspect 3D model from database using SLB Petrel & Eclipse
2. **Reservoir Characterization**: Create a detailed reservoir model using CMG software. It is necessary to include defined reservoir structure, fluid distribution and define rock and fluid properties, like porosity, permeability, and fluid saturation. It assists to identify the possible location of reserves and to evaluate the reservoir performance under different scenarios.
3. **Reservoir Simulation and Modeling**: Apply the reservoir model in order to assess production with different developed strategies such as primary, secondary and tertiary recovery which would yield the most recovery with respect to well economics and challenges posed by the environment.
4. **Well Planning and Design**: Assess and design the number, type, and spatial distribution of different wells among the injectors, producers and observation wells needed to meet production targets. It is done by choosing drilling technologies, completion methods, and well trajectories needed to penetrate different zones in the reservoir effectively.
5. **Production System Design**: Design the surface facilities that are needed for the production of oil and gas, which include gathering systems, separators, pumps, compressors, and pipelines. It also deals with planning of gas potential sales, water handling, and also the processing facilities required.
6. **Economic Evaluation**: Carry out- of the development plan in relation to its economic analysis and also submission of estimates for costs on capital (CAPEX), operations (OPEX), calculated income and uncertainties involved in the plan. Sensitivity analysis is developed to see whether the plan could hold together in the face of varying oil and gas price scenarios.
7. **Environmental and Regulatory Compliance**: Ensure that the plan complies with environmental, governmental regulations and industry standards. This may involve

conducting an Environmental Impact Assessment (EIA), obtaining necessary permissions, and planning for waste management, emissions control, and site restoration.

8. **Risk Assessment and Contingency Planning**: Identify operational and technical uncertainties throughout the life cycle of the project like environment and economic risks ideally developed for urgent situations in order to address an area where failures and interruptions may occur.

9. **Implementation and Monitoring Plan**: Prepare a proper, detailed working plan together with chronological manner for initiation involving drill, completion, and construction of facilities. This last step will also ensure the establishment of appropriate monitoring systems that allow careful evaluation of the reservoir as well as production for comparison with what was expected, so that plans can be modified as the case may be.

10. **Field Optimization and Enhancement**: After the first oil production, the production and reservoir performance must be evaluated continuously in order to recover as much oil as possible. It is important to adjust surface facilities and plan secondary recovery techniques and evaluate possible Enhanced Oil Recovery methods to maximize profitability of the reservoir as production proceeds.

Problem Statement

The Norne Field faces the dual challenge of declining production efficiency and complex reservoir heterogeneity, necessitating the development of an advanced FDP. This plan must explore pioneering EOR processes to maximize recovery and extend the productive life of the field, while remaining economically practical, meeting regulations, and being environmentally responsible.

Chapter 1. Data Gathering and Initial Analysis

Norne Field is an oil and gas field offshore Norway in the Norwegian Sea and a quite famous one with a rather complex organisation of Jurassic-age sandstone reservoirs. The primary reservoirs are the Ile and Tofte formations, which contain oil, and the Garn formation, which primarily holds gas. It has been a significant offshore oil and gas development operated by Equinor (formerly Statoil). Initially, the field's production was expected to last until 2014, but advancements in technology and successful implementation of Enhanced Oil Recovery (EOR) techniques extended the field's life. According to more recent reports the Norne field still functions but at a lower production rate than what was recorded during its peak years. The growth of the field has been significantly extended mainly due to the discovery of satellite fields and the application of new technologies aimed at improving the recovery factor. To this end, the Norne production facilities have continued to operate due to these connected satellite fields of Skuld and Marulk. That being said, the current and the foreseeable future developments of the field will to a great extent be dictated by the economic viability of such developments, the state of technology, government policies and the state of the infrastructure.

1.1 Geological Data

Norne Field which is found in the Norwegian Sea is made up of Jurassic sandstone reservoirs within Type I structural traps created by tilted fault blocks. Structural maps of a region indicate that there are multiple fault blocks which enhances compartmentalization of the reservoir. Available core samples of Norne suggest there were fluvial and shallow marine depositional environments which caused porosity and permeability to vary. These lithological studies highlight heterogeneity in the reservoir and as such have an impact of fluid distribution and flow characteristics in the reservoir.

In the Norne Field area, the reservoir is further described to comprise three to four distinct formations with differing formation types. This stratification, in turn influences how the reservoir is compartmentalized, how fluids are distributed within it as well as their flow characteristics hence explaining why specific practices are required in drilling and recovering in every formation. Such an understanding of the ranges is important for asset maximization

and therefore sustainability in production since volumetric flows between the wells are sensitive to porosity, permeability, fluid and fluid contacts across the field.

Garn Formation: This formation is predominantly gas-bearing, with variable permeability across different zones. The gas-rich nature of the Garn Formation requires specific strategies for gas production and management to optimize hydrocarbon recovery and prevent premature gas breakthrough.

Ile and Tofte Formations: These are the primary oil-bearing formations within the Norne Field, containing significant volumes of recoverable oil. The Ile and Tofte formations are the main targets for oil production, benefiting from favorable porosity and permeability that facilitate efficient oil flow.

Tilje Formation: Situated lower in the stratigraphic section, the Tilje Formation is characterized by relatively low permeability. Although it forms part of the reservoir, its limited permeability affects flow rates and requires careful consideration when planning extraction methods, especially if targeting extended or secondary recovery strategies.

1.2 Geophysical Data

Geophysical analysis of the Norne Field has involved extensive 3D seismic surveys, which help define reservoir boundaries, major fault lines, and structural complexities. Key seismic attributes, including amplitude and velocity, have been employed to assess reservoir thickness, fluid contacts, and zones with potential hydrocarbon accumulation. For monitoring reservoir dynamics over time, 4D seismic (time-lapse seismic) is used, which allows the observation of changes in fluid movement, especially useful for assessing water flooding patterns and the effectiveness of Enhanced Oil Recovery (EOR) strategies.

1.3 Petrophysical Data

In terms of petrophysical data, well logs such as gamma-ray, resistivity, neutron, and density logs have provided crucial information on the field's porosity, permeability, and fluid saturation. These petrophysical insights help in identifying net pay zones and estimating the volume of hydrocarbons in place, essential for planning efficient production. Nuclear

Magnetic Resonance (NMR) logs further enhance the understanding of pore size distribution, which plays a critical role in fluid flow and recovery efficiency across different parts of the reservoir.

1.4 Reservoir Characterization

Reservoir engineering plays an important role in a FDP as it serves as a fundamental of the reservoir to determine and control the hydrocarbon recovery. Reservoir engineering utilizes principles of fluid flow, thermodynamics, and reservoir behavior to give a detailed characterization of a reservoir; fluid type, distribution and pressure behavior. This understanding is critical for building a model that can simulate reservoir behavior to meet both the short-term and long-term production targets of the FDP.

Another aim of reservoir engineering in an FDP is to measure reserve and probable production. This includes the integration of historical production data with the help of modeling techniques, including reservoir simulation to assess the effects of development concepts, including primary, secondary and enhanced oil recovery(EOR) methods. These models help to choose mechanisms for appropriate extraction as well as provide forecasts on how many wells should be installed and in what form to optimally drain the reservoir with minimal wastage.

Reservoir engineering plays a crucial role in economic planning for the FDP. When the other parameters like the production rates, decline curves and cumulative recovery are forecasted, the engineer is in a position to offer vital contributions to help with revenue generation and evaluation of projects economic feasibility. This information helps to develop financial analysis in FDP that is important for decision-making by executives, stakeholders and investors. Further, through reservoir-engineering data, it is possible to estimate the surface facilities, equipment and infrastructures that may be required to achieve the desired production rates and pressure management

Lastly, reservoir engineering provides information which helps the company to manage risks in an FDP, including technical risks, such as pressure decline, fluid breakthrough or

compartmentalization in the reservoir. Knowledge of these risks helps the reservoir engineers to prepare management strategies and backup operational plans to keep the production high and avoid incidents that are costly to undertake.

1.4.1 Reservoir Rock and Fluid Properties

Table 1.4.1. Rock and Fluid properties of Norne Field's cut segment.

Property	Numerical value
Depth	2500-2700 meters
Lithology	Sandstone
Porosity	25-40 %
Permeability	20-2500 mD
Average permeability	500-1500 mD
Water Saturation	~16%
Wettability	Predominantly water-wet
Oil-Water contact TVD	8700 ft
Viscosity	6 x 10^-4 Pa·s
Average fluid API	34-35° API

Table 1.4.2. PVT Analysis.

Parameter	Value

Reservoir Fluid Types	Black Oil
Reservoir Pressure	3900 psi
Reservoir Temperature	207°F
Bubble point pressure	3600 psi
Oil formation volume factor	~1.2 m^3/STM
GOR	~120 Sm^3/Sm^3
Oil Compressibility	~ 10^-5 bar

Chapter 2. Geology and Petrophysics

2.1. Geological Background

The Norne Oilfield is located 200 km off the coast of Norway, in the North Sea. Founded in 1991, the Oilfield occupies the blocks 6608/10 and 6508/1 in the Nordland II area, which is situated in the Northern part of the Norwegian Continental Shelf. (Cruz, 2015). This area is associated with abundant hydrocarbon reserves, which counts a total of 125 fields that were producing since 1971 (Norwegian Petroleum, 2024). Figure 2.1.1. illustrates the precise location of the Norne Oilfield.

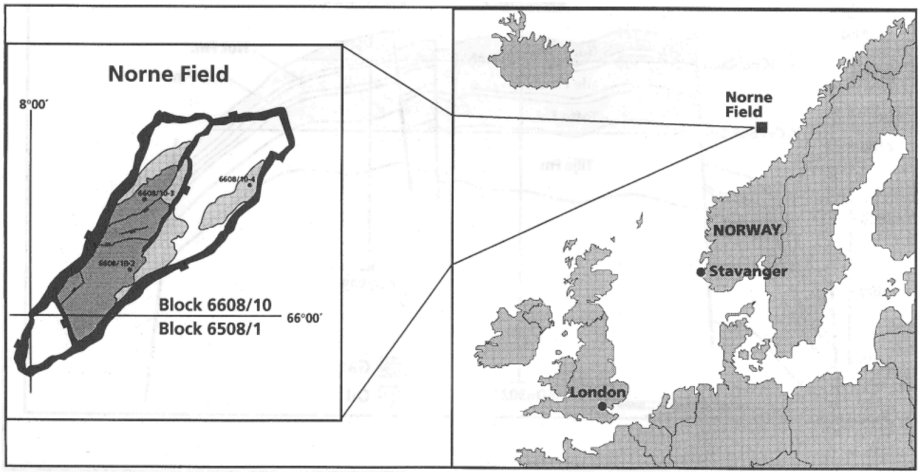

Figure 2.1.1. The location of Norne Oilfield (Gjerstad et al., 1995)

The Oilfield is located in a series of horsts and graben, which is due the very complex fault system and active tectonics in that region. It lies on the transition of two structural elements at the Revfallet Fault Complex area: Dønna Terrace and the Nordland Ridge (Cruz, 2015). This is greatly demonstrated in the figure 2.1.2. below, highlighting the location of the Norne Field.

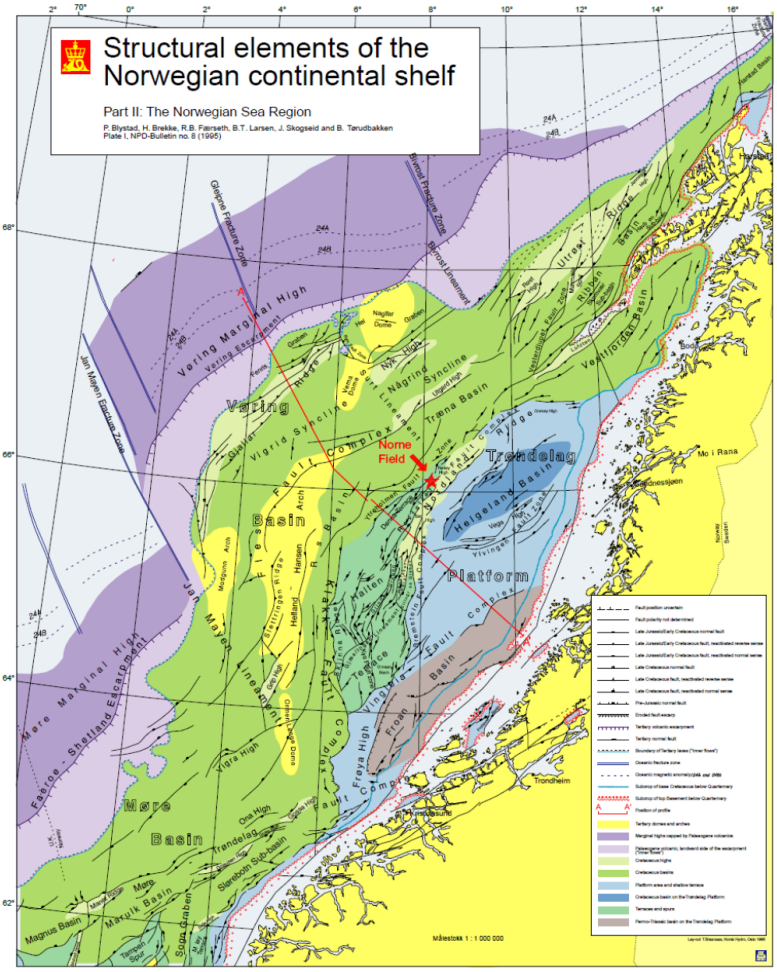

Figure 2.1.2. The structural map of the mid-Norwegian margin (Cruz, 2015)

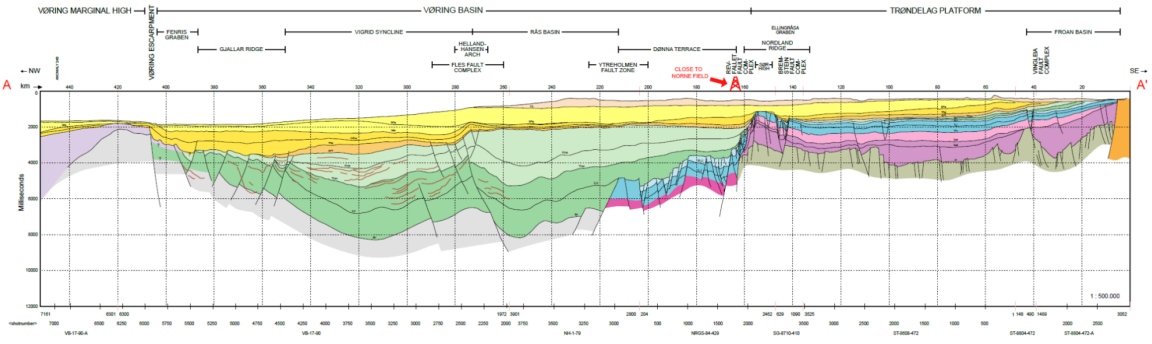

Figure 2.1.3. The profile of the mid-Norwegian margin (Cruz, 2015)

2.2. Stratigraphic Overview

The Norne Oilfield that is located on the horst blocks nine kilometers in length and 3 kilometers in width has four key formations. These are Garn, Ile, Tofte, and Tilje in the increasing order of depth (Rwechungura et al., 2010). The division between these formations is demonstrated in figure 2.2.

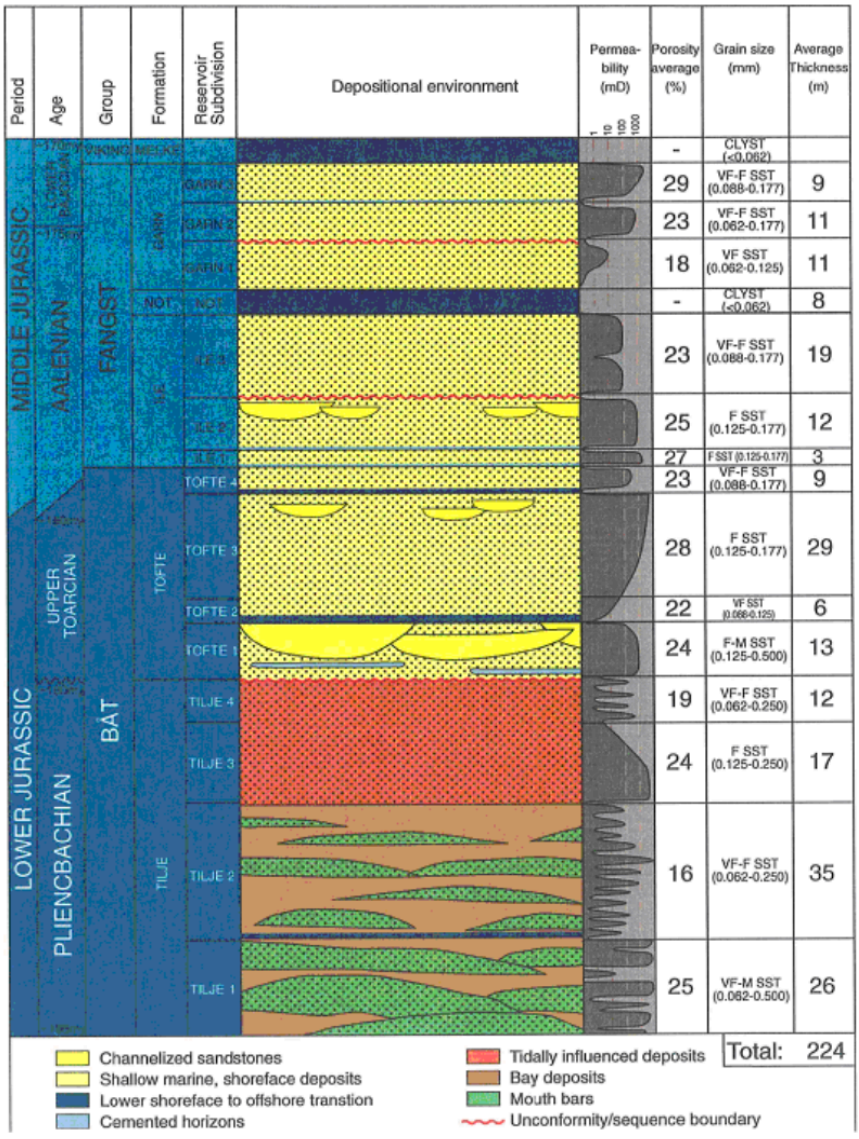

Figure 2.2. Stratigraphic subdivision of the Norne Field (Rwechungura et al., 2010)

The hydrocarbon column of 135 meters is located at the Ile, Tofte, Garn formations, which predominantly are fine-grained sandstones at the depths of 2500-2700 meters. The hydrocarbons originated from the high organic content source rock that is estimated to be from the Spekk formation from the period of Late Jurassic and Åre Formation from the period of Early Jurassic. The trapping mechanism takes place in the Melke Formation due to the impermeable cap rock sealing the reservoir. Another impermeable formation is the Not formation, which splits and isolates the Garn and Ile formations (Rwechungura et al., 2010).

2.3. Oilfield Segmentation

The Norne Field lies on a complex fault system that consists of horsts and grabens. Because of this, it splits into two separate oil compartments: the Norne Main Structure that includes segments Norne-C, Norne-D, and Norne-E, and the Northeast Segment that includes the Norne-G segment (Islam et al., 2018). This segmentation is clearly illustrated in the figure 2.3. In 1991, it was estimated that 97% of oil reserves of the field were held in the Norne Main Structure. Within this field development plan, the Norne-C segment was chosen from the Norne Main Structure, as it holds about 80% of the total oil from this field (Akpan, 2015) and contains the most available datasets for the analysis.

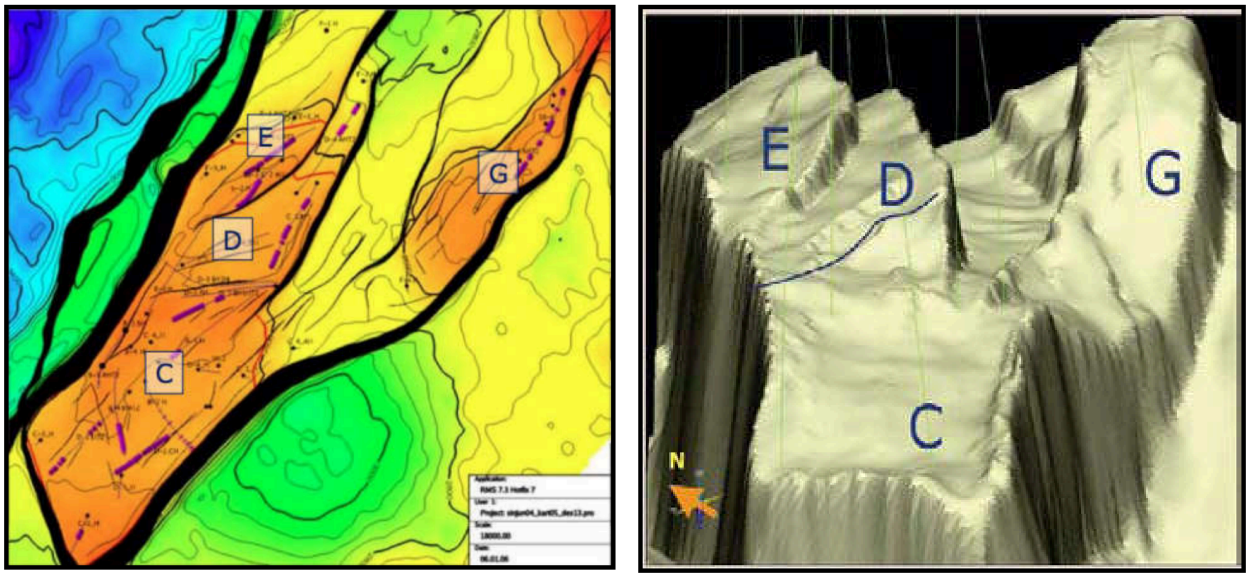

Figure 2.3. The segmentation of the Norne Field (Islam et al., 2018)

2.4. Well Log Analysis in Techlog Software

In order to create a comprehensive field development plan, a thorough well log analysis needs to be performed. It was chosen that it will be done using the Techlog Software, courtesy of Schlumberger Ltd. In this section, the methodology behind the analysis, results, and discussion will be presented.

2.4.1. Methodology for Well Log Analysis

The Norne Oilfield lacked open source well logs in lasio format, which is suitable for various softwares, so it was decided to find an analogous oilfield in the North Sea with the available data. The Volve Oilfield was chosen for this step. After completing the full analysis, the results of this case study will be presented and compared to actual data of the Norne Field.

The dataset included three corresponding logs from wells 15/9-F-1A, 15/9-F-1B, and 15/9-F-1C, which included the following logs:

- GR - Gamma Ray log
- CALI - Caliper log
- BS - Drill Bit Size log
- NPHI - Neutron Porosity log
- RHOB - Bulk Density log
- RACEHM - Deep Resistivity log

From these logs, the following properties will be found:

- Wellbore integrity
- VShale volume
- Lithology zonation
- Fluid zonatoin
- Total and effective porosity
- Water saturation

- Permeability

The procedure will now be described with steps.

Step 1: Import the data

Click on the “Import”  icon. Then, click on the “Browse”  icon in the project browser section:

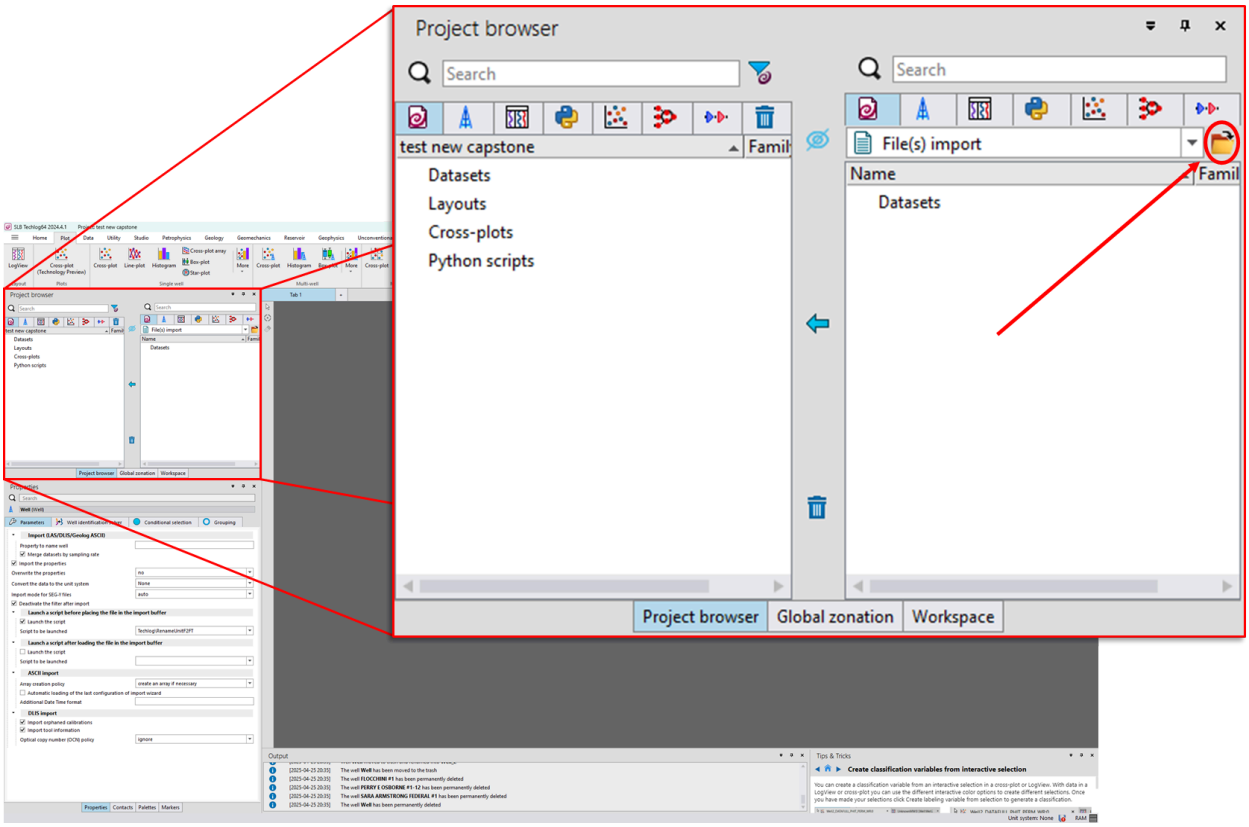

Figure 2.4.1. Data Importing in Techlog

Step 2: Transfer the dataset into Project dataset

Highlight the 3 wells datasets and click on the blue arrow:

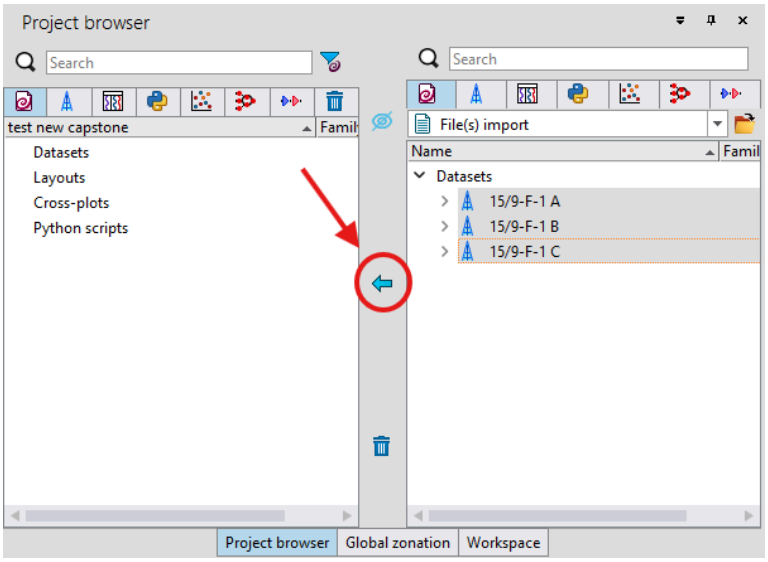

Figure 2.4.2. Project dataset transfer

Step 3: Plot the logs

On “Plot” section, click on the “LogView” icon  and drag and drop the logs.

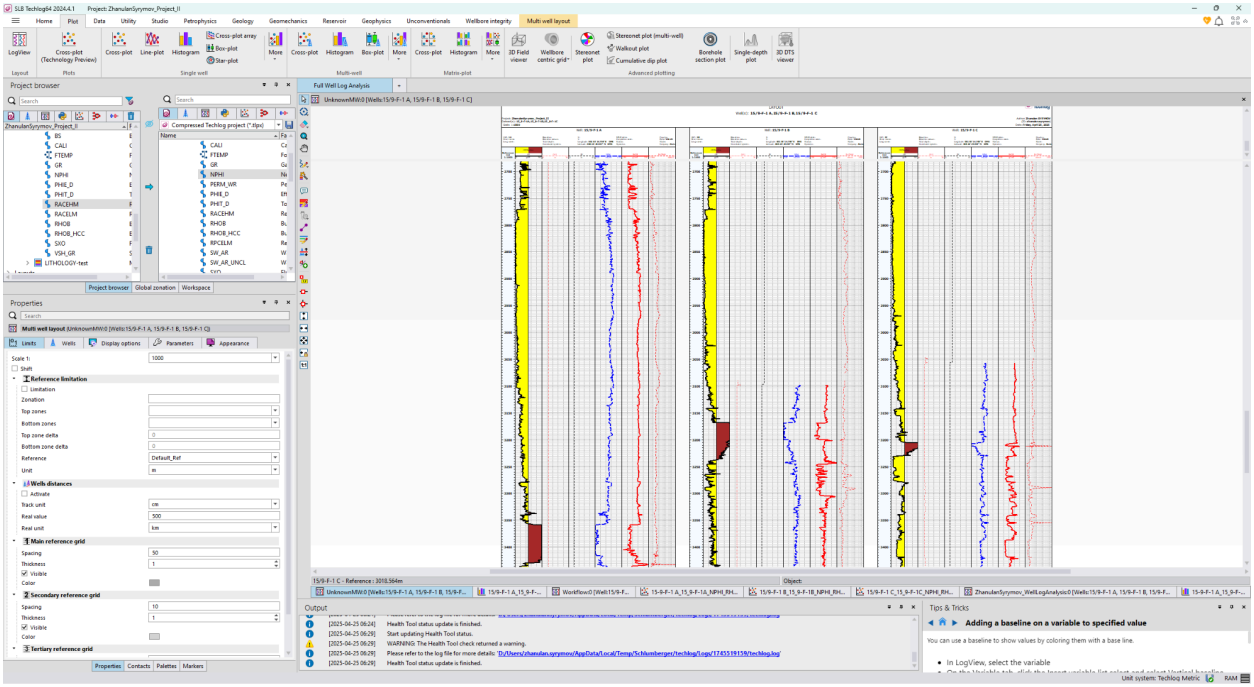

Figure 2.4.3. Initial Log data on the Volve Field

The logs are plotted, however they lack any analysis, so the process will start on a blank tab.

Step 4: Wellbore integrity analysis

In this step, plot and correlate the caliper (CALI) log with the Drill Bit size (BS) log. It is important to keep the limits of the well log plot the same (6-16 in). After plotting, click on both logs while holding shift, right click, and click on the "Insert area fill between the variables" icon.

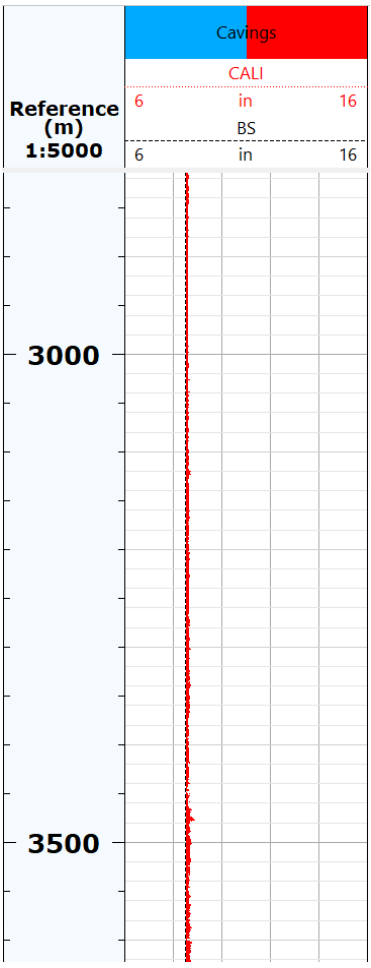

Figure 2.4.3. Cavings and washout zone identification

Step 5: Plot the Gamma Ray Log

Drag and drop the Gamma Ray (GR) log. After, select the limits 0-150 gAPI and by right clicking on the log, select the “Insert vertical baseline” icon. This will be needed to clearly identify the porous zones and shale zones.

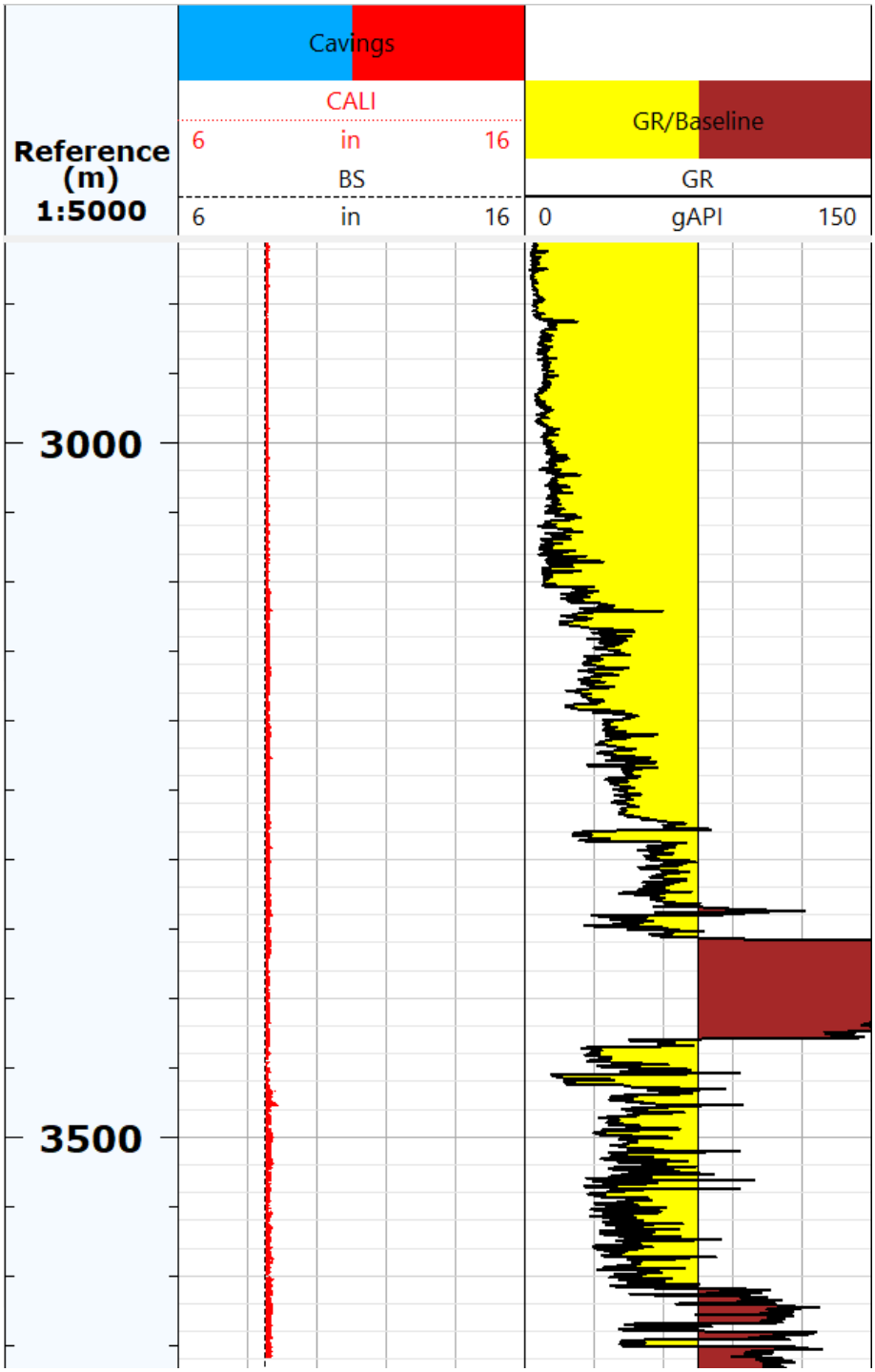

Figure 2.4.4. Gamma Ray (GR) Log

Step 6: Bulk density (RHOB) log vs. Neutron Porosity (NPHI) log

Plot first the RHOB log, and then plot NPHI log on top of it. Select the color of NPHI log line to be a red dashed line, and for RHOB black solid line. Repeat the process as for CALI vs. BS logs. Select the colors to be green and cyan. Green will account for the so called "Gas Effect".

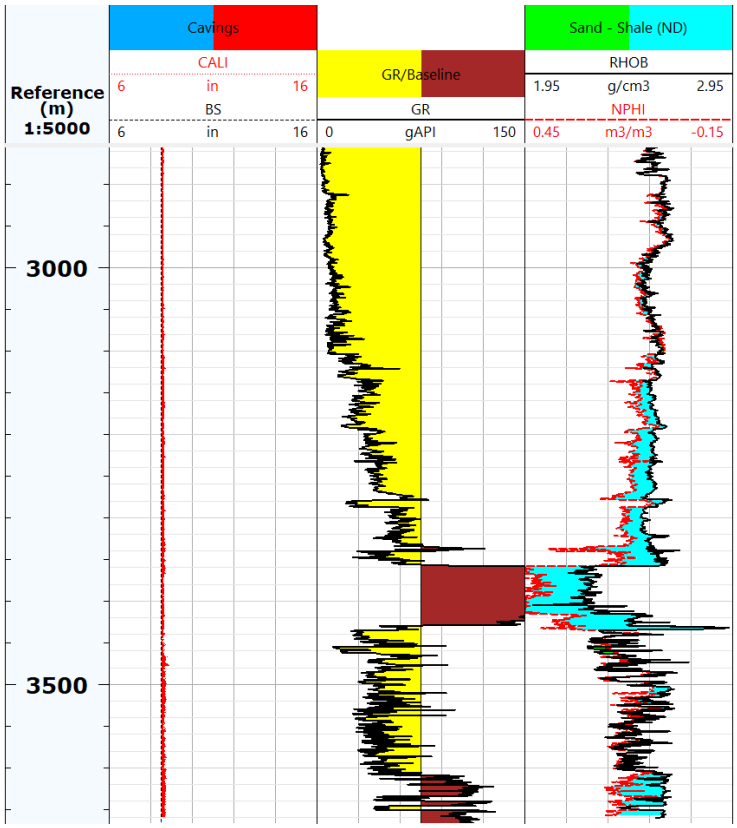

Figure 2.4.5. RHOB vs. NPHI logs

Step 7: Temperature log

In the Petrophysics section, click on the “Precomputations” icon and select “Formation temperature”. There, a workflow window will appear. In that window, the depth log needs to be selected:

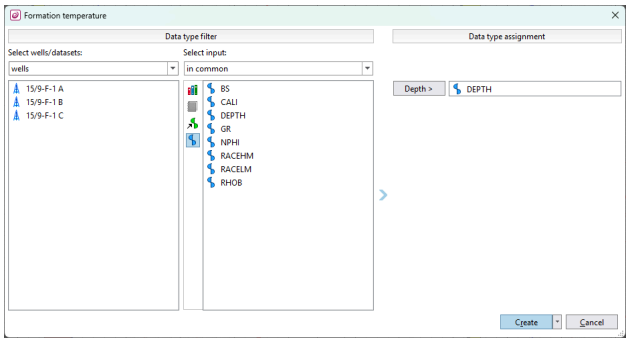

Figure 2.4.6. Formation temperature determination

After creating the workflow, the datasets need to be drag and dropped:

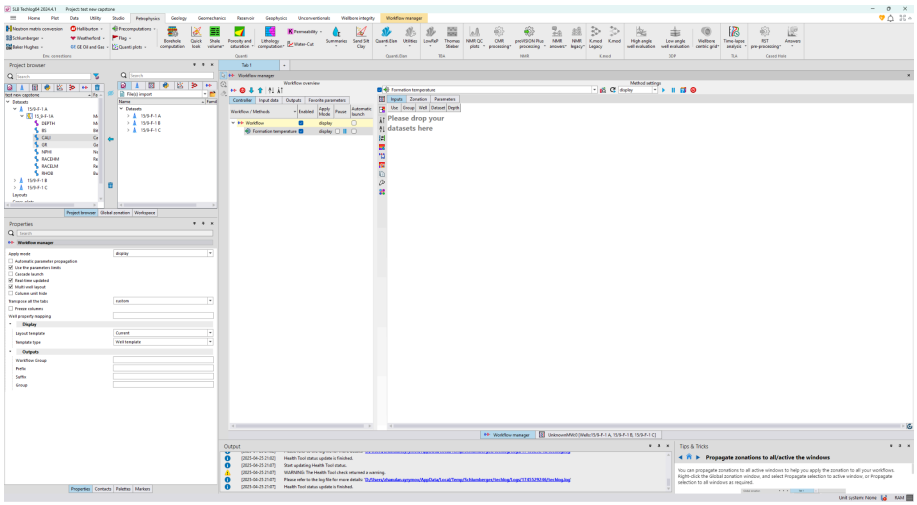

Figure 2.4.7. Workflow manager for the temperature

There, select the “Display and save” option and click on the “Launch” icon.

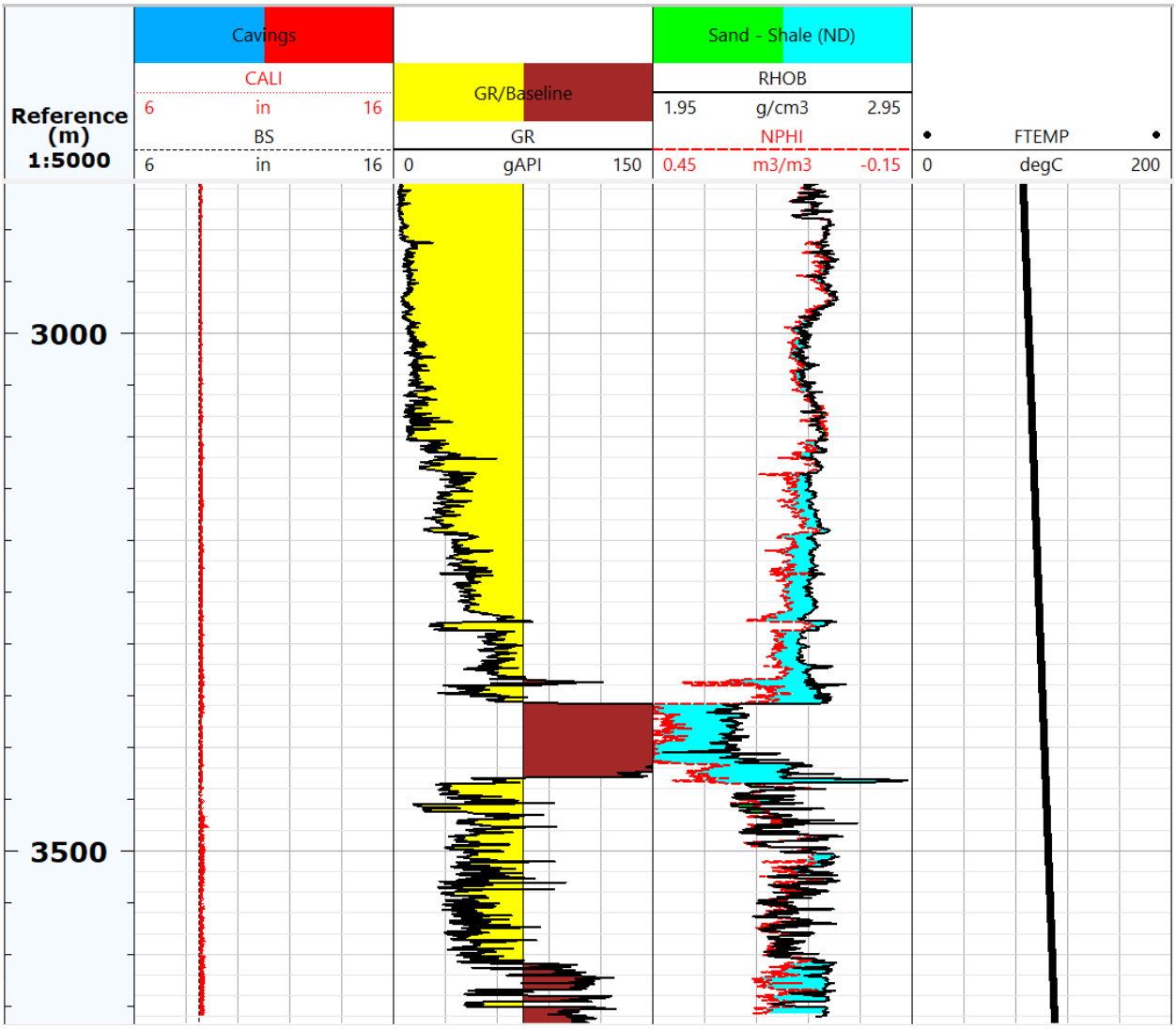

Figure 2.4.8. Formation temperature curve

Step 8: Lithology

For this step, the scatter plot of NPHI vs. RHOB needs to be created. To do this, in the "Plot" section, select the "Cross Plot"  icon. A window for the plotting will appear. There, the NPHI log has to be dropped in the x-axis and RHOB has to be dropped on the y-axis. After that, the Schlumberger pre-made correlation has to be integrated:

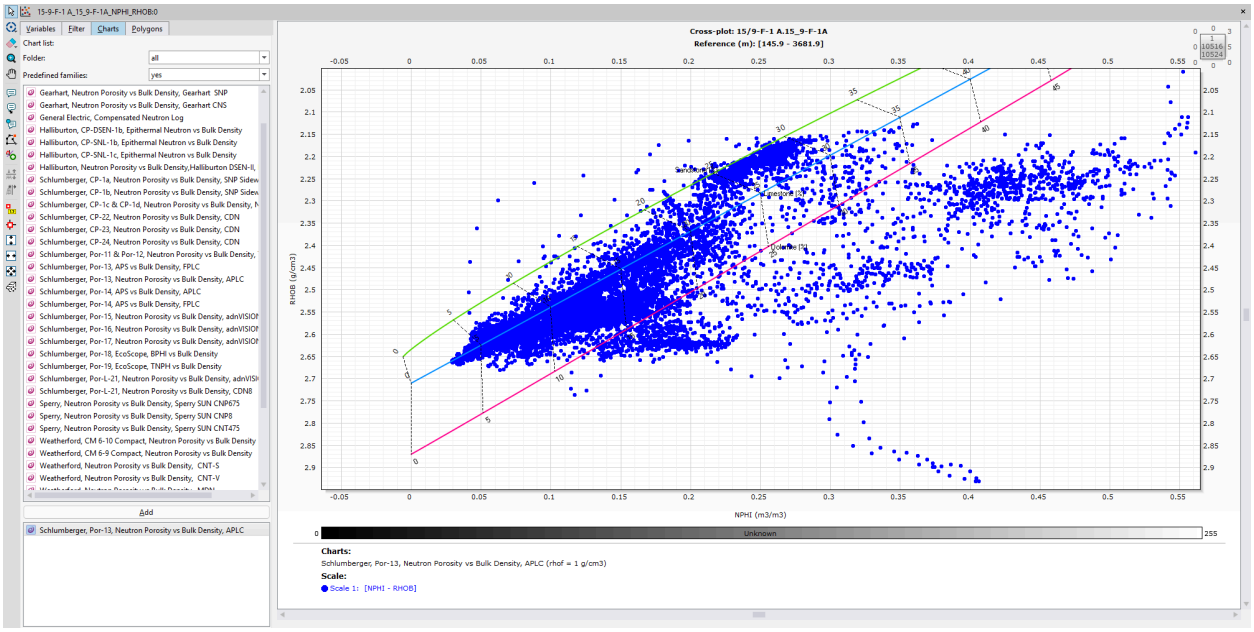

Figure 2.4.9. NPHI vs. RHOB scatter plot

There, the "Interactive selection" needs to be used. Assigning three different colour for Sandstone, Limestone, and Dolomite, select the corresponding values that lie beneath the correlation lines like the following:

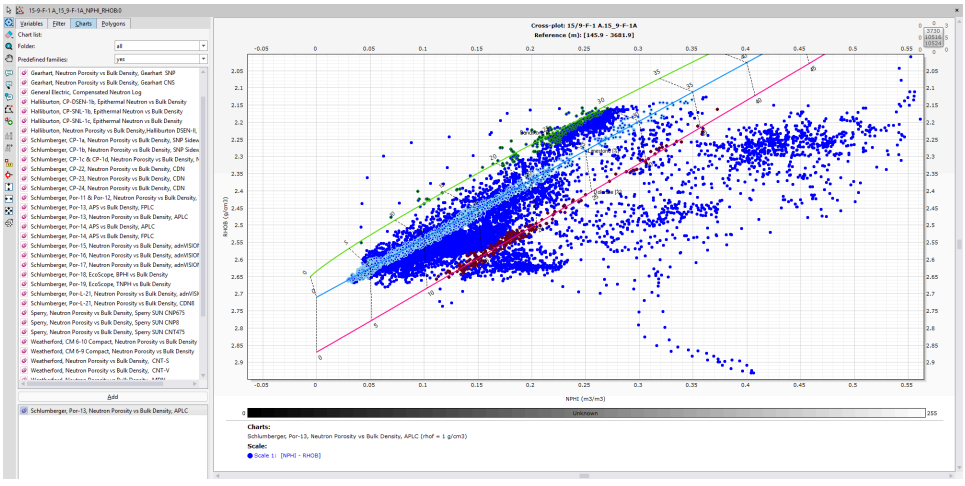

Figure 2.4.10. Correlated NPHI vs. RHOB scatter plot

These actions highlighted the sections in the basic logview panel allowing us to complete the lithology analysis:

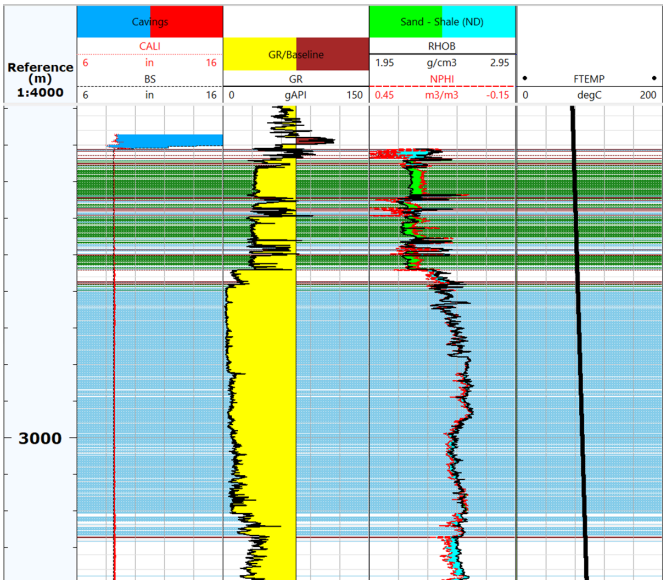

Figure 2.4.11. Lithology analysis in Techlog

From here, click on the “Create and edit zones over logview"  icon.

After creating a new zonation labeled as “Lithology”, create zones for Sandstone, Limestone, Dolomite, and Shale. Then, assign each zonation depending on the correlation highlights and other well logs (GR) for shale zones.

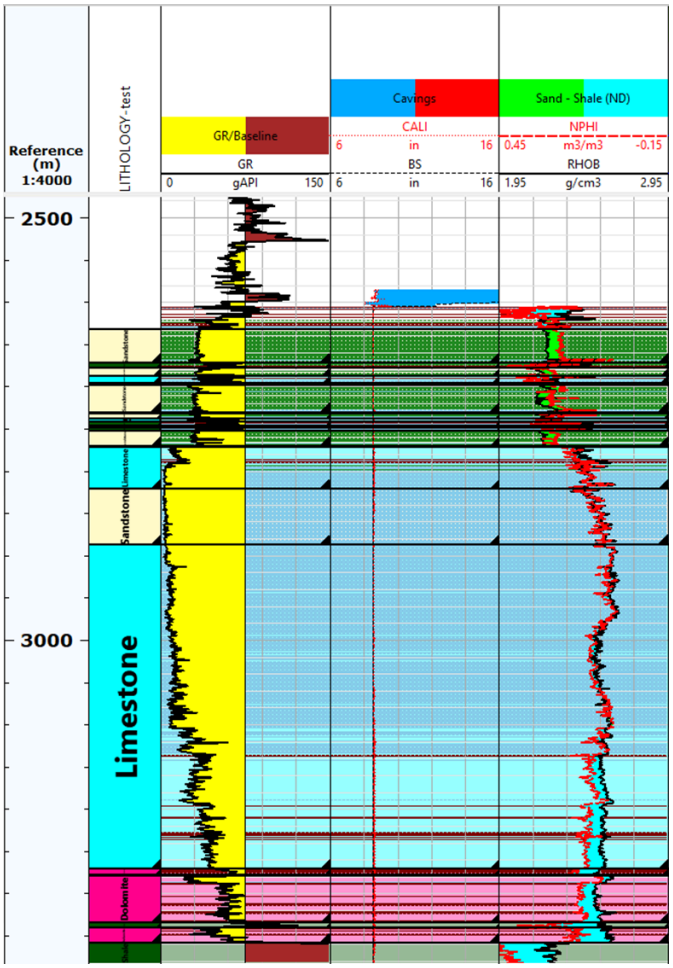

Figure 2.4.12. Formation lithology analysis

Step 9: VShale volume logs

For this step, in “Petrophysics” section, select “Shale Volume”  icon. There, select the “Gamma Ray” approach. The procedure will be the same, as for the formation temperature, where the Gamma Ray (GR) log needs to be selected. After that, proceed to the workflow manager window, and drag and drop the data, and launch the workflow:

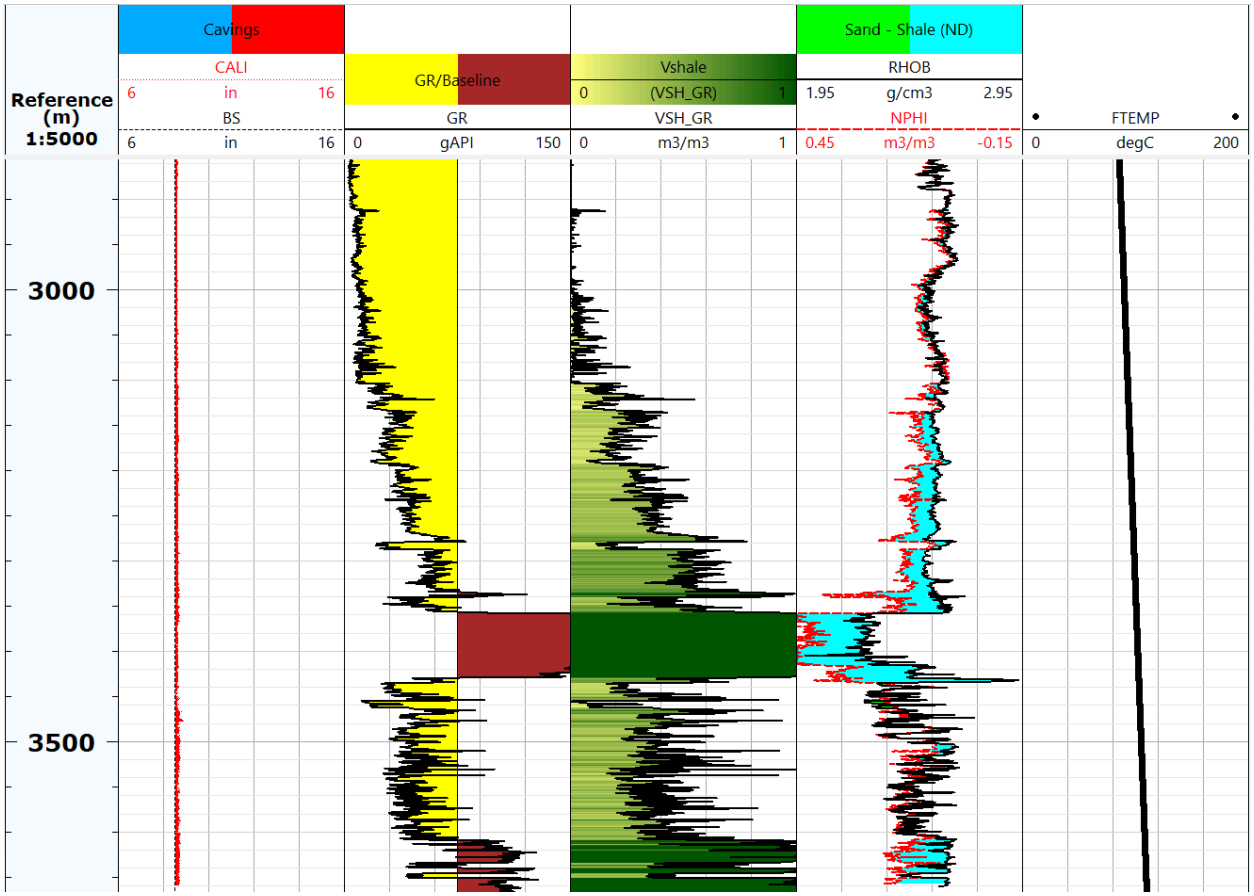

Figure 2.4.13. VShale log

Step 10: Resistivity log

Plot the RACEHM/RACELM logs. Select logarithmic scale and limits of 0.2 to 2000 ohm*m:

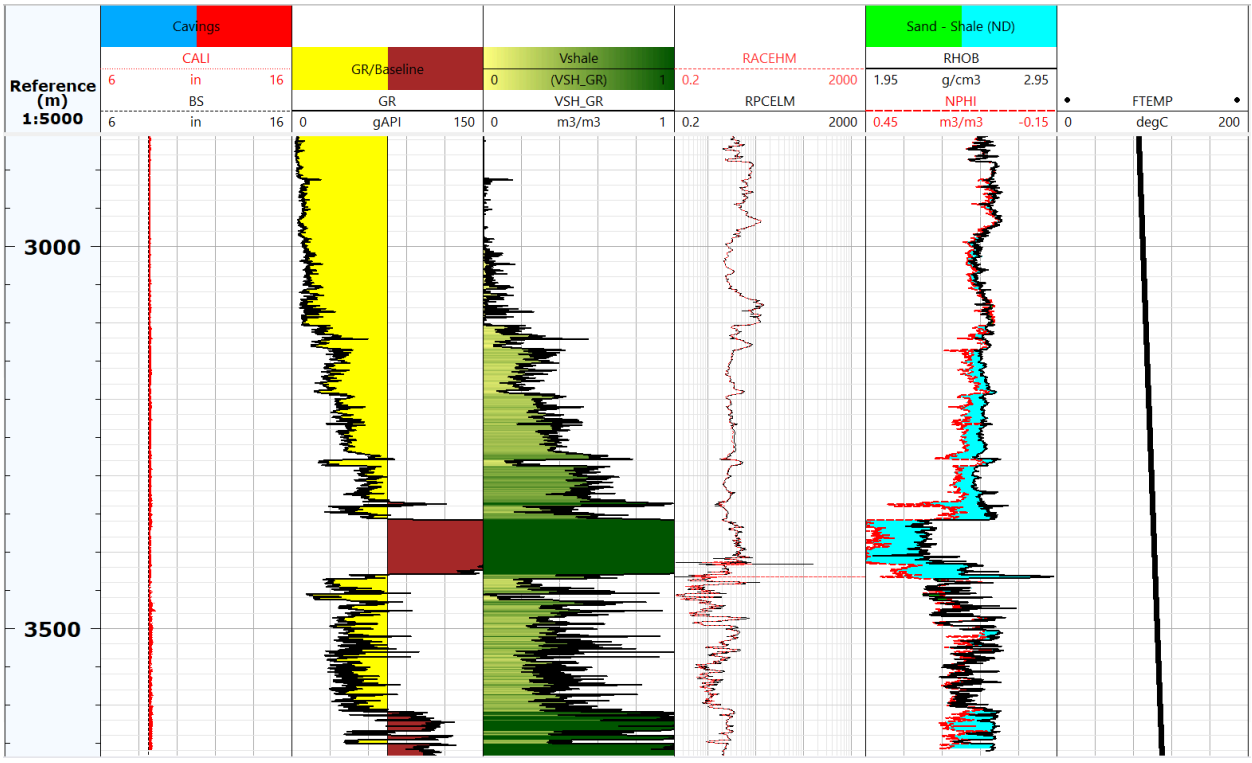

Figure 2.4.14. Resistivity logs

Step 11: Effective and Total Porosity logs

To determine these porosities, in the “Petrophysics section” select the “Effective Porosity” and “Total Porosity” choosing “Neutron-Density” approach. After moving on to the workflow manager, the zonation has to be applied. There, the constants for the corresponding zones have to be filled in for matrix densities, brine densities. After that, launch the workflow:

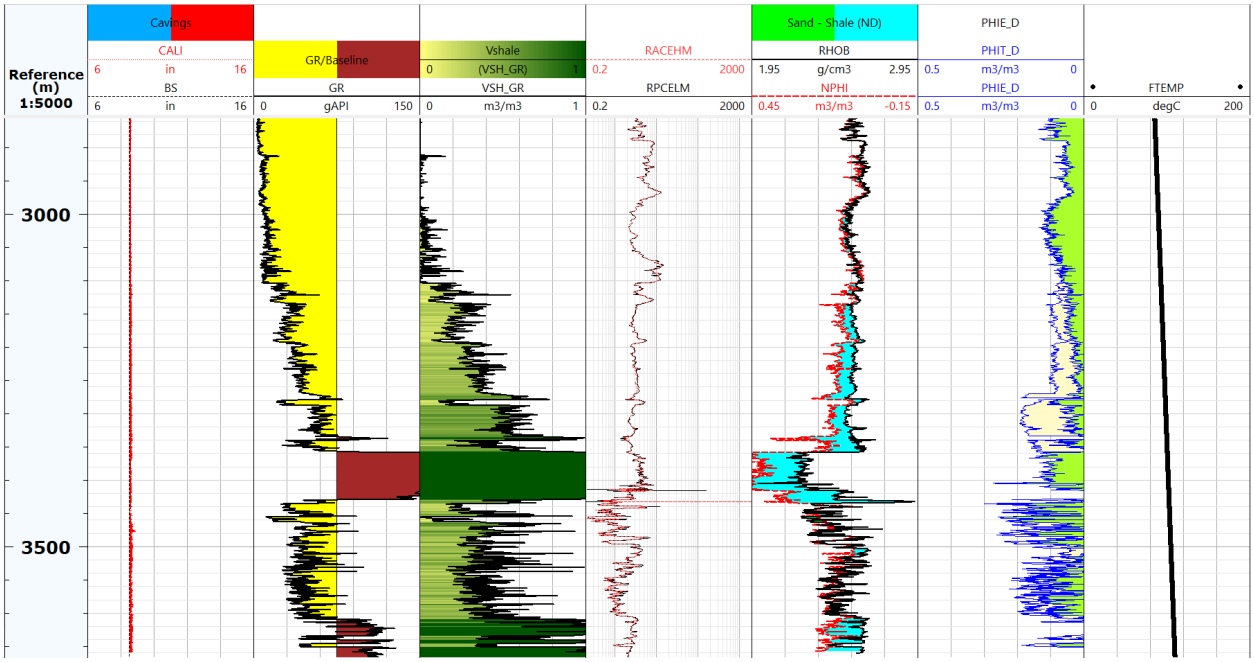

Figure 2.4.15. Effective and Total Porosity logs

Step 12: Permeability and Water Saturation logs

For this step, in "Petrophysics" section, select the "Permeability" icon and in "Porosity and Saturation" click on "Saturation" icon and select "Archie" approach. Proceed to the workflow. For the permeability, the Willie-Rose correlation will be used.

The Willie-Rose correlation equation is defined as following (Archie, 1942):

$$K = P \times \frac{\Phi^{Q}}{S_{wir}^{R}} \quad (1)$$

Where:

- K - Permeability
- P, Q, R - Empirical constant that are derived from lab
- Φ - Total Porosity

- S_{wir}^{R} - Irreducible water saturation

For this step, the constants come included in the lasio file, and the irreducible water saturation will be assumed to be equal to 0.2.

The Archie equation is given as following (Xin, 2001):

$$S_w = \sqrt[n]{\frac{a \times R_w}{R_t \Phi^m}} \tag{2}$$

Where:

- S_w - Water saturation
- R_w - Resistivity of formation water
- Φ - Total porosity
- R_t - True formation resistivity
- a - Empirical constant
- m - Cementation exponent
- n - Saturation exponent

For this step, the average constant will be taken, which are usually equal to 2.

Proceeding with the workflow gives us the results:

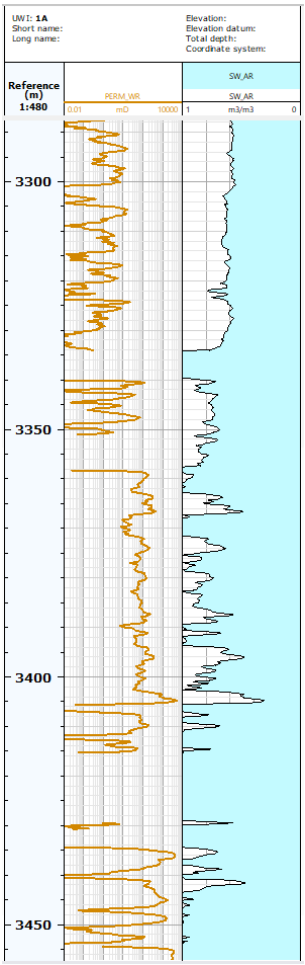

Figure 2.4.16. Permeability and Water Saturation logs

Step 13: Fluid zonation identification

For this step, various logs will be used. The most important of them are Resistivity logs, NPHI vs. RHOB and Lithology. Also, the principles such as “Gas effect”, “Football effect” will be used. The following procedure will be used:

- Low resistivity and NPHI vs. RHOB curves close to each other - Water zone
- High resistivity and NPHI vs. RHOB curves close to each other - Oil zone
- High resistivity and NPHI vs. RHOB criss-cross with high difference - Gas zone

After following this procedure, the following zones were identified:

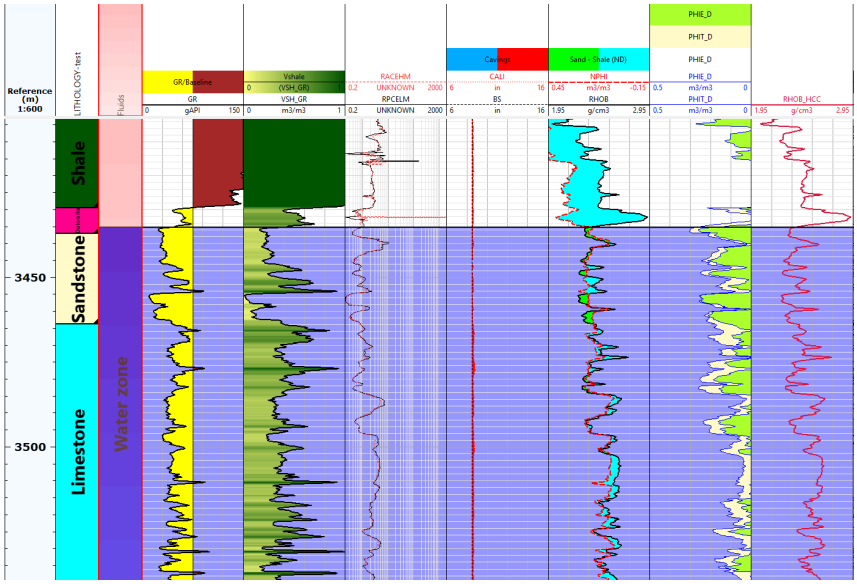

Figure 2.4.17. Water zone

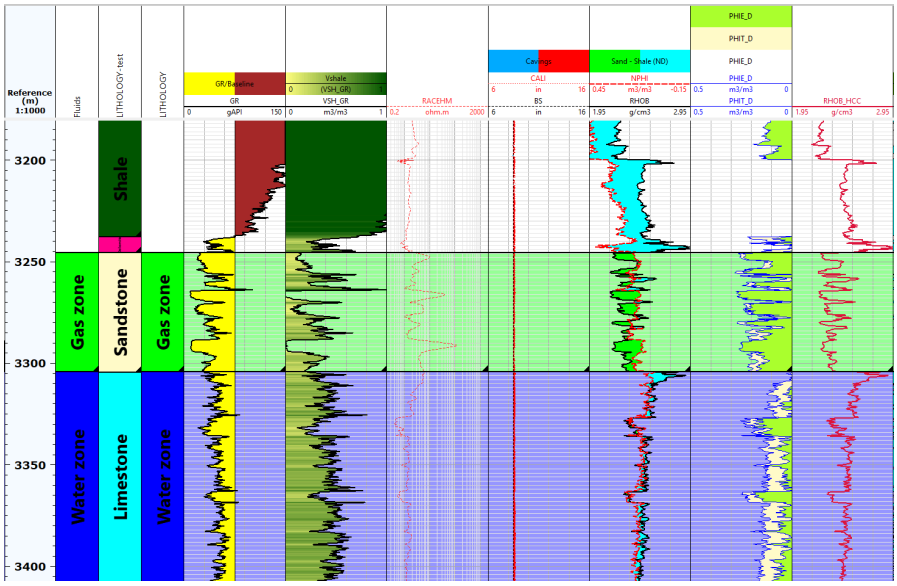

Figure 2.4.18. Gas Water contact zone

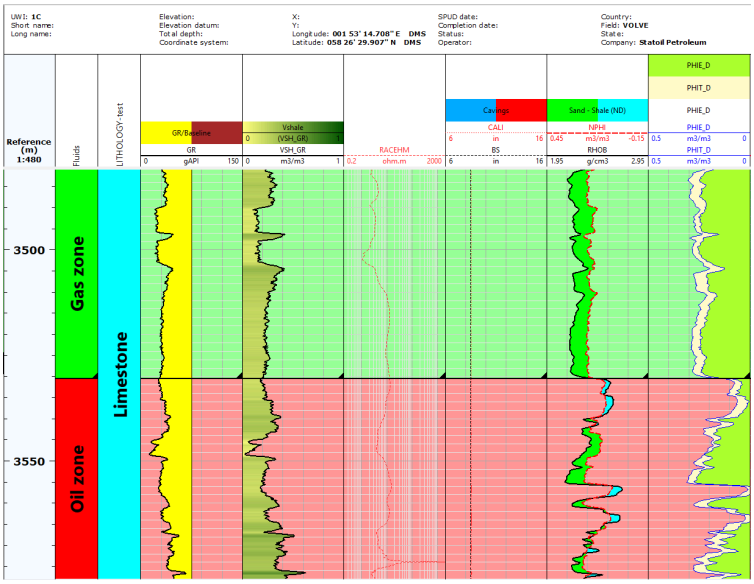

Figure 2.4.19. Gas Oil contact zone

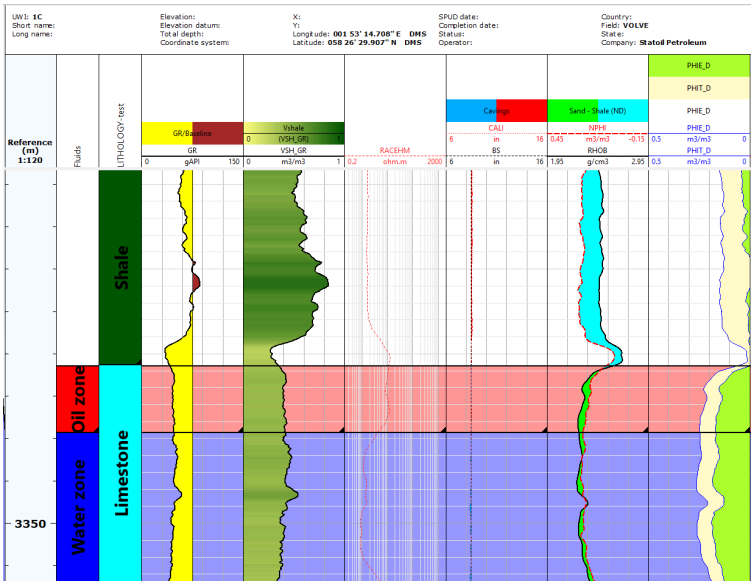

Figure 2.4.20. Oil Water contact zone

2.4.2. Well Log Analysis Results

After repeating the procedure for all three wells, the following results were obtained:

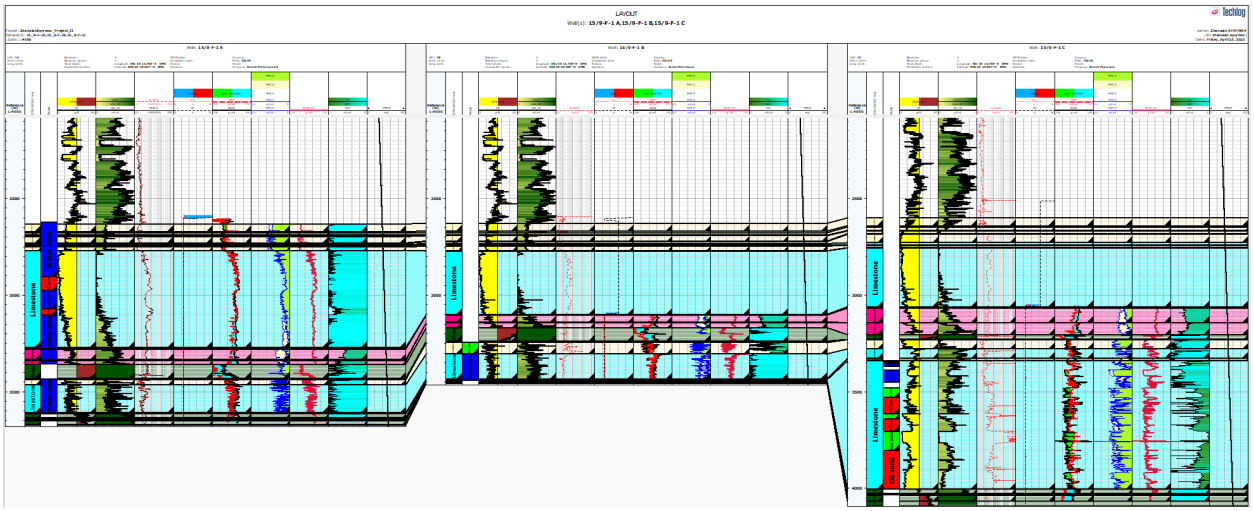

Figure 2.4.21. Full well log analysis in Petrel

The porosities, permeability, vshale, and other curves will be presented as histogram plots with corresponding statistics:

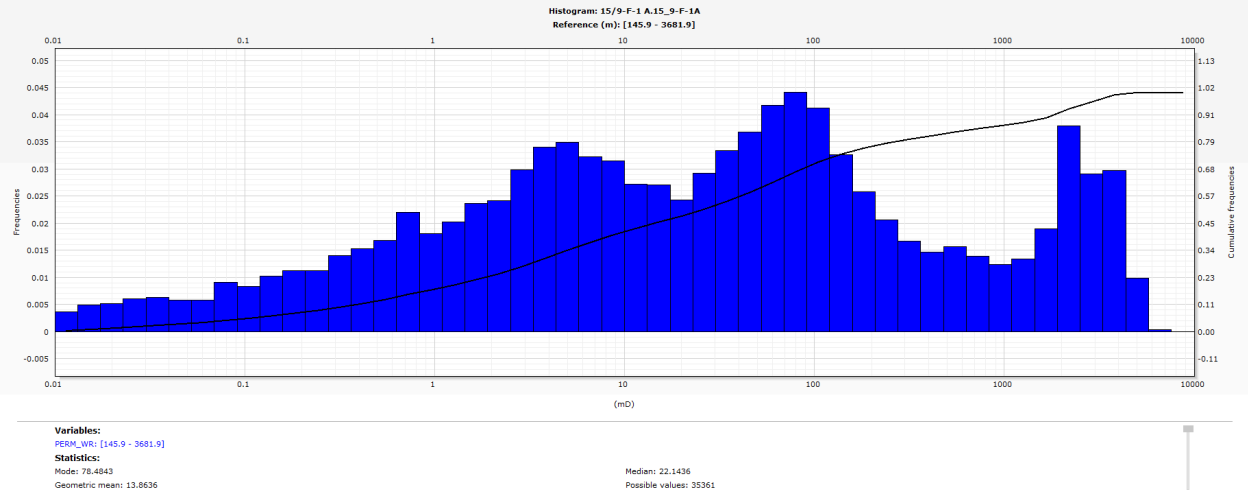

Figure 2.4.22. Permeability histogram plot

Table 2.4.1. Permeability statistics

Variables : 15/9-F-1 A.15_9-F-1A.PERM_WR		
Statistics		
Mode : 78.4843	Arithmetic mean : 428.703	Geometric mean : 13.8636
Median : 22.1436	Average deviation : 629.147	Q1[10%] : 0.141996
Number of values : 35361	Standard deviation : 975.911	Q2[25%] : 1.89072
Number of missing values : 26316	Variance : 952403	Q3[50%] : 22.1436
Min value : 5.31859e-16	Skewness : 2.6947	Q4[75%] : 154.159
Max value : 6405.5	Kurtosis : 6.6415	Q5[90%] : 1932.36

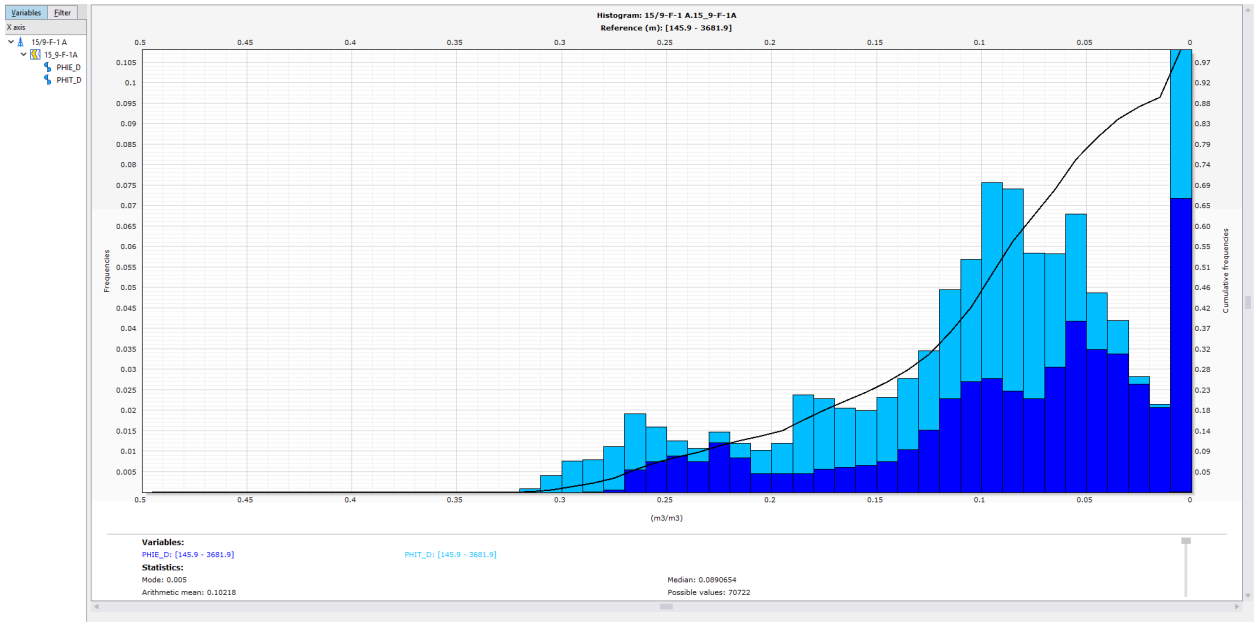

Figure 2.4.23. Total and Effective porosity histogram plots

Table 2.4.2. Total and Effective porosity statistics

Variables : 15/9-F-1 A.15_9-F-1A.PHIE_D,15/9-F-1 A.15_9-F-1A.PHIT_D		
Statistics (cumulated)		
Mode : 0.005	Arithmetic mean : 0.10218	Geometric mean : 0.0901416
Median : 0.0890654	Average deviation : 0.0587456	Q1[10%] : 0.00341295
Number of values : 70722	Standard deviation : 0.0749391	Q2[25%] : 0.0502623
Number of missing values : 50142	Variance : 0.00561587	Q3[50%] : 0.0890654
Min value : 0	Skewness : 0.783886	Q4[75%] : 0.139414
Max value : 0.329304	Kurtosis : -0.0115732	Q5[90%] : 0.222647

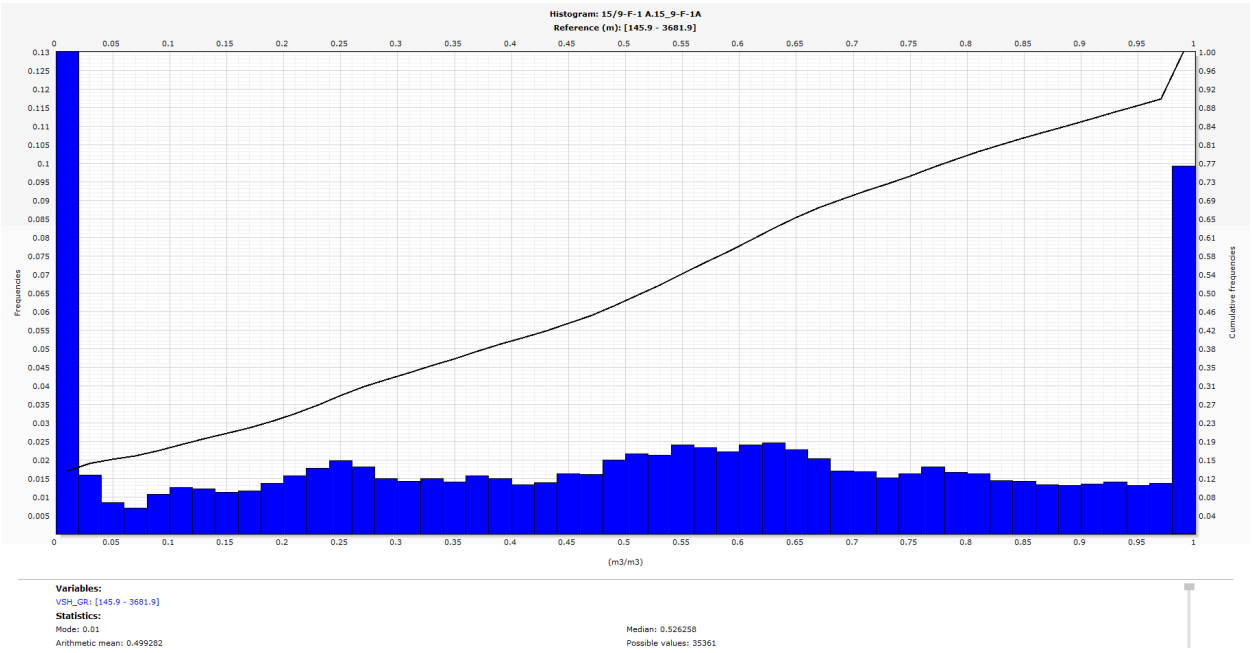

Figure 2.4.24. VShale histogram plot

Table 2.4.3. VShale statistics

Variables : 15/9-F-1 A.15_9-F-1A.VSH_GR		
Statistics		
Mode : 0.01	Arithmetic mean : 0.499282	Geometric mean : 0.414665
Median : 0.526258	Average deviation : 0.281365	Q1[10%] : 0
Number of values : 35361	Standard deviation : 0.327742	Q2[25%] : 0.221221
Number of missing values : 690	Variance : 0.107415	Q3[50%] : 0.526258
Min value : 0	Skewness : -0.0614528	Q4[75%] : 0.769365
Max value : 1	Kurtosis : -1.20251	Q5[90%] : 0.978851

2.4.3. Discussion of Well Log Analysis

Caliper and Drill bit comparison analysis shows that there is almost no difference in these wirelines, which suggest that the wellbore integrity is maintained at significantly high state. No caving and washout zones were identified.

Lithology analysis shows that there are predominantly limestone and sandstone formation zones with the presence of shale zones in between. The high values for VShale and Gamma ray support the Shale zonation, while the Schlumberger correlations for NPHI vs. RHOB scatter plot support the accuracy of the lithology identification.

As for the fluid zonation procedure, while it was accurate at defining the saturated fluid, there were still zones with the sequence of Oil-Water-Oil-Water or Gas-Oil-Gas-Oil zones. This may happen for a reason that there might be a thin impermeable layer that prevents the balancing of this fluid columns, or there might have been an error due to the miscalibration of the well logging equipment.

To analyze the accuracy of the porosity and permeability data, it will be compared to actual data from the Norne Field. The figure 2.4.25 presents the geological zonation and rock properties values for the Norne field.

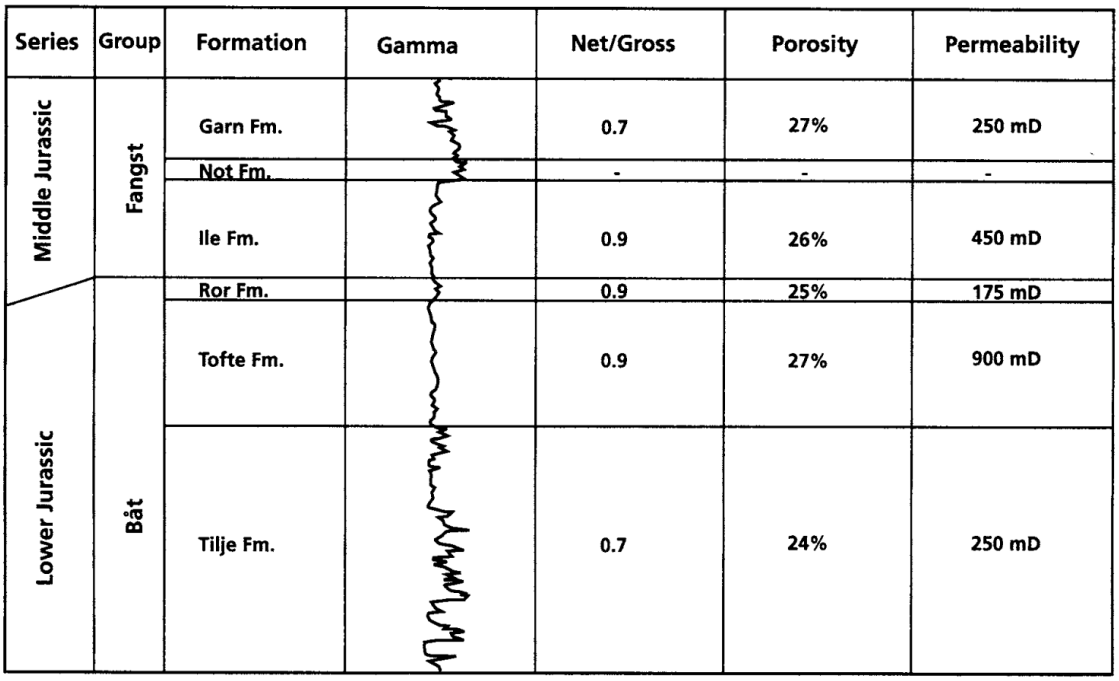

Figure 2.4.25. Actual geological zonation and rock properties of the Norne Field (Gjerstad et al., 1995)

It can be seen that while the permeability values might match at an average of 500 mD, the values for porosity differ significantly. That is why these values will be neglected, and the actual values will be used further instead.

2.5. Seismic Data and Fault System of the Norne Field

During the exploration of the Norne Field, there were many seismic tests conducted for the reservoir, aiming for understanding the fault system of the field. The figure 2.5.1. will show the inline seismic section of the Norne Field showcasing Segment Norne-E and Norne-C.

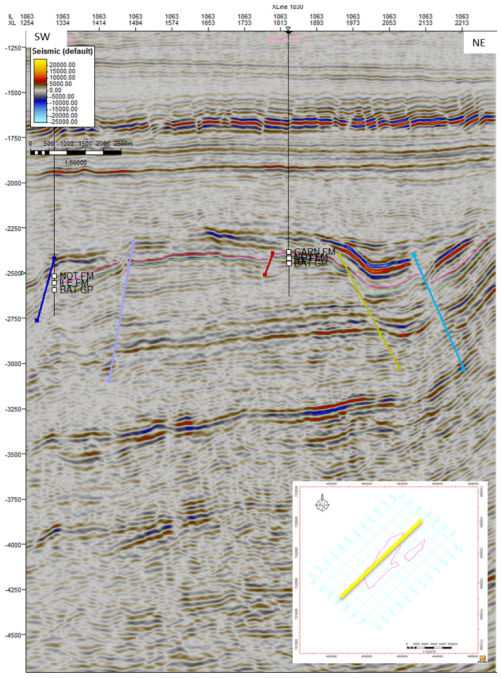

Figure 2.5.1. The inline seismic section of the Norne Field (Cruz, 2015)

Interpreting this seismic image gives us the following results:

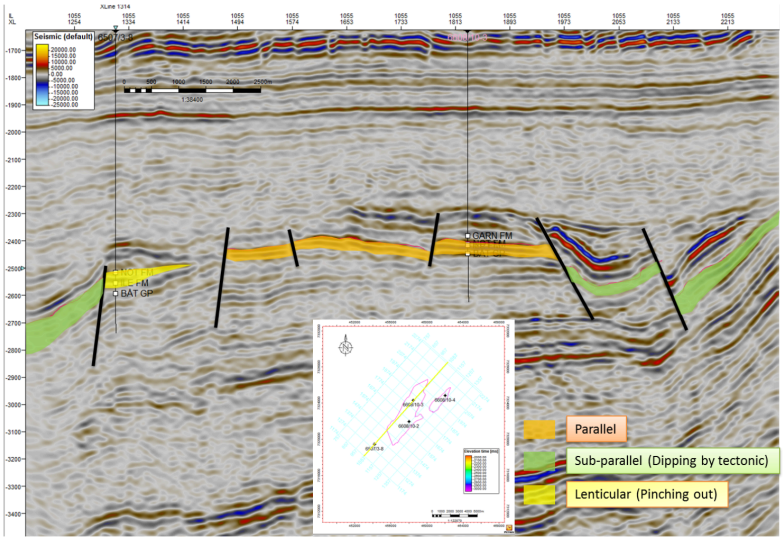

Figure 2.5.2. Interpretation of the Seismic image (Cruz, 2015)

Using all this data, the fault model and seismic maps were created:

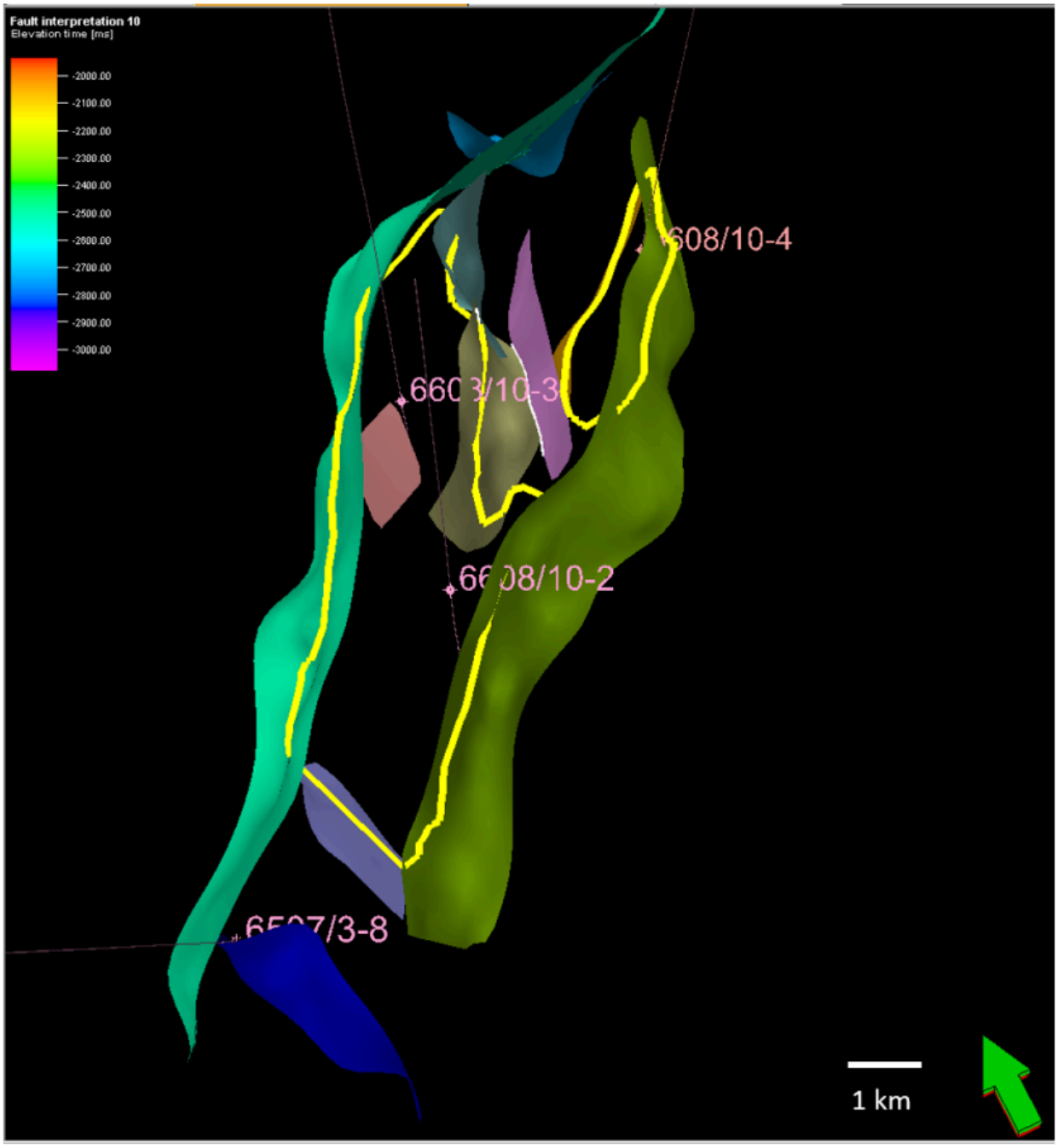

Figure 2.5.3. Norne Oilfield fault model (Cruz, 2015)

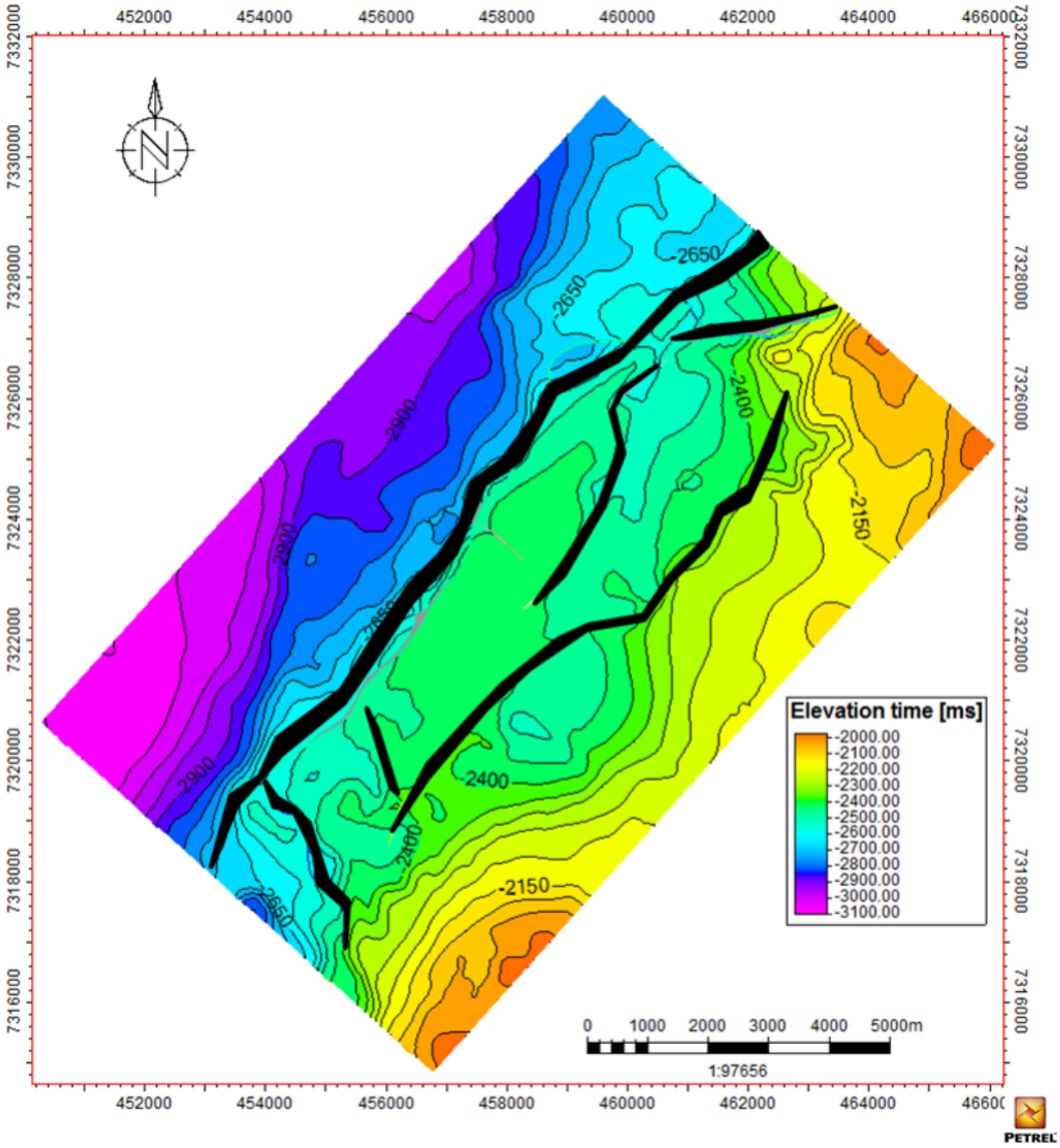

Figure 2.5.4. Norne Oilfield seismic map (Cruz, 2015)

This data was used for the interpretation of the history and tectonic activities of the field. It was found that the rifting occurred multiple times: during Permian, Late Jurassic-Late Cretaceuos times. This created a fault system that is dominated by extensional faults. On the contrary, the formation of horst blocks, in which the reservoir is associated with the series of

normal faults, which are mostly oriented in the North-Eastern direction. There were also minor faults that spread to 2-5 kilometers laterally identified in the region.

The data that was found and determined in this section was provided to other departments. Many datasets that are not mentioned in this section were provided directly and introduced in the corresponding chapters. This includes the rock and fluid properties, their distribution of values, which will be used for the Monte Carlo Analysis, the net thickness and key hazardous zones, which will be used in drilling and completion engineering. Number of wells, their depths, types, and costs will be discussed in other sections, and introduced by other corresponding departments. The static and dynamic model included all the necessary data for the analysis in the initial dataset.

Chapter 3. Reservoir Engineering

3.1 Drive Mechanisms

The Norne Field uses several drive mechanisms to recover oil, and the main focus is on C and E segments. During the initial stages of the development, water and gas injection formed two of the main approaches to support reservoir pressure and recovery factor. The field initially mainly focused on water flooding, which is also a type of secondary recovery method it used to maintain pressure and enhance the density of the oil and water phase. Nevertheless, beyond this period, the field faced the challenge of high water cut together with reduced production rates, and as a result, EOR methods were in need to be implemented .

Since water injection only was not sufficient to achieve targeted recovery factor, it was planned to inject gas together with water to enhance sweep efficiency and to avoid early water breakthrough problems particularly in complex heterogeneous parts of the field. For instance, according to Akpan, (2012) in the Norne C-segment, there was both gas and water injection to sustain the right pressure, as well as support displacement of the oil in the formation to the production well. This drive mechanism was complemented by careful positioning of injectors and horizontal producers to ensure efficient reservoir contact and delay on the gas breakthrough.

3.2 Enhanced Oil Recovery

Enhanced Oil Recovery (EOR) is a group of techniques designed to increase the amount of oil that can be produced from the reservoir above the levels that can be achieved using the primary and secondary recovery methods alone. Typically, EOR methods involve thermal recovery, gas injection and chemical flooding. These methods are essential for extending the life of oil fields, increasing recovery effectiveness, and lowering the need for new well drilling. The importance of EOR in petroleum engineering is to increase the recovery of oil from mature or declining reservoirs, where conventional methods may have become ineffective (Amirbayov, 2014). EOR improves the economic viability of oil fields, and extends productive life of reservoirs. EOR is thus an indispensable means of maintaining oil production and minimizing new drilling’s environmental footprint. The EOR projects are

very costly, and subject to a large number of risks, including price of oil and poor performance of the methods. EOR projects are a success or failure depending on the EOR technique chosen for a given reservoir.

Table 3.2.1. Effectiveness of every EOR technique for 0.6, 0.7 and 0.8 oil saturations (Pendaeli 2019).

Oil saturation	0.6	0.7	0.8
method	Criteria fit		
Gas injections methods			
N2 injection	40%	40%	50%
H2 injection	50%	50%	50%
CO2 injection	67%	67%	67%
Immiscible injection	67%	67%	83%
Chemical flooding methods			
Polymer flooding	60%	60%	70%
SP/ASP flooding	91%	91%	91%
Thermal recovery methods			
Steam flooding	60%	70%	70%
IN-situ combustion	75%	75%	83%

Pendaeli (2019), focused on evaluating the EOR methods for the Norne field E-Segment using the Eclipse 100 simulation model. From table 3.2.1, it is clear that EOR screening results are in favor of ASP flooding as it shows the highest criteria fit. Immiscible injection and in situ combustion showed second highest results. Nevertheless, even though those methods were quite successful in oil production, they were considered quite costly methods.

The author suggested using the polymer injection method as it requires less investments and ends up with the highest investment return or positive NPV.

According to Abrahamsen (2012) it was concluded that the Norne field, particularly the Ile formation, is a strong candidate for chemical flooding due to its high oil saturation and substantial original oil in place. He assessed different EOR methods by using Eclipse reservoir simulation software. He suggested that polymer flooding would be the most effective method for Norne C-Segment, with an expected Net Present Value (NPV) of 406 million USD by 2022. Because it greatly increases mobility control and sweep efficiency within the reservoir, this approach was determined to be the most economically feasible. Additionally, the author stressed that alkaline flooding and surfactant alone were less effective. In most cases, surfactants produced negative net present values (NPVs) because they were unable to generate enough additional oil to cover the cost of chemicals. Comparing alkaline flooding to surfactant flooding, the former had less of an effect on boosting oil recovery.

According to the synthetic model used for optimization, polymer flooding produced the highest recovery factor (RF) and outperformed other techniques in terms of oil mobilization, particularly when the concentration was 0.05 weight percent. Because surfactants and alkaline agents are expensive, the best chemical combination in the ASP system did not perform noticeably better than polymer flooding. Furthermore, it was discovered that polymer flooding, a feature of the Norne C-Segment, was especially successful in heterogeneous reservoirs.

Table 3.2.2. Fields similar to Norne Field.

Field	**Statfjord Field (North Sea, Norway/UK)**	**Troll Field (North Sea, Norway)**	**Gullfaks Field (North Sea, Norway)**	**Brent Field (North Sea, UK)**	**Snorre Field (North Sea, Norway)**

Reservoir Type	Sandstone (Jurassic period)	sandstone (Jurassic period)	sandstone (Jurassic period)	Sandstone (Jurassic period)	sandstone (Jurassic period)
Fluid (° API)	38-40° API	Troll East: ~56° API (gas), Troll West: 30-33° API (oil)	37-39	38-40	28-33
Content	Mainly oil with associated gas	Gas and oil (split between Troll East and Troll West)	Oil + associated gas	Primarily oil with significant associated gas.	Oil with associated gas
Pressure (bar)	290-320	160-200	200-250	250-350	300-350
Depth (meters)	2,500-2,800	1,350-1,550	1,700-2,300	2,500	2,000-2,500
Temperature (°C)	80-90	60-70	90-100	85-90	80-90
Porosity (%)	20-25	25-30	20-22	18-25	20-25
Permeability (mD)	1,000-2,000	1,000-2,000	500-2,000	1,000-2,000	200-1,000
Drive mechanisms	Water injection and natural aquifer drive	Gas cap expansion and water injection	Waterflooding and natural aquifer support	Waterflooding and gas cap expansion	Water injection and gas injection (WAG)
EOR	Waterflooding	Primarily natural depletion + water injection in the oil zones	Water injection	Water injection, gas injection, and hydrocarbon gas recycling	Water alternating gas (WAG) injection is applied

3.3 Well Test

Fluid flow is enhanced across some of the fracture formations in the Norne field such as in the Ile and Garn formations. The rocks contorting from tectonic events usually create the natural fractures that permit oil and gas to move through pathways in the rocks. The influence on well performance, but in particular on wellbore productivity and the effectiveness of EOR techniques, is due to the presence of fractures. In the case of fractures, they can provide increased permeability close to the wellbore, although such fractures sometimes provide better oil recovery through better fluid movement.

Table 3.3.1. Initial conditions for build up test

Parameter	Value
Porosity (%)	28
Viscosity (mPa*s)	0.63
Total compressibility (1/kPa)	2.14E-6
Oil formation volume factor (Rm3/Sm3)	1.3
Wellbore radius (m)	0.108
Height (m)	22.9
Temperature (degree C)	98.4

Table 3.3.2. Initial conditions converted to oil field units

Given Values	
parameter	value
porosity	0.28
viscosity, cp	0.63
ct, 1/psi	0.00000031
bo	1.3
rw, ft	0.35433
h, ft	75.46
q, bbl/day	6164.2

From Table 3.3.1 we took parameters and values and converted them into oil field units to create a Horner time plot. Figure 3.3.2 shows the horner time plot which helped us to find out the slope which we included into the permeability formula form Figure 3.3.3. After we have found the skin factor using the formula from Figure 3.3.4.

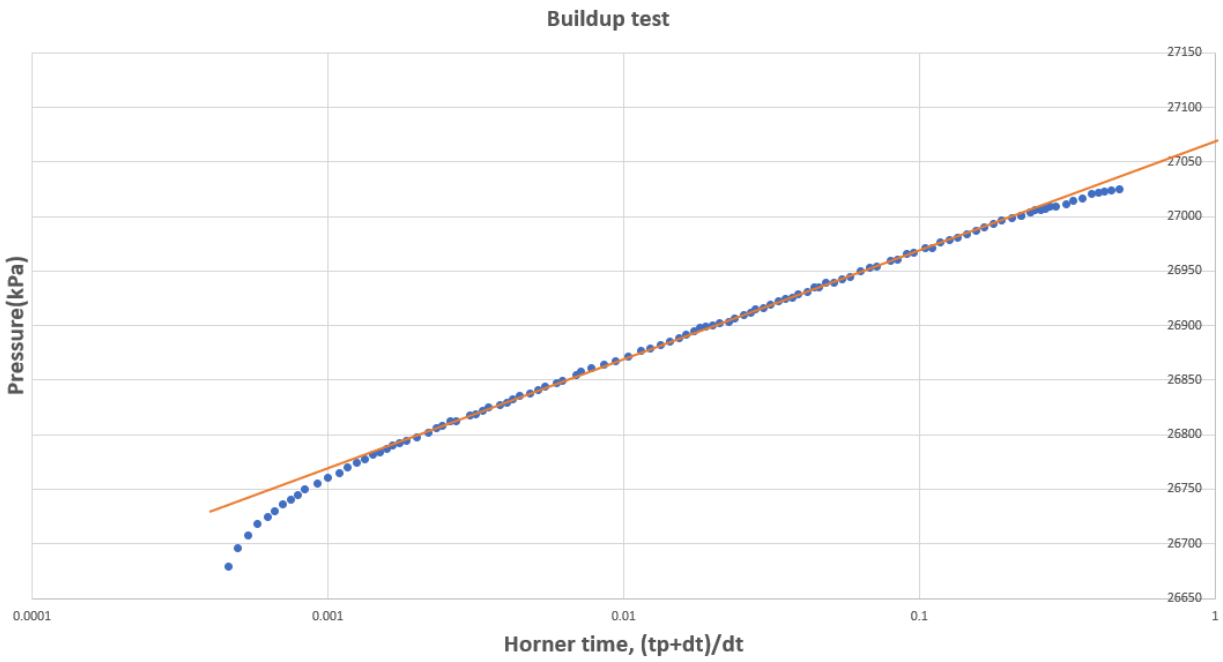

Figure 3.3.2. Horner time vs pressure plot

$$k = 162.6\frac{qB\mu}{mh}$$

Figure 3.3.3. Formula to find out permeability

$$s = 1.151\left[\frac{(p_{1\,\mathrm{hr}} - p_{wf})}{m} - \log\left(\frac{k}{\phi\mu c_t r_w^2}\right) + 3.23\right].$$

Figure 3.3.4. formula to find out skin factor form build up test

Table 3.3.3. Results from buildup test

Results	
m(slope)	14
p(1hr)	27068
k	777.0274
s	5.227174

The permeability of the reservoir from the buildup test analysis is 777 md and it is considered good for a heavy oil reservoir. It can be seen from Table 3.3.3. In general, it would mean that better fluid flow would be achieved in comparison with reservoirs of lower permeability. However, heavy oil has a high viscosity, which could increase resistance to flow. Nonetheless, the higher permeability increases the likelihood of success for enhanced recovery techniques. Because of its moderate permeability (777 md), waterflooding would probably be the first secondary recovery method investigated for the reservoir. Waterflooding is used to increase pressure in the reservoir and force oil towards producing wells. In heavy oil reservoirs, the injected water often does not sweep the oil due to immobility mismatch between oil and water, leading to low oil driving efficiency (Lake, 1989). While still some pressure support to waterflooding, it would not aid much in oil recovery without other methods. Furthermore, the positive skin factor (5.22) may hinder water flooding by inhibiting water from displacing the oil near the wellbore. Low skin factor and associated improvement in the efficiency of waterflooding would probably result in a need for well stimulation prior to such stages.

Injection of CO2, a tertiary recovery method, is known well as it reduces oil viscosity and improves pressure maintenance. At some pressures and temperatures, CO2 is miscible with oil and is capable of increasing the viscosity of the heavy oil and allowing it to move though the reservoir more easily. CO2 injection has become very common in heavy oil reservoirs where steam injection is not possible or where the additional pressure is required (Cuenca, 2017).

Formation damage or friction is occurring that reduces well productivity as indicated by the positive skin factor of 5.22. Well stimulation techniques like acidizing or hydraulic fracturing

should be considered to improve well productivity and enable the best use of secondary and tertiary recovery methods. Acidizing can increase the permeability around the wellbore, especially if the damage is due to scaling or formation damage. It aids in the dissolution of minerals that may block the flow of oil and increase well productivity and aid in the operations of water flooding or other EOR techniques (Ahmed & McKinney, 2011). If the formation is tight or if there exists low permeability zones near the wellbore, hydraulic fracturing could be considered. Hydro fracturing is accomplished by fracturing the rock to impede the flow of oil towards the wellbore and thereby improve performance of secondary and tertiary recovery techniques (Economides & Nolte, 2000).

3.4 Monte Carlo Simulation

Monte Carlo simulation is a statistical method that can help to simulate and evaluate the probability of different outcomes. In reservoir engineering, Monte Carlo simulation is used to measure the uncertainty in reservoir performance and rock and fluid properties. By applying Monte Carlo simulations, reservoir engineers can predict a range of potential production outcomes, maximize development plans, and make better decisions (Jafarpour et al., 2014).

In the estimation of Original Oil in Place (OOIP), Monte Carlo simulations are very useful since they allow us to use uncertainties related to the reservoir's geological characteristics and fluid distribution. The method involves generating many realizations of the reservoir to account for the variability of critical parameters such as porosity, oil formation volume factor, net-to-gross ratio, and water saturation. So, engineers and scientists can obtain a distribution of potential OOIP values, providing a better representation of the probable outcomes (Khalil et al., 2018). As a result, by applying Monte Carlo Simulation, it becomes easier to evaluate and improve the reservoir characterization. From the formula below, it can be seen that in order to simulate the OOIP, it is necessary to apply parameters like reservoir area, net pay, rock porosity, water saturation and oil formation volume factor.

$$OOIP = 7758 * A * h * \phi * (1 - S_{wc}) * \frac{1}{Bo}$$

The simulation was done twice for the entire Norne field and particularly for the C-segment of the Norne field. The results can be seen from figure 3.3.1 and figure 3.3.2. To do the simulation, random normal, random triangular and random uniform distributions were used with 10000 numbers of simulation for both cases.

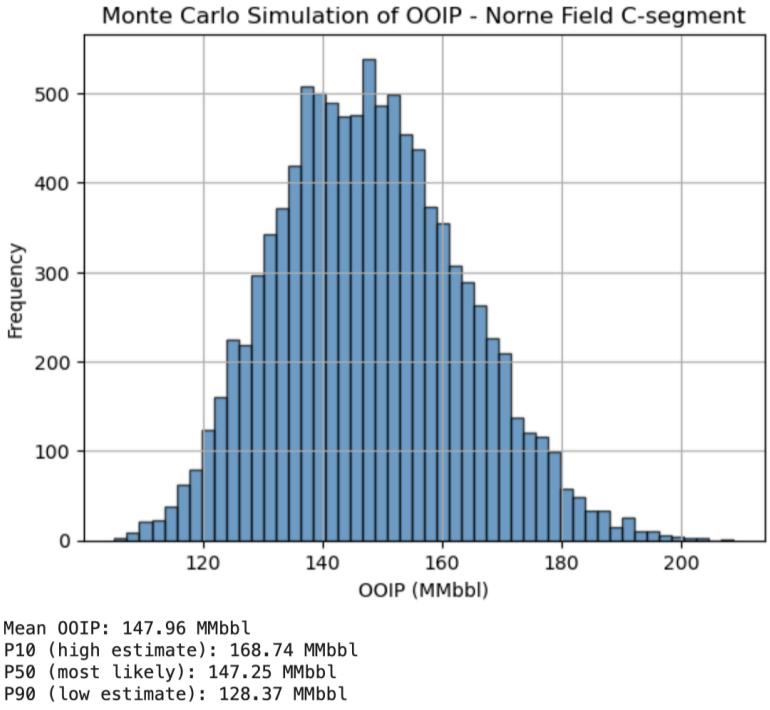

Figure 3.4.1. Monte Carlo simulation for C-segment

The Monte Carlo simulation of figure 3.4.1 is used to make an estimate of the Original Oil in Place (OOIP) of the C-segment of the Norne Field. The simulation takes into consideration the system uncertainty and variability to provide an estimate of the range of potential values for OOIP. X-axis is the set of possible values for OOIP, this set indicates how the estimated oil reserves vary. The Y-axis is how often each specific value of OOIP occurred, where taller bars indicate that certain values occurred more often in the simulation. It shows that the most likely OOIP value is around 147.25 MMbbl, with the range between 128.37 MMbbl and 168.74 MMbbl. The simulation shows the uncertainty of oil reserve estimation, giving a general idea of the likely outcomes.

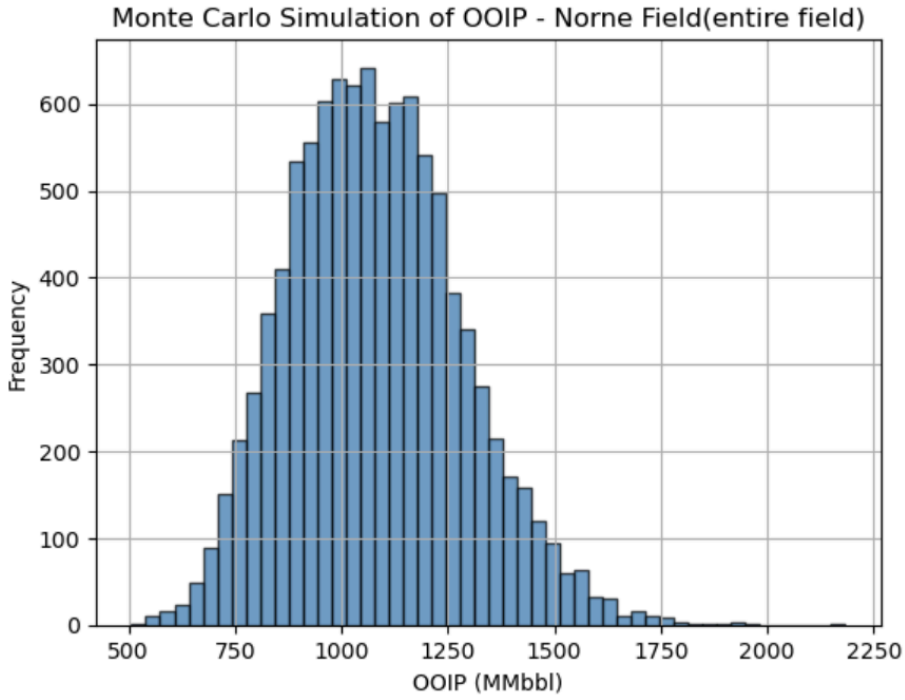

Figure 3.4.2. Monte Carlo simulation for entire field

The figure 3.4.2 shows the result of a Monte Carlo simulation to determine the OOIP in the entire Norne Field. The X-axis contains the values of potential OOIP from around 500 MMbbl to over 2000 MMbbl.

The figure's primary statistics include the mean OOIP, which is equal to 1079.86 MMbbl. The P10 value is 1346.09 MMbbl. There is a 50% chance that the actual OOIP will be higher or lower than the P50 value, which is 1068.14 MMbbl and represents the most likely estimate. The P90 value of OOIP is 825.97 MMbbl. With a range of 825.97 MMbbl for the low estimate and 1346.09 MMbbl for the high estimate, the distribution of values suggests that the most likely OOIP for the Norne Field is approximately 1068 MMbbl.

3.5 Decline Curve Analysis

The Decline Curve Analysis (DCA) is a common and easy way of predicting the future oil and gas production rates using the historical data. However, it takes for granted that after a first productive interval, output will continue to follow a known course. So, it is possible to extrapolate to deduce future performance (Falcon, 2021). The role of this method is very important for determining the ultimate recovery and remaining reserves of a reservoir.

DCA's prime purpose is to project the future production, in case reliable historical data are available. It helps in determining the amount of remaining reserves of a well, planning production strategies, predicting the economic life of a well, and optimizing the well's management. Finally, DCA is used to determine the most effective well intervention or re-stimulation effort times.

In DCA, various declining models are used and the most common is the exponential decline. It further assumes that the rate at which production declines is at a constant rate as time moves forward. DCA coupled with reservoir models can give a comprehensive production forecast of a well's production throughout its life and aid in deciding optimal production strategies (Arps, 1945). However, DCA has limitations. The accuracy depends heavily on availability of historical production data, which are seldom available. What's more, the method becomes less effective in reservoirs that are not declining at a constant rate (that is, those experiencing sudden pressure drops or such heterogeneity). According to Ghalambor (2011), DCA is also not well suited for unconventional reservoirs, such as shale or tight oil plays, where production behavior deviates much from the conventional expectations and warrants more complex modeling practices.

The Exponential Decline method is used for our case. And the formula below is applied to estimate the decline rate:

$$q_0 = q_i e^{-Dt}$$

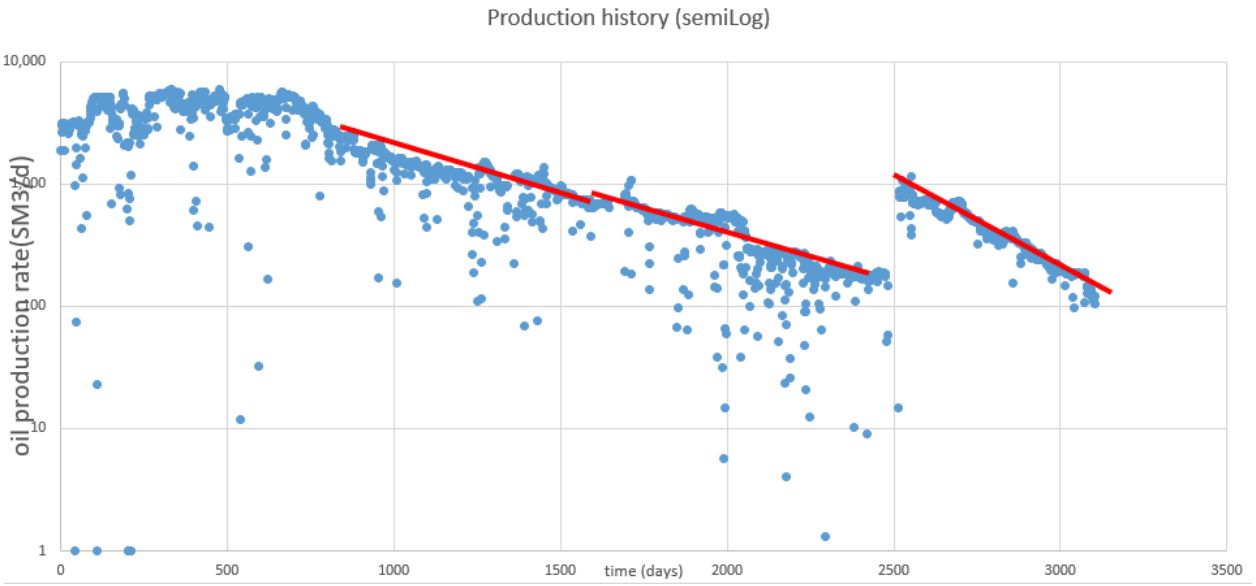

Figure 3.5.1. Oil production history in semi log graph

Figure 3.5.1 is the oil production history of the well which helps to choose the best time period for DCA estimations. It is known that it would be better to choose the latest decline segment because it interprets the latest reservoir conditions such as choke size and pressure. From the graph it can be seen that there was a well stimulation as it shows significant rise in production approximately between day 2500 and 2510. That is why it is better to choose the latest segment for DCA.

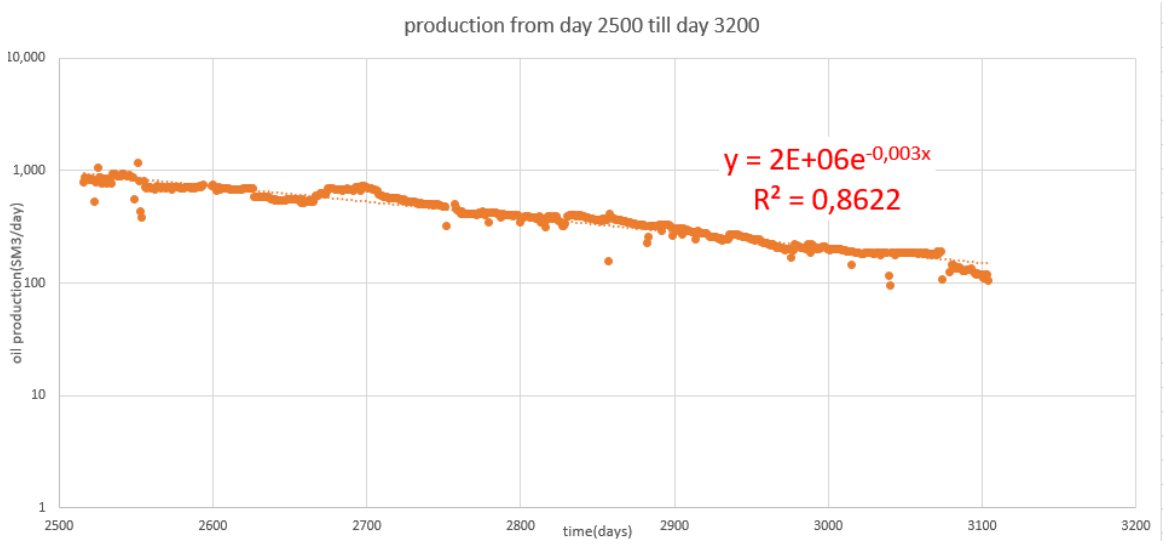

Figure 3.5.2. DCA applied to latest segment with found decline rate

After error analysis and finding the decline trend through the exponential decline method, it is required to find out the daily decline rate which is 0.3% while decline rate per year will be 66.8%.

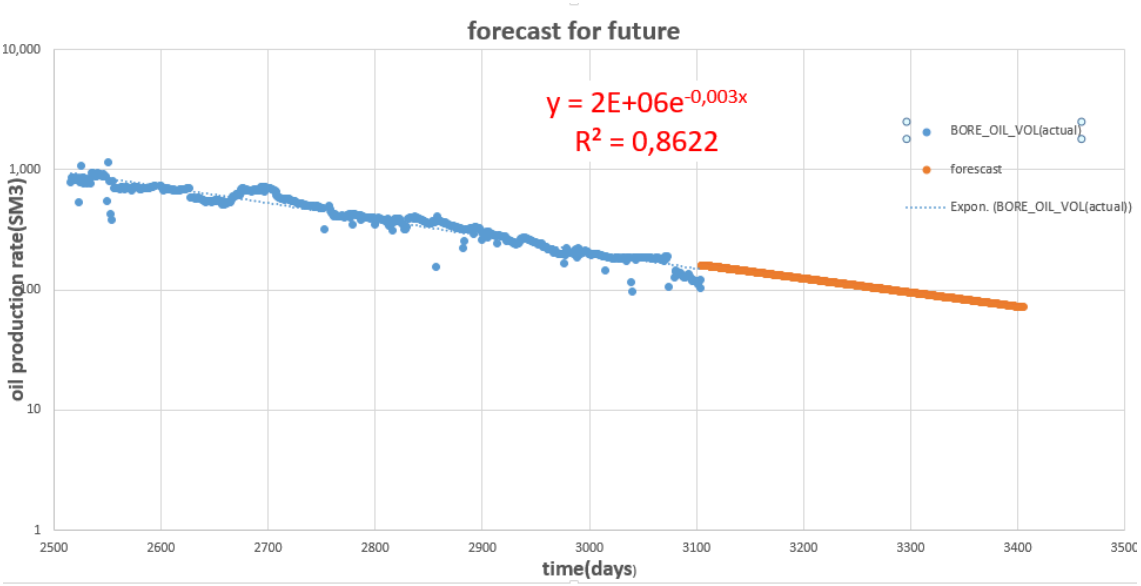

Figure 3.5.3. DCA with prediction in oil production

From the semi log graph in the figure 3.5.3, the orange line shows the future oil production rate for the well. On day 3285, the oil production rate will fall below 100 meter cubes per day. By analyzing the DCA graph it becomes possible to find out the economic limit of the well.

Chapter 4. Reservoir Simulation.

4.1. Static Modeling

Static modeling is a critical component of reservoir characterization that involves constructing a detailed, static representation of the reservoir before making any further actions (such as reservoir simulation, EOR, production, etc.). This model is very important for understanding subsurface geology and helps to develop a dynamic model, which is used

for simulating fluid flow and reservoir performance. Static models integrate geological, geophysical, and petrophysical data to create a comprehensive picture of the reservoir's static features such as rock properties, fluid distribution, and structural configuration.

Objectives

- To achieve a high-resolution and accurate representation of the reservoir's geological framework;
- Distribute petrophysical properties like porosity, permeability, and saturation throughout the reservoir model as accurately as possible;
- To quantify uncertainties in the reservoir model and evaluate their impact on field development planning;
- Integrate data from various sources such as seismic, well logs, and core samples to enhance the reliability of the reservoir model.

Methodology

- Gathering and synthesizing data from well logs, core samples, and seismic surveys.
- Constructing a 3D geological framework that defines the reservoir boundaries & structural features;
- Distributing key reservoir properties such as porosity, permeability, and fluid saturations using static modelling tools;
- Transferring static model to CMG software, to recreate reservoir's segment and fill it with necessary data;
- Managing conflicts that will arise during creating a structural model and transferring it to another software.

Expected Outcomes

- Static model that provides a detailed understanding of the reservoir geology, geometry and property distribution, which will help in the optimization of the field development plan;
- Decisions regarding well placement, production strategies, and recovery techniques based on a reliable model of the reservoir;

- Identification and management of risks associated with geological uncertainties, ensuring that development strategies are resilient and adaptive.

4.1.1. Data Collection and Integration

Well Log Data

The collection of well log data is a very important part of creating our reservoir's characteristics. Gamma Ray is used to identify lithology and differentiate between shales and sandstones or carbonates, helping to define reservoir zones.

Resistivity Logs provide information on fluid content and hydrocarbon saturation by distinguishing porous, hydrocarbon-bearing zones from water-bearing zones.

Combination of Neutron, Density logs are essential for estimating porosity, which is critical for reservoir characterization. The difference or average between neutron and density porosity logs helps refine porosity estimates and identify gas zones (e.g., neutron-density crossover indicating gas).

By integrating these varied data sources, the reservoir's grid should be containing all the necessary information for creating a reservoir simulation. However, due to the confidentiality of Norne field's operational process, well logs for the whole field are not available online.

Core Samples

Core sampling is a direct method of reservoir evaluation. RCAL would reveal data on porosity, permeability and fluid saturations, which are, as previously mentioned, to understand reservoir quality and possible performance. Nevertheless, SCAL reveals insights on measurements like P_c and k_r. They are crucial for detailed flow simulations and recovery factor optimization. These core insights should have been integrated with log data to improve the model's grid and enhance predictive accuracy, if those data would be available in open source.

Seismic Data

Analysis of seismic data includes interpretation of 3D surveys which provide high-resolution imagery of the subsurface geology, which could be very handy for overall reservoir's estimation. It is used to construct detailed structural models and for stratigraphic interpretations and to detect fluid contacts, assess reservoir continuity, and identify compartmentalization, which can significantly impact field development strategies.

Structural Framework

The structural framework of the reservoir is originally modeled using faults and horizon layers, with implementation of both seismic interpretations and well data. This framework helps in understanding the geomechanical behavior of the reservoir, including the influence of faults on fluid migration. It allows us to look at the reservoir itself from a different angle, visually evaluate it. Detailed structural modeling is very important for optimizing well placement and predicting production behavior. Norne field's open source data is provided with a dataset to simulate its behaviour. The majority of data, that should be originally obtained with above mentioned methods, was taken from this very model in SLB Petrel software, since it contains all the necessary information.

Petrophysical Analysis

Petrophysical analysis begins with the assessment of porosity, permeability and fluid saturations, ideally using data from core measurements, well logs & seismic imaging. Direct measurements from cores provide the most reliable data, while indirect estimations from logs are less reliable and offer extensive coverage across the whole reservoir. However, as was mentioned above, we do not have any of those, so we will extract these values from the structural model in Petrel (the process will be described later). This analysis of petrophysical properties is crucial as they directly influence the reservoir's capacity to store and transmit fluids.

In the case of the Norne Field, the necessary data was collected and presented as an open-source archive, containing files to run an Eclipse simulation.

4.1.2. Model Extraction

First of all, it was crucial to extract the data using Schlumberger Simulation Launcher (further SSL). In order to do that, .DATA file was required, which was found on the site of Norwegian University of Science and Technology (https://www.ipt.ntnu.no/~norne/wiki1/doku.php?id=english:nornebenchmarkcase2). It was included into the archive and contained all the necessary information to proceed further.

The .DATA file, as well as all the other, include files were downloaded from an open database source. For our field, the production began in November 1997, and it is continued for 10 consecutive years, simulating the fluid flow in 3D and also providing all the necessary graphs, dimensions, coordinates and providing an enhanced comparison between the wells, visually showing how they were placed, changed and everything related to the oil, gas and water saturations, productions and etc.

In order to complete this simulation, we need to open SSL, and choose the “ECLIPSE” option from the Simulators tab.

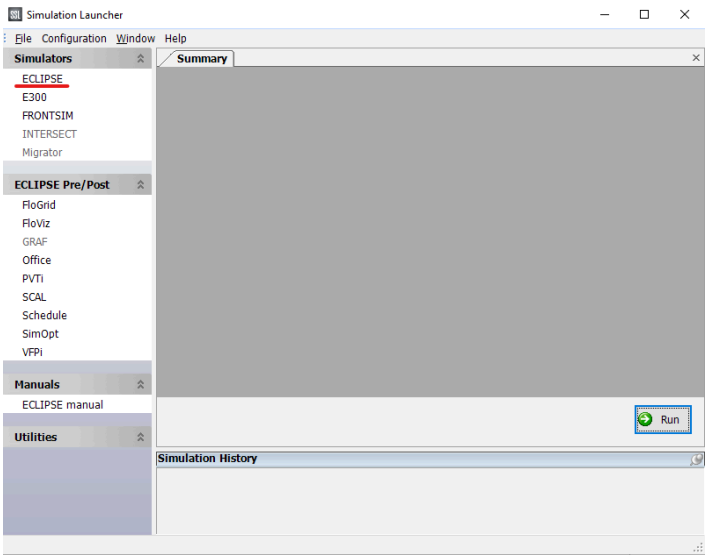

Figure 4.1.1. Eclipse Simulation Launcher.

Once opened, the dataset should be imported to proceed work on. Simply press “Add Dataset…”, choose the .DATA file “NORNE_ATW2013.DATA”, and click the Run button.

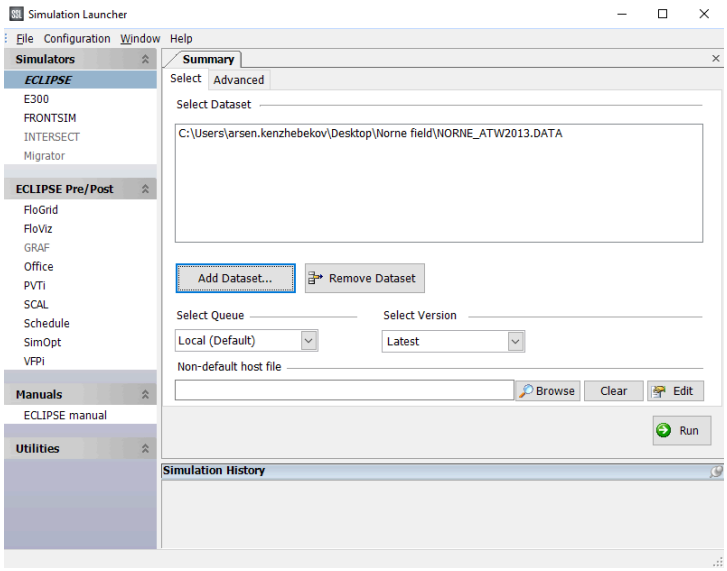

Figure 4.1.2. Extraction of .DATA file.

The output files define the model's grid, attributes (such as porosity and permeability), fluid parameters, wells, and production/injection schedules. Petrel E&P Software Platform was used in order to inspect and extrapolate output files. The inside function of “ECLIPSE Office” was used to illustrate the model with all the graphs and 2/3D representations. Changing the upper tab to the “Simulation”, and then proceeding with the “Legacy” button option, the “ECLIPSE Office” is opened. The .DATA file for the Norne field is the primary control file that sets up the whole reservoir simulation. It includes key simulation instructions, grid setup, fluid properties, fault configurations, and well performance data. This file essentially guides the simulator through each step, specifying reservoir geometry, rock and fluid properties, production parameters, and output requirements. It was also inspected as the text file for further work and useful discoveries.

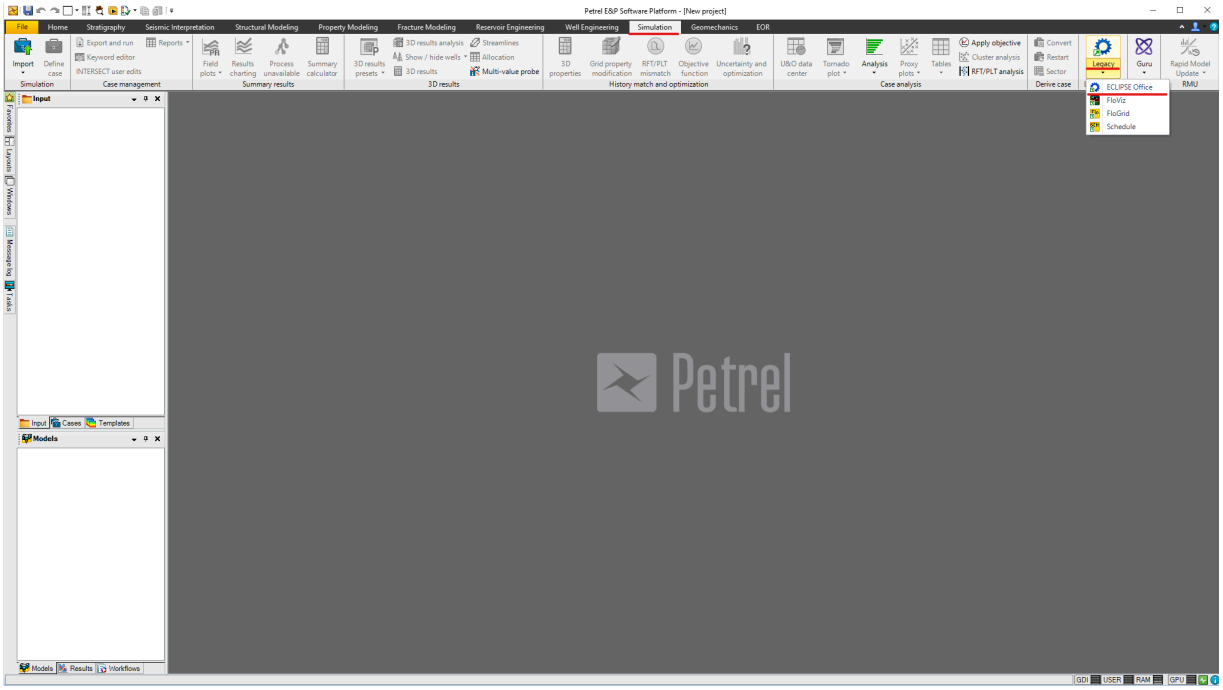

Figure 4.2.1. Opening of the Eclipse Office.

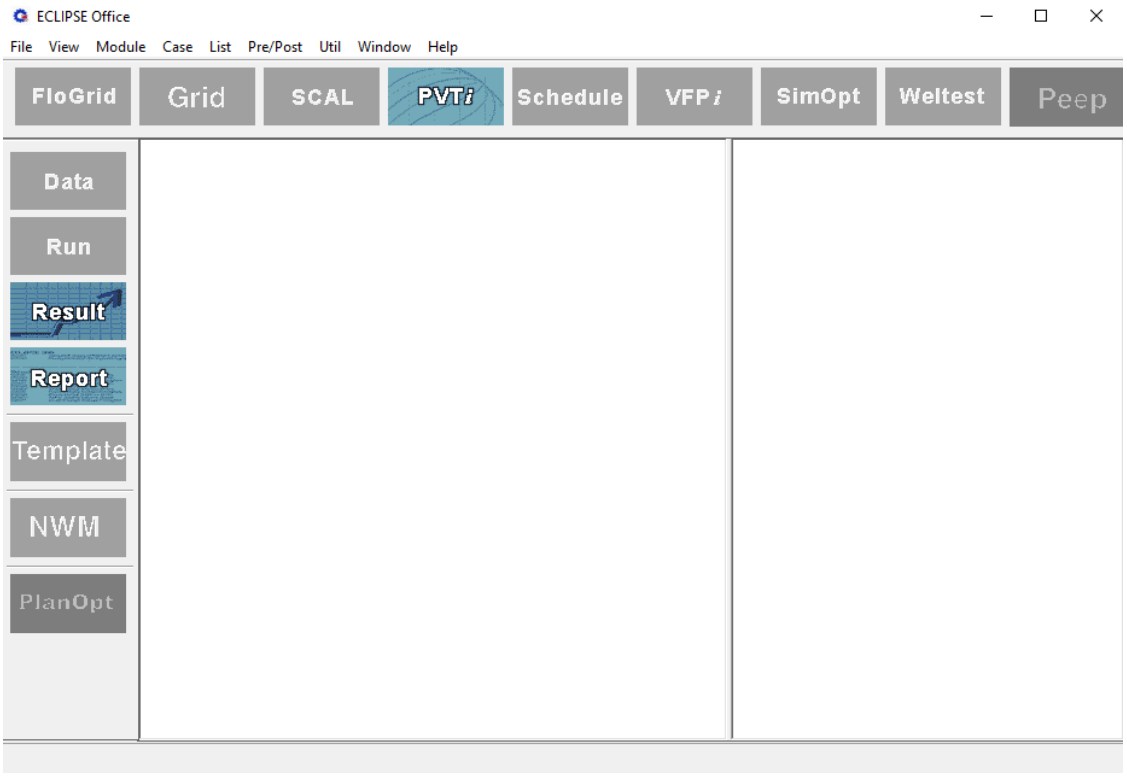

Figure 4.2.2. Eclipse Office for plotting.

It presents us with the operational tab with results and report buttons available. After clicking the results button, all vectors should be loaded. In order to do this, following steps should be completed:

- Open “Results” tab;
- File → Open → SUMMARY → Load All Vectors;
- From the list of extracted files, choose “NORNE_ATW2013.SMSPEC” file;
- The same step should be now repeated for: GRID, Solution & RFT.

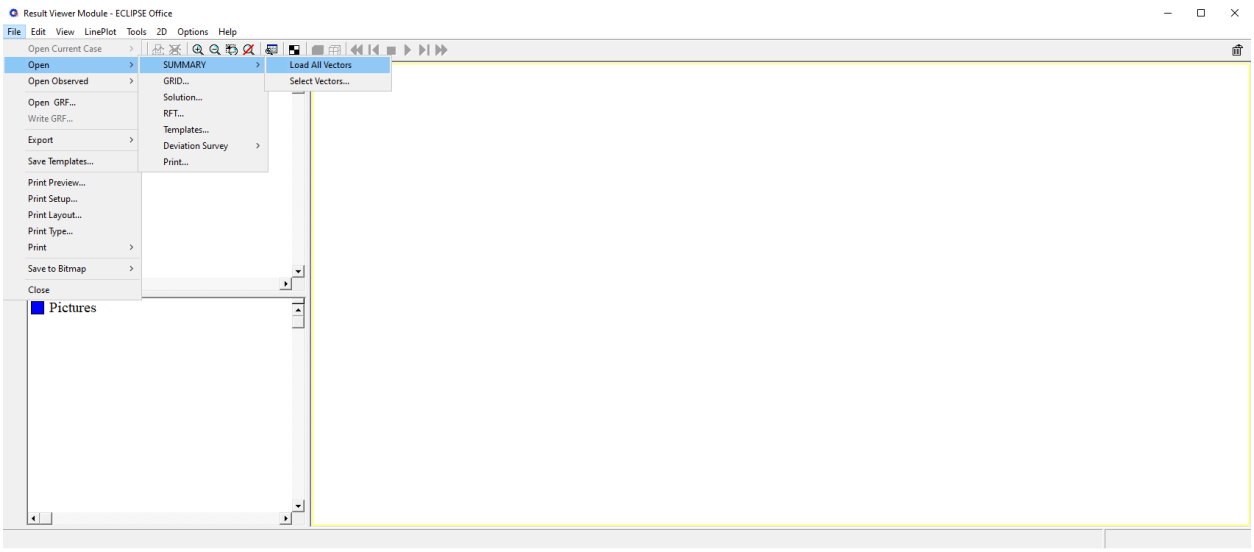

Figure 4.2.3. Loading vectors.

After vectors and the grid were successfully uploaded, a list of imported files will appear on the left side of the window.

Figure 4.2.4. Uploaded data.

Let’s look at a few examples of simulation outputs:

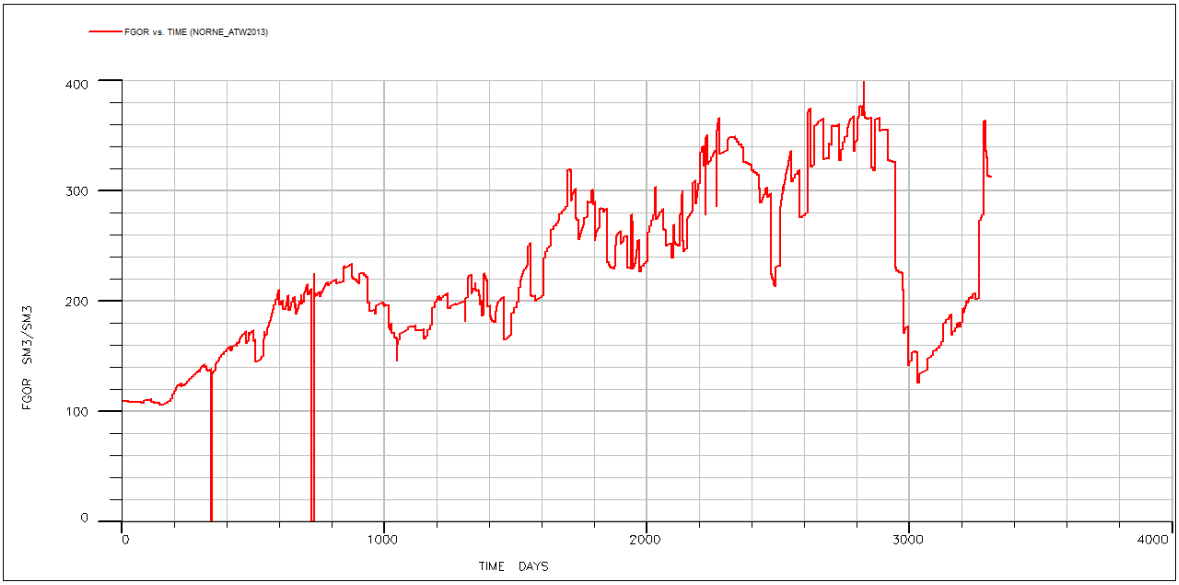

Figure 4.3.1. GOR vs. Time Days plot.

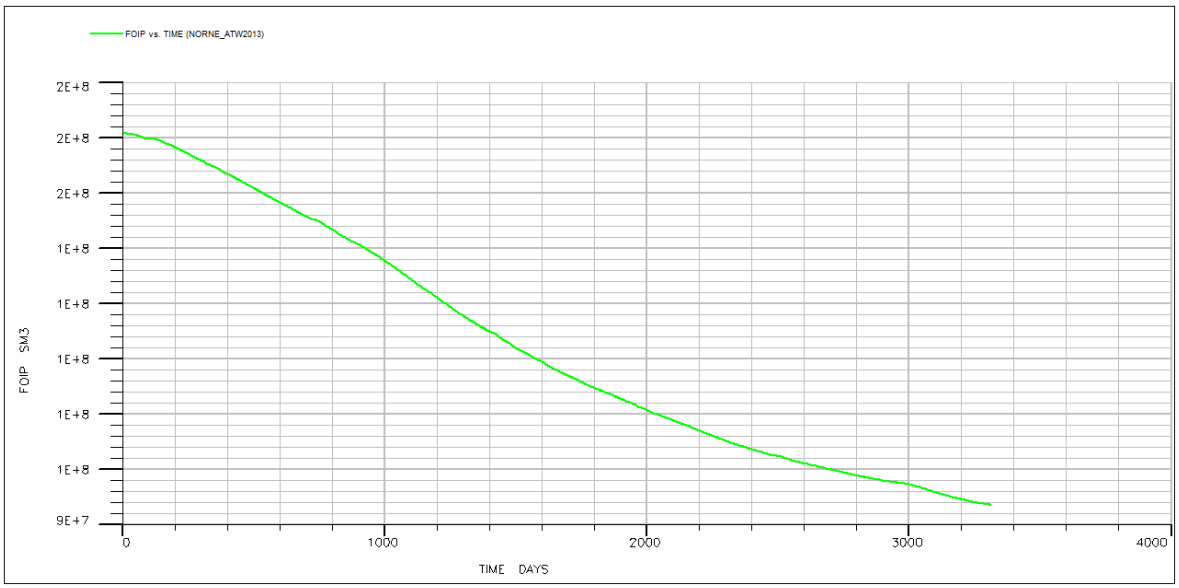

Figure 4.3.2. Oil in place vs. Time Days plot.

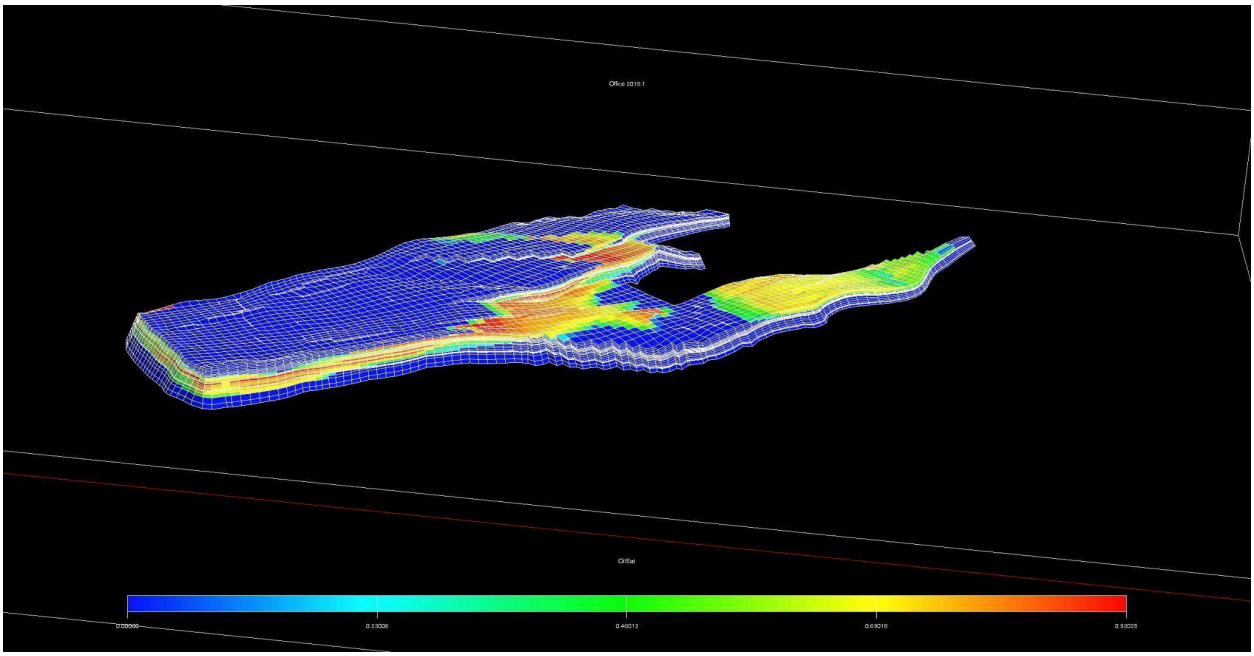

Figure 4.3.3. 3D static model of the Norne field in Eclipse Office.

However, the Eclipse Office is not rich with different kinds of instruments, so Petrel itself was preferred to be chosen to proceed to the next steps. We do the import of the same datafile into the Petrel itself, and get the following:

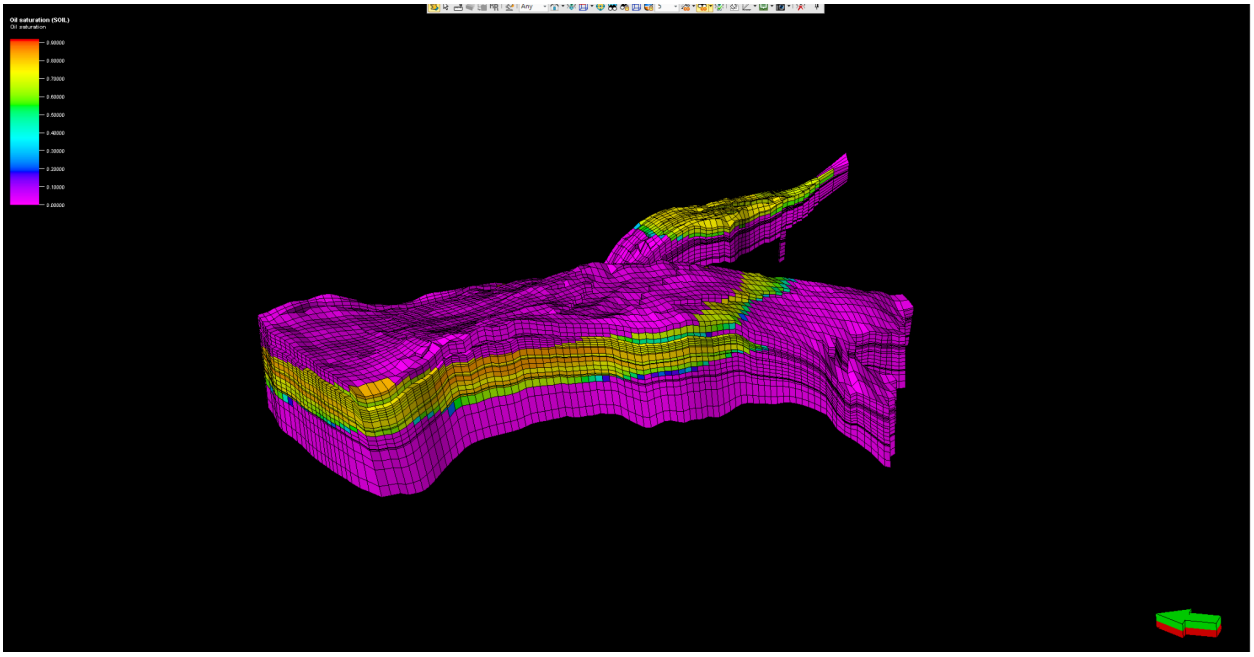

Figure 2.4.1. 3D static model of the Norne field in Petrel.

As we can see from this model, the oil saturation values are high in the middle layers, so we will consider layers 8-9 to 14-15, where the majority of the field's oil reserves are located.

4.1.3. Structural Modelling

Now, in order to create our model we will export Petrel' model to CMG. As well known, CMG has a limitation of 10.000 cells, so the best choice in case of the Norne field would be to cut a certain part of the reservoir, and recreate the model. We start from creating a boundary plane.

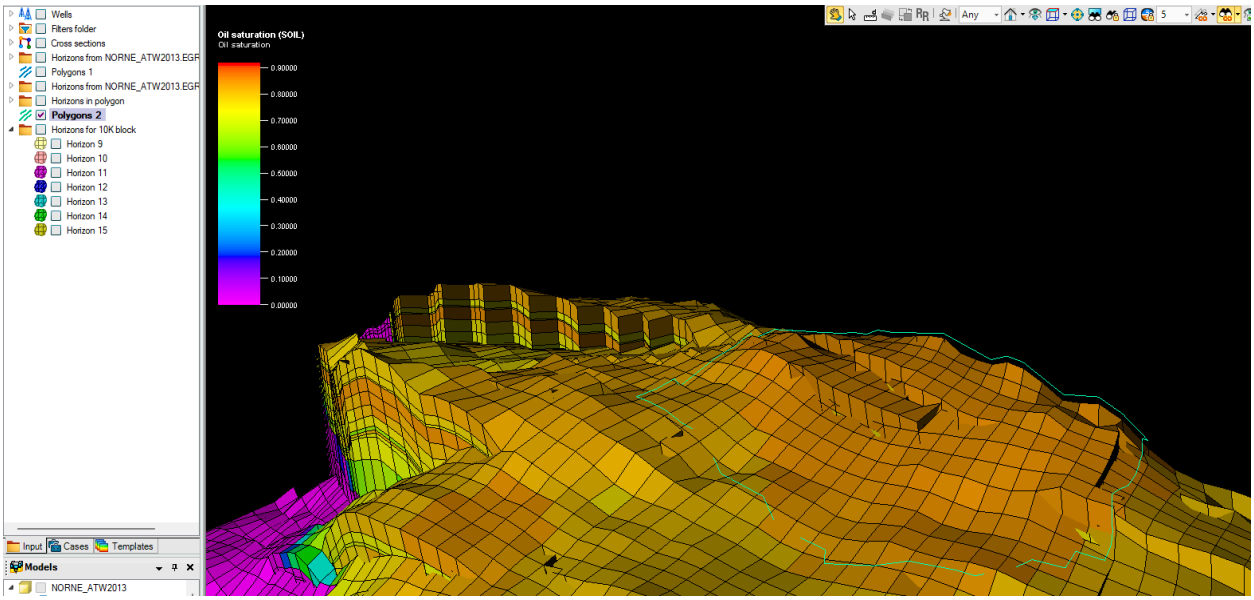

Figure 4.4.2. Polygon creation.

Then, we make a surface in order to create a 3D-grid afterwards.

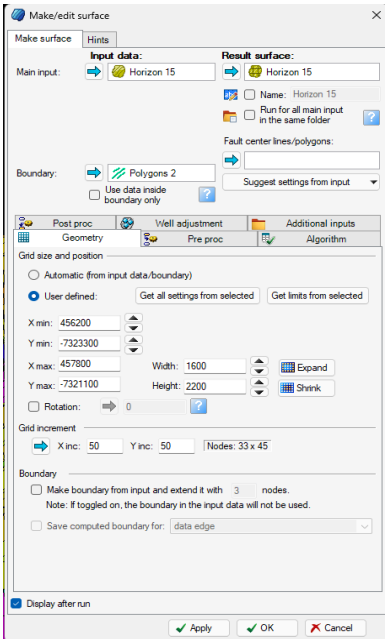

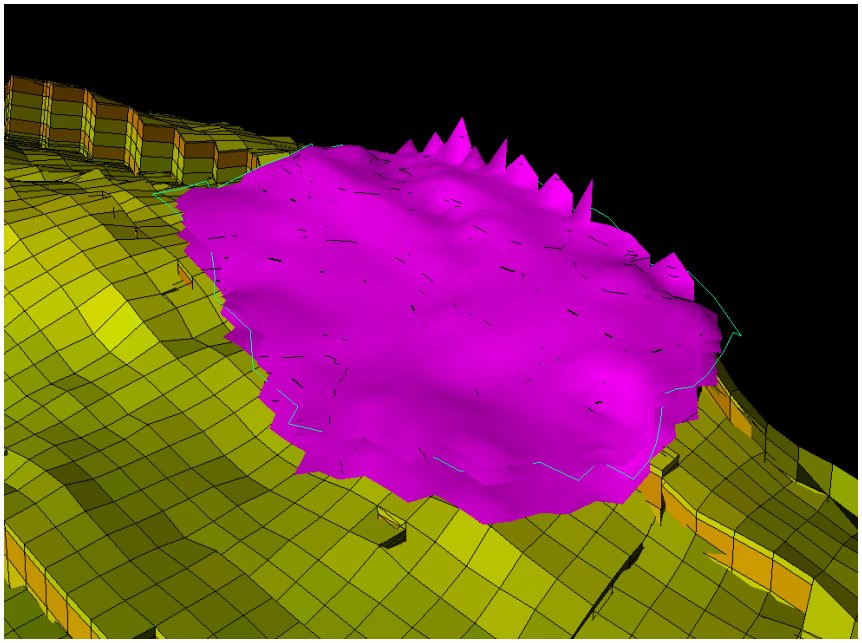

Figure 4.4.3. Make/Edit surface tab.

Then, we create a structural model itself, using the “Structural Modeling” tab on top. We define a model and a simple grid.

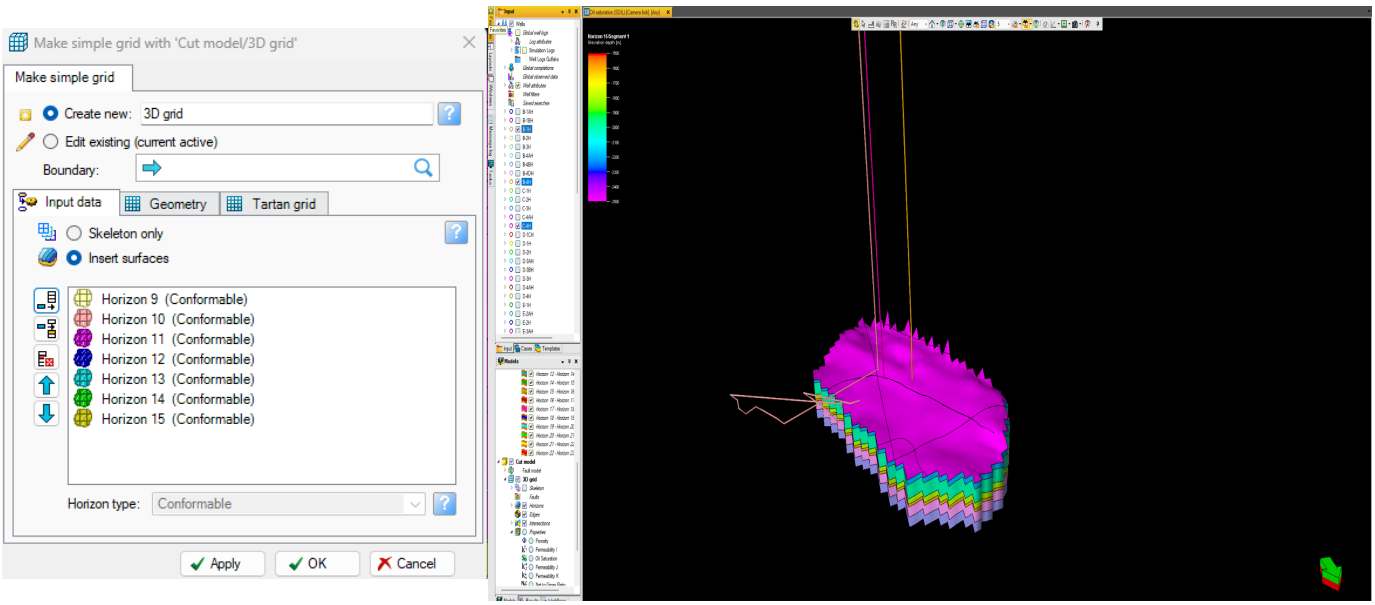

Figure 4.4.4. Making a simple grid.

We can observe the simple grid that was made as an output of the above described process and 3 wells that align perfectly with the model that we will use. It contains 6888 cells, which is good for work in CMG, and wells B-1H, B-4H as producers, and C-4H as an injector. Those 3 wells are chosen for the sensitivity analysis in the Reservoir Simulation part of this Field Development Plan. This includes: well placement optimization, injection rates change, injection fluid type. Since the gas production is moderate and is not a primary goal for production, it could be used for re-injection to increase possible production of the oil. Those changes are essential for decreasing operational costs and increasing profit.

Now, due to absence of any well logs, properties were assigned randomly by calculating the mean and standard deviation, and assigning them to each cell. These following variables are: porosity, permeability I, J and K, pressure, oil and water saturations. Those properties were assigned within the Petrel itself using the Geometrical Property Modelling tool. It is very important to name properties properly, since it will make easier for CMG to determine properties automatically in future.

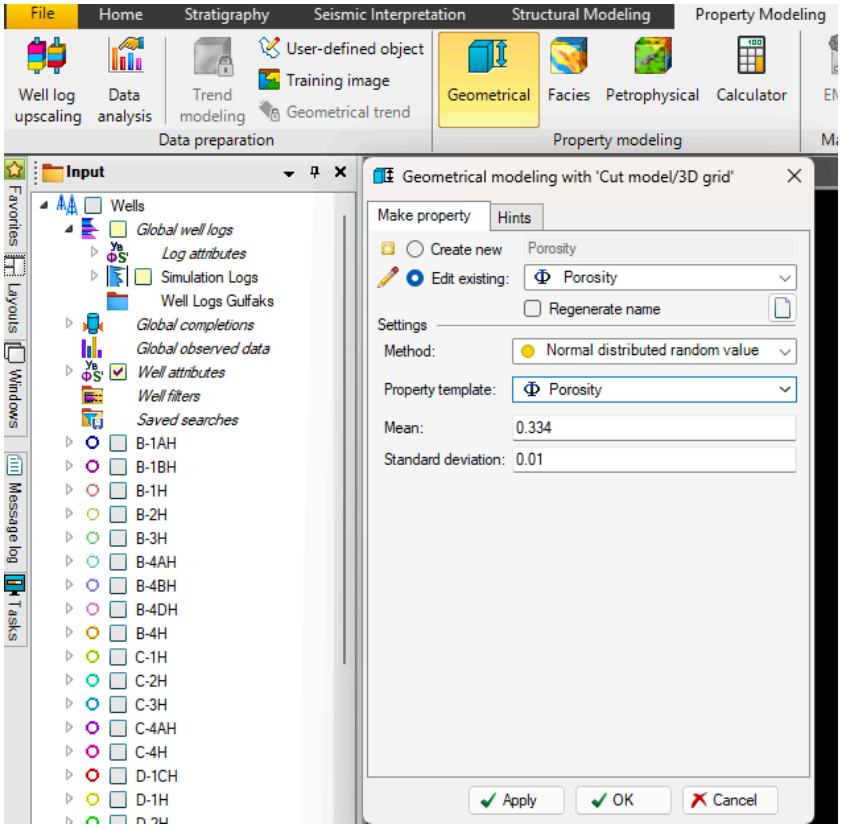

Figure 4.4.5. Geometrical Property Modelling.

As was mentioned, it will randomly assign properties for each cell within the range of inputted values, allowing us to create a grid, which cells have properties. As could be seen on the *Figure 1.7.6.,* porosity is normally distributed near the value of 0.344.

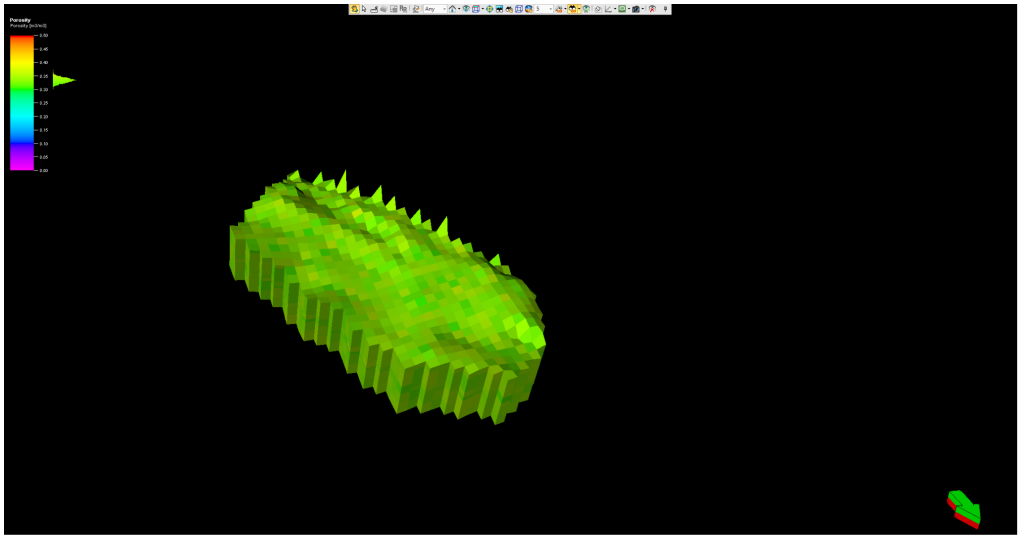

Figure 4.4.6. Normal distributed random values of porosity.

Now this process should be repeated for each property, since each cell has to contain these essential properties to properly run the simulation in further steps.

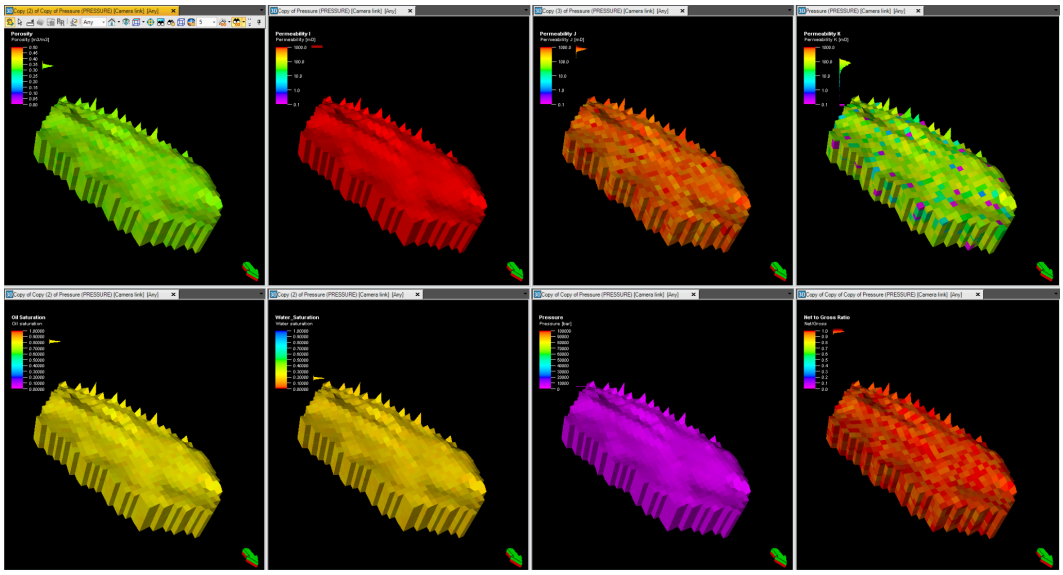

Figure 4.4.7. 8 properties assigned to each cell.

4.1.4. Rescue model

The static model itself is already completed and fully assigned with vital parameters. However, Petrel does not support reservoir simulation without a specific license, so in order to overcome this, we will use a CMG simulator. Projects saved in SLB Petrel are only compatible with SLB products. So, to transfer the grid model from Petrel to CMG we will use the RESCUE model. Rescue model is a file format that can be used to move reservoir information and grid between different simulations softwares. As was mentioned, earlier, it will contain not only necessary properties for the grid (porosity, permeability and other), but also wells' information and trajectories as well. This is a common practice to use such a method. For example, Juan C. in 2024 while working with The Illinois Basin Decatur Project did the same transfer using the rescue model.

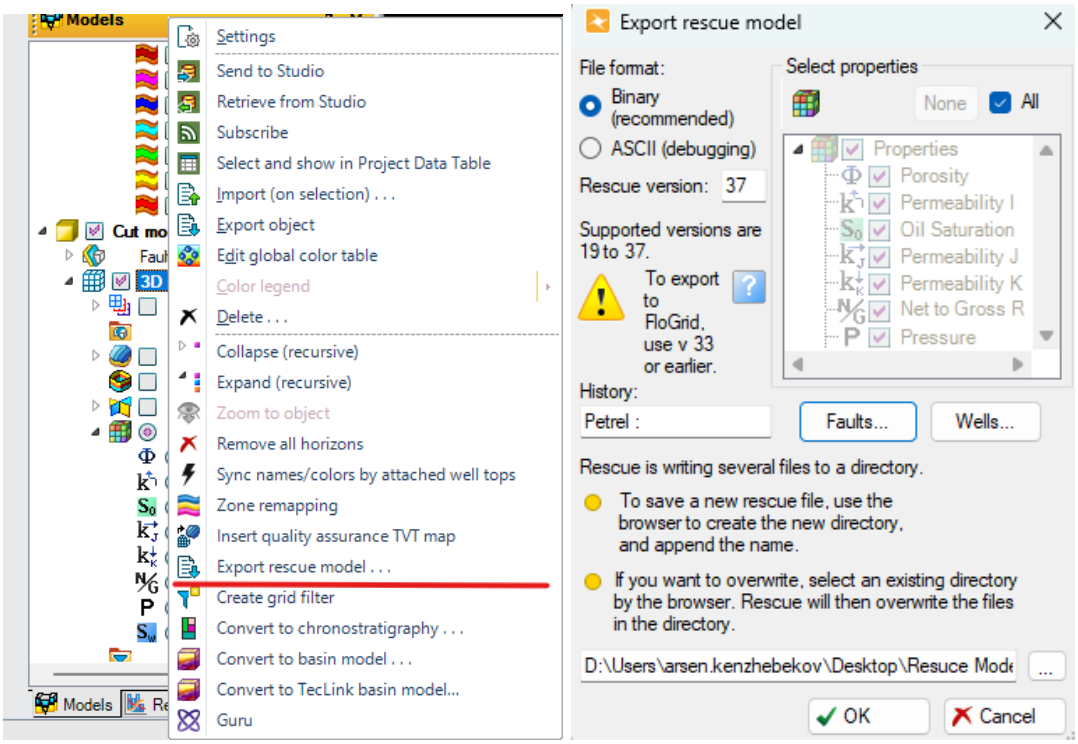

Figure 4.4.8. Exporting process of rescue model.

After it is extracted, a lot of files will be present in the destination folder. All of them would be necessary during model import. As was mentioned above, CMG should be launched to import the model itself. So we click “New”, choose IMEX simulator (STARS would be more preferable, however, due to the lack of data we could not run it properly), field units and a Single porosity model. Set the simulation start date on January 1st, 1998, we neglect the first 1.5 months of production, starting in November. Confirm it and head to the model import. Click “Reservoir”, then “RESCUE” and “Open RESCUE file…” and choose the main file. CMG will ask to select blockunits from the model.

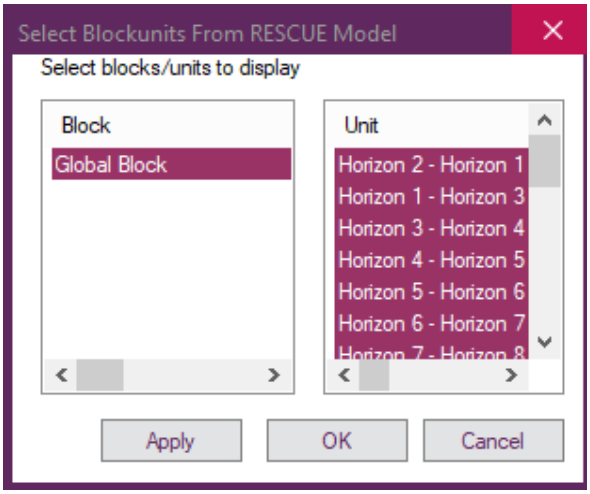

Figure 4.5.1. Selection of layers.

Since Horizons 8-9 to 14-15 were chosen, we should only import them, others do not contain any information. Click “OK”. It should not cause any problems. Next follows Rescue property importer. Previously, proper property naming was already mentioned, and now, it will allow CMG to automatically correlate each imported property with itselves inner properties. Otherwise, it should be correlated manually (pressure to pressure, porosity to porosity and so on).

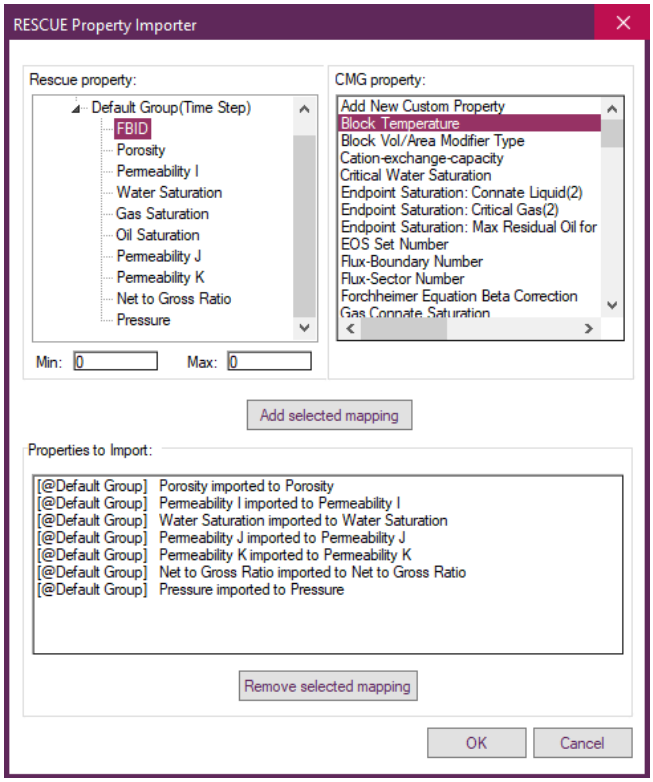

Figure 4.5.2. Rescue property importer.

To further enhance the Norne field reservoir simulation model, additional components and considerations will be further incorporated. However, though properties were assigned normally, it was still done randomly, that is why some values might lay out of their logical ranges. In that case, we just give them mean values (which we were using during geometrical property modelling).

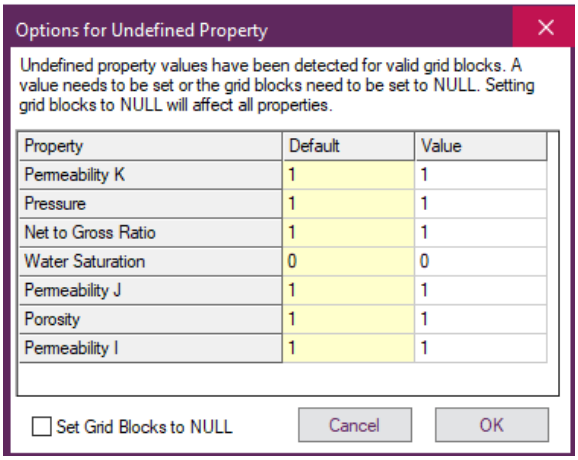

Figure 4.5.3. Undefined properties assignment.

After that, follow the trajectories import, and since we do not need any wells beside B-1H, B-4H and C-4H, we just deselect them. Important, after that we press “Finish & Perf” in order to automatically create wells based on their trajectories.

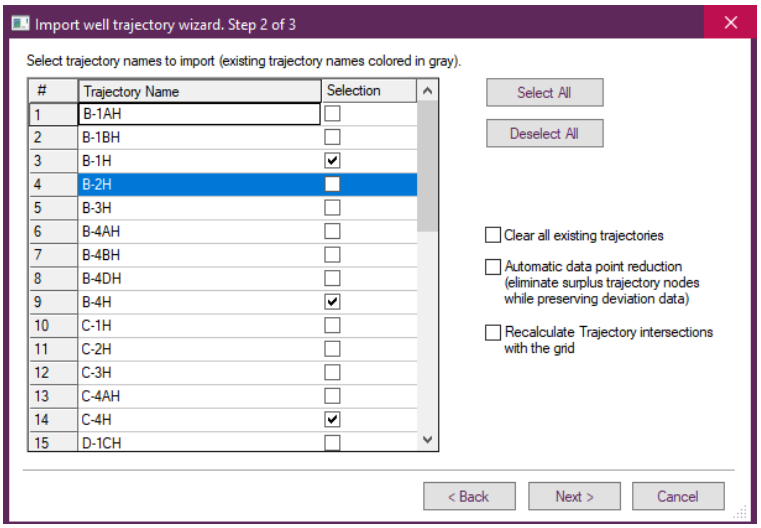

Figure 4.5.4. Well trajectories import wizard.

In the perforations tab, we click “Quick Perf” to automatically and quickly do perforations for our wells. Software will fill in all the necessary data based on what it has. Click “OK”.

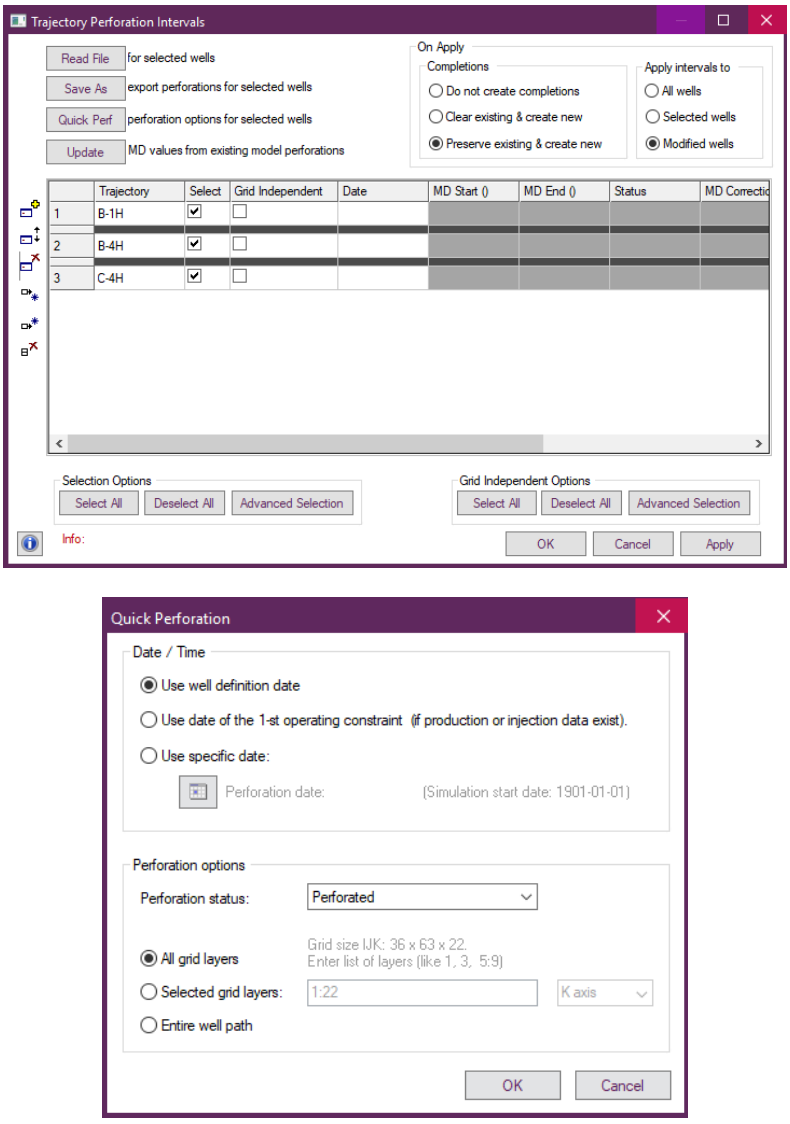

Figure 4.5.5. Perforations manager.

That is it for rescue model importing, now all the missing values should be inserted, and model will be ready for dynamic reservoir simulation.

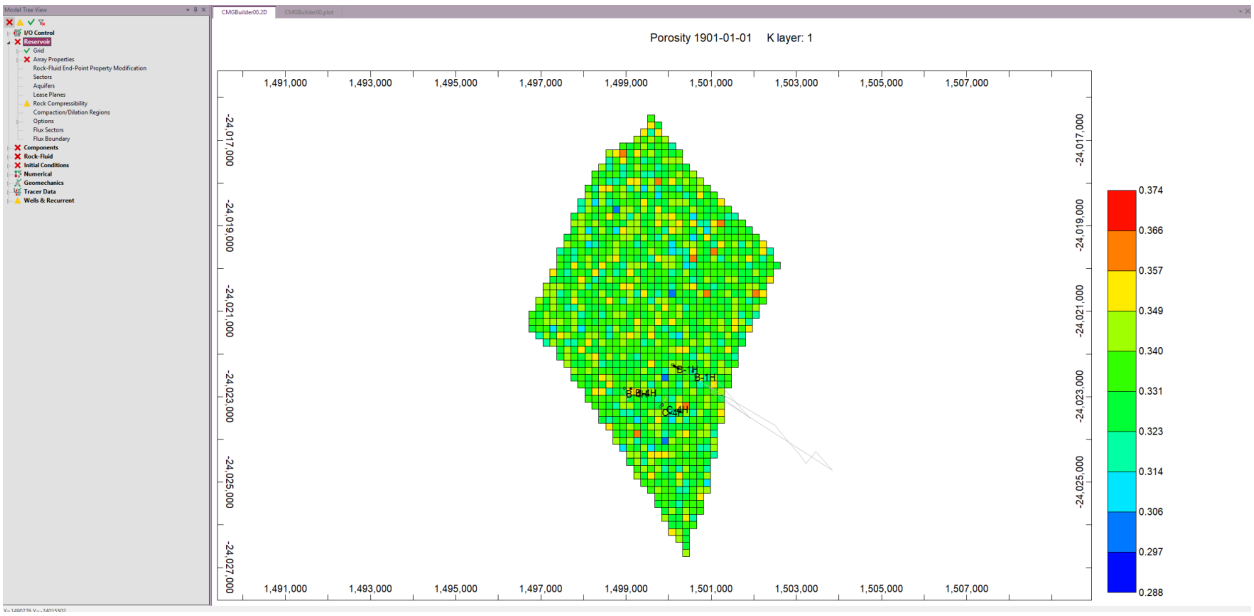

Figure 4.5.6. Rescue model imported into CMG.

4.1.5. Completing model in CMG

Missing data, which is required for completion, contains following:

- Array properties;
- Component properties;
- Rock Fluid Types;
- Initial Conditions;
- Wells & Recurrent data.

Array properties are missing bubble point pressure, which is 2650 psi. Component properties are missing data on which liquid is located within the reservoir, so we create a BLACKOIL model and fill in the missing values.

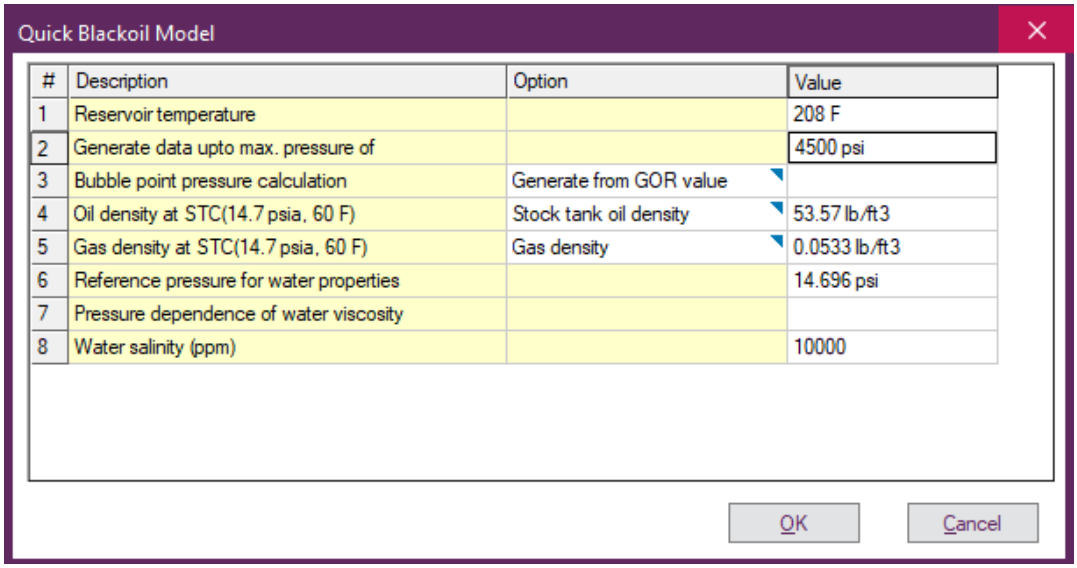

Figure 4.6.1. Blackoil model creation.

Rock types tab requires information on: water saturation, liquid saturation, relative permeabilities of water and gas, and wettability. 2 tables are created: Water-Oil table & Liquid-Gas table, each requires S_w, k_{rw}, k_{row} and S_l, k_{rg}, k_{rog} respectively. All these values were obtained during examination of .data files which were initially used to be imported into Eclipse Office/Petrel.

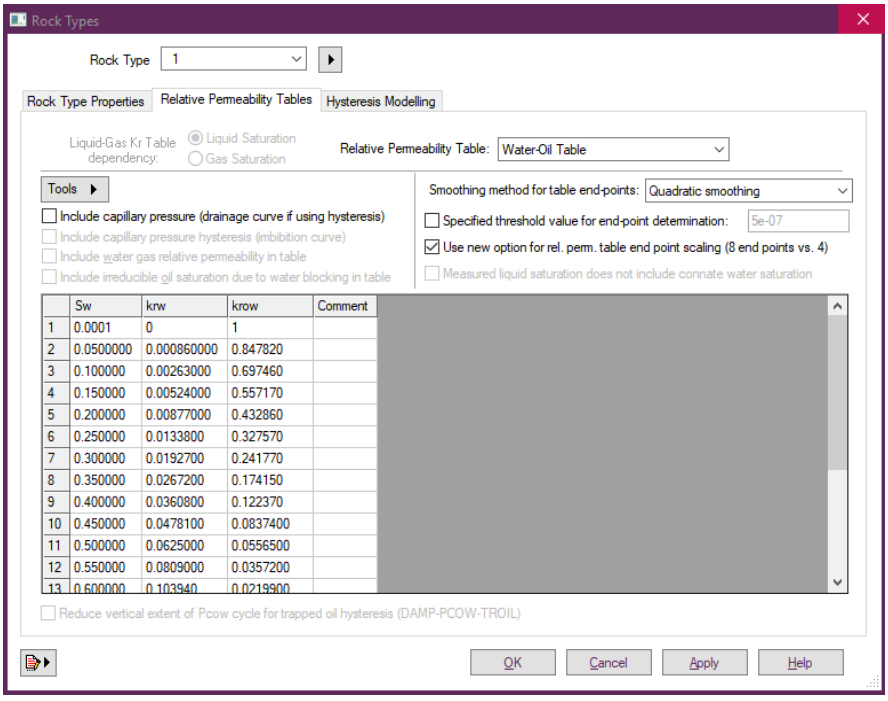

Figure 4.6.2. Rock types assignment.

The next step is to set initial conditions for the model for it to work and model oil extraction properly. Referring back to the Petrel model, all necessary information could be obtained. Pressure of the reservoir at the reference depth varies from 3850 to 3950 psi, so averaging these values would result in 3900 psi. The oil water contact is located on the depth of 8700 ft, so the value is pasted into the corresponding box DWOC. Since the gas cap of the Norne field was located way higher, it was not considered and included into grid properties. So out of 3 options, “Water, Oil” is chosen in what reservoir contains initially.

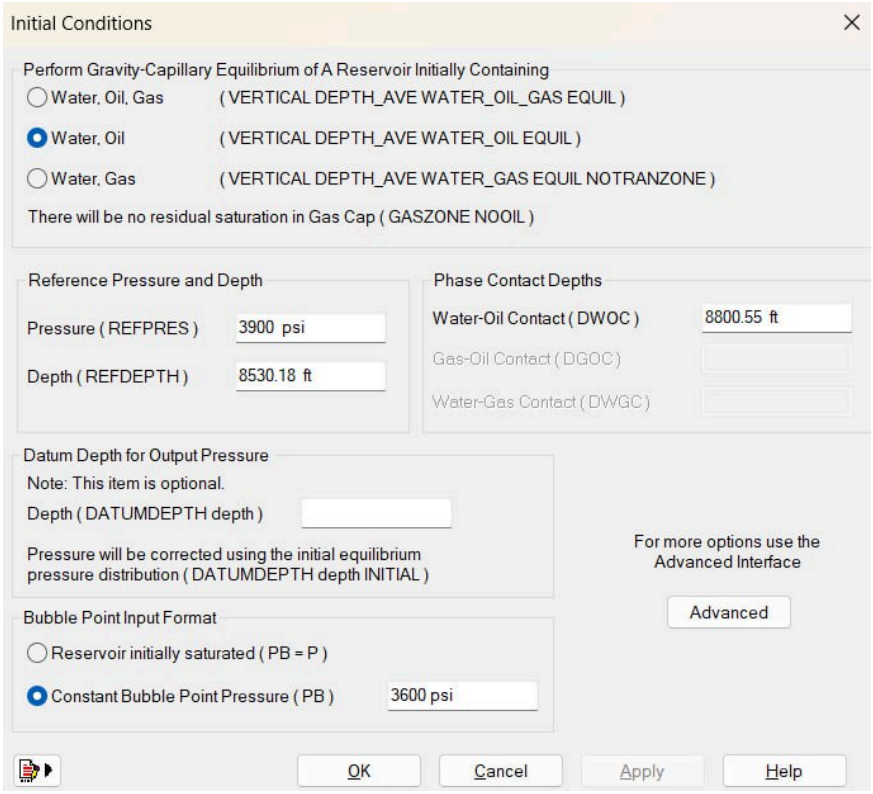

Figure 4.6.3. Initial conditions setting.

The next, very important step, was to set suitable constraints for both injector and producer wells. Constraint of optimal oil production rate was provided by a production engineer using Pipesim simulation, which should be very good for great indicators in future and a balance between fast production and reservoir’s life length. Minimal pressure is set for production wells (B-1H & B-4H) in order to avoid too low values and not exceed Bubble point

pressure's level of 2650 psi, 100 psi is a safety factor. On the other hand, the injection well's injection rate was not capped, however, it has a limitation of 6900 psi bottom hole pressure. Norne field's fracturing pressure is not publicly discovered, so there was a decision to find minimum and maximum P_f values of reservoirs that contain black oil (as Norne field does) and average them. That is indeed very rough, however, there was no data at all. Max & min values reached 10600 and 6800 psi respectively, so averaging them and taking 20% safety factor resulted in 6960 psi.

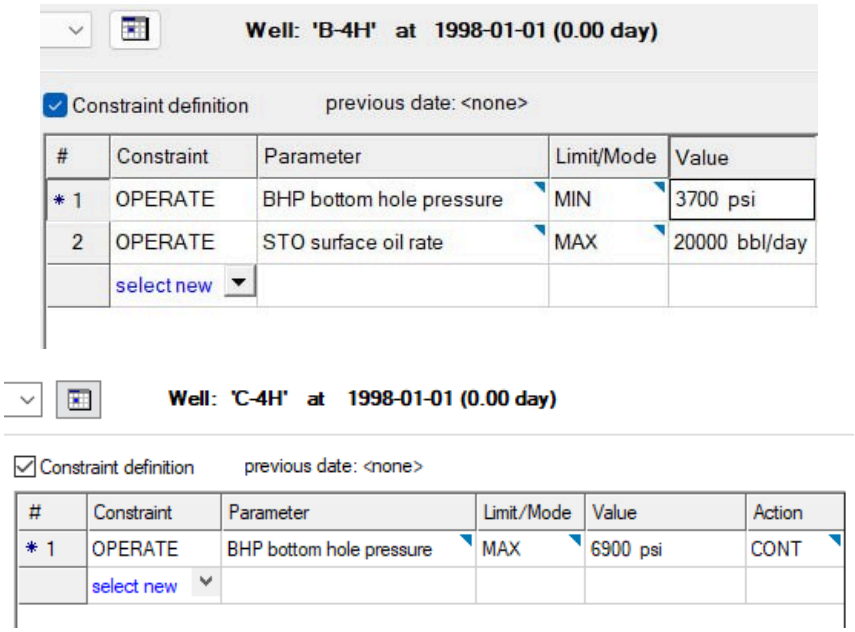

Figure 4.6.4. Constraints set for wells (upper - producer, lower - injector)

A few things remained to complete before running a simulation. One of them is to complete perforations. As was mentioned before, wells have their trajectories, so CMG made perforations on its own through the formation that was recreated. It was important to check whether those perforations were made properly or not. That step was also discussed with the production engineer of our development team.

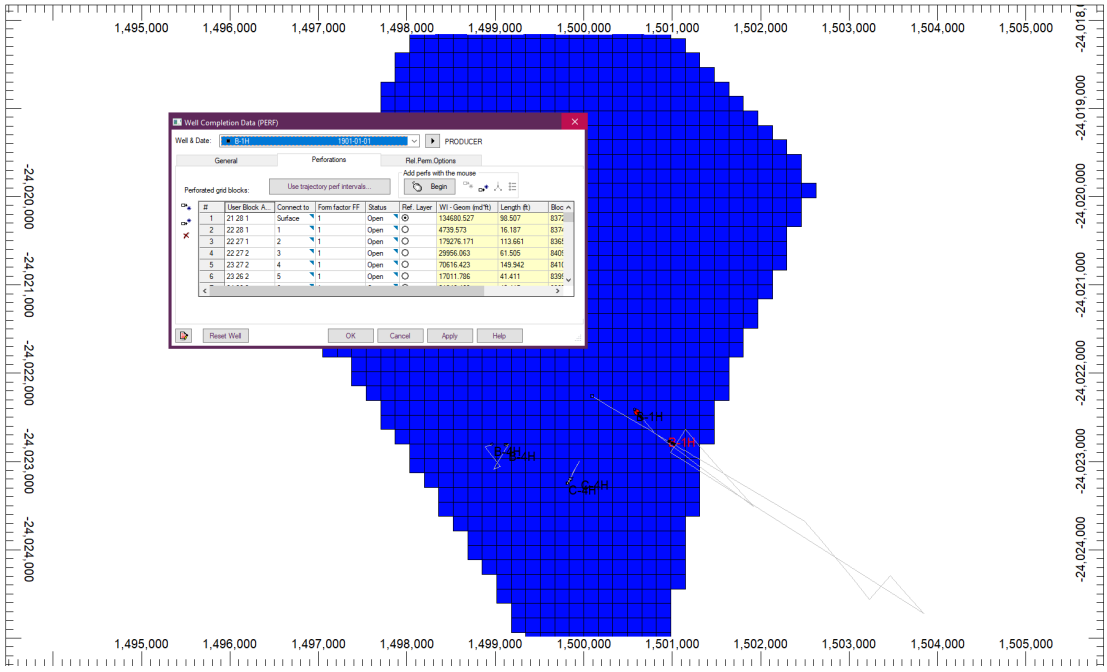

Figure 4.6.5. Perforations check.

The very last step that CMG should get is simulation dates. Since our team decided to examine production since 1998, January 1st was set as a starting date. The 10 year period means that the production must be stopped on January 1, 2008. The time step of 1 month was chosen as a "golden mean" between the accuracy and simulation runtime. 1 day timestep would obviously result in very accurate results, however, the time required to complete simulations would be enormous. 1 year timestep, on the other hand, would take seconds to run but would be very rough.

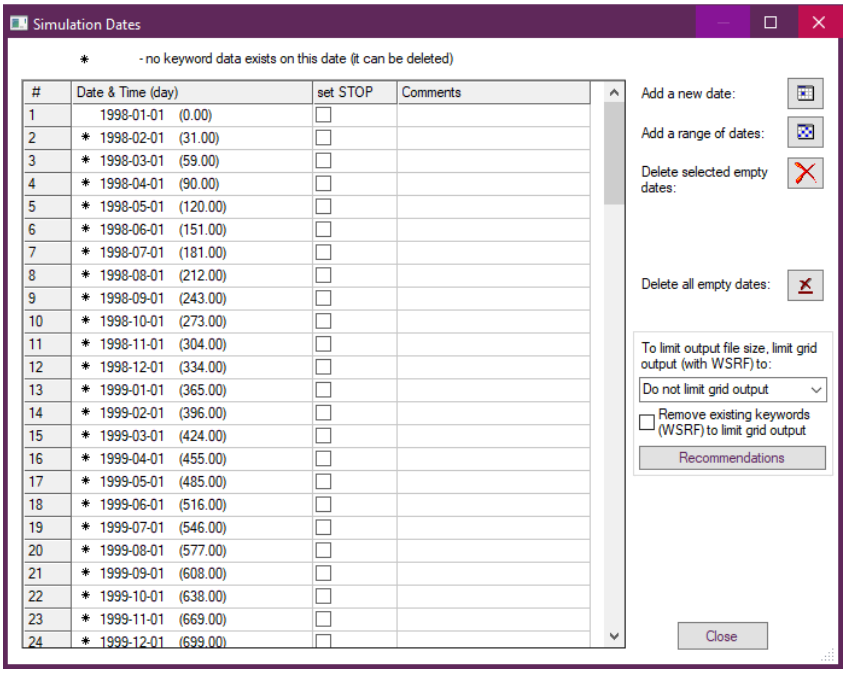

Figure 4.6.6. Dates selection.

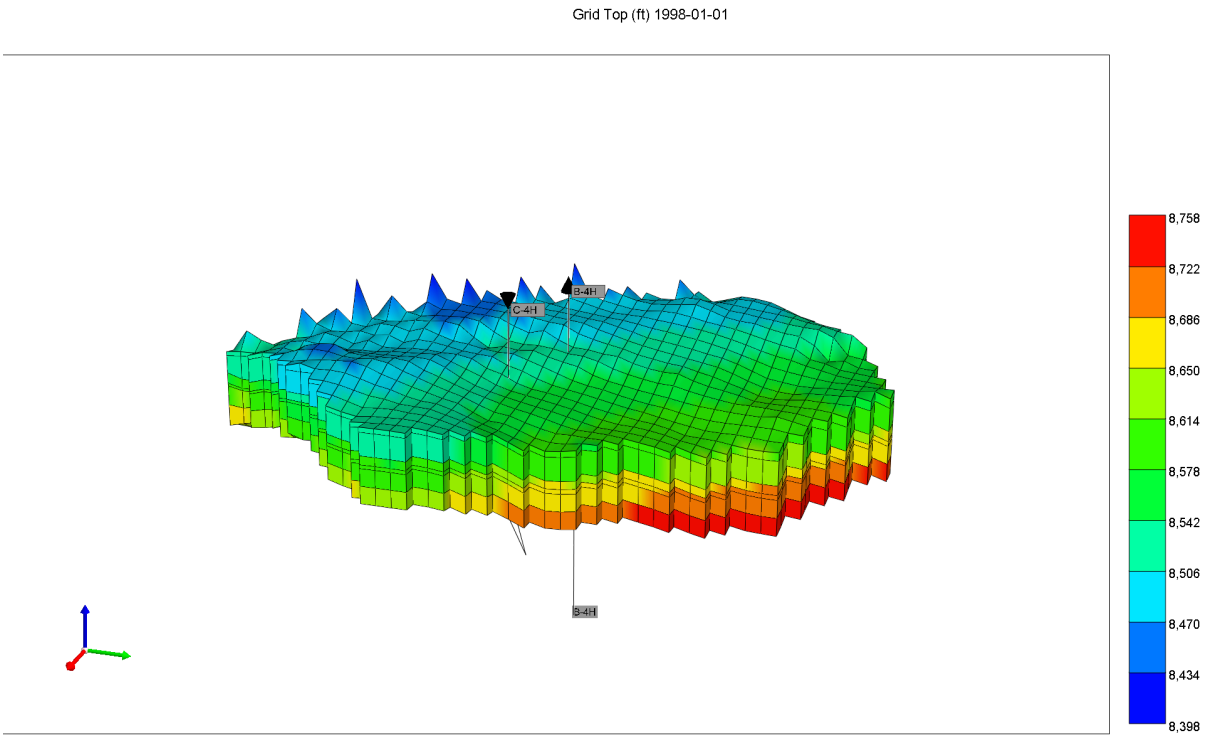

Figure 4.6.7. 3D model of completely transferred grid.

The model, from now on, is fully operational and ready to be run in order to get reservoir simulation results.

4.2. Reservoir Simulation

The simulation reservoir engineering job was to run a simulation program using the presented/found data. It was an important element of the Capstone project process since simulation is essential for developing both a static and dynamic model of the given field, which is the Norne field in Norway. Simulation progress enables other team members to complete their jobs. For example, a reservoir engineer receives the PVT, well location, fluid composition, and pressure control, whereas a production engineer receives the output, pressure control, and placement of production wells, as well as injection information. The drilling and well completion reservoir engineer benefits from simulation because it helps him comprehend the process for well placement as well as the pressure data surrounding those wells and inside the formation itself.

4.2.1. Dynamic Modeling

Reservoir Rock Properties

Permeability (PERMX, PERMY, PERMZ):
Permeability in the x, y, and z axes is one of the most important factors in determining fluid flow inside the reservoir. The simulation can alter the permeability characteristics at certain layers and locations to evaluate the impact of horizontal and vertical permeability on recovery and fluid flow. Such analysis helps reveal how penetration perpendicular to the isopach affects the production and even helps optimally determine the position and the distance between the wells.

Porosity:
Porosity also controls the reservoir's storage capacity which in turn affects the total amount of oil in place. It is possible to note changes in the recovery potential as well as changes in the flow behavior when concentrations of porosity are changed for different regions of the model. The parameter variation in this case study is of utmost importance because it helps explain the change in the amount of recoverable oil and gas to be drilled in the particular region.

Fluid Properties

Viscosity of Oil, Water, and Gas:

The phase mobility of fluids is predominantly influenced by the viscosities of the fluids involved. Given the economically reasonable limits of values, the simulation model was able to vary the viscosity of the fluids used in order to determine their effect on the flow rate and the recovery rate. Higher values of viscosity would hamper fluid movement whilst low values would enhance mobility thus resulting in changing production and sweep efficiencies during the injection processes. Viscosity sensitivity study aids in the optimization of recovery procedures, especially in zones with high oil or gas viscosity.

Gas-Oil Ratio (GOR):

The gas-oil ratio influences reservoir drive mechanisms, including pressure maintenance and gas saturation levels. By changing the GOR, the simulation can determine the effect on production rates, gas management, and total recovery efficiency. This GOR parameter sensitivity is very important in planning whether the gas should be injected or recycled, the inclusion of gas recycling of the solution is not advisable.

Relative Permeability and Capillary Pressure

Relative Permeability Curves (kr):

Graphs of relative permeability characterize how much flow each fluid phase is able to sustain due to capillary effects as the saturation increases. By modifying these curves in the simulations, we observe the effects of fluid interactions on multiphase flow and recovery. This type of sensitivity analysis is relevant when evaluating water and gas injection methods as different relative permeability parameters determine the efficiency of the injected fluids displacing the oil.

Capillary Pressure Curves:

Fluid occupancy inside the rock matrix pores is controlled by capillary pressure. The simulation may also show what happens when several values of capillary pressure are selected in order to alter fluid flow patterns, for example, under waterflooding. Capillary pressure ranges allow designing appropriate water injection rates and strategies so that the oil is displaced and water penetration is reduced.

Well and Injection Parameters

Water Injection Rate:

The water injection rates may be varied on the simulation so that their effects on pressure maintenance, sweep efficiency, etc., and recovery in total may be studied. Primarily the highest water injection ratio recommended is sufficient to cause oil displacement and yet prevent early water breakthrough. This kind of sensibility analysis is very important to come up with viable and usable waterflooding methods that ensure the desired level of pressure in the reservoir and get the best out of the water used.

Gas Injection Rate:

The rates of gas injection are essential for pressure maintenance and oil efficiency displacement much the same as is the case with water injection. Application of gas injection rate change allows the simulation to determine the efficiency of gas used , especially for miscible gas injection. This sensitivity helps to know the best possible rate of gas injection that could be used in the reservoir for certain zones of pressure maintenance and for better recovery as well.

- **Reservoir Simulation Models**: The static geological and petrophysical models are also made first in order to build dynamic reservoir simulation models, which are the ones designed to show fluid's and a certain distance over time's pressure behavior . Those simulations are conducted with software such as Eclipse, or CMG. The models forecast how a reservoir would respond to stimulation from various production conditions.
- **History Matching**: The dynamics in the model are adjusted in such a way that historical production data is utilized and the reservoir performance over time is captured during the calibration of the model. A more acceptable model is built by reconciling the differences between the actual production and the anticipated production levels.
- **Forecasting**: The history matched model is then utilized for estimating the future performance of the reservoir for different management strategies like drilling additional wells, water flooding, and Enhanced Oil Recovery (EOR) techniques among others.

4.2.2. Initial dynamic reservoir model

As it was described by a static model engineer above, we managed to get our hands on the rescue model that we transferred into the CMG, where after some considerations and a careful analysis as well as discussion with other engineers we defined wells, completions for those wells and placed them as accordingly to the original oil field as we could. During that process we had encountered multiple problems which included: Poor initial reservoir pressure (due to an inability to transfer the gas cap and the water layer from the petrel model), well placement issues, gas saturations distribution issues. Besides all of that, we managed to define 1 production well and 1 injector well. After that, I consulted with production engineers to get the optimal flow rates and completion designs. Flow rates were used as constraints for the well definitions. Completion designes were utilized as closer as possible to the real case considering all the restrictions that CMG software has. After that, we carefully evaluated the most realistic and optimal well placement by looking at the static model in petrel with all the wells visible.

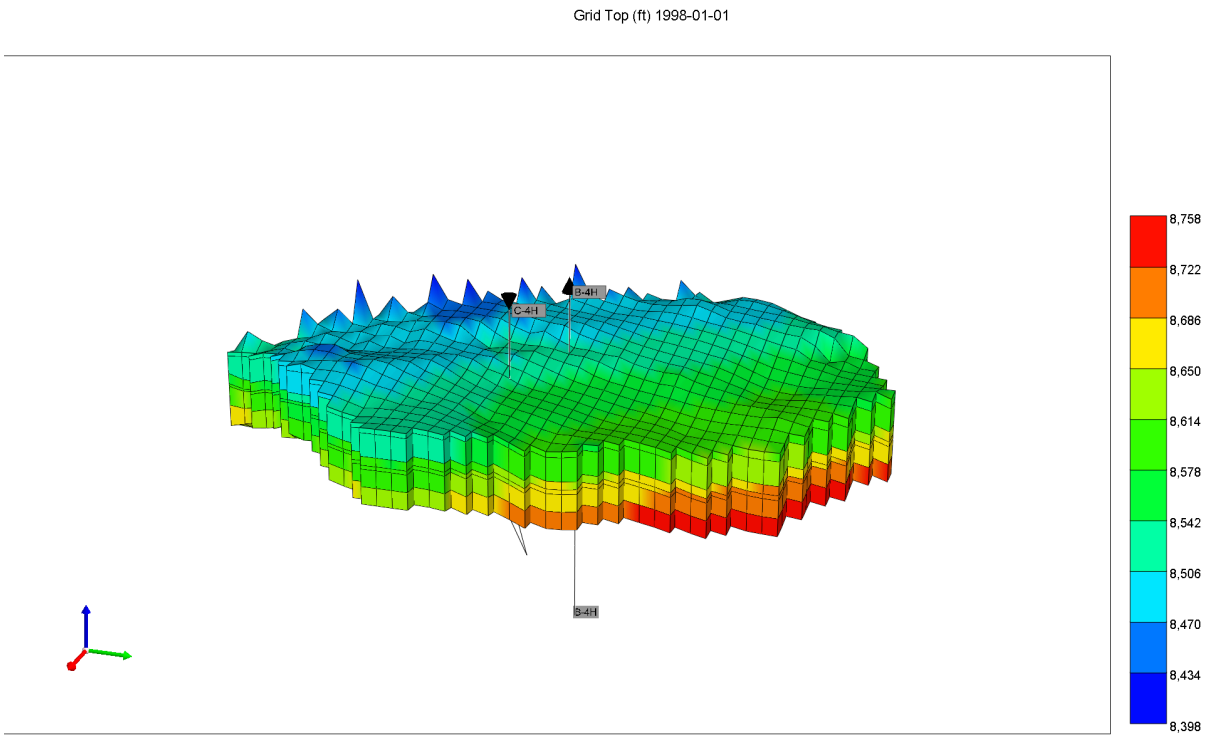

Figure 4.7.1. Initial model.

To successfully transfer the well trajectories, we had to account for the NULL blocks as well as the grid itself. So it was settled that we would try to perforate on our own.

The injector was set to be a gas injector with the type of injection: MOBWEIGHT. This decision was advised by the reservoir engineers as it is clear that the Norne field had a lot of excess gas in the reservoir initially and it was economically viable to inject it in the beginning.

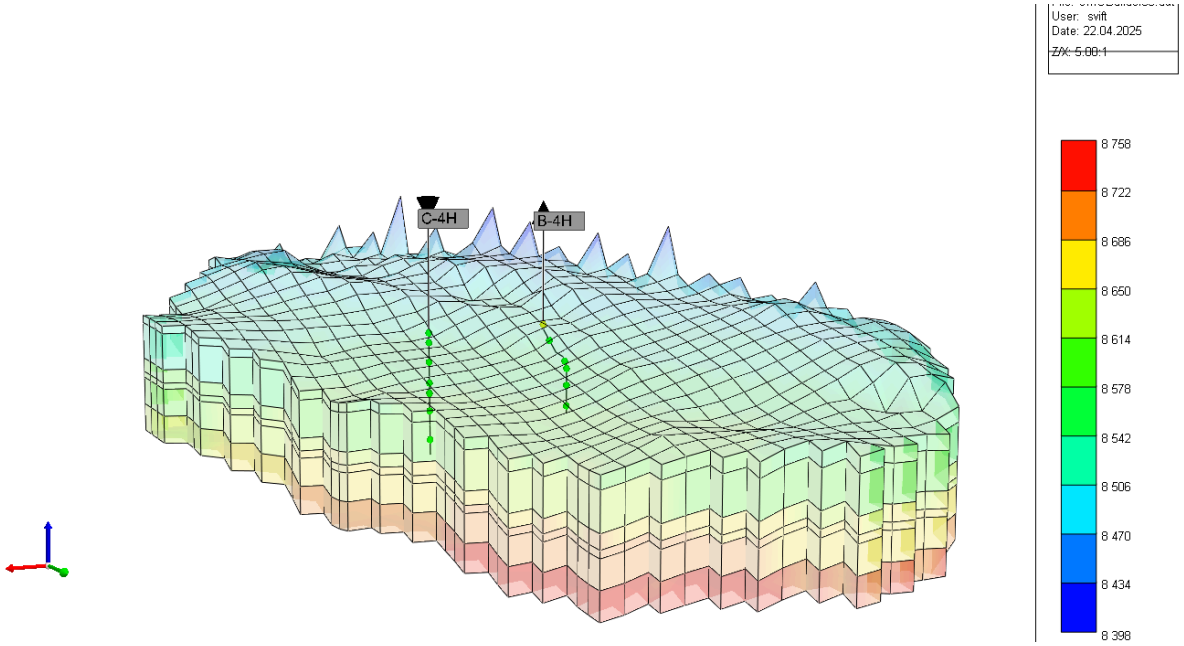

Figure 4.7.2. Initial wells placement.

Position of the wells were determined by the initial petrel model.

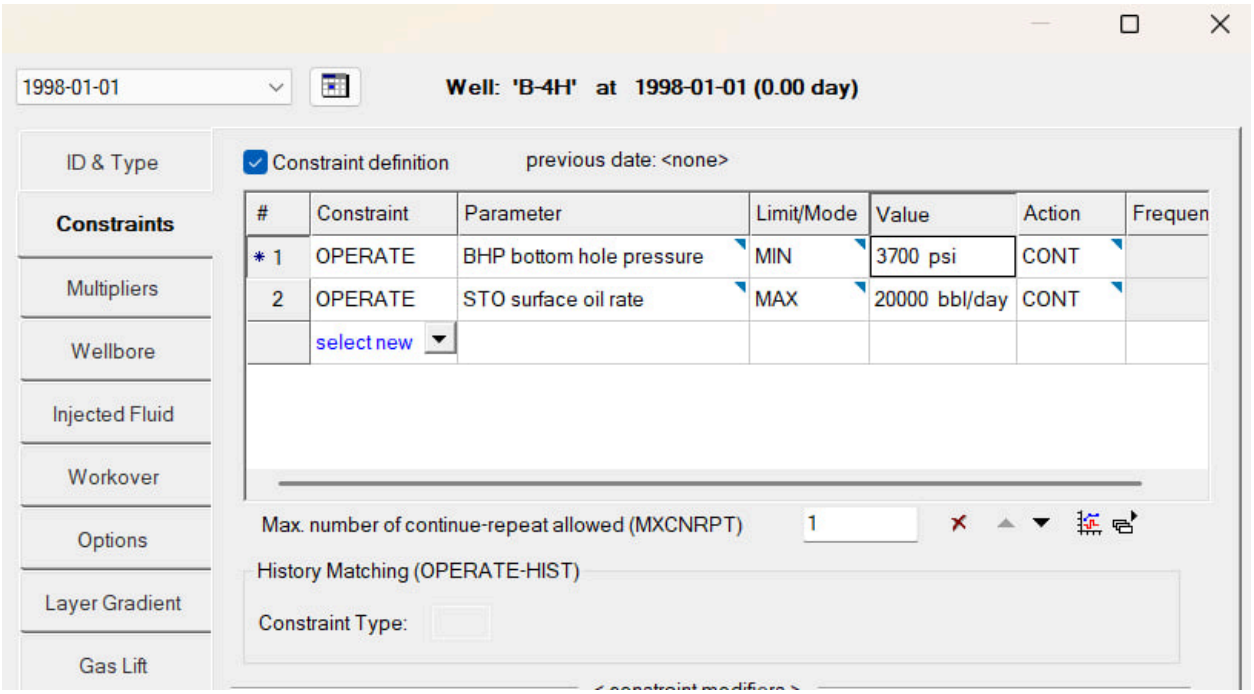

Figure 4.7.3. Well B-4H Constraint definition.

The constraints were set as type OPERATE and the parameters were chosen as BHP bottom hole pressure and STO surface oil rate. For BHP min mode and value of 3700 psi with a CONT action and for STO max mode and value of 20000 bbl/day with a CONT action.

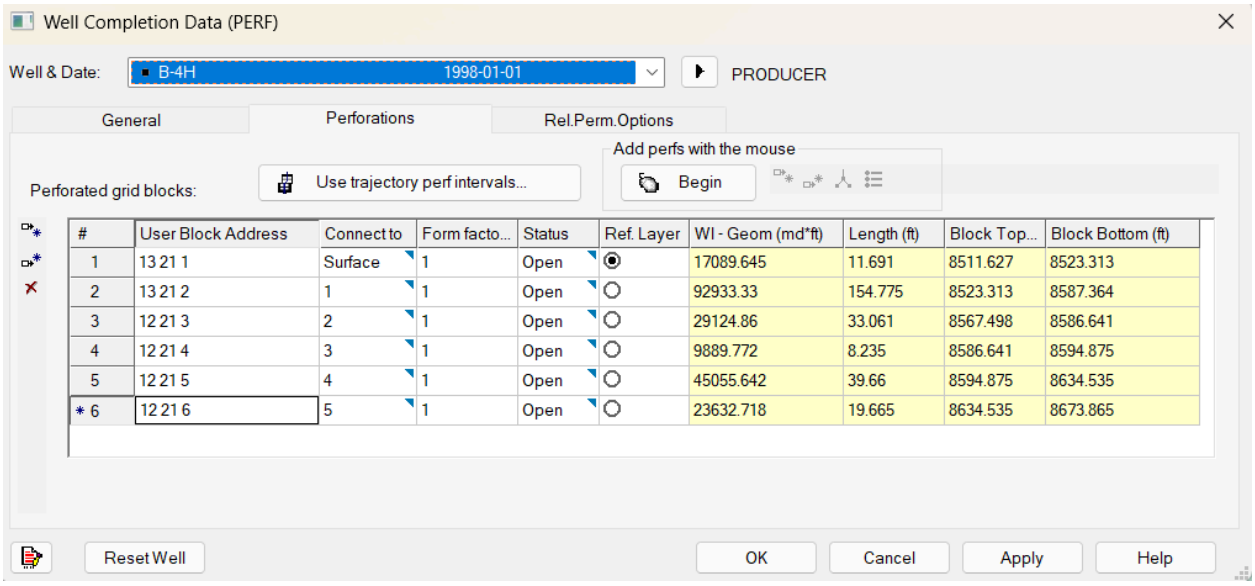

Figure 4.7.4. Well B-4H completion data.

Perforations coordinates for B-4H well with a reference layer set as the highest layer.

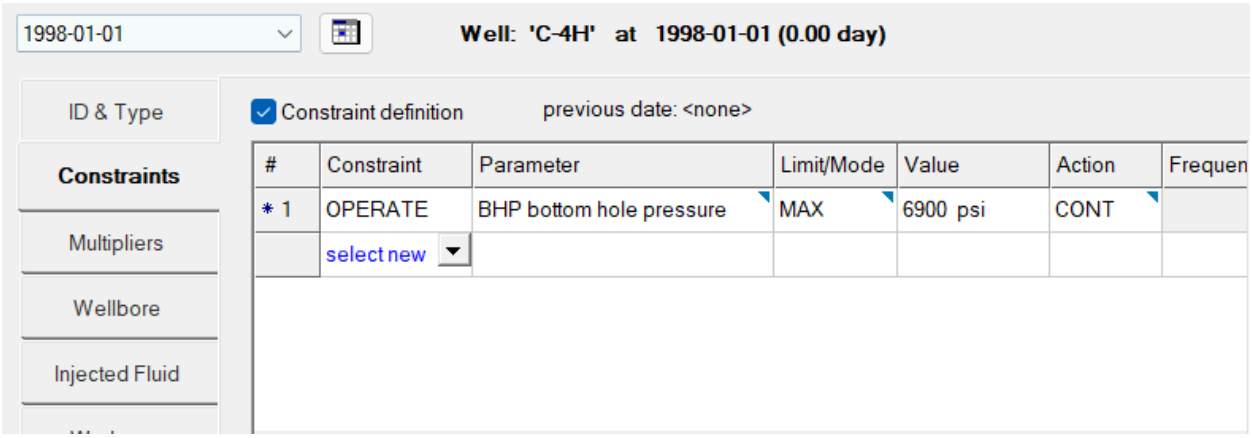

Figure 4.7.5. Well C-4H constrain definition.

Constraint for the injector well C-4H is an OPERATE constraint with a BHP at max mode with 6900 psi value with a CONT action.

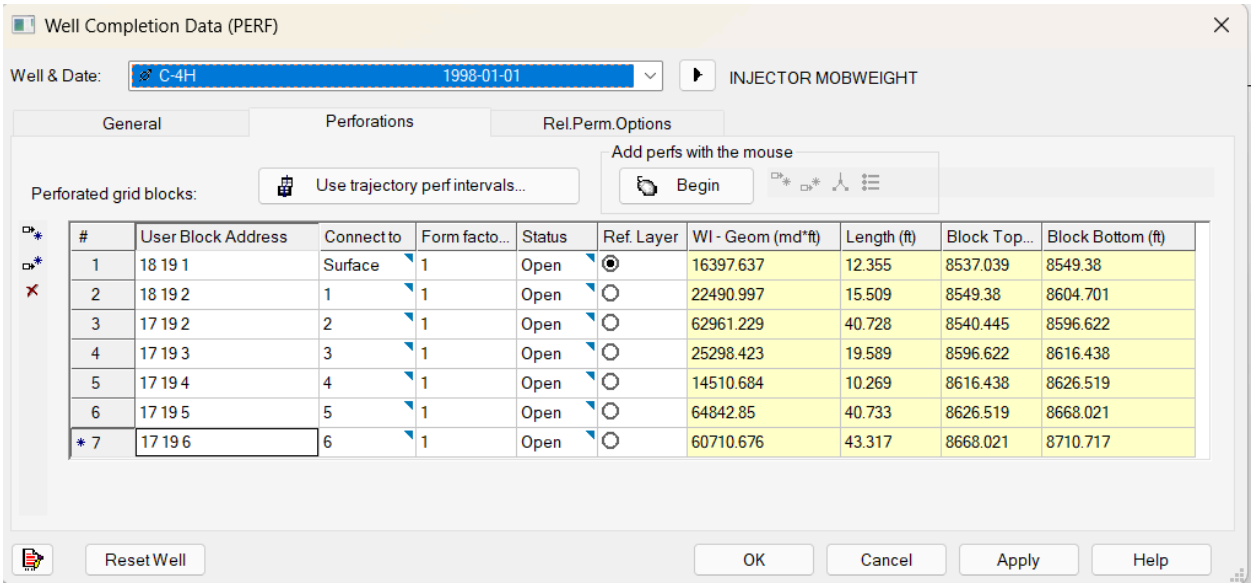

Figure 4.7.6. Well C-4H completion data.

Perforation coordinates for C-4H well with a reference layer set as the highest layer.

The perforations were done by hand due to the fact the the trajectories imported from the petrel model were accounted for all the layers in the whole reservoir. And because only the part of the reservoir was transferred into the CMG software, the trajectories were going out of the grid which resulted in errors and an inability to run the simulation. So the completion design was suggested by the production engineer.

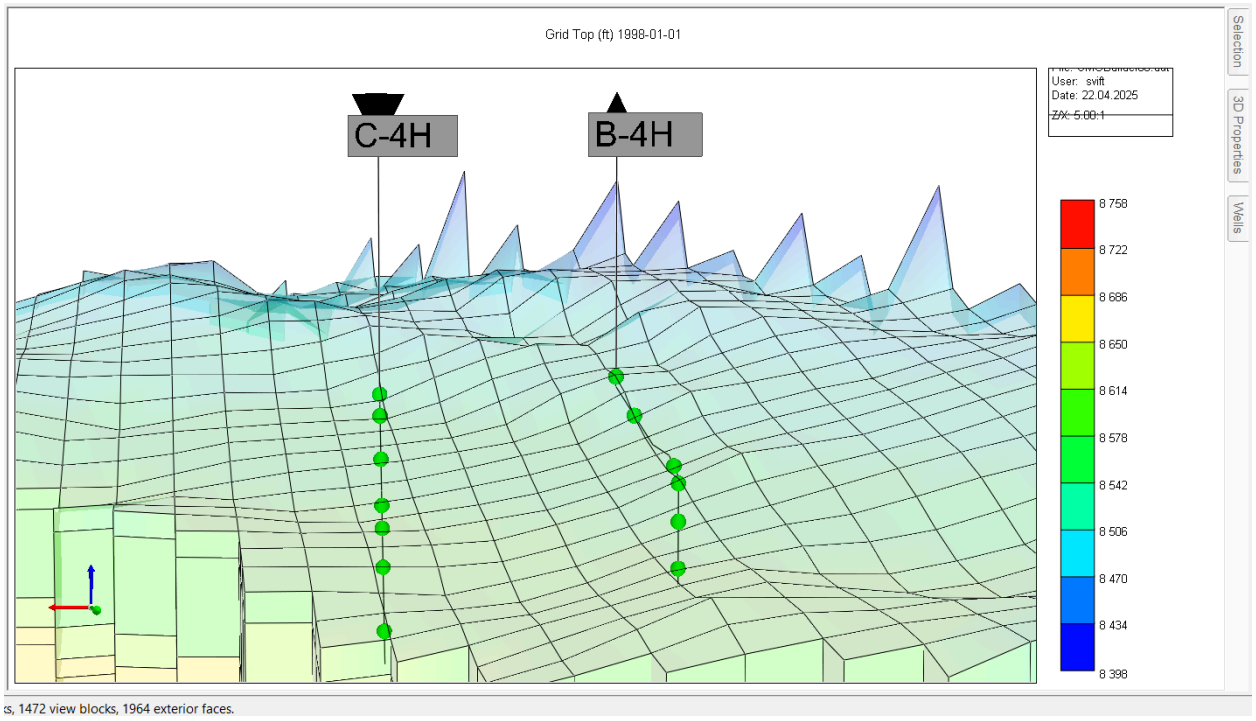

Figure 4.7.7. Well's perforations.

The C-4H well is an injector well with gas as an injected fluid at a true vertical depth of 8708 ft. B-4H well is the producer at a true vertical depth of 8757 ft.

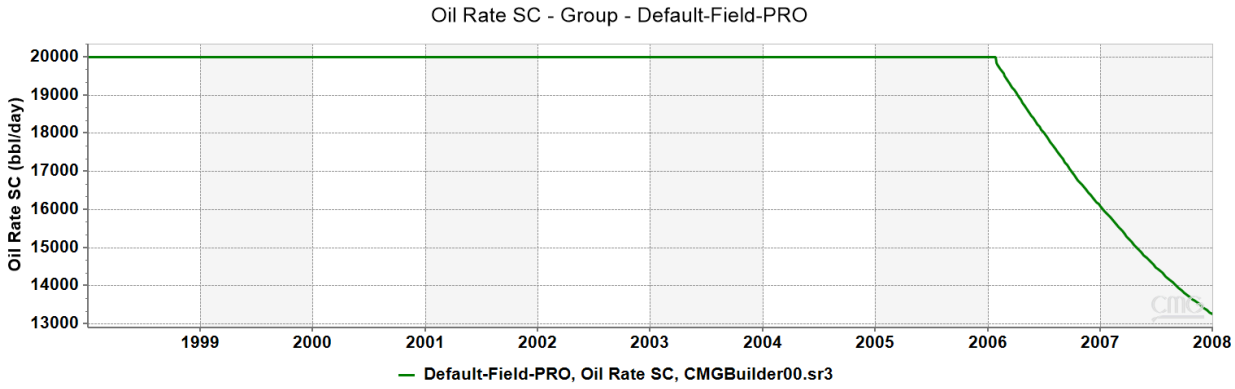

Figure 4.7.8. Oil rate of the initial model.

The oil production rate remained constant at approximately 20000 barrels per day from 1998 to late 2005. This indicates a stable plateau phase,maintained through gas injection which kept the reservoir pressure stable. After that starting in 2006, a gradual decline in oil production has started, falling to around 13000 barrels per day by the end at 2008. This decline was further analysed and was take into account for future sensitivity analysis. It should be noted that the constraint set to 20000 barrels per day is what keeping the production well from depleting the reservoir too fast.

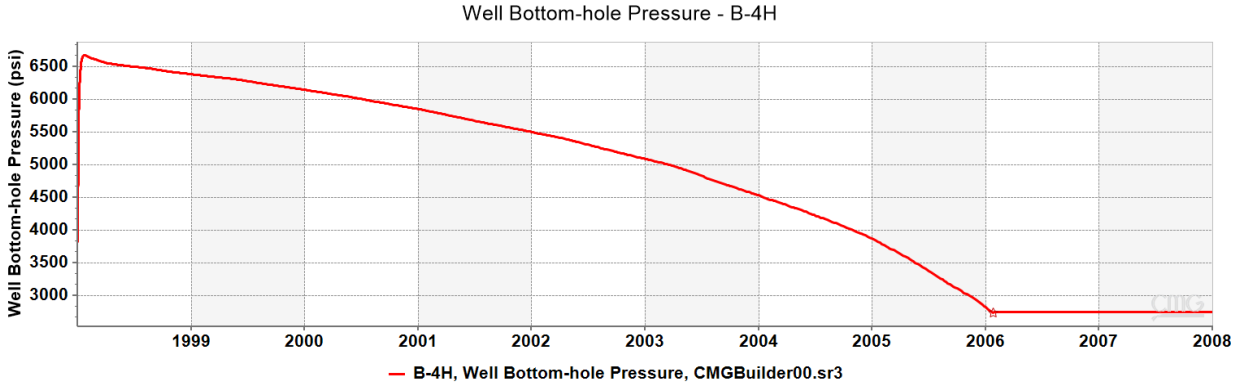

Figure 4.7.9. Wells' BHP of the initial model.

It can be observed here that the bottom-hole pressure for well B-4H began at around 6600 psi in 1998 and steadily declined over the years, reaching just below 3000 psi by 2006. After that it had reached an operational limit set at 2750 psi. The constant pressure after 2006 suggests no further production activity from the well until the last day of the simulation.

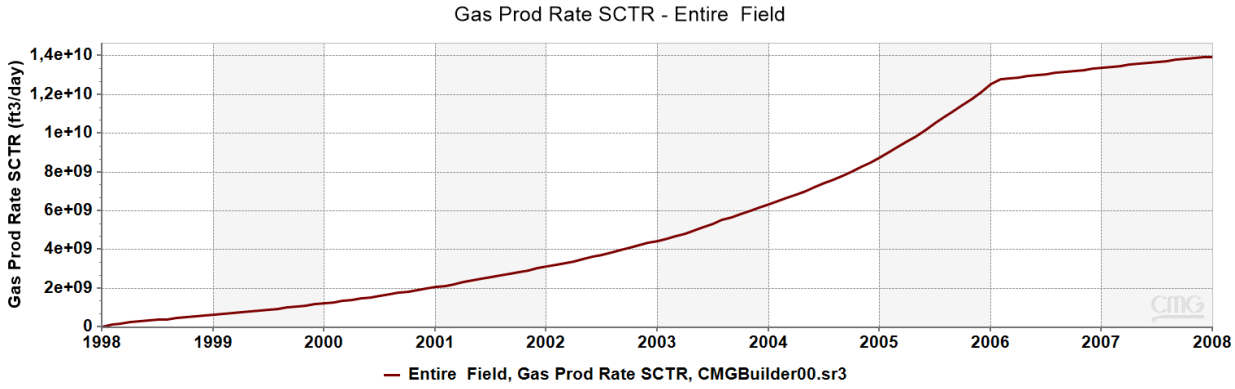

Figure 4.7.10. Gas production rate of the initial model.

The gas production rate for the entire field shows a steady and continuous increase from 1998 to 2008, starting near zero and reaching approximately 1.4 × 10^3 ft^3/day by the end of the simulation. This trend reflects consistent gas injection throughout the entire period, as indicated. Even though gas was injected from the beginning, the production curve shows that gas production gradually increased over time, with a notable sharp increase around 2006, followed by a flatenning. This suggests that gas that was injected continuously has broke through to the producers, eventually becoming a big part of the produced flow.

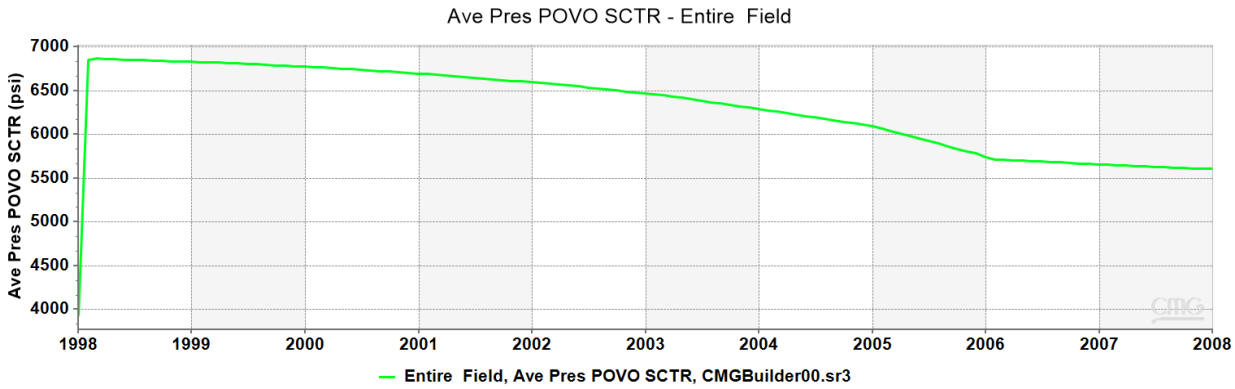

Figure 4.7.11. Average pressure of the reservoir's model.

The average reservoir pressure started from 3900 to 6900 psi in 1998 due to the injection operational constraint and gradually declined to around 5800 psi by the end. Gas is injected continuously but the pressure is still gradually dropped, which means that production is higher now than the pressure support. The decline become much smoother after 2006, suggesting possible gas breakthrough and recycling, with less net reservoir energy loss.

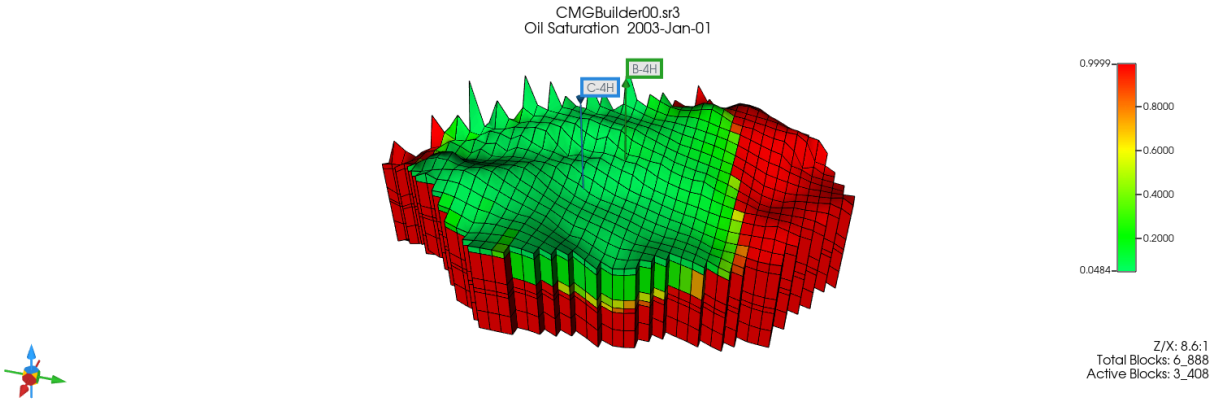

Figure 4.7.12. Initial model's oil saturation in 2003.

As of January 1, 2003, the green areas in the reservoir show where most of the oil has already been produced, while the red areas still contain a lot of oil. Around the production well B-4H, there is mostly green, meaning this area has been producing oil effectively. Near the injection well, there is still a lot of oil remains there. This shows that the gas injection is helping push oil toward the producer, but some parts of the reservoir still have oil that hasn't been reached yet.

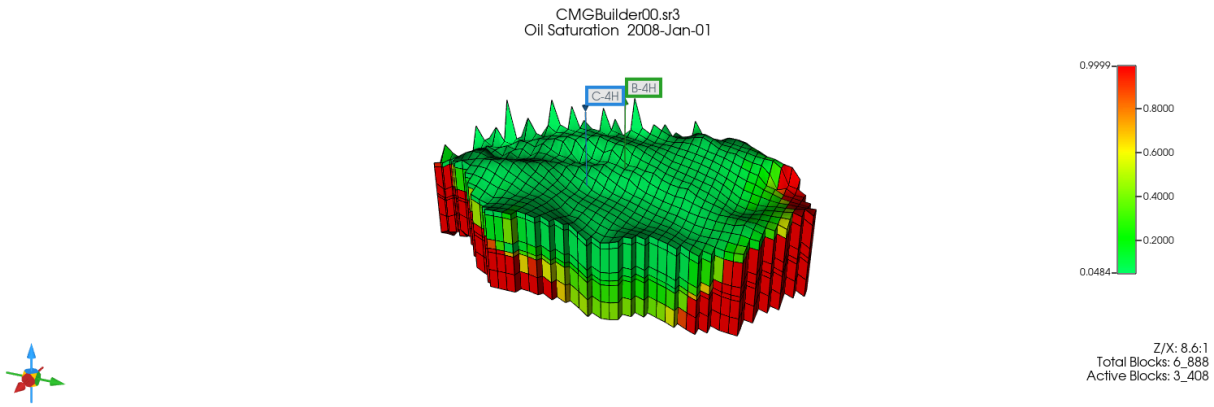

Figure 4.7.13. Initial model's oil saturation in 2008.

As of January 1, 2008 (the end of the simulation), the oil saturation show that most of the reservoir around well B-4H has turned green, meaning oil has been successfully swept out in that region. In contrast, large red areas still remain in the outer parts of the reservoir, especially far from the injection well C-4H. This means a lot of oil is still left in the reservoir. Further adding new wells, changing the well placement, changing constraints, adding aquifer could help to more optimally sweep all the oil from the reservoir

4.2.3. Sensitivity Analysis

Objective

The main objective of a sensitivity analysis was to identify how each variables affected the reservoir

Methodology

The specific feature of our work was that we did not create the model from scratch, due to a lack of data necessary to build a model that would closely match the real case. As a result, we could not use the CMOST utility, and we had to change all variables manually. These variables included the presence of an aquifer, the number of wells, their location, their optimal placement, flow rates, constraints, and so on. Once the objective was defined—namely, identifying the variable we would change to study its impact on oil production—the original file was saved, and a copy was created in which the new variables

were introduced. These variables, in turn, were adjusted based on insights gained from previous changes.

Analysis

Scenario 1: Flow rates

Objective

To study the effect of the production rate constraints on the field.

Cases Analyzed:

Case 1: Production rate 20000 bbl/day

Case 2: Production rate changed to 10000 bbl/day

Case 3: Production rate change to 40000 bbl/day

Outcomes:

Case 1:

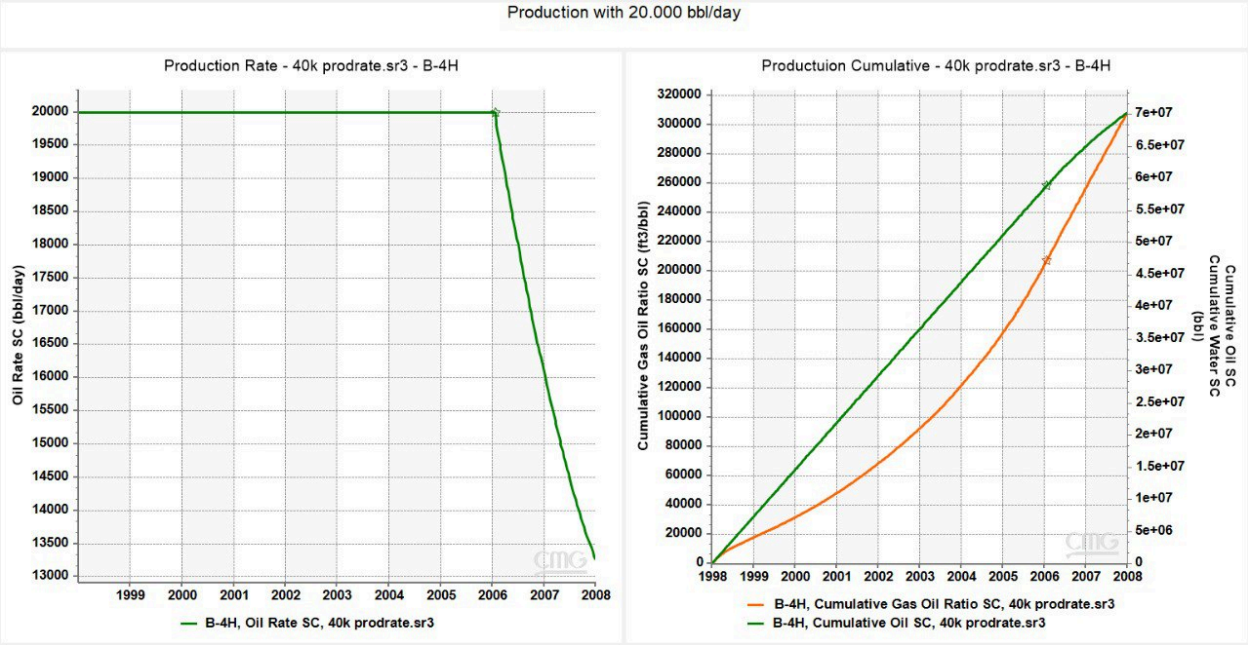

Figure 4.8.1. Production with 20000 bbl/day.

In the first scenario with a production rate of 20000 bbl/day, oil production remains the same until 2006, after which it declines sharply. This suggests a well-maintained plateau phase followed by reservoir pressure depletion. The cumulative oil and gas production grow steadily, reaching approximately 70 million barrels of oil by 2008. Cumulative gas production shows late-stage gas breakthrough because of declining reservoir pressure which is efficient in a long term. This case is set as an initial and it shows a stable, yet not fully recovered reservoir with a lot of oul left unswept.

Case 2:

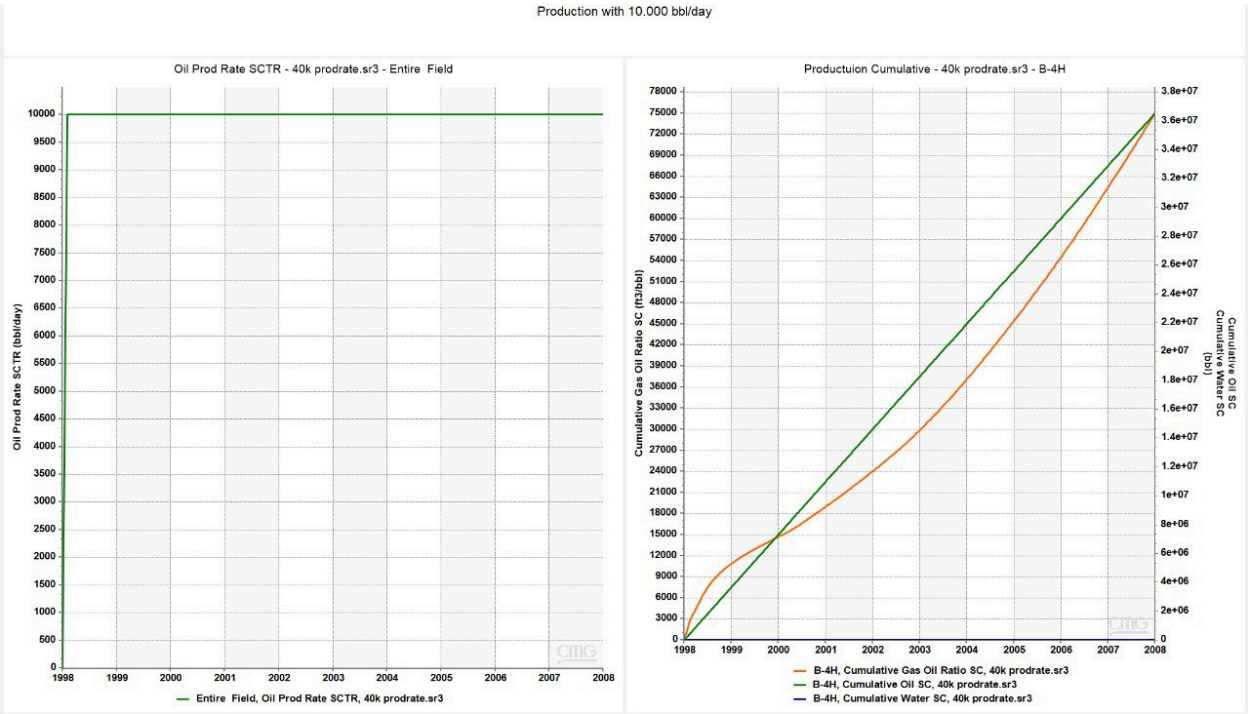

Figure 4.8.2. Production with 10000 bbl/day.

In the second scenario, the field produces constantly at 10000 bbl/day for the entire field life. This production rate helps to maintain good reservoir pressure and to delay gas and water breakthrough. However, the total cumulative oil produced is much lower, approximately by half, 36 million barrels. The gas-oil ratio grows slowly, indicating a more balanced and pressure-stable production profile. But considering that the oil rate never dropped the reservoir never depleted in a span of 10 years. So the flow rate set as 10000 barrels per day is not enough for the reservoir to efficiently recover oil.

Case 3:

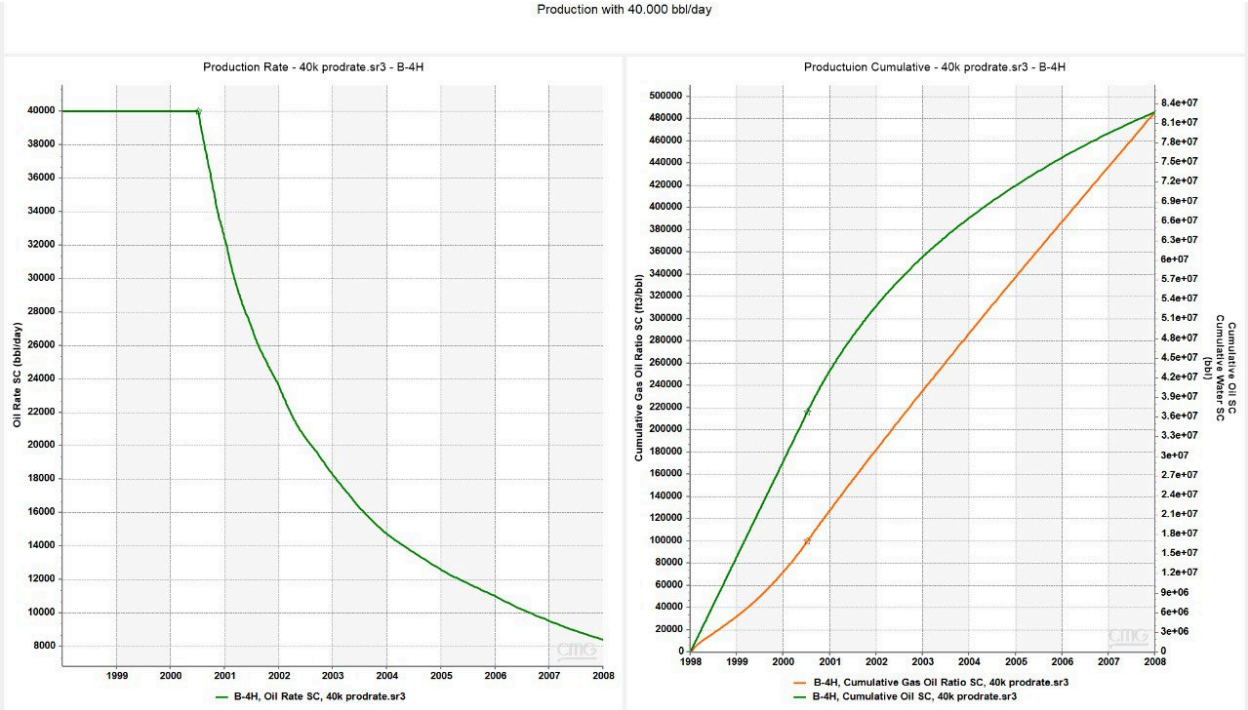

Figure 4.8.3. Production with 40000 bbl/day.

In the third scenario, production begins at a high rate of 40000 bbl/day but drops quickly after the early years, indicating rapid reservoir depletion and pressure loss. It is cleat that this approach results in the highest cumulative oil recovery over 84 million barrels by the end, it also speeds up the gas breakthrough, as seen from the sharp increase in the gas-oil ratio. This aggressive strategy yields the most oil early but reduces long-term efficiency due to fast energy decline. Overal this operational constraint is the most efficient in terms of recovered cumulative oil.

Conclusion:

The oil production operational constraint has a significant impact on reservoir performance over time. A high production rate, such as 40000 bbl/day, leads to rapid pressure depletion, early gas breakthrough, and faster decline in production, even though it provides for high oil

volumes in the short term. On the other hand, a low production rate of 10000 bbl/day, presents a more stable reservoir pressure, delays gas breakthrough, and maintains a more stable production profile, but results in a much lower cumulative oil recovery. A moderate rate, such as 20000 bbl/day, provides a more balanced solution for production making it smoother for several years before declining. Overall, higher production rates make the reservoir depleat faster, while lower rates keep the pressure more stable,but undermines the potential recovery. Choosing the optimal constraint involves a choice between early cash flow or long-term recovery efficiency.

Scenario 2: Optimization of Well Spacing and Placement

Objective:

To study how the well placement and spacing affects the reservoir

Cases Analyzed:

Before proceeding another producer was added to make the analysis more reasonable and handle reservoirs reserves better

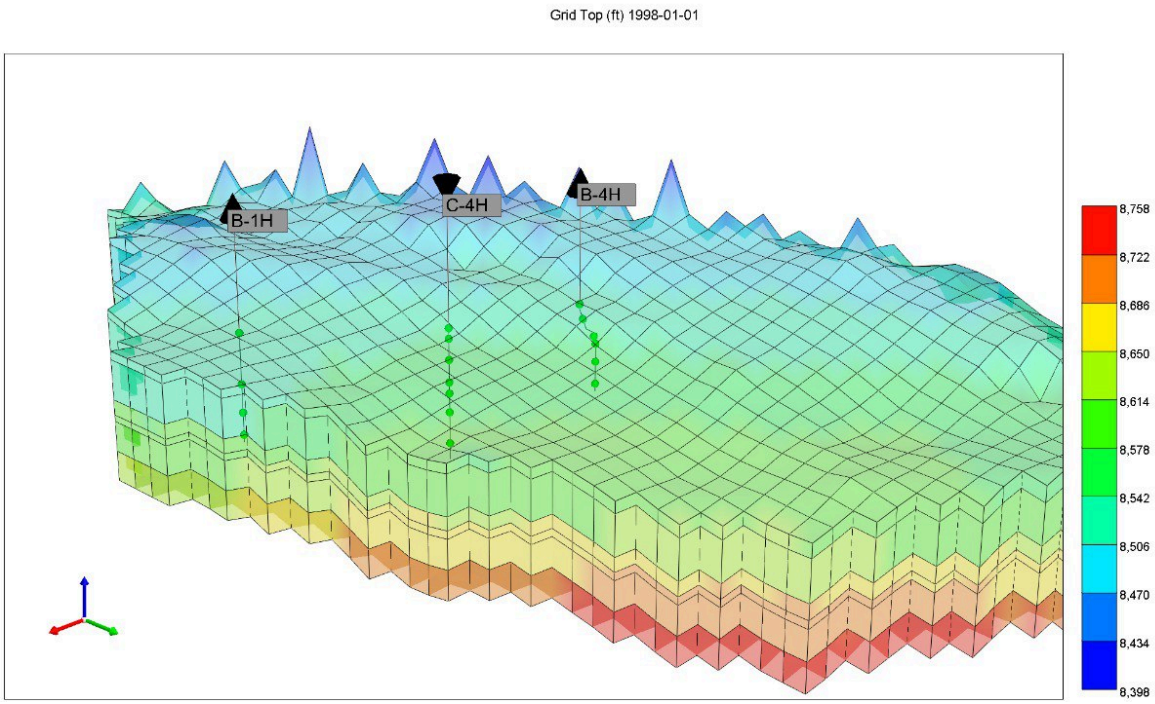

Figure 4.8.4. B-1H well' location.

Case 1: Production wells close to a changed position of an injector

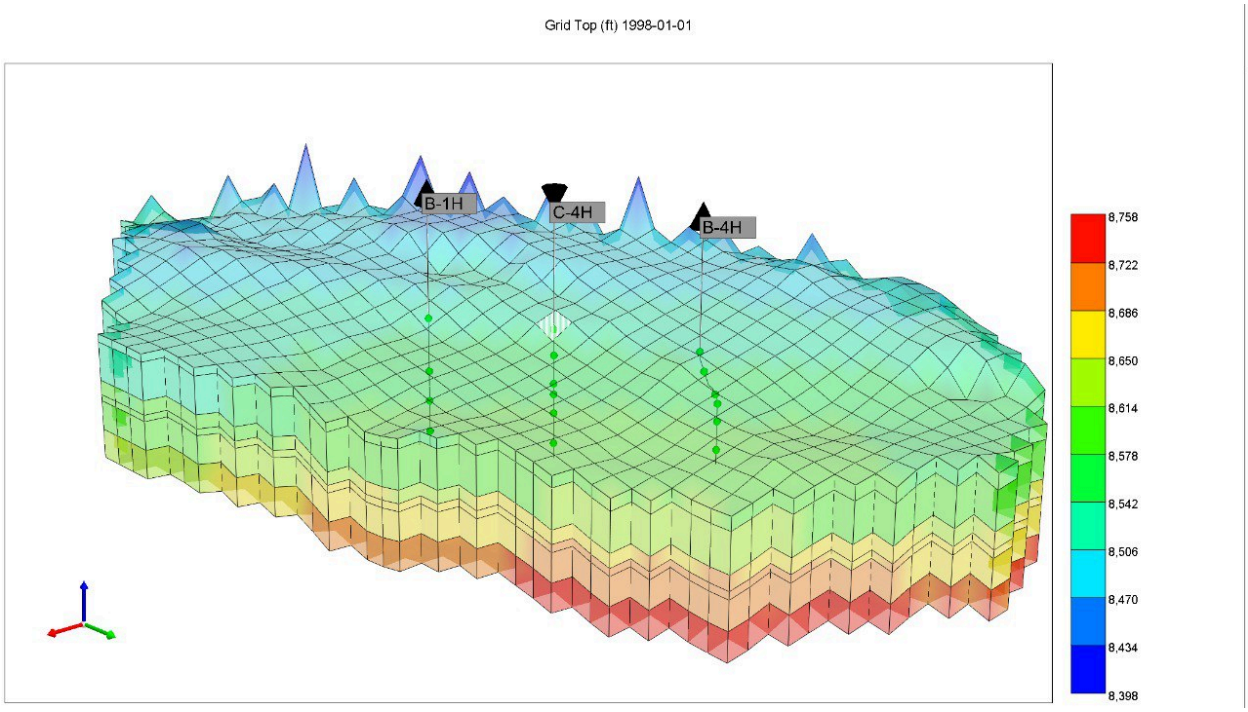

Figure 4.8.5. Close distance.

Originally, the position of the injector was more to the left, but it was decided to move it to the center for more possibilities of well placements and especially spacings. Also, off the record, it was studied that this way the production is more stable and the oil is swept more uniformly across the whole reservoir.

Case 2: Production wells on a moderate distance from a changed position of an injector

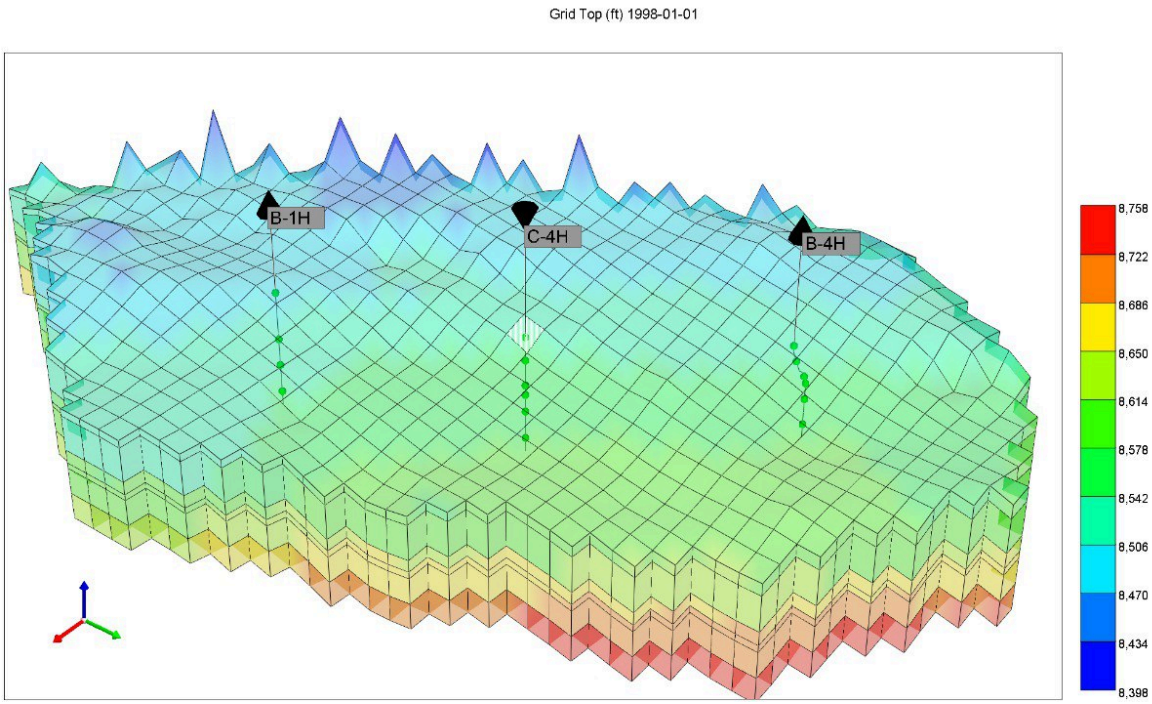

Figure 4.8.6. Moderate distance.

On the figure 4.8.6. We see that both production wells were placed on an equal distance from the injector and were spread more widely, but not so much. The distance is considered to be moderate.

Case 3: Production wells on large distance from a changed position of an injector

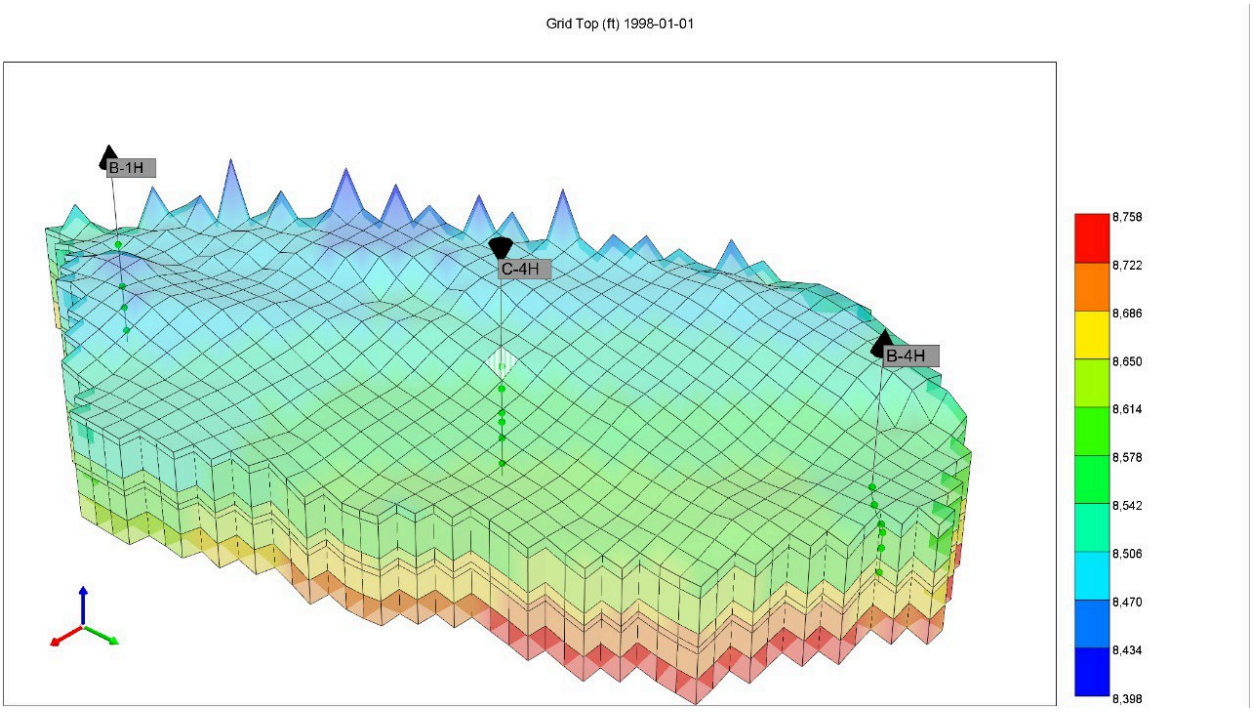

Figure 4.8.7. Far distance.

On the figure 4.8.7. The well placement was set to be on the edges of the reservoir. Considering how strong the injection rate, this case is expected to be the most promising.

Outcomes:

Addition of another producer:

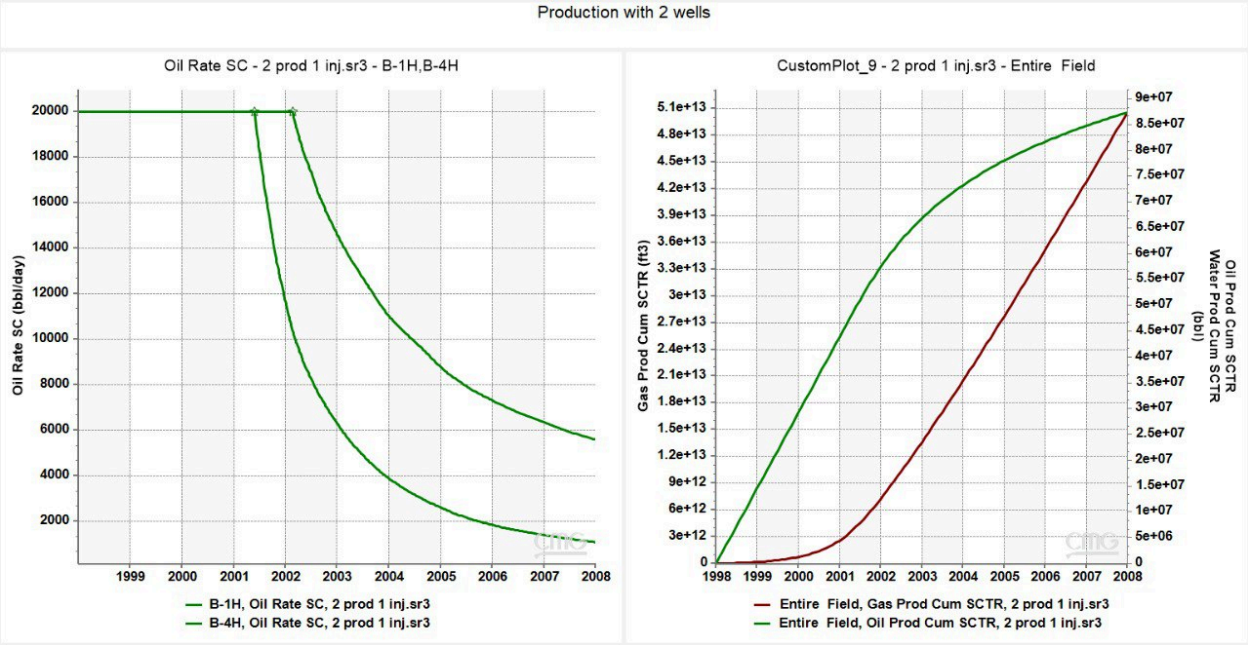

Figure 4.8.8. Production rate with 2nd well.

The effect of another producer is obvious, now that there is another way for the fluid to come out of the reservoir, the oil production is more efficient and the pressure profile is much more stable.

Case 1:

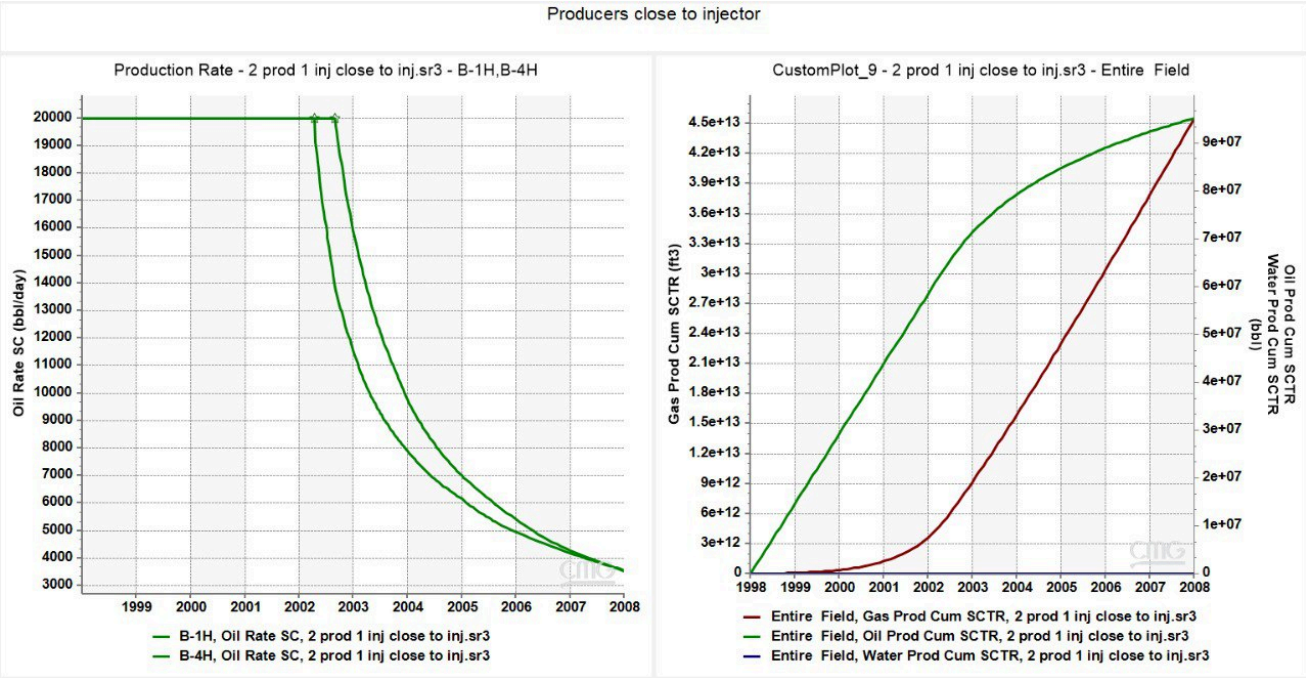

Figure 4.8.9. Production rates of case 1.

From the figure 4.8.9. it is clear that the injector being placed closer to the injector and new position of the injector is much more suitable. The production rate became to slow down and drop gradually later at 2002 rather than in the previous case at 2001.

Case 2:

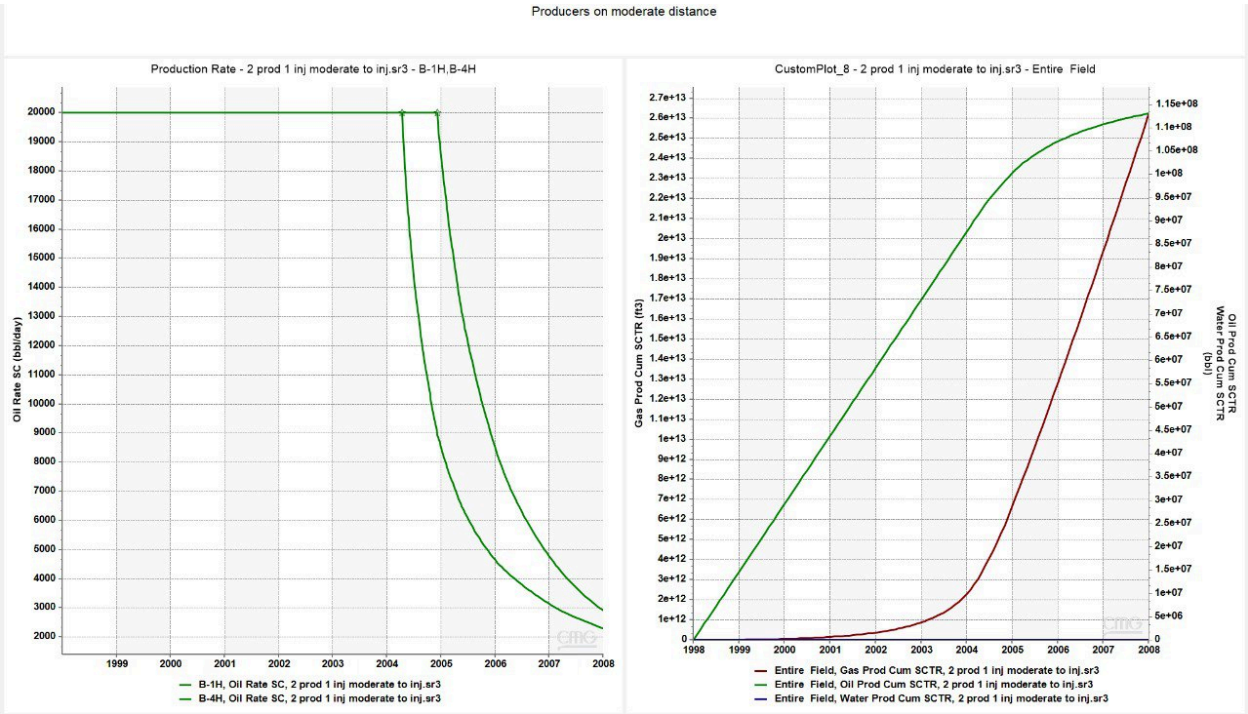

Figure 4.8.10. Production rates of case 2.

In this case, while placing the producers closer to the injector is what seems the logical decision due to the fact that the oil would be swept more accurately and would goi to the production wells faster, it can be observed from the figure 4.8.10. that with a moderate distance the production rate begins to fall off only at the year 2004 which is much later that in the case 1 (2002)

Case 3:

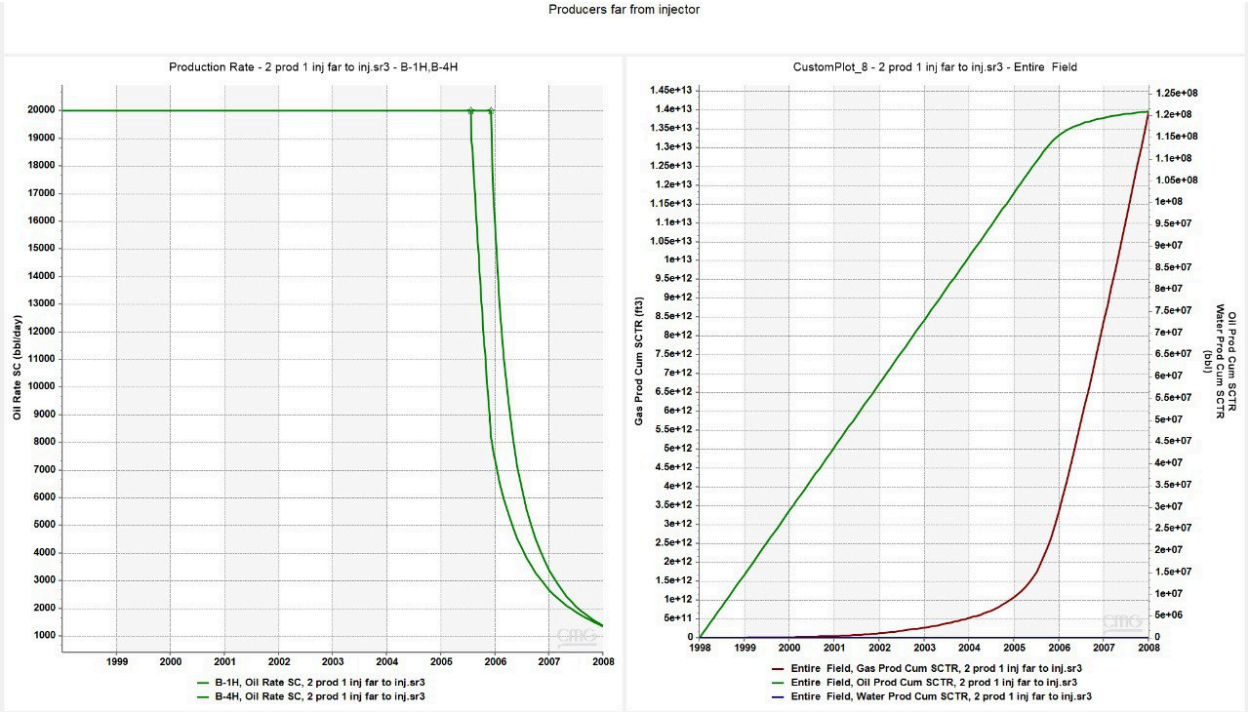

Figure 4.8.11. Production rates of case 3.

In this case, the figure 4.8.11. suggests that the producers being placed at the edges of the reservoir on an equal distance from the injector is what is considered to be the most efficient and preferable way of placing the wells. It can be seen that the gradual drop of the production rate began at mid 2005 which is much later that in both previous cases.

Conclusion:

When the injector is placed close to the producers, oil production rates decline rapidly after 2002, and cumulative oil production reaches around 90 million STB. Gas production also increases steadily but starts to plateau earlier compared to the other scenarios. In the case 2, the oil production rate decline is more steady, and cumulative oil production increases to about 115 million STB, which hints to a more balanced displacement and a much more later

gas breakthrough. When the wells are located far from the injector, cumulative oil production reaches the highest value of approximately 125 million STB. This means that a larger well spacing (case 3) leads to a more effective sweep and higher overall recovery as the cumulative plots suggest, with gas production also becoming more stable. Therefore, it is concluded that with a bigger spacing the injection and producer wells there is an improvement in oil recovery and gas breakthrough happens at a later time which makes it a more favorable decision. For further evaluation, case number 3 will be taken as a basis.

Scenario 3: Aquifer

Objective:

To study the impact of an aquifer on the reservoir.

Cases Analyzed:

The newly added well's (B-1H) perforations were changed to match the old producer well. Instead of a vertically perforated well it is now a horizontal one.

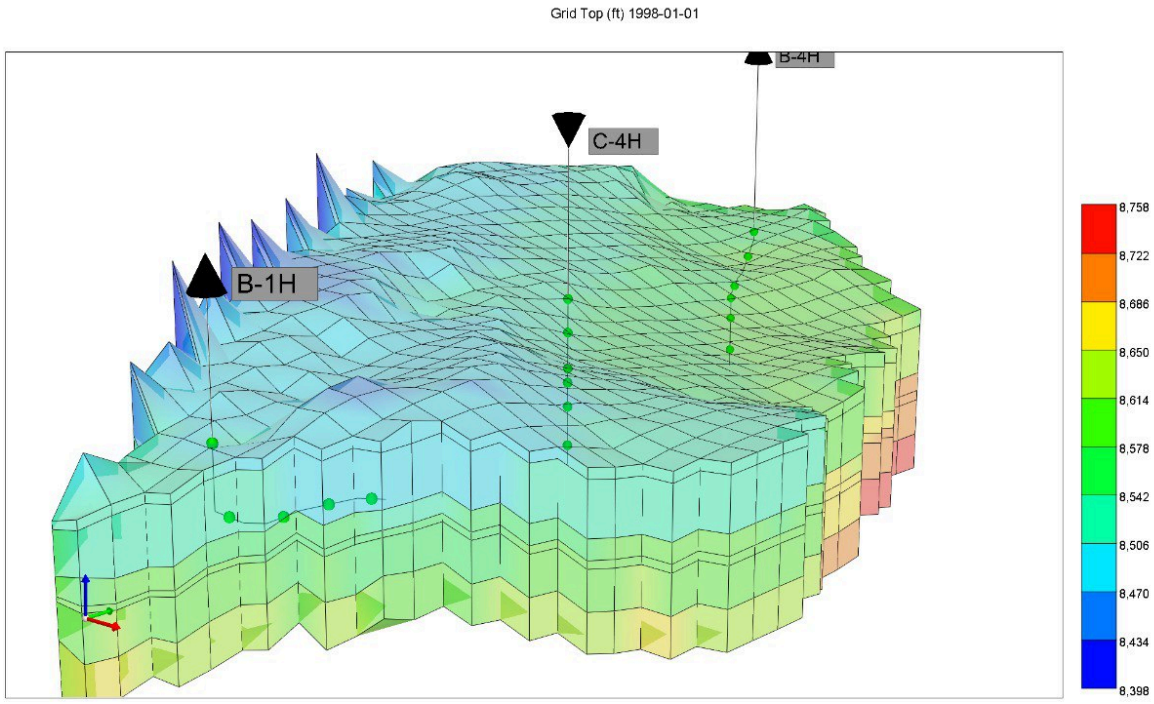

Figure 4.8.12. B-1H well's altered perforations.

Case 1: Addition of an aquifer

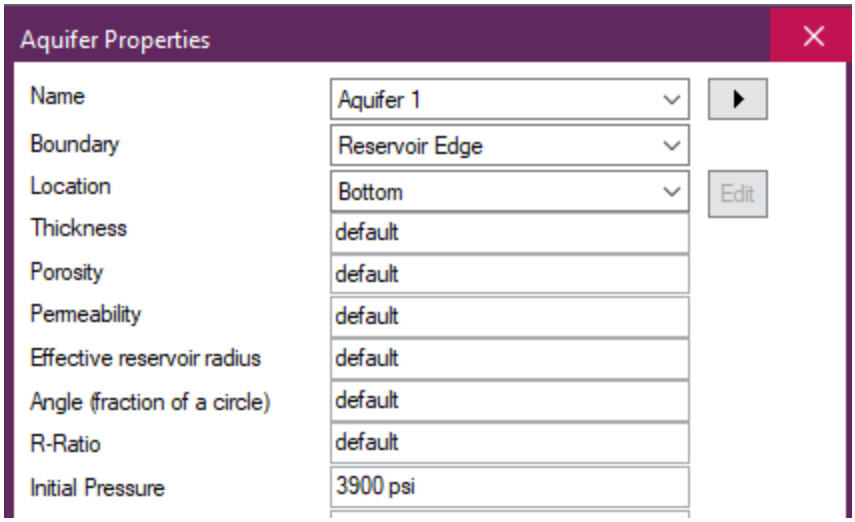

Figure 4.8.13. Aquifer properties definition.

The aquifer properties were assigned as default with an initial pressure set as 3900 psi. Location was set as Bottom and bounded to the reservoir edge. The reason behind this solution is that the real case of the Norne field, in particular the part of the reservoir that was selected for an analysis consists of a layer of water on the lower horizons. But, the rescue model was unable to transfer it properly as all the values were assigned randomly due to the lack of data, so the aquifer was set as located at the bottom of the reservoir.

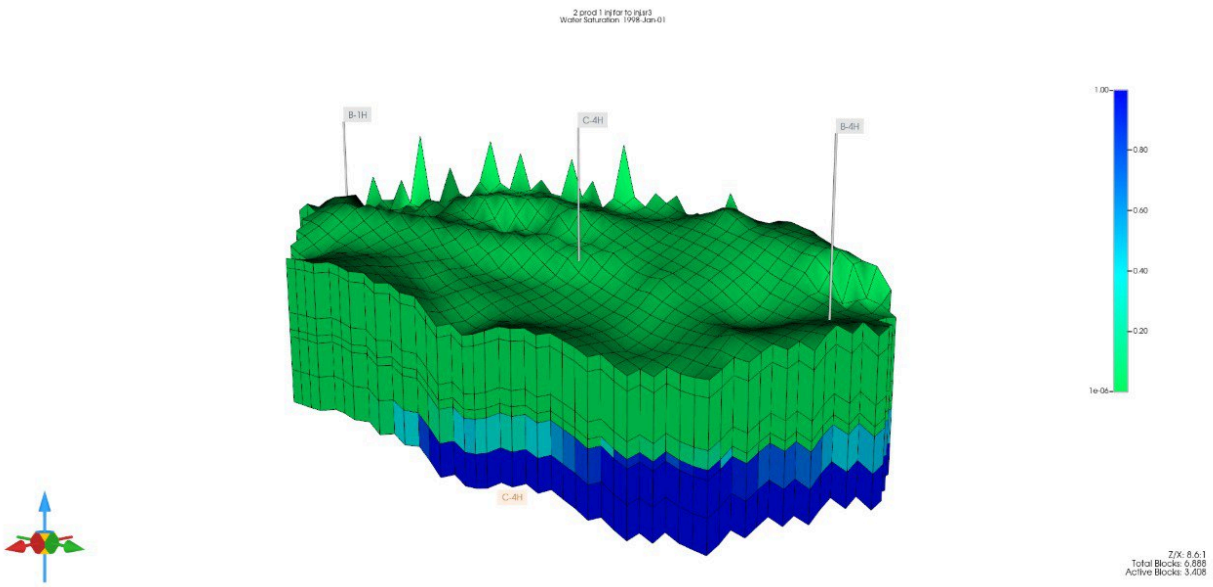

Figure 4.8.14. Water saturation of the field.

According to the figure 4.8.14. the position of an aquifer can be observed. It is located closer to the well B-4H.

Outcomes:

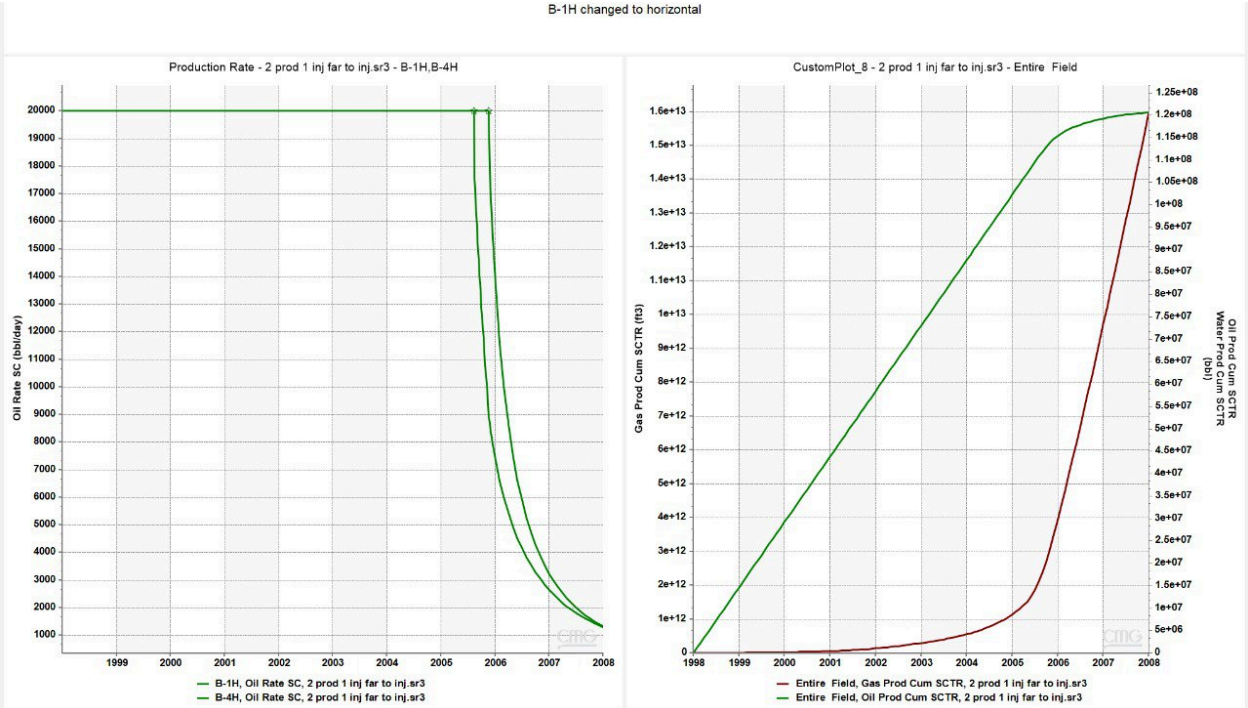

Figure 4.8.15. B-1H well's production rates with new perforations.

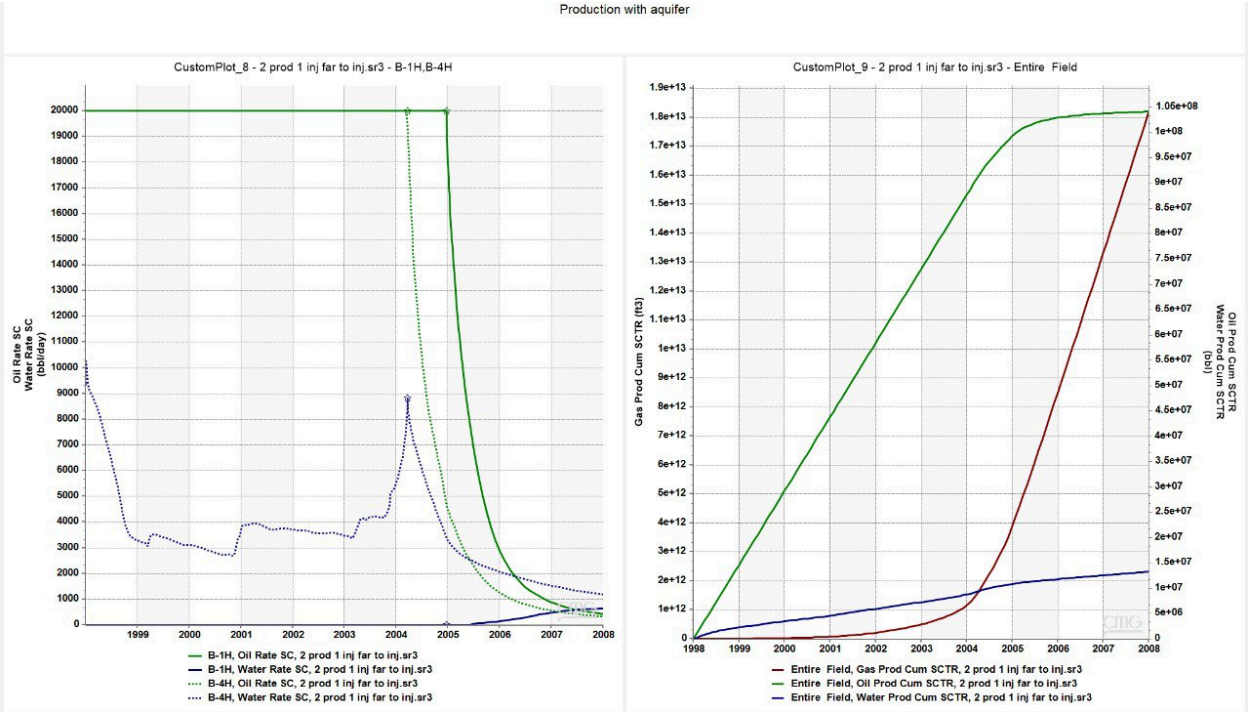

Figure 4.8.16. Production rates with an aquifer.

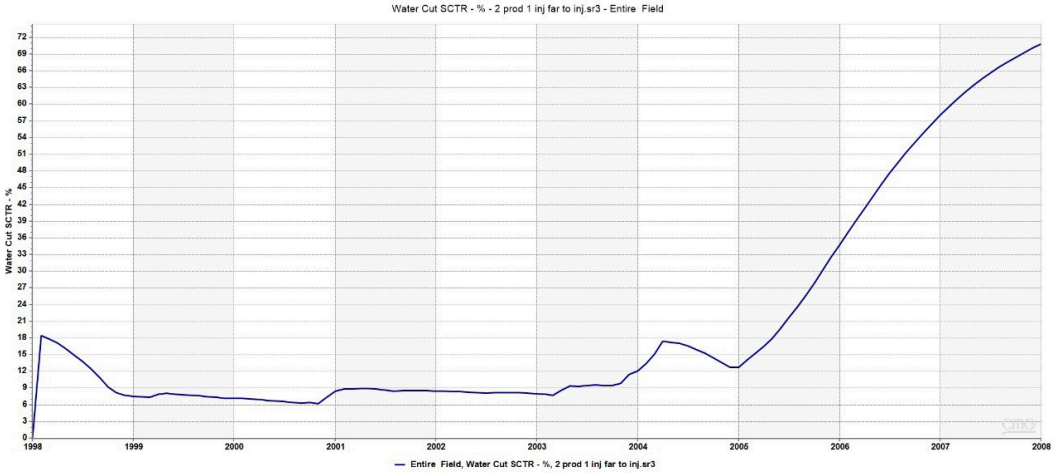

Figure 4.8.17. Water cut with an aquifer.

After adding the aquifer, from the figure 4.8.17. it is clear that the production rates were corrected as well as the water saturation rises, the water cut is also now present and affects how the reservoir is behaving. First of all, the pressure distribution became more stable as it can be seen from the gas to oil cumulative production curves (smoother). Second of all, The water cut became more stable as well. It rose to an adequate level and kept almost constant until the water breakthrough in 2006.

In the version with no aquifer the natural pressure drive was too low and it was needed to pump the reservoir with injectors at the very beginning to recover oil at all. With an addition of an aquifer it is safe to assume that the drive at the beginning is now capable to overcome that and start the production without an injection at first.

Also, while the production rate for one of the wells dropped down, the cumulative oil production also decreased from 1.2*10^8 bbl to approximately 1.05*10^8 bbl. Even though this indicates that less amount of oil is recovered, it is more reasonable to assume that this case is representative of a more real scenario. Showing how the presence of water source disturbs the total recoverable amount of oil while still keeping the pressure profile of the whole reservoir more in tact.

Conclusion:

As far as the outcomes go it is indeed the position of an aquifer that play a crucial role. At this point, the location of the aquifer is set to reservoir edge, but, even though the edge is set to bottom, the lower layers of the reservoir in our scope are not flat, which makes it difficult to spread it evenly. Also, a big impact is made by the water oil contact. We had to account for the fact that the model is only a part of the whole reservoir, so the water oil contact was set to 8700 instead of 8800 which is the real value that was obtained by our reservoir engineer Arlan. This water oil contact, correlating with the depth of our chosen layers of the reservoir in question, allowed us to create the closest possible model of the aquifer. Newly added aquifer is not only a water source but a great initial drive mechanism which helped to maintain better pressure profiles and make the production more stable.

Scenario 4: Water injection

Objective

To study the effect of a water injection

Cases Analyzed:

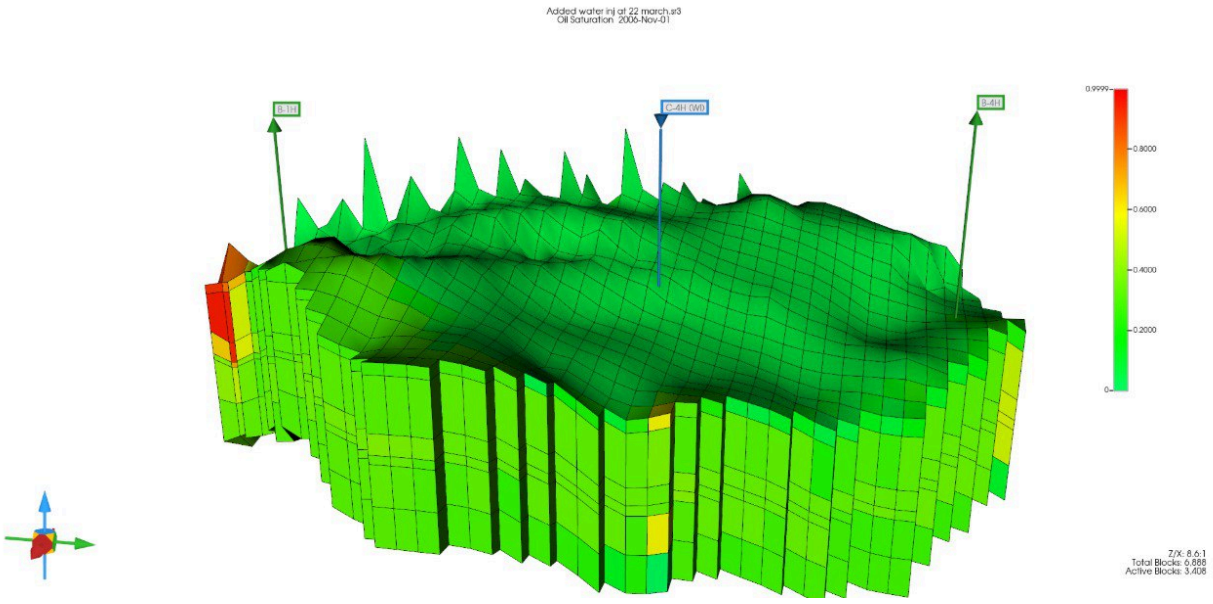

Figure 4.8.18. Water injector well's location.

On the figure 4.8.18. we can see the location of that well. Because there was no way to inject to different fluids from the same injection well it was designed so that the newly defined well had the exact same perforations and locations, but was never defined before the gas injection ended. So the definition of that well became only after 2004, March 22nd. This was done to support an economically viable claim that it would be invaluable to put another injection well rather than just changing the injection fluid type. So, with all that said, this newly defined injection well can be regarded as the exact same well.

Outcomes:

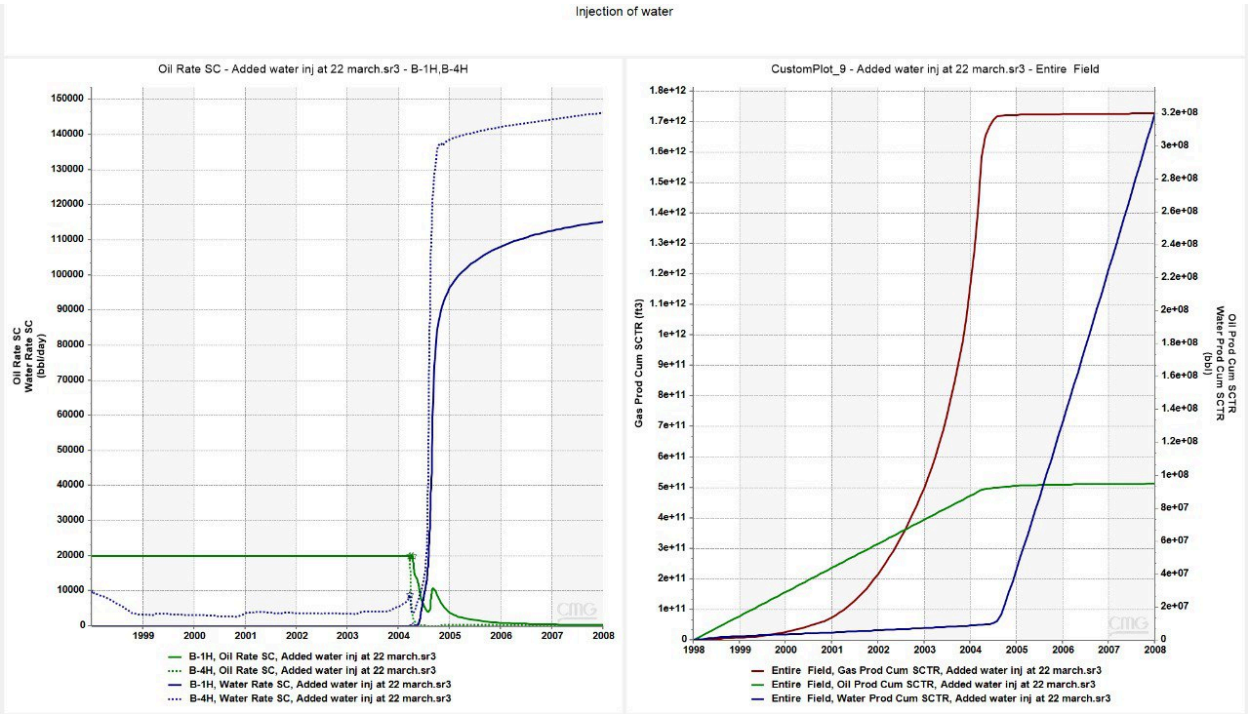

Figure 4.8.19. Production rates with water injection.

Wells B-4H and B-1H are analysed on the figure 4.8.19. and the overall field behavior is also looked at. Water injection started on 22 March, 2004, and its impact is visible in the production trends for the whole simulation period from start to finish. In the left plot, which shows the oil and water production rates for wells B-1H and B-4H, it is clear that water injection resulted in a steep increase in oil output. Before the year 2004, the oil production from both wells remained almost constant at approximately 20000 barrels per day. But right after the start of water injection, it increased slightly and then went down for the well B-4H and there was a complete water breakthrough at the well B-1H which Regarding water production, there is a sharp increase in both wells. Before the water injection, water production was almost negligible due to the specification of our simulation which is directly affected by the fact that the part with only oil was extracted from the whole reservoir. After injection, B-4H began producing water at rates exceeding 140000 barrels per day which is an extreme value, meaning a potential water breakthrough might be happening at that time stamp. This suggests a trade-off between enhanced oil recovery and the onset of excessive water production, which may lead to challenges related to water handling and separation. Water production of the well B-1H is exceeding 100000 barrels per day. This range is

connected to the fact that the aquifer is much closer to B-4H. The conclusion that is made here is that well placement should be analysed and be regarded with the aquifer present. Well spacing is directly affected by the presence and location of an aquifer. As we can see from the graphs, the oil rate of the well B-4H drops significantly because it is very close to the position of the aquifer, and that is why the water breakthrough happens too soon which also lowers down the cumulative water production.

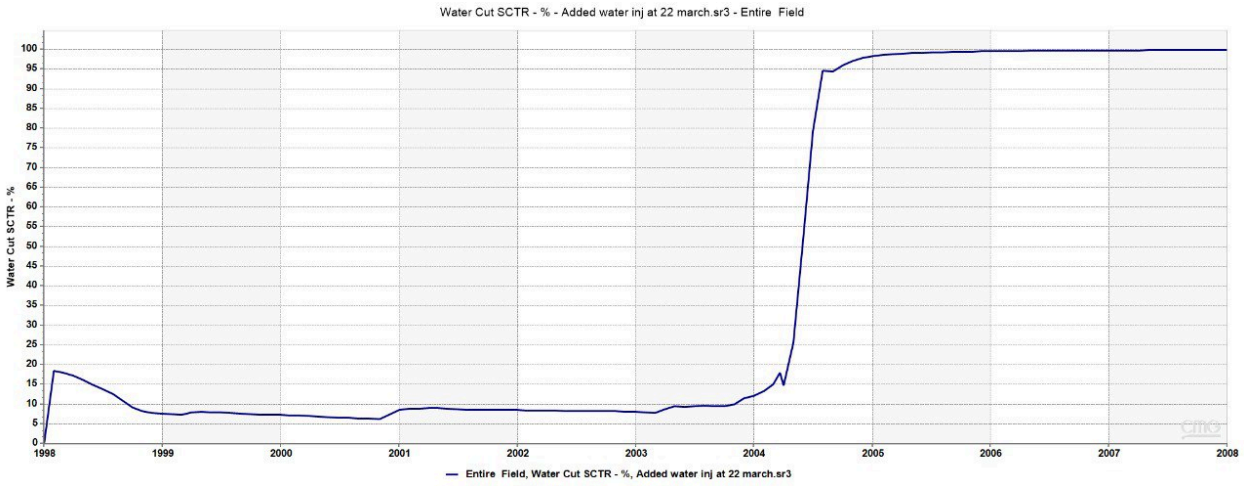

Figure 4.8.20. Water cut with a water injection.

Conclusion:

To conclude, initial gas injection was done as a base model due to the fact that the real field had an excess gas production in the beginning. Accounting for the whole reservoir, the thick layer of gas, which was not taken into consideration in the dynamic model, was reinjected back into the reservoir. This process was done until the moment gas prodctuin was not exceding and that time stamp is approximated to year 2004. After that, it is only logical to stop the gas injection and try to water flood the reservoir. Additionally, it is not economically feasible to insert a completely new well to inject another type of fluid, and even though it is not possible in the CMG to stop injection of a certain fluid at a specific time and start

injecting another one, the case was analysis as if the same well is both a gas injector in the beginning and a water injector at the end. The biggest conclusion to make was that according to the sudden production rate drop to almost zero of the well B-4H, which is located right above the aquifer, the water breakthrough happens to soon. So, it is now clear that the wells' placement should be optimized with accordance of the position of the aquifer. As it is important to control such sudden water outbursts. In addition to that point, the water injection rates should also be controlled. Only setting the BHP operating constraint for the water injection well is not accurate as it is essential to also control the amount of water that is pumped in.

Key Features and Usefulness

The sensitivity analysis was done not only to evaluate the impact of each variable but also to try and improve the oil recovery of the field, as well as to study and examine the possible scenarios and how to overcome different issues that might come up during the field life. During the whole procedure it was necessary to make some adjustments to match the real field case as much as possible. But it is worth mentioning that some of the limitations were in the way of making a one hundred percent decision on some of the factors affecting the reservoir. Nonetheless, it is most certainly the most accurate and precise sensitivity analysis that could have been done in the case of Norne field.

4.2.4. Phase Behavior Analysis using WinProp model:

Objective:

To do a phase behavior analysis using software.

Methodology:

It is worth mentioning that oil composition is used while modelling reservoir in STARS simulator. However, since we were dealing with insufficient data IMEX was our choice. Imex does not require any compositional parameters, but was asking whether we invistigate blackoil, lightoil or gas reservoir

No. of components: 14 Constant Volume Shift

No.	Component	HC	Pc (Atm)	Tc (Deg. K)	Acentric fact.	MW	Vol. Shift	V Shift Coef1 (1/deg C)
1	N2	0	33.5	126.2	0.04	28.013	0	0
2	CO2	3	72.8	304.2	0.225	44.01	0	0
3	CH4	1	45.4	190.6	0.008	16.043	0	0
4	C2H6	1	48.2	305.4	0.098	30.07	0	0
5	C3H8	1	41.9	369.8	0.152	44.097	0	0
6	IC4	1	36	408.1	0.176	58.124	0	0
7	NC4	1	37.5	425.2	0.193	58.124	0	0
8	IC5	1	33.4	460.4	0.227	72.151	0	0
9	NC5	1	33.3	469.6	0.251	72.151	0	0
10	FC6	1	32.46	507.5	0.27504	86	0	0
11	FC7	1	30.970000493...	543.2	0.308301	96	0	0
12	FC8	1	29.12	570.5	0.351327	107	0	0
13	FC9	1	26.94	598.5	0.390781	121	0	0
14	FC10	1	25.010000493...	622.1	0.443774	134	0	0

Figure 4.9.1. Component Selection/Properties of the Norne field.

Component	Primary
N2	0.32
CO2	0.69
CH4	43.9
C2H6	3.96
C3H8	2.18
IC4	0.47
NC4	0.93
IC5	0.44
NC5	0.48
FC6	0.88
FC7	2.55
FC8	4.16
FC9	3.08
FC10	35.96
Sum	100

Figure 4.9.2. Component Composition of the Norne field.

The reservoir fluid is composed of light hydrocarbons, heavy fractions, and trace amounts of non-hydrocarbon gases. The main components are methane (43.9 percent), ethane (3.96 percent), and propane (2.18 percent). Heavy hydrocarbons account for 47.58 percent of the composition, indicating that heavy components are present in large numbers. Non-hydrocarbon gases, such as nitrogen (0.32 percent) and carbon dioxide (0.69 percent), are present in trace levels.

The critical properties of fundamental components show that methane has a critical pressure of 4.54 MPa and a critical temperature of 190.6 K. Heavy fractions, such as C9-C10, with critical pressures ranging from 26.94 to 25.01 MPa and critical temperatures more than 600 K. Heavy hydrocarbons increase the risk of condensate banking, while low concentrations of non-hydrocarbon gases reduce concerns about CO_2 corrosion and nitrogen dilution.

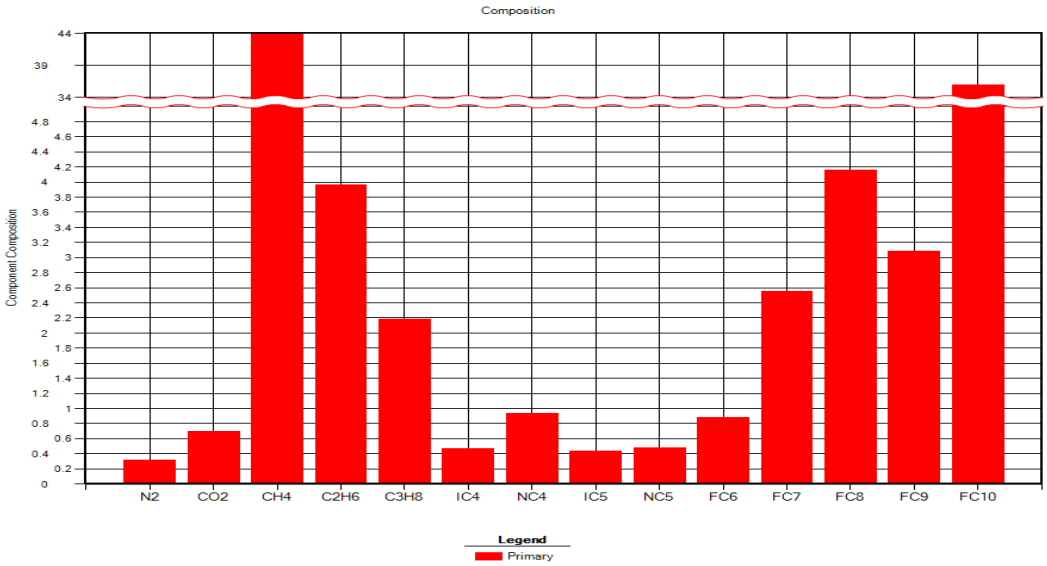

Figure 4.9.3. Composition plot.

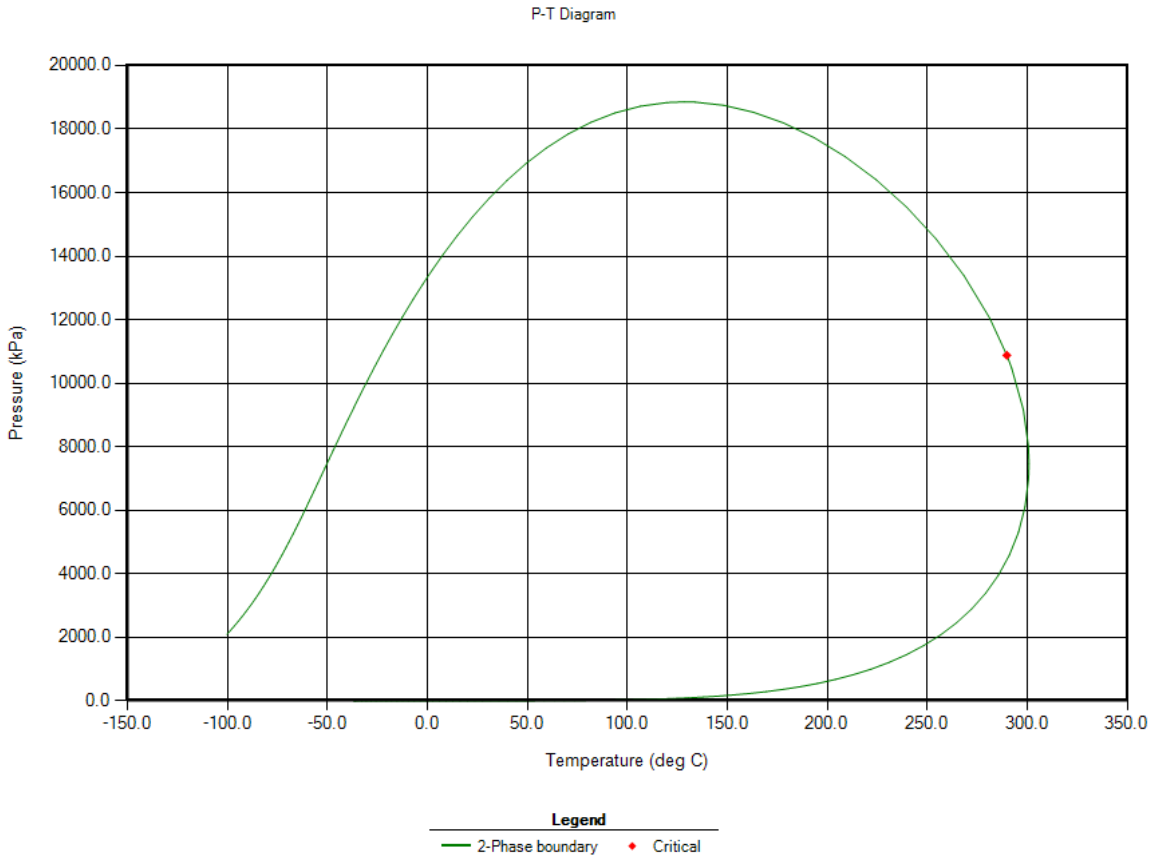

Figure 4.9.4. 2-Phase boundary P-T Diagram.

The pressure-temperature phase diagram shows a dome-shaped two-phase area with a critical point about 290 degrees Celsius and 10.88 MPa. The bubble point pressure at 100 degrees Celsius is 18.63 MPa (2650 psi, 189 bar) which well corresponds with the bubble point pressure obtained from the Petrel software's Pressure vs Depth graphs. Suggesting gas evolution as pressure drops below this level. The dew point at 15.5 degrees Celsius and 101.35 kPa causes a substantial phase split, with 52.3% moving to the vapor phase. At reservoir temperatures of around 120 degrees Celsius and 22.5 MPa, the fluid remains a single-phase, undersaturated liquid.

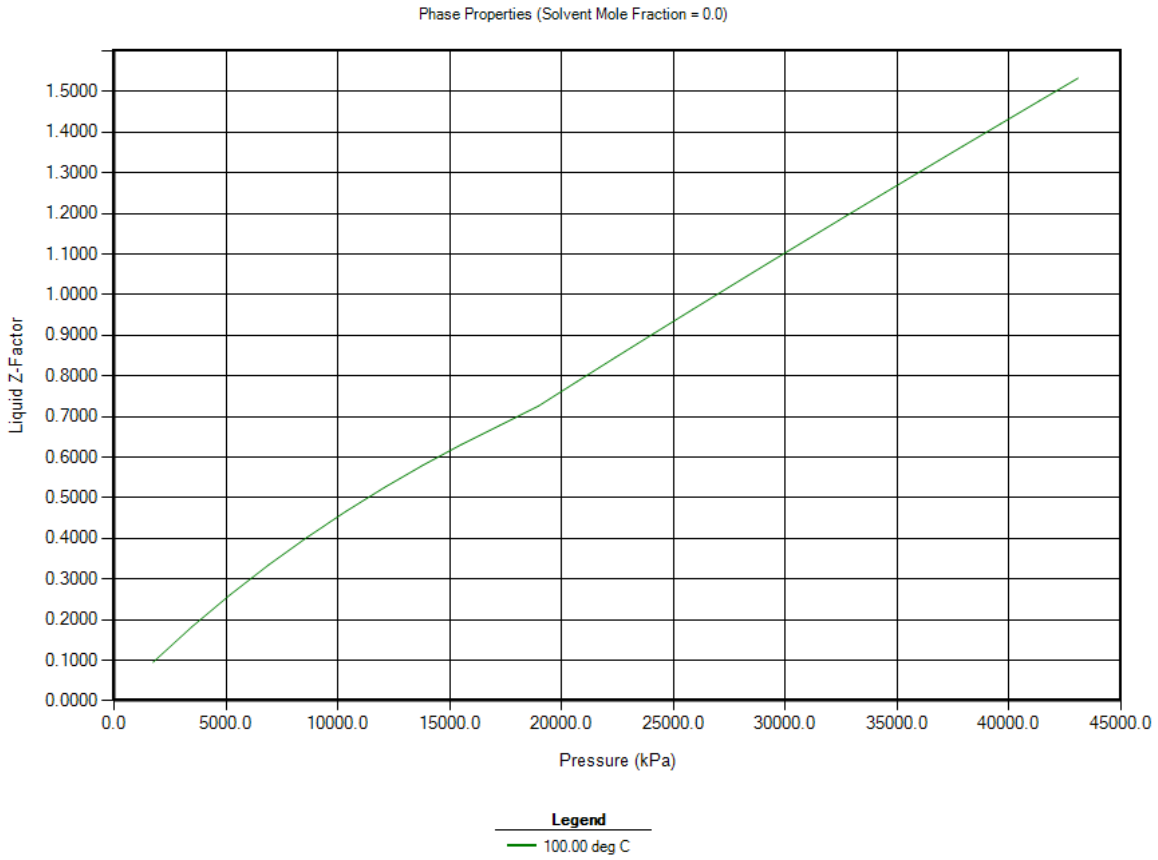

Figure 4.9.5. Phase Properties. Liquid Z-Factor.

When the pressure is low, the Z-factor value is less than 1.0, showing that the fluid behaves like a thick liquid with low compressibility. When the pressure increases, the z-factor increases as well, and the compressibility increases correspondingly. This trend indicates that the fluid expands when pressure is dropped. At pressures of 20,000 kPa, the Z-factor approaches roughly 0.7, which corresponds with the values found in volatile oil reservoirs. As the pressure rises above this range, the Z-factor approaches and exceeds 1.0, indicating a change to a more compressible phase, possibly reaching supercritical behavior at extremely high pressures.

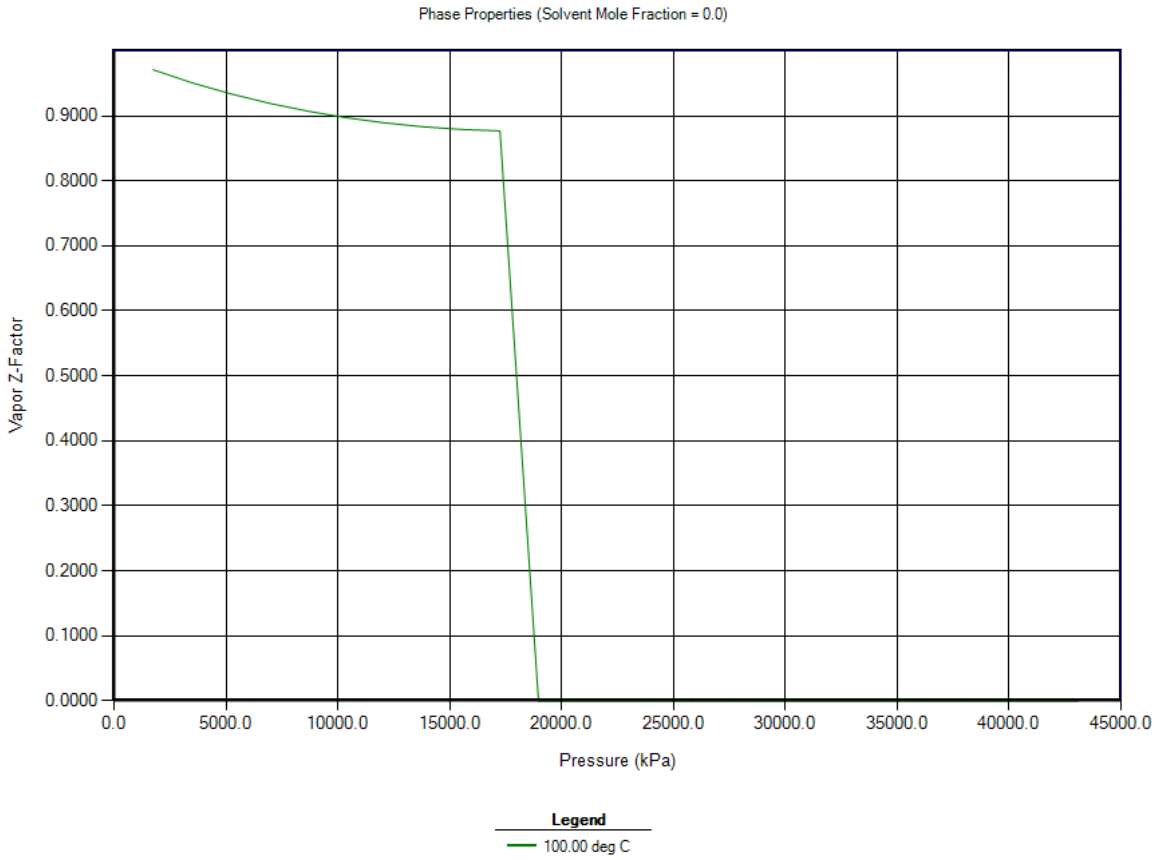

Figure 4.9.6. Phase Properties. Vapor Z-Factor.

At low pressures, the vapor Z-factor is close to 0.9, indicating that the gas phase behaves as an ideal gas with minimal deviations from the standard conditions. As pressure increases, the Z-factor gradually decreases, suggesting reduced gas expansibility. Around 18,000 to 20,000 kPa, the Z-factor goes quickly to zero. This sharp fall decline shows that the gas phase is approaching condensation and will change into the liquid phase. At higher pressures, the gas phase is no longer present, indicating that the system has completely transitioned to a liquid state. Large drop in the Z-factor at higher pressures highlights the importance of maintaining pressures above this critical range to avoid excessive gas-liquid phase transition losses.

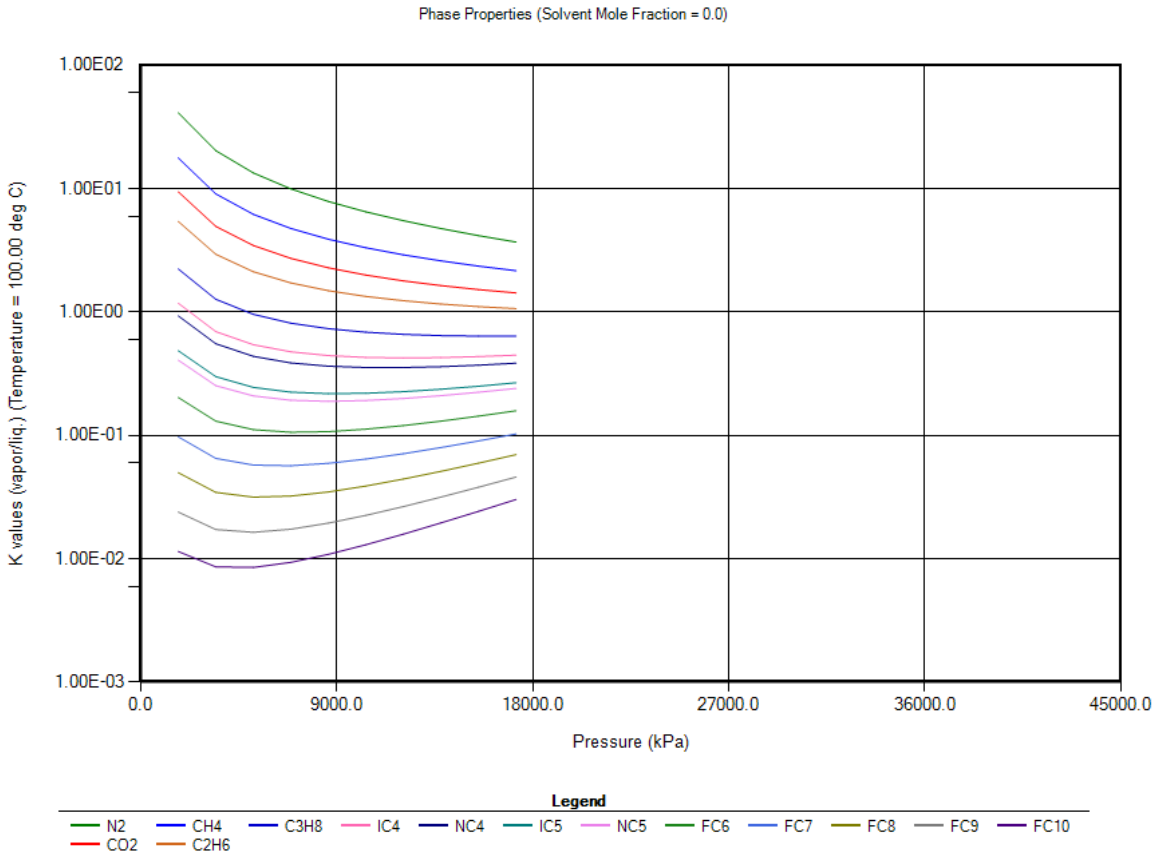

Figure 4.9.7. Phase Properties. K values (vapor/liq.).

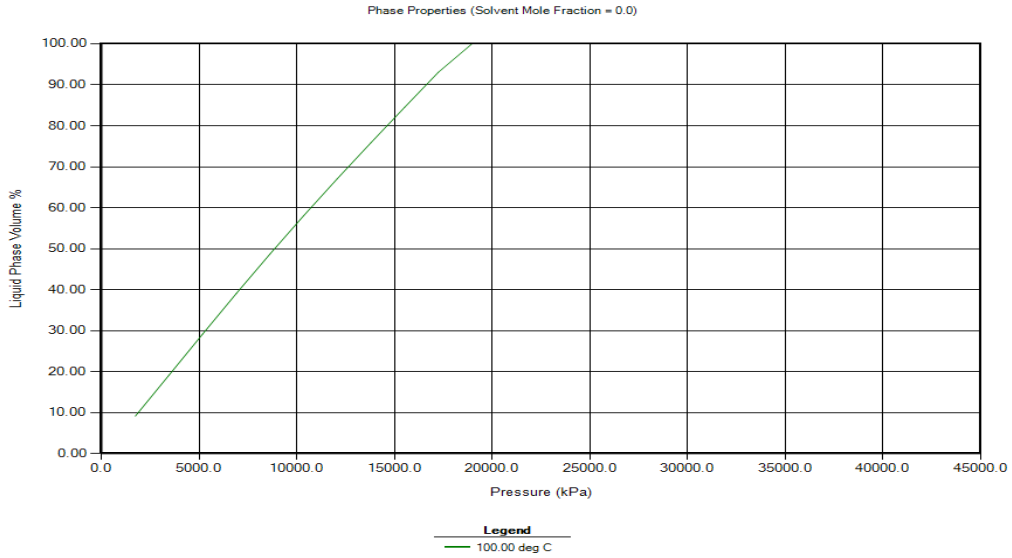

Figure 4.9.8. Phase Properties. Liquid Phase Volume.

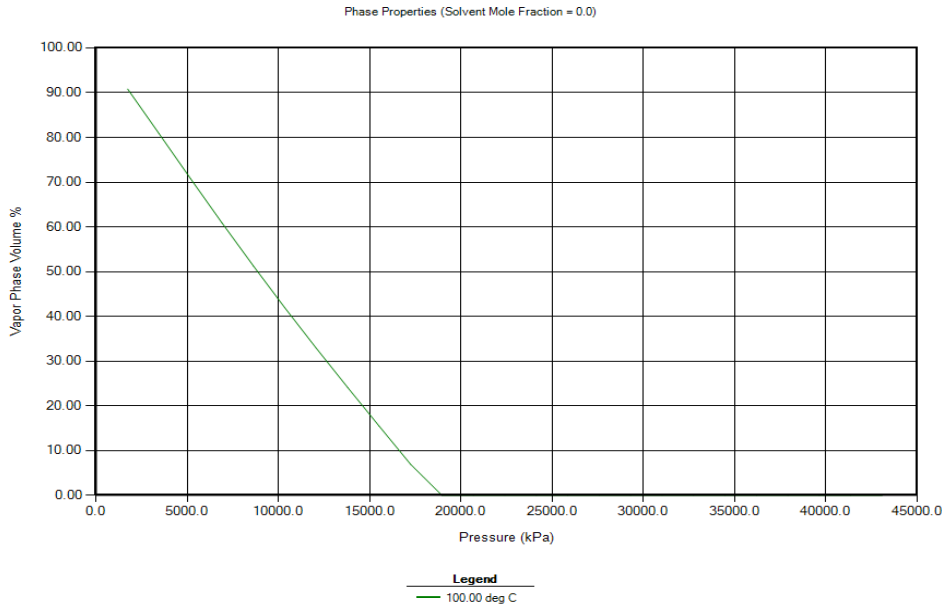

Figure 4.9.9. Phase Properties. Vapor Phase Volume.

Recommendations for an EOR

One of the main difficulties in the Norne Field, from the WinProp software, is gas liberation at lower pressures, which can lead to retrograde condensation in the reservoir and wellbore. This can lead to dropout in production tubing and surface facilities. Furthermore, the fluid's high methane content can cause foamy oil state, reducing efficiency of separation and causing operational issues in processing. Another key challenge is the existence of heavy hydrocarbons, notably the C9-C10 fractions, which are more likely to precipitate under reservoir conditions. These heavy fractions may cause wax and asphaltene precipitations, which can clog flow channels, limit permeability, and lower production rates One of the main takeaways that the software helped to understand is that it is crucial for the Norne Field to Ensure adequate flow So that is why enhanced oil recovery (EOR) techniques need to be implemented. All the obtained and analyzed data using WinProp software suggests that Gas reinjection should be considered as the main EOR strategy because it would significantly help to maintain reservoir pressure, not to mention the fact the the Norne Field production consists of not only oil but gas as well, which may be efficiently used to improve oil mobility, enhance swelling, and lower viscosity.

Water alternating gas (WAG) injection is also a very suitable technique to maximize sweep efficiency and control mobility. This method involves alternating water and gas injections to maintain pressure while enhancing contact with the reservoir fluids. Nitrogen or lean gas injection can also be considered to sustain reservoir pressure and optimize displacement efficiency. Other EOR techniques like steam, surfactant or polymer floodings are rather unlikely to be implemented because they are not particularly well suited for a “gas” related problems in the production.

Chapter 5. Upstream Processing

5.1.1 Drilling and Completion

Methodology

The methodology that has been used for the well completion and drilling part in the Norne Field is based on an extensive review of technical papers, literature, field data review and analysis. The steps are as follows:

Data Gathering Methods

1. **Literature Review:**

Publicly available reports, scientific papers, and field development studies were collected relevant to the Norne Field. These papers summarized information for geological, petrophysical, and reservoir characteristics. Key sources include the following publications: "The Norne Field Development" and "The Norne Field - Exploitation Strategies."

2. **Field Development Reports:**

Technical reports from operators such as Factpages were reviewed to gain insight into well construction strategies, completion designs, and drilling methodologies specifically for the Norne Field. Those papers include information related to rig selection, cement circulation equipment, well schematics as well as the leak off test data for them.

Field Overview and Well Characteristics

The history of the Norne field begins in 1991 in the offshore region of the Norwegian coastal area. It consists of reservoirs that contain oil and gas columns of the Lower to Middle Jurassic age. At the depth of around 2,525 meters into the reservoir a flat horst block can be observed (John A. 1995). There are three key formations that are rich in hydrocarbon content. Namely they are the Ile and Tofte formations that contain oil, and the Garn formation with gas. The reservoir displays excellent permeability in the range between 100 to 2,500 millidarcies (md). Such values indicate high conductivity which makes it suitable for horizontal drilling which enables efficient hydrocarbon drainage.

Well Construction Strategy

In the production of Norne wells, the well structure was planned and designed in such a way as to enhance recovery while minimizing gas and water breakthrough concerns. As part of the field's first phase development proposal, there were twenty wells suggested among which were two gas injectors, seven water injectors and eleven production wells. This was later optimized to 14 development wells based on reservoir performance studies, consisting of 7 production wells, 5 water injection wells, and 2 gas injectors (Helge M. et al. 1995).

One of the crucial steps in the well development plan was to switch from deviated wells to horizontal ones. This decision allowed the project to achieve several benefits. Namely, the life of wells was prolonged due to the inhibition of gas and water breakthroughs which in return resulted in increased production. The horizontal sections varied in length, with production wells extending up to 1,200 meters and gas injectors between 200 and 500 meters (Helge M. et al. 1995). This procedure allowed to decrease the number of wells but more importantly it brought 6,000 barrels of additional oil from each well. Besides, the cost and complexity of the project further decreased due to commingling production from two wells into a single flowline. This helped to minimize flowline installations (John A. 1995).

Drilling Techniques:

- Extended Reach Drilling (ERD): The ERD techniques have been applicable in reaching distant parts of the reservoir from a solitary platform site. By horizontally increasing the well orientation, the reach of the Norne field allows for constructing fewer platforms, hence reducing costs and impact on the environment. ERD allows greater access to reservoir zones without new surface locations.
- Managed Pressure Drilling: MPD technology helps in controlling downhole pressure precisely, which is especially useful in mitigating damage and maintaining stability, which reduces nonproductive time and the possibility of kicks or losses.

Casing and Liner Design:

- Two types of wellbore construction 'liner' and 'casing' borehole construction methods which are antithetic to the geomechanical characteristics of the field are used in the

construction of Norne wells. For the purposes of resisting the reservoir pressures and preventing inflatable collapse of the well, high strength steel formation casing pipes are used.

- In certain instances, anti-corrosion liners may also be fitted because of the potential damage to the well integrity by the presence of corrosive oil fluids. Throughout a well's life span, with appropriate selection of casing and liner materials, changes in temperature and pressure can be withstood without compromising safety and allowing for stability in operation.

Completion Design

Brechan and Sangesland (2019) claim that the completion technique was focused on preserving well integrity while making adjustments for the production environment. The necessity to make future well workovers easier led to the adoption of a 7-inch monobore system as the general completion arrangement for Norne. The use of horizontal Christmas trees, rather than conventional systems, provided significant time savings during completion operations and supported high production rates (John A. 1995).

Completion design in the Norne field was also focused on delaying the breakthrough of gas from the gas cap and water from the water injection zones. Water injectors were placed in the Tilje formation at the lower sections to prevent sulfate scaling and reservoir souring caused by extensive seawater circulation (Helge M. et al. 1995). Gas injectors, placed in the upper Garn formation, were positioned to maximize injectivity while maintaining an optimal distance from the production wells, mitigating the risk of early gas breakthrough (Helge M. et al. 1995). It was envisioned that these completion strategies would be further optimized during field operations, through ongoing reservoir data that would inform future interventions.

Multilateral Wells: According to John (1995), Norne had extensively applied the multilateral completions where a single main wellbore has many branches extending into the reservoir. This is to get maximum reservoir contact, which becomes valuable in fields like Norne, where reservoir heterogeneity would minimize drainage in such simpler designs.

Intelligent Well Completions: Our team customized well for both vertical and horizontal directions. These wells will be of an intelligent completion, therefore providing the facility for real-time monitoring and control. Downhole sensors monitor pressure and flow rates, enabling selective zone management, which will enhance production (Brechan and Sangesland, 2019). It is an essential technique in controlling the variance of pressure and permeability within the reservoir because it provides variable flow adjustments based on real-time data.

Application of AI in Well Completion and Drilling

For the Norne Field, AI can further improve well design and operational efficiency. For instance, digital twins-a virtual model of the reservoir and all the structure on it-enable predictive analytics for optimizing completion designs and monitoring well integrity, which will be discussed in length down the report (Wanasinghe, 2020). AI applications also extend to real-time decision-making processes in MPD operations for preventing the formation damage and loss of well stability. The integration of AI applications provides better precision of operations, reduces non-productive time, and allows for proactive management of various technical problems associated with sand control and decline in reservoir pressure.

5.1.2 Rig Type Selection

For the Norne Field, which has water depths ranging between 2500 to 2700 meters, Semi-submersibles and Drillships are the most viable options. Semi-submersibles provide better stability, while Drillships offer greater mobility and deeper drilling capabilities.

Rig Sizing & Capacity

Since the Norne Field is a deepwater field, the rig must be capable of operating in significant water depths. A semi-submersible rig or drillship is the best choice, as both can handle deepwater conditions effectively. Estimated water depth in the Norne Field: 380 m (1,247 ft). The rig should be rated for at least 500 m (1,640 ft) to provide operational flexibility.

The TVD for the Norne Field wells is around 8,200 ft. The selected rig must have a drilling depth capability exceeding 10,000 ft to accommodate potential sidetracks or deeper formations.

Environmental & Site Preparation

The Norwegian Sea experiences harsh weather conditions, including strong winds and high waves. Typical wave height: 5–7 meters (16–23 feet). Wind speeds: 20–30 knots during storms.

Requirements for the rig's smooth operation:

- A rig with high heave compensation capabilities.
- Weather-resistant mooring and anchoring systems.
- Emergency disconnect features for quick evacuation in extreme conditions.

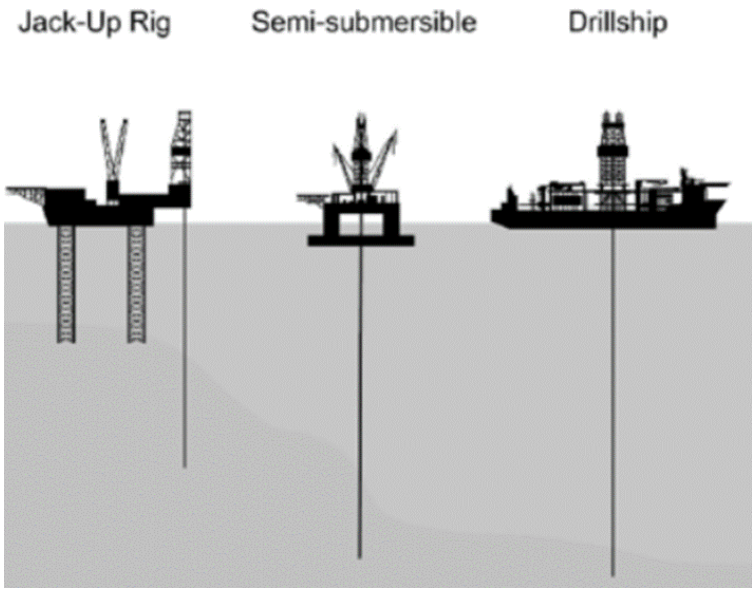

Figure 5.1.1. Rig types

For this project semi-submersible rigs and drillships are the most suitable options. Semi-submersible rigs offer high stability in rough seas by using partially submerged

pontoons and dynamic positioning systems. They are ideal for deep-water drilling and can withstand harsh environmental conditions. Drillships, on the other hand, provide higher mobility and are equipped with advanced dynamic positioning systems to maintain their location over the well. Given the deep-water conditions and expected drilling challenges, a semi-submersible rig will be chosen for this project due to its stability and operational efficiency.

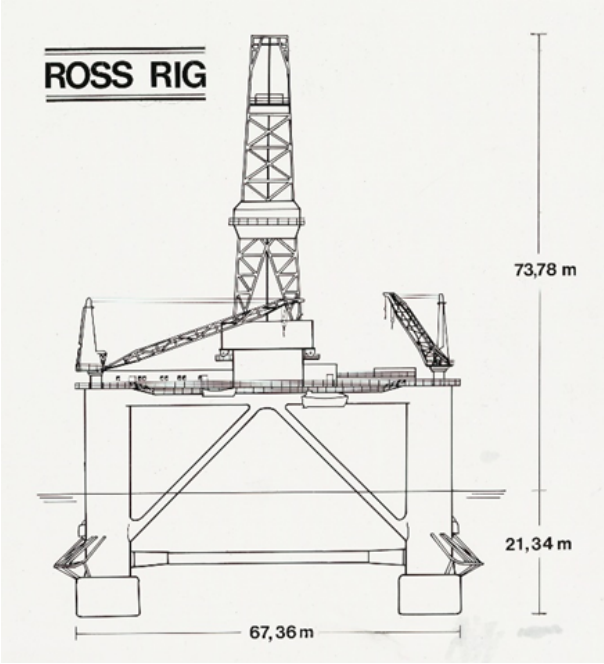

Figure 5.1.2. Ross Rig (https://equinor.industriminne.no/rigget-for-suksess-ross-rig)

5.1.3 Cement Circulation

Cementing is critical for well integrity, ensuring zonal isolation, casing support, and formation stability. The process involves pumping cement slurry down the casing and up the annulus, creating a barrier to prevent fluid migration between formations. Proper cement circulation prevents well control issues such as gas or water influx, reduces casing corrosion, and enhances structural stability. In offshore environments, cementing is even more crucial due to high hydrostatic pressures and corrosive seawater exposure. The cement job must be

properly designed, with centralizers ensuring uniform placement and testing conducted to verify proper bonding.

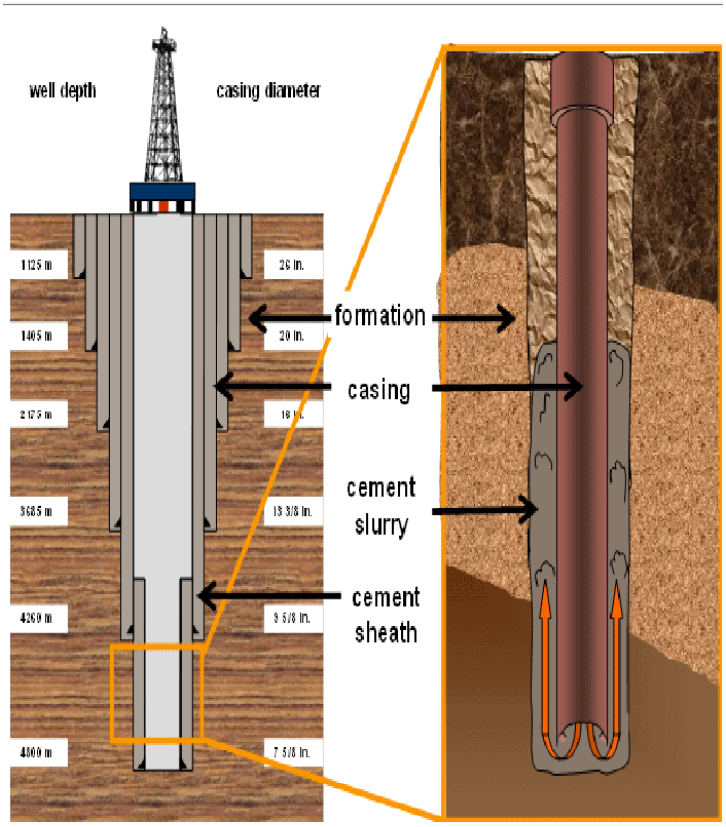

Figure 5.1.3. Wellbore Cementing

(https://www.drillingcourse.com/2015/12/introduction-to-cementing.html)

5.1.4 Completion Type Selection

For this capstone project, a cased-hole completion is selected due to the field's sand production issues. This completion method involves running production casing and cementing it in place, followed by perforation to connect the reservoir to the wellbore. The cased-hole completion provides well control, reduces formation damage, and offers flexibility for sand control measures (Andrews et al., 2008). It also allows for better zonal isolation and selective production. Given the reservoir conditions and sand production concerns, this method is the most effective and reliable.

The following two images represent the Seabed and Wellbore schematics for one of our wells in the Segment C.

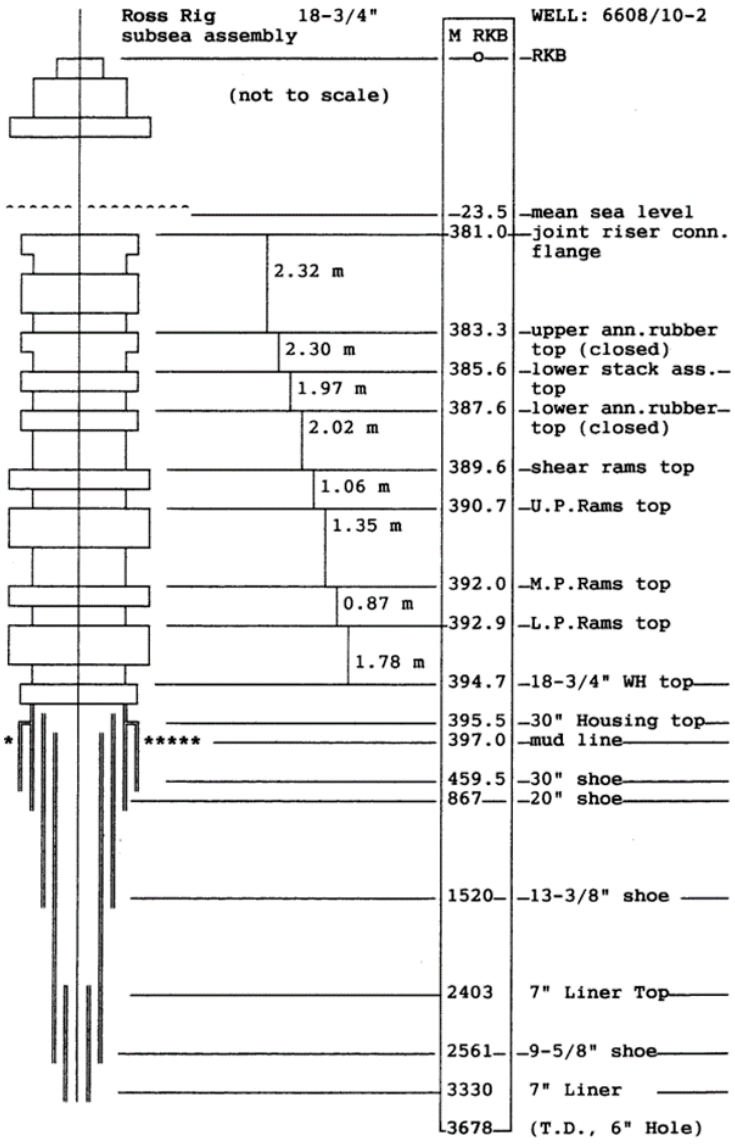

Figure 5.1.4. Subsea schematic 6608/10-02

Table 5.1.1. Leak Off test results for Well 6608/10-2

Casing type	Casing diam.[inch]	Casing depth [m]	Hole diam. [inch]	Hole depth [m]	LOT/FIT mud eqv. [g/cm3]	Formation test type
CONDUCTOR	30	459.0	36	460.0	0.00	LOT
INTERM.	20	867.0	26	870.0	1.41	LOT
INTERM.	13 ⅜	1520.0	17 ½	1522.0	1.86	LOT
INTERM	9 ⅝	2561.0	12 ¼	2564.0	1.95	LOT
LINER	7	3330.0	8 ½	3678.0	1.82	LOT

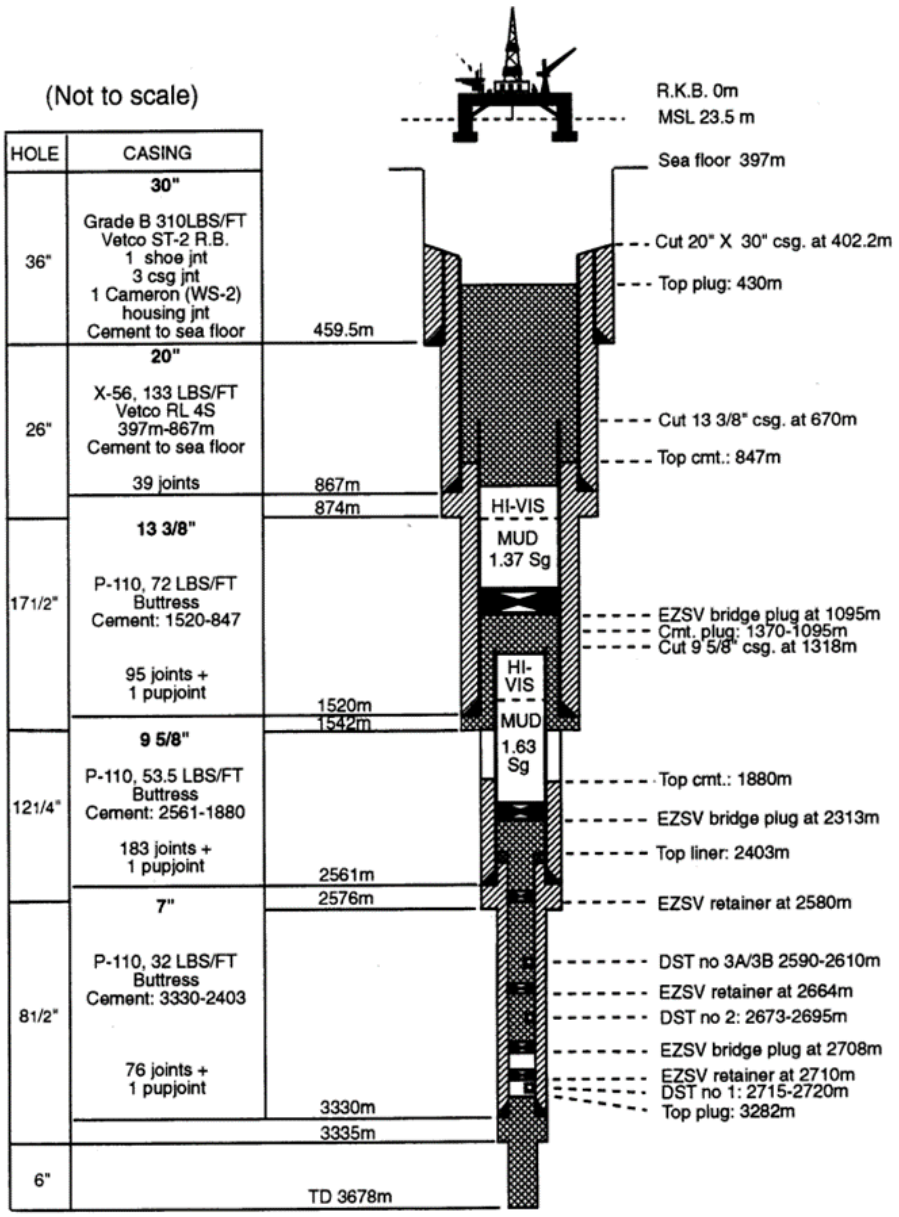

Figure 5.1.5. Wellbore schematic 6608/10-2

Table 5.1.2. Leak Off test results for Well 6608/10-3

Casing type	Casing diam.[inch]	Casing depth [m]	Hole diam. [inch]	Hole depth [m]	LOT/FIT mud eqv. [g/cm3]	Formation test type
CONDUC	30	466.0	36	466.0	0.00	LOT

TOR						
INTERM.	20	863.0	26	863.0	1.40	LOT
INTERM.	13 ⅜	1574.0	17 ½	1574.0	1.85	LOT
INTERM	9 ⅝	2542.0	12 ¼	2542.0	1.97	LOT
LINER	7	2921.0	8 ½	2921.0	0.00	LOT

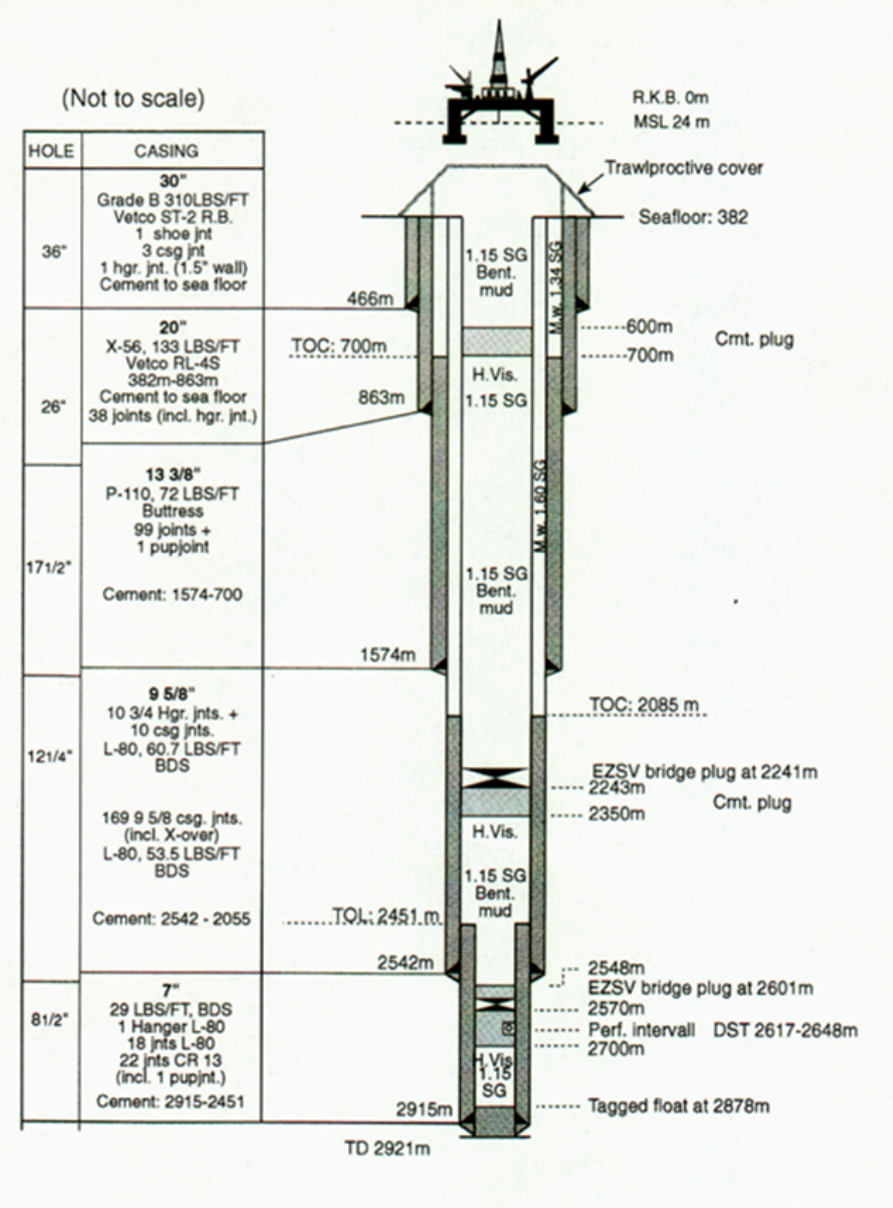
(Not to scale)
HOLE
CASING
36"
30"
Grade B 310LBS/FT
Vetco ST-2 R.B.
1 shoe jnt
3 csg jnt
1 hgr. jnt. (1.5" wall)
Cement to sea floor
26"
20"
X-56, 133 LBS/FT
Vetco RL-4S
382m-863m
Cement to sea floor
38 joints (incl. hgr. jnt.)
17 1/2"
13 3/8"
P-110, 72 LBS/FT
Buttress
99 joints +
1 pupjoint
Cement: 1574-700
12 1/4"
9 5/8"
10 3/4 Hgr. jnts. +
10 csg jnts.
L-80, 60.7 LBS/FT
BDS
169 9 5/8 csg. jnts.
(incl. X-over)
L-80, 53.5 LBS/FT
BDS
Cement: 2542 - 2055
8 1/2"
7"
29 LBS/FT, BDS
1 Hanger L-80
18 jnts L-80
22 jnts CR 13
(incl. 1 pupjnt.)
Cement: 2915-2451
R.K.B. 0m
MSL 24 m
Trawlproctive cover
Seafloor: 382
466m
TOC: 700m
863m
1574m
TOL: 2451 m
2542m
2915m
TD 2921m
1.15 SG
Bent.
mud
Mw 1.34 SG
Mw 1.69 SG
H.Vis.
1.15 SG
600m
700m
Cmt. plug
TOC: 2085 m
EZSV bridge plug at 2241m
2243m
2350m
Cmt. plug
2548m
EZSV bridge plug at 2601m
2570m
Perf. intervall DST 2617-2648m
2700m
Tagged float at 2878m

Figure 5.1.6. Wellbore schematic 6608/10-3

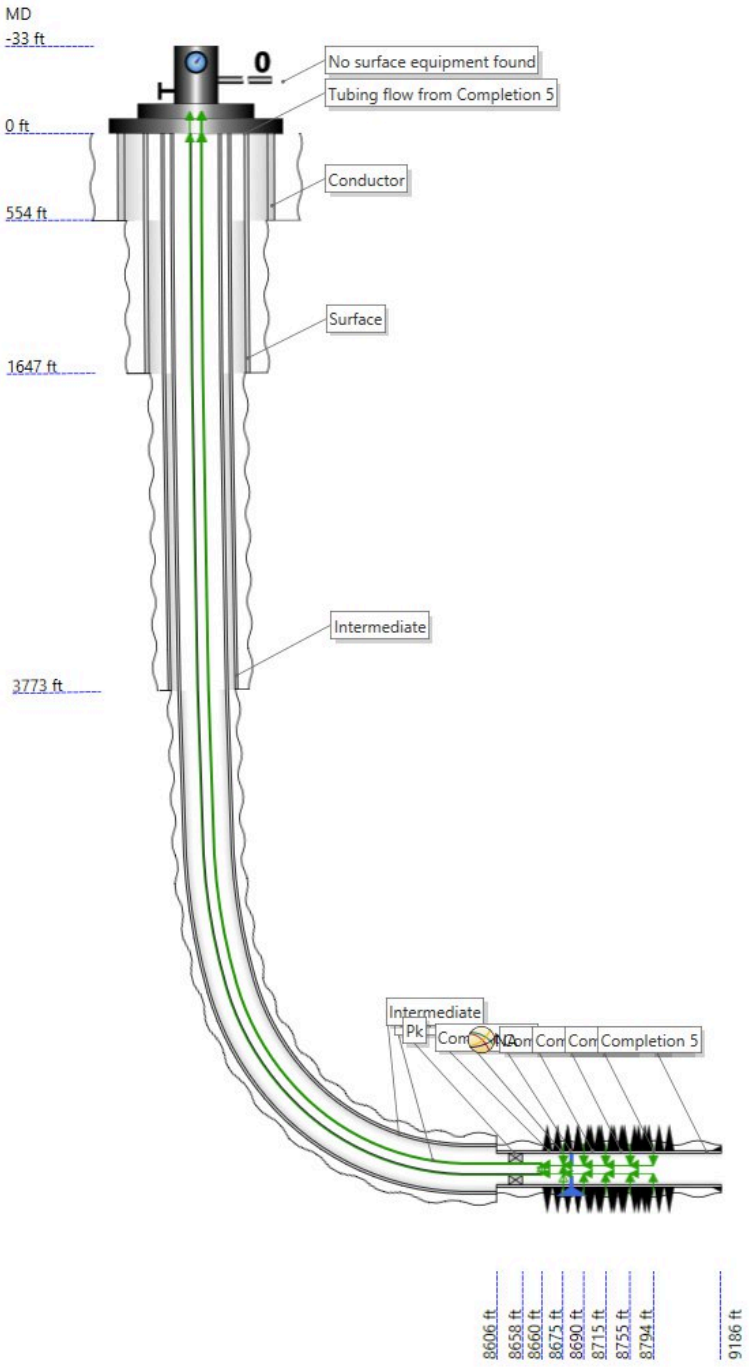

Figure 5.1.7. Horizontal well schematic by our team

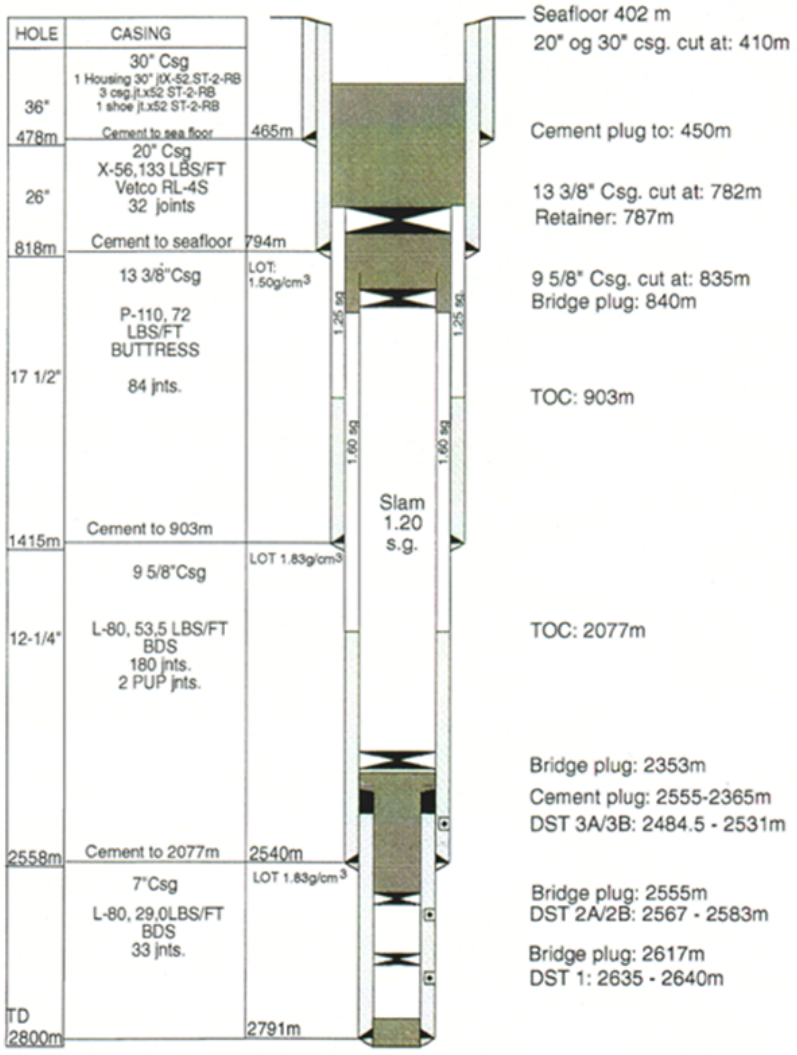

Figure 5.1.8. Casing design for Injection well proposed by the company

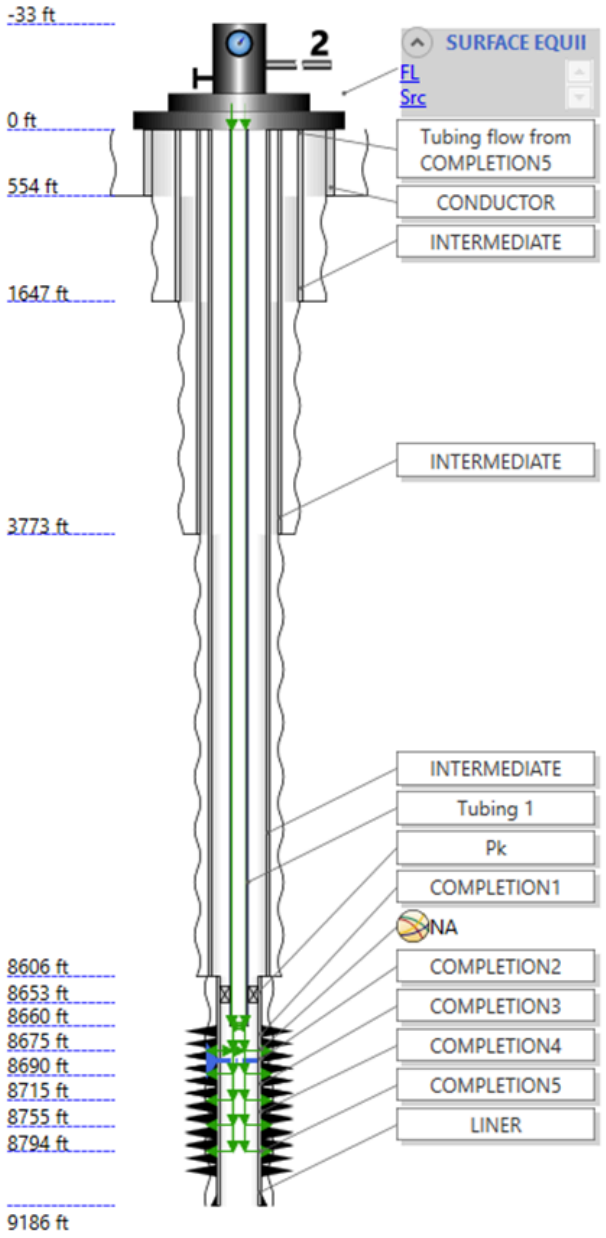

Figure 5.1.9. Casing design for Injection well proposed by our team

Table 5.1.3. Summary of the planned wells

Well Name	Well Type	Role	Target Formation	TVD (m)	MD (m)	Well Orientation

B-4H	Oil producer	Production	Ile & Garn	2669.134	2589.886	Horizontal
B-1H	Oil Producer	Production	Garn	2608.478	2960.522	Vertical
C-4H	Water Injector Gas Injector	Pressure support Artificial lift	Garn Ile	2654.198 2654.198	2656.027 2656.027	Vertical

5.1.5 Perforation Method

Perforation is a critical step in well completion, allowing hydrocarbons to flow from the reservoir into the wellbore. Since the Norne field employs cased-hole completions with sand screens or gravel packs in the production zones perforations are necessary because the production casing or liner seals off the reservoir rock, and perforation creates pathways for hydrocarbons to flow into the wellbore.

In this project, perforation guns will be used to create precise, high-energy perforation tunnels through the casing and cement into the formation. The selection of exact charge size, penetration depth, and shot density can be seen in the table below. Perforation will be conducted under underbalanced conditions to avoid formation damage and enhance productivity. Proper gun deployment and safety protocols will be followed to ensure efficiency and well integrity.

Table 5.1.4. Requirements for perforating gun

Parameter	**Selected value**
Gun Size	3 ⅜” - 4 ½”
Charge Type	Deep Penetrating Charge
Penetration Depth	18 inches
Shot Density	4 shots per foot

Phasing	$60^o - 90^o$

5.1.6 Sand Control Measures

To address sand production issues, gravel packing will be implemented as the primary sand control method. This involves pumping sized gravel into the annular space between the production casing and a wire-wrapped screen. The gravel pack filters out formation sand while allowing hydrocarbons to flow freely. This method is effective in preventing wellbore collapse, reducing erosion of downhole equipment, and ensuring stable production rates. Gravel packing will be designed based on particle size distribution and formation strength.

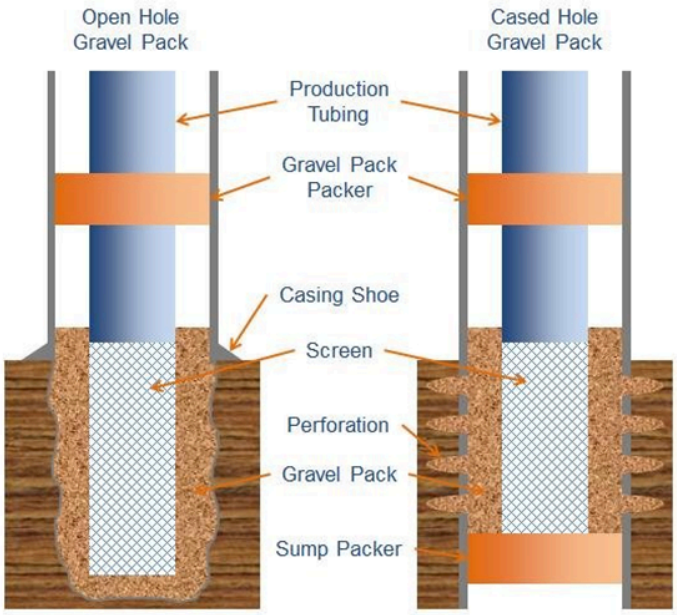

Figure 5.1.10. Gravel packs

As an alternative to that Oriented perforating sand prevention measure can be implemented (Andrews et al., 2008). Since the main contributing factors to sand production are Reservoir

Pressure Depletion and High Production Rates avoiding these factors by oriented perforation can be crucial. According to Andrews et al. (2008), experience in fields shows over 350 bars of depletion has been prevented due to this technique. When it comes to the amount of deferred sand the following results have been obtained.

Table 5.1.5. Deferred production due to sand production

	Wells shot without orientating systems	Wells shot with orientating systems
Total oil Production (Sm^3/d)	6800	12700
Production potential with 100% choke (Sm^3/d)	11000	13700
Deferred production (Sm^3/d)	4200	1000

5.1.7 Pump Selection for Artificial Lift

Since natural reservoir pressure may not be sufficient for optimal production, artificial lift will be utilized. The selection process involves evaluating fluid properties, production rates, and reservoir pressure Considering the offshore environment, high-pressure formations, and depth of operations, the Triplex Mud Pump is the most suitable option for the following reasons:

- High pressure-handling capacity for deep drilling. Pressure range that can be safely handled up to 5,000-7,000 psi
- Compact and efficient design, ideal for offshore platforms. Horsepower range is 1,000-1,200 HP
- Reliability and easy maintenance due to fewer moving parts compared to other pump types. Time between successive maintenance exceeds 1,000 hours

Table 5.1.6. Pump types and their description

Pump type	Desing	Operation	Characteristics	Applications
Duplex Mud Pump	Two pistons or plungers	Each piston completes a suction and discharge cycle	Moderate flow rates and pressures; bulky design	Historically used in drilling, now largely replaced
Triplex Mud Pump	Three pistons or plungers	Phased sequence ensures continuous smooth flow	High efficiency, compact, handles high pressures	Standard in modern drilling operations
Quintuplex Mud Pump	Five pistons or plungers	Even smoother flow with reduced pulsation	Higher flow rates and pressures; larger footprint	Demanding drilling operations requiring high flow
Hydraulic Mud Pump	Uses hydraulic fluid to drive pistons	Smooth, pulsation-free operation	High-pressure capability, complex system	Used where minimal vibration is required
Diaphragm Mud Pump	Flexible diaphragm to move fluid	Expansion and contraction create suction & discharge	Handles abrasive or corrosive fluids, lower flow	Mining, construction, handling chemically aggressive fluids
Peristaltic Mud Pump	Rotor squeezes a flexible tube	Peristaltic motion moves fluid	Gentle action, good for shear-sensitive fluids	Specialized mining, construction, slurry handling

5.1.8 Drilling Mud Selection

When it comes to the wellbore stability, pressure control and removal of the cuttings, the drilling mud fulfills a crucial role in it. For this particular project, the combination of water-based mud, oil-based mud and synthetic-based mud will be used depending on the location in the wellbore. Entire upper section of the wellbore will operate under water based mud due to the environmental concerns near the surface. In sections with high-pressure zones or unstable formations, oil-based mud will be implemented where stability and performance are critical. The last but not least Synthetic-Based Mud will be selectively used depending on

the region of the wellbore we are dealing with. It is often used in environmentally sensitive offshore fields like Norne. Its advantage lies in its ability to combine the performance of OBM with reduced environmental impact. It also has low toxicity and ease of disposal in compliance with offshore regulations.

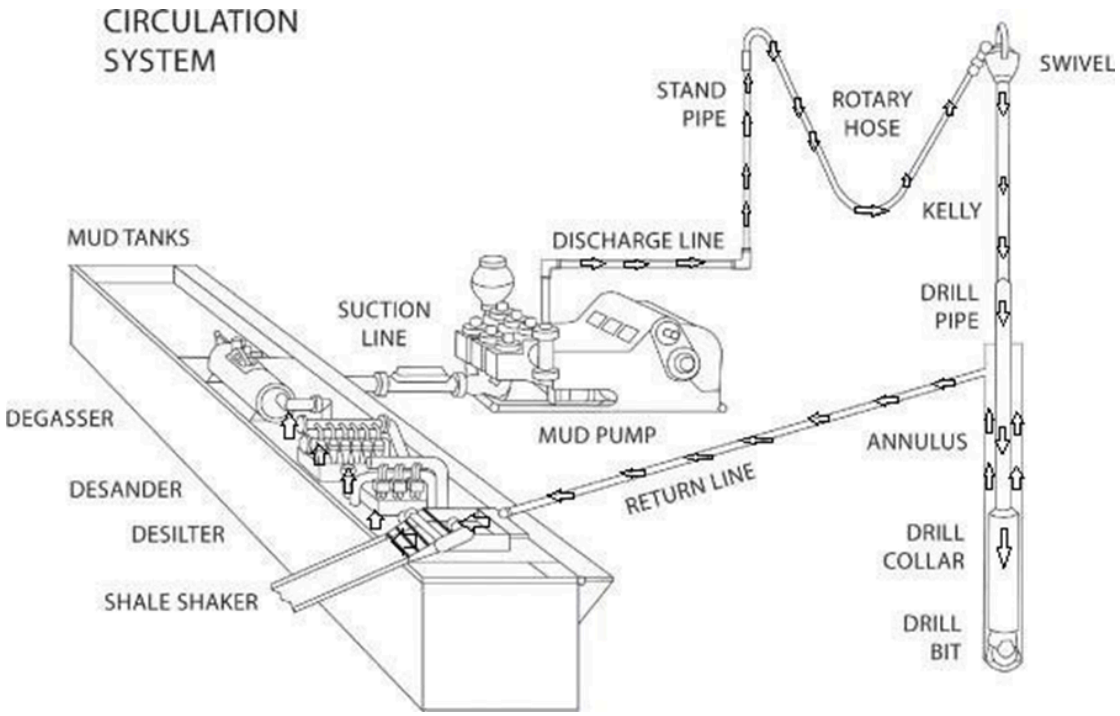

Figure 5.1.11. Mud circulation system (DOI: 10.54729/2959-331X.1002)

5.1.9 Tubing Selection

Tubing selection is based on reservoir pressure, production rates, and fluid properties. High-strength steel tubing with appropriate diameter and wall thickness will be used to withstand downhole conditions and minimize flow restrictions. Tubing design includes corrosion-resistant alloys if required, along with threaded connections for easy assembly. Tubing anchors and packers will be used to maintain well control and prevent fluid migration. Specification related to the tubing parameters can be found from the following table.

Table 5.1.7. Requirements for the Tubing parameters

Parameter	Selected values
Tubing Outer Diameter (OD)	3.5” - 5.5”
Inner Diameter (ID)	2.5”- 4.5”
Wall Thickness	0.25”- 0.5”
Material	Corrosion resistant high strength steel

Figure 5.1.12. Tubing with corrosion resistant alloys

5.1.10 Drilling Calculations

The following partcontains detailed calculations for the following drilling parameters based on the formula sheet obtained through past course experience:

1. Pressure Gradient & Hydrostatic Pressure.
2. Converting Pressure to Mud Weight.
3. Finding Specific Gravity (SG)

4. Maximum Allowable Mud Weight (Leak-off Test)
5. Annular Velocity
6. Strokes per Minute for Specific Annular Velocity
7. Amount of Cuttings Drilled per Foot
8. Buoyancy Factor
9. Cost per Foot

3.10.1 Converting Pressure to Mud Weight

Mud Weight (ppg) = Pressure (psi) ÷ (0.052 × TVD (ft))

For a pressure of 3,916 psi and TVD of 8200 ft:

Mud Weight = 3,916÷ (0.052 × 8200) = 9.18 ppg

Sources used:

https://cdn.dal.ca/content/dam/dalhousie/pdf/sites/sustainable-energy/Dalhousie_MINUS%20CO2.pdf?utm_source=chatgpt.com

https://keffi.nsuk.edu.ng/bitstreams/6d4c51c9-4aec-40f0-a39e-1fb150bea5b4/download?utm_source=chatgpt.com

3.10.2 Pressure Gradient and Hydrostatic Pressure

Pressure Gradient (psi/ft) = Mud Weight (ppg) × 0.052

For a mud weight of 9.18 ppg:

Pressure Gradient = 9.18 × 0.052 = 0.477psi/ft

Hydrostatic Pressure (HP) = Mud Weight (ppg) × 0.052 × True Vertical Depth (TVD, ft)

- Mud weight of 9.18 ppg
- TVD of 8,200 ft

HP = 9.18 × 0.052 × 8,200 = 3914.35 psi

3.10.3 Finding Specific Gravity (S.G)

S.G = Pressure Gradient (psi/ft) ÷ 0.433

For a pressure gradient of 0.477 psi/ft:

S.G = 0.477 ÷ 0.433 = 1.1

3.10.4 Maximum Allowable Mud Weight from Leak-off Test

The leak off- the pressure at which the formation just below the casing shoe will fracture and allow fluid to "leak off" into the formation. Okland et al. (2002) points out the importance of conducting leak-off tests for extended periods of time to prevent the circulation loss during drilling. Unlike conventional leak-off tests, XLOTs (extended leak off tests) provide additional data on fracture propagation and closure pressures, allowing for a more accurate understanding of formation strength and stress conditions.

Mud Weight (ppg) = (Leak-off Pressure (psi) ÷ (0.052 × TVD (ft))) + Initial Mud Weight (ppg)

·Leak-off pressure of 3400 psi https://www.aade.org/application/files/1115/7261/8801/AADE-11-NTCE-24.pdf

- TVD of 8200 ft
- Initial mud weight of 9.18 ppg:

Mud Weight = (3400 ÷ (0.052 × 8200)) + 9.18 = 17,15 ppg

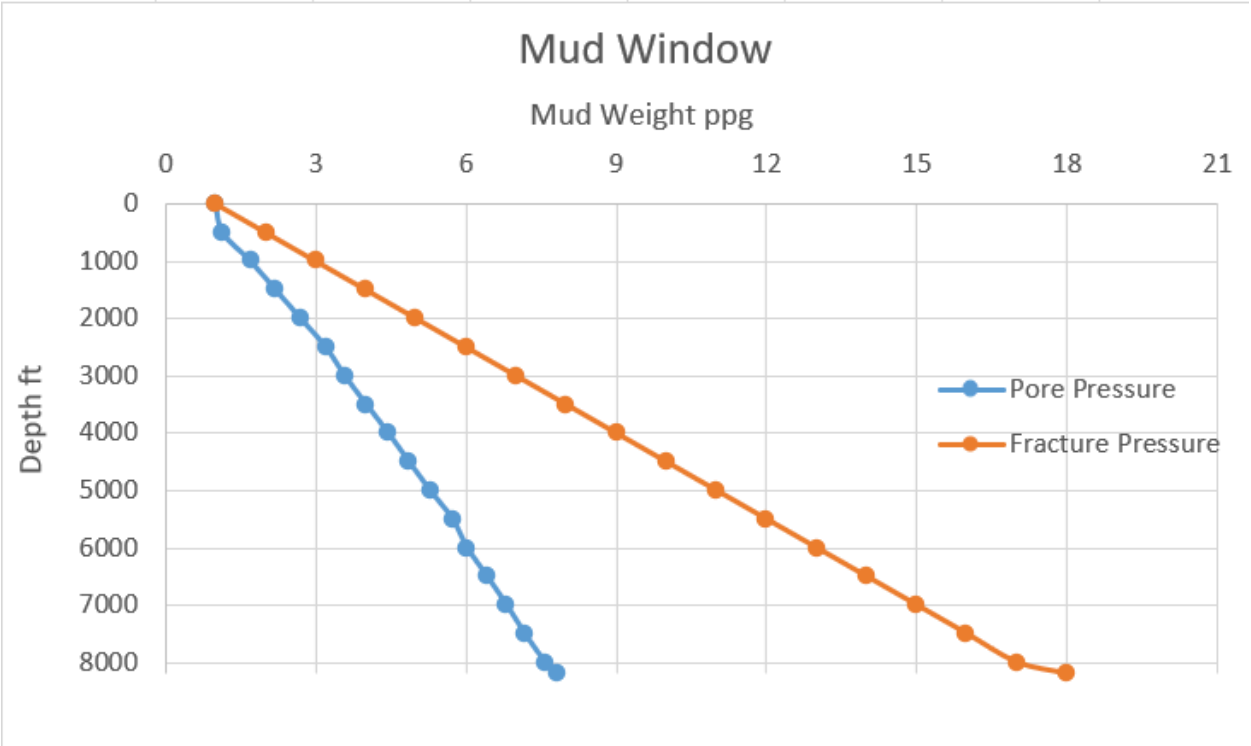

Figure 5.1.13. Mud Window

Labeling:

1) Blue line- lower limit

2) Orange line- upper limit

3) Everything in between - operating mud weight range

Annular Velocity

Annular Velocity (AV) = Pump Output (bbl/min) ÷ Annular Capacity (bbl/ft)

· Pump output of 12.6 bbl/min

· Annular capacity of 0.1261 bbl/ft

AV = 12.6 ÷ 0.1261 = 99.92 ft/min

Strokes per Minute for a Specific Annular Velocity

SPM = (Annular Velocity (ft/min) × Annular Capacity (bbl/ft)) ÷ Pump Output (bbl/stk)

- Annular velocity of 120 ft/min
- Annular capacity of 0.1261 bbl/ft
- Pump output of 0.14 bbl/stk

SPM = (120 × 0.1261) ÷ 0.14 = 108.1

Amount of Cuttings Drilled per Foot of Hole Drilled (HSE)

Barrels of Cuttings = Capacity (bbl/ft) × (1 - Porosity)

- A hole capacity of 0.146 bbl/ft
- Porosity of 20%

Cuttings = 0.146 × (1 - 0.20) = 0.1168 bbl/ft

Buoyancy Factor

BF = (65.5 - Mud Weight (ppg)) ÷ 65.5

For a mud weight of 15.0 ppg:

BF = (65.5 – 9.18) ÷ 65.5 = 0.86

Cost per Foot

Cost per Foot = (Bit Cost + Rig Cost × (Rotating Time + Round Trip Time)) ÷ Footage per Bit

- A bit cost of $2500
- A rig cost of $900/hour
- Rotating time of 65 hours

· Round trip time of 6 hours

· Footage per bit of 1300 ft:

Cost per Foot = (2500 + 900 × (65 + 6)) ÷ 1300 = $51.08/ft

5.1.11 Drill string calculations

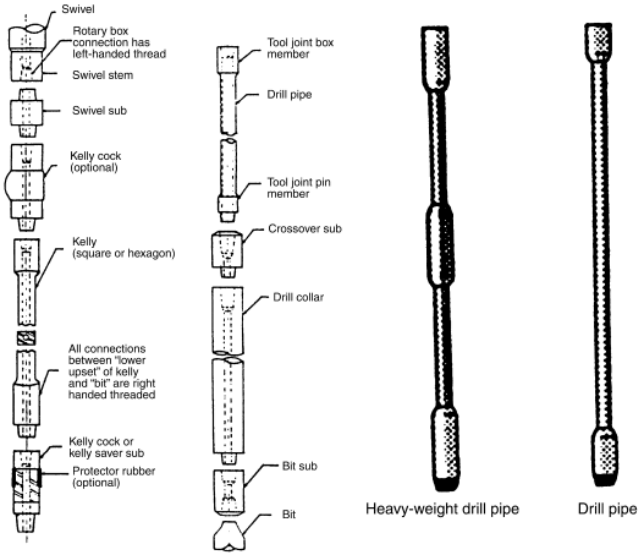

Figure 5.1.14. Drill string design

There are **4 basic requirements** which must be met when designing a drill string:

· The collapse, burst and tensile strength of the drill string components must not be exceeded

· The bending stresses within the drill string must be minimized - control I/C ratio

· The drill collars must be able to provide all the weight required for drilling - DC must be sufficient

· The BHA must be stabilized to control direction of the well-design assembly appropriately

Bending stress (I/C ratio):

Section Modulus = I / C = Moment of Inertia / External Radius of Tube

- Moment of 25,000 ft-lbs
- Distance of 1.5 ft
- Section Modulus of 300 in^3:

$$\sigma = (25{,}000 \times 1.5) / 300 = 125 \text{ psi}$$

Drill collar weight:

The length of DC must be sufficient to provide WOB and overcome buoyant force

DC Length for WOB:

$$L\_WOB = WOB \text{ (lb)} / (DC \text{ weight (lb/ft)} \times BF)$$

- WOB of 40,000 lbs
- DC Weight of 700 lbs/ft,
- Buoyancy Factor of 0.86:

$$L\_WOB = 40{,}000 / (700 \times 0.86) = 66.45 \text{ ft}$$

DC Length for Buoyant force:

$$L\_Bf = (DP \text{ Weight in Air (lb)} - DP \text{ Wet Weight (lb)}) / (DC \text{ weight (lb/ft)} \times BF)$$

- Weight in Air of 120,000 lbs
- Wet Weight of DP of 90,000 lbs
- DC Weight of 700 lbs/ft,
- Buoyancy Factor of 0.86

$$L\_Bf = (120{,}000 - 90{,}000) / (700 \times 0.86) = 49.83 \text{ ft}$$

Total length should then be increased by 15%

$$L\_Bf \times 1.15 = 57.3 \text{ ft}$$

Summary of Results:

1 Bending Stress (σ) = **125 psi**
2 Required Drill Collar Length for WOB = **66.45 ft**
3 Required Drill Collar Length to Overcome Buoyancy = **49.83 ft**
4 Adjusted Buoyancy Length with 15% Safety Margin = **57.3 ft**
5 Final Drill Collar Length (WOB + Adjusted Buoyancy) = **~124 ft**

5.1.12 Drill bit selection

PDC (Polycrystalline diamond compact)- is perfect for sedimentary rocks as shales, limestone, and weakly cemented sandstones which is exactly what we have in Norne field. The shearing action is the most efficient cutting mechanism which requires the least energy to drill. The PDC cutter's self-sharpening effect results in long bit life and high rates of penetration

Figure 5.1.15. PDC drill bit

5.1.13 Drill Pipe selection design

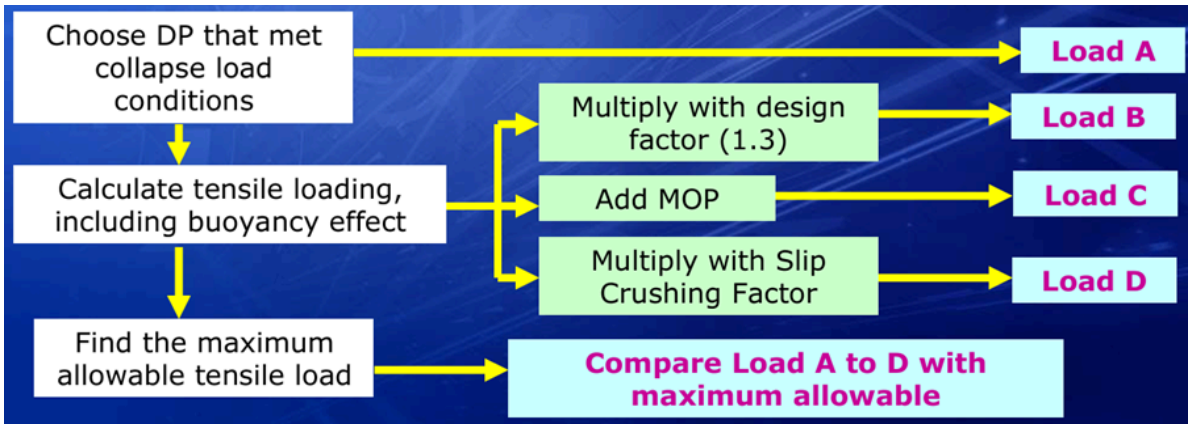

Figure 5.1.16. Drill Pipe selection procedure

1) Calculate Tensile Loading, Including Buoyancy Effect

Tensile Load (T) = (Total Weight × Buoyancy Factor)

- Total Weight of 150,000 lbs
- Buoyancy Factor of 0.86

$$T = 150{,}000 \times 0.86 = 129{,}000 \text{ lbs}$$

2) Maximum Allowable Tensile Load

API Grade E-75 selected with the following properties:

- Minimum Yield Strength = 75,000 psi
- Nominal Pipe Size = 5"
- Nominal Wall Thickness = 0.362"
- Cross-sectional Area = 7.07 in²

Formula:

Maximum Allowable Tensile Load = Cross-sectional Area × Minimum Yield Strength

- Tmax = Maximum Allowable Tensile Load

- Cross-sectional Area = 7.07 in²
- Minimum Yield Strength = 75,000 psi

Maximum Allowable Tensile Load = 7.07 × 75,000 = 530,250 lbs

3) Multiply with Design Factor (1.3)

Formula:

Allowable Load = Maximum Allowable Tensile Load / 1.3

Allowable Load = 530,250 / 1.3 = 407,884.62 lbs

4) Add Maximum Operating Pressure (MOP)

Formula:

MOP Load = MOP × Cross-sectional Area

- Max operating pressure = 5,000 psi
- Cross-sectional Area = 7.07 in²

MOP Load = 5,000 × 7.07 = 35,350 lbs

Total Allowable Load = Allowable Load + MOP Load

Total Allowable Load = 407,884.62 + 35,350 = 443,234.62 lbs

5) Multiply with Slip Crushing Factor

Formula:

Final Allowable Load = Total Allowable Load × Slip Crushing Factor

- Slip Crushing Factor = 0.9

Final Allowable Load = 443,234.62 × 0.9 = 398,911.16 lbs

Summary of Results

- 1 Tensile Load (T) = 129,000 lbs
- 2 Maximum Allowable Tensile Load = 530,250 lbs
- 3 Allowable Load with Design Factor = 407,884.62 lbs
- 4 Total Allowable Load (including MOP) = 443,234.62 lbs
- 5 Final Allowable Load (including Slip Crushing Factor) = 398,9111.16 lbs

5.1.14 Challenges and Mitigation Strategies

The development of the Norne Field came with a number of technical challenges such as water and gas breakthrough amongst other production related issues as well as dealing with associated uncertainty with the reservoir. A crucial part of mitigating these risks included real-time updating of reservoir data and ongoing simulations to update well trajectories and optimize production. Further, application of flexible risers and flowlines adapted to the topography of the seabed-rendered by Iceberg scours-minimized the risk to damage infrastructure on production (John A. 1995).

The other challenge was well integrity throughout its lifecycle. Digital well integrity tools, as outlined in the digital well planning document, provided a forward-looking approach to well construction and management. The tool then automated many of the engineering calculations required for well integrity and allowed continuous monitoring of the wells through the integration of subsurface data that ensured long-term safety and performance of the wells (Brechan and Sangesland, 2019).

Reservoir Pressure Decline:

- As the field reaches maturity, reservoir pressure decreases and therefore production rates decline. The Norne field has implemented strategies using gas and water injection to maintain pressure and enhance oil recovery.

- The design of these wells supports those injection techniques: injection wells are placed appropriately, and their completions are injection-compatible to avoid well damage and maximize recovery.

5.1.15 Recent Advancements and Industry Practices

Autonomous Inflow Control Devices (AICDs):

- Among the more recent inflow control devices are the AICDs, which have been made available in the industry since the start of the Norne field. AICDs could help improve oil recovery by automatically adjusting flow rates based on reservoir conditions, especially useful in handling water and gas breakthroughs in multilateral wells.
- AICDs could be implemented that would allow finer flow control, reducing water or gas production, and optimizing overall production efficiency.

Digital Twins and Predictive Analytics:

- In place of the actual Norne field, a digital twin of Norne field can also be utilized in simulating field operations, predicting well maintenance and monitoring older infrastructure (Wanasinghe, 2020).
- Predictive analytics can enhance production optimization strategies by encouraging operators to modify actions driven by data analysis, thereby safeguarding production, if early signs of reservoir or well performance related problems are detected.

Surface facilities

Our surface facilities were designed based on insights from the drilling and completion phase. The selection of ESP, Gas Lift, and horizontal wells directly influenced the required chokes and downstream pressure systems. Flow rate estimates guided the sizing of the separator, compressor, and pumps. The three-phase separator splits hydrocarbons into gas, oil, and drilling mud, each directed via appropriate flowlines to final destinations using a compressor and pumps. Equipment power needs were estimated based on assumed flow and pressure conditions, with compressor power in the range of 150–400 kW and pump powers between 20–70 kW.

Figure 5.1.17. Surface Facilities

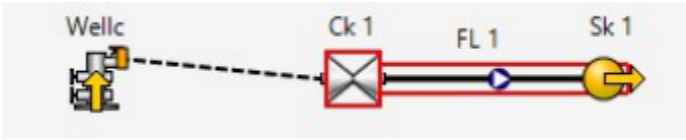

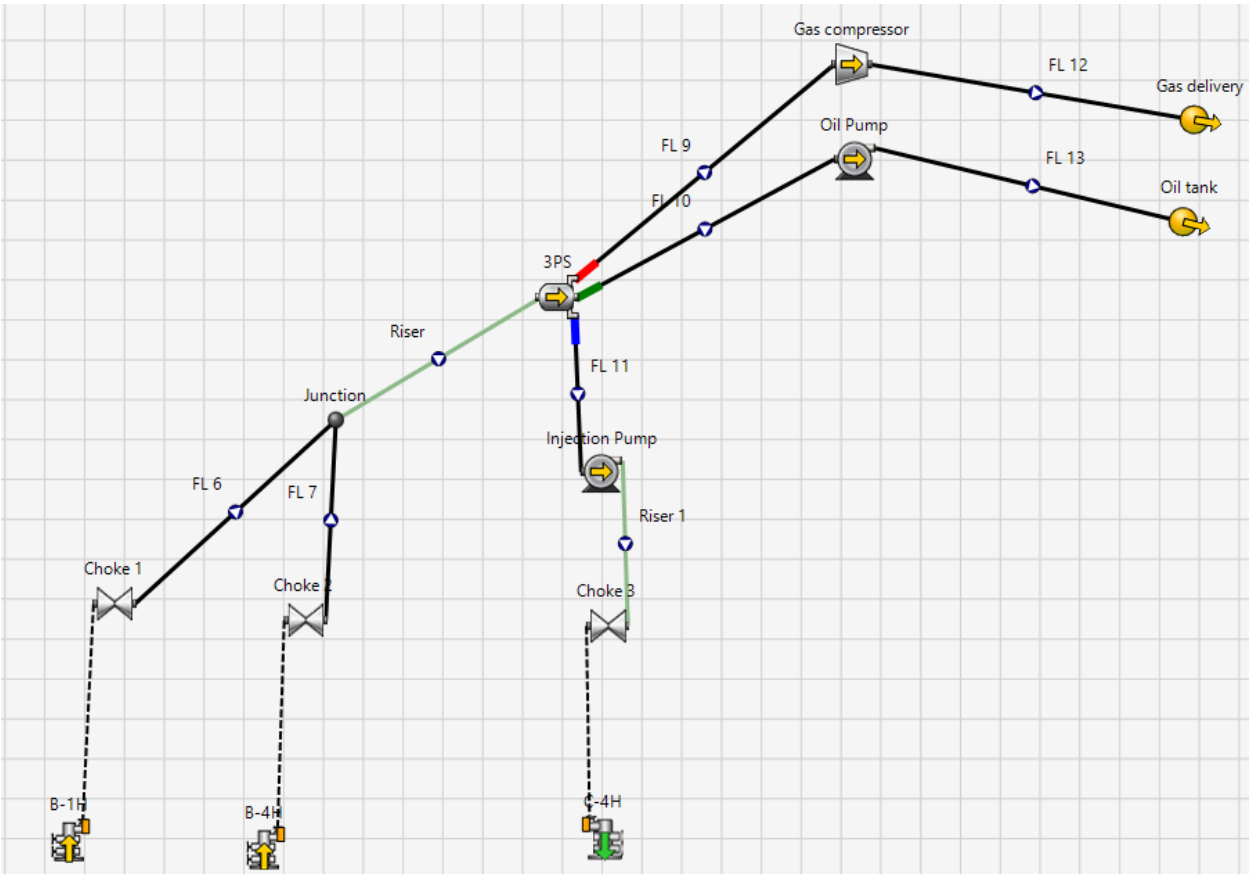

Figure 5.1.18. Equipment of Downstream

Chapter 6. Application of Machine Learning in production analysis:

6.1 Machine Learning Algorithms

6.1.1 Random Forest Regression

Random Forest Regression (RFR) is a machine learning algorithm that uses an ensemble of decision trees to make predictions of continuous values. It operates by training many decision trees on random subsets of data and then aggregating their predictions to produce a final output. The ensemble method serves to enhance the accuracy and stability of the model over using single decision trees. In Random Forest, each tree is trained on a bootstrapped sample, which is a random sample with replacement of the original sample; it can be seen from figure 6.1.1. In this manner, the model is able to generalize better and not overfit to specific points. The final prediction is usually the mean of the predictions of all individual trees, which reduces variance and enhances the overall performance of the model (Breiman, 2001). A random subset of the features is tested at each decision node in the decision tree for splitting. This randomness makes the trees diverse and also reduces correlation between the trees, thus the "forest" is better than one decision tree (Breiman, 2001). Random Forest models are less overfit than individual decision trees. Since the overall prediction depends on averaging predictions from numerous models, it has a tendency to reduce any spikes or biases of individual trees and generalize even further on out-of-sample data (Liaw & Wiener, 2002). One of the major advantages of Random Forest Regression is that it is more stable. Random Forest is less prone to overfitting, particularly in noisy feature or high-interaction relationship datasets. Random Forest can also determine the contribution of various features to predicting the target variable, which can prove useful in feature selection (Breiman, 2001). Random Forest, unlike most other machine learning models, does not require feature scaling because decision trees are invariant to the scale of features. However, Random Forest Regression also has its drawbacks. The model can be extremely large and computationally expensive due to the ensemble nature of the method, so inference is slow compared to simpler models. Furthermore, while one decision tree is easy to interpret, Random Forest models are less transparent because the output that results is an average of multiple trees, which is harder to understand how decisions are made.

$$RFR = 1/T \sum_{t=1}^{T} h_t(x)$$

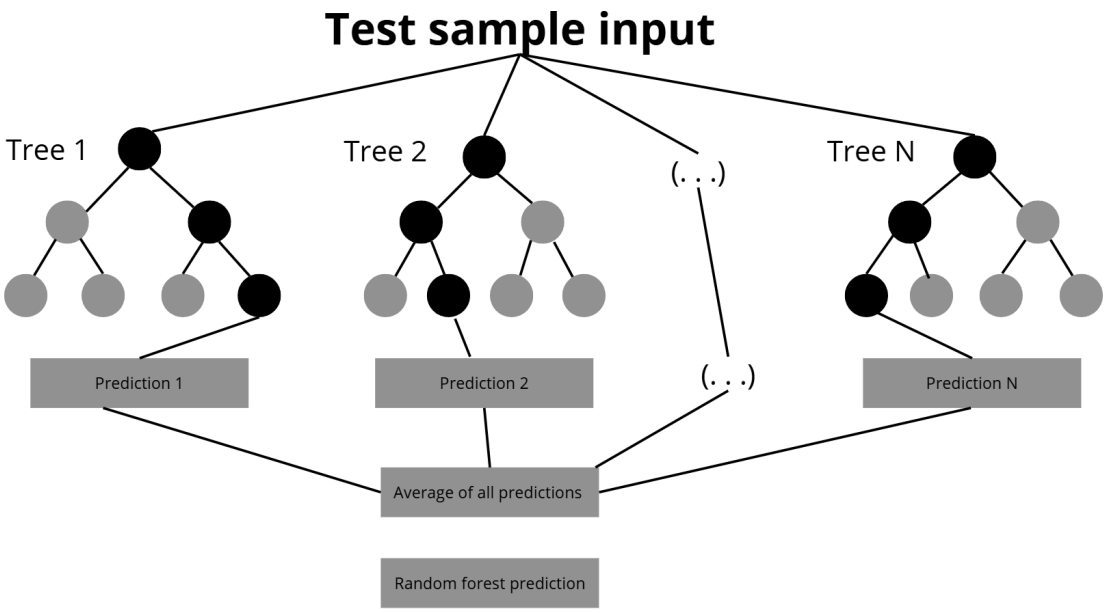

Figure 6.1.1. Random Forest mechanism

6.1.2 Linear Regression

Linear Regression is likely the simplest and most popular technique in machine learning and statistics. Linear Regression is utilized to fit a dependent variable to one or more independent variables. The central idea of linear regression is to identify the best-fit straight line (for simple linear regression) or hyperplane (for multiple regression) that characterizes the relationship between the variables. In its most fundamental form, simple linear regression attempts to provide a description between two variables using a model representing a straight line through the data. The mathematical formula for simple linear regression is represented in figure 6.1.2:

$$y = \beta_0 + \beta_1 x_1 + \beta_2 x_2 + \ldots + \beta_n x_n + \epsilon$$

Figure 6.1.2. Formula of simple linear regression

The simplicity and interpretability of linear regression are two of its main advantages. The model is reasonably simple to describe and interpret because the coefficients clearly show the direction and magnitude of the relationship between the independent and dependent variables. Additionally, linear regression is computationally efficient, which makes it ideal for large-scale database analysis. However, there are certain drawbacks to linear regression. It will not function as well if the relationship is actually non-linear because it is predicated on the idea of a linear relationship. Additionally, outliers can have a disproportionate impact on the model's fit, and linear regression is sensitive to them. High correlations between independent variables in multiple regression can lead to coefficient estimate instability and render the model useless.

6.1.3 Artificial Neural Networks

Artificial Neural Networks (ANNs) are a category of Machine Learning algorithms which is based on the operation of biological neural networks of the human brain. ANN are used in a wide range of applications involving regression, classification and pattern recognition. An ANN contains the concept of interconnected layers of nodes, also known as neurons. Inputs are received by each neuron, the neuron performs an activation function on the inputs and passes the output to the next layer of neurons. In general, from the figure 6.1.3, the architecture has three types of layers: an input layer, hidden layers, and an output layer. The data features are fed into the input layer, which is transformed into one or more hidden layers. Each of these connections has a weight that is adjusted during training to minimize the error in prediction of the network. Training an ANN involves the use of a dataset to apply it iteratively to adjust these weights to a result called backpropagation. It calculates the difference between the predicted and the known values and back propagates the error through the network to correct the weights (generally by means of optimization algorithms such as gradient descent). As ANNs can learn complex, non-linear relationships in data, they are powerful models. The advantage of ANNs is in their versatility, as they are capable of approximating any continuous function, with which they are suitable for problem solving where traditional models do not apply. ANNs are very useful in tasks like image

classification, natural language processing and time series forecasting. One of the greatest advantages of ANNs is that they can learn automatically from data and no feature engineering is needed by manual. High computational costs are one of the difficulties faced by ANNs, which necessitates big datasets and powerful computers.

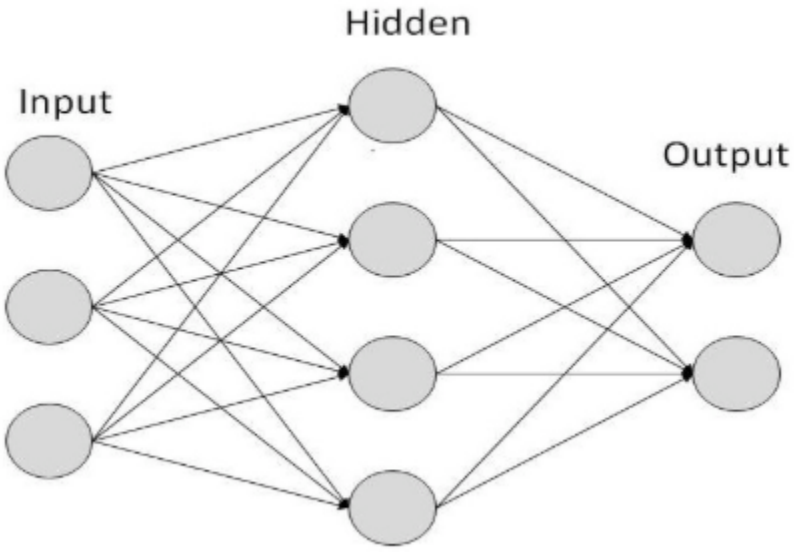

Figure 6.1.3. The structure of an ANN algorithm

6.2 Performance Metrics

6.2.1 Mean Absolute Error

Mean Absolute Error (MAE) is a popular way of assessing the success of a set of predictions in regression. It is necessary to take the average of the absolute differences between the predicted values and the actual values, which is what it is calculated by. The MAE does not consider the direction of errors, thus it only measures their magnitude. MAE is mathematically calculated as the sum of the absolute errors divided by number of observations. This is particularly useful because it is easy to interpret and the result is in the same units as the data being predicted. MAE does have a disadvantage: it is robust to outliers, in the sense that it does not square errors and treats all errors equally (Willmott & Matsuura, 2005). While this metric doesn't penalize larger errors as much as other metrics

such as the Root Mean Squared Error (RMSE) or Mean Squared Error (MSE), its drawback is that it does not provide any information on error. For this reason, MAE may not be as sensitive to large discrepancy in prediction as models with squared error terms.

$$MAE = \frac{1}{n}\sum_{i=1}^{n} |y_i - \hat{y}_i|$$

6.2.2 Mean Squared Error

Mean Squared Error (MSE) is a commonly used metric to measure the average squared error between the predicted and actual values. Summing the squared residuals and then dividing by the number of observations is calculated. Squaring the errors amplifies the impact of large deviations, and therefore MSE is often used when it is important to penalise large errors (Hyndman & Koehler, 2006). MSE is very useful at highlighting large differences between predicted and actual values, but to understand it directly can be quite difficult as it is obtained in squared units. MSE is also sensitive to outliers just like RMSE so extreme errors can disproportionately affect it. The weakness of this is that in real world applications, MSE is not very intuitive, while it is a powerful metric to use when one wants to minimize large errors.

$$MSE = \frac{1}{n}\sum^{n}(y_i - \hat{y}_i)^2$$

6.2.3 Root Mean Square Error

Another metric to evaluate the performance of a regression model is Root Mean Squared Error (RMSE), that is the square root of MSE. The square root of the average squared differences between predicted and actual values is the expression of magnitude of error. It is useful because it makes the magnitude of error interpretable, in the same units as the original data, as RMSE does. It is more sensitive to outliers. Unlike MAE, RMSE penalizes larger errors more heavily as a result of the squaring of differences (Chai & Draxler, 2014). This is a good measure of RMSE, since large errors are undesirable, but it also causes RMSE to be inflated by large deviations from the actual values or outliers. As a result, RMSE is more

useful when trying to predict models that have high error implications that will affect the outcome, e.g. in production forecasting or financial modeling.

$$\text{RMSE} = \sqrt{\frac{1}{n}\sum_{i=1}^{n}(y_i - \hat{y}_i)^2}$$

6.2.4 R-Square

R-Square (R^2) is a statistical metric which measures how well a regression model fits the data. It is calculated by 1 minus the residual sum of squares divided by total sum of squares, where the residual sum of squares is the sum of squared differences between the observed values and the predicted values and the total sum of squares is the sum of squared values between the observed and mean of the observed values. R^2 tells how much variance in the dependent variable this explanatory variable explains. The R^2 value of 1 means that the model has a perfect variance, while 0 means that there is no variance (Draper & Smith, 1998). Although R^2 is a useful metric to evaluate fitness of the model, it does have a few drawbacks. For example, R^2 does not penalize overfitting and so, adding more variables in the model can increase R^2 artificially even if the model is poor. Moreover, R^2 is not informative in case the model is poorly specified, and insensitive to outliers, which implies that R^2 is not always a good measure in the sense of true predictive accuracy of the model (Field, 2013).

$$\text{R\^2} = 1 - \frac{\sum_{i=1}^{n}(y_i - \hat{y}_i)^2}{\sum_{i=1}^{n}(y_i - \bar{y}_i)^2}$$

Table 6.2. Results

	Train (80%)			Test (20%)		
Metrics	Linear Regression	Random Forest Regression	Artificial Neural Network	Linear Regression	Random Forest Regression	Artificial Neural Network
MAE	1667.84	33.34	3275.44	1794.22	99.34	3539.2

RMSE	2111.69	139.89	4433.79	2268.65	414.01	4876.65
MSE	4459255.64	19569.07	19658496.04	5146760.58	171402.41	23781749.65
R2	0.86	0.99939	0.943	0.8485	0.99495	0.92726

Chapter 7. Production Engineering

7.1 Production Engineering

This section describes the result of an evaluation of an integrated production system by the use of Schlumberger's PIPESIM software, a robust industry standard nodal analysis and steady state multiphase flow simulation software. Three strategically selected wells from the field, which are vertical production well (B-4H), horizontal production well (B-1H) and an injection well (C-4H) are studied. The purpose of that is to evaluate and optimize their operational performance under changing subsurface and surface conditions.

It was then shown through nodal analysis simulations that the best operating points for each production well were defined in order to have both realistic, hydrocarbon producing rates, and safe, bottomhole pressures in order to sustain hydrocarbon production. Simulations for CO_2 and water injection scenarios were conducted for the injection, and direct comparison of injectivity performance and long term pressure support efficiency is enabled. Both cases were designed so as to keep the impacts of the injected fluid isolated.

The analysis including a series of sensitivity studies to pressure – flow correlations and their interaction with tubing diameter, tubing roughness, water cut and reservoir pressure depletion were developed to assess system behavior in detail. Results from these investigations showed inflow and outflow performance characteristics and constraint on reservoir conditions.

With the increase in production, pressure depletion and rising water cut became a challenge to natural flow which could only be solved by the use of artificial lift systems. Three types of lifts, Electric Submersible Pumps (ESP), Sucker rod Pumps (SRP) and Gas Lift Systems, were designed and analyzed. IPR and VLP curve intersections were used to evaluate the performance of each system, and sensitivities of the operational system such as pump frequency, plunger diameter, stroke length and gas injection rates are also considered. This helped us understand what would be the most effective solutions to restore productivity under depleted conditions.

Ultimately, this overall analysis aims to achieve all the information necessary to understand the well operation under different conditions. The findings provide a solid basis for decision making in field development planning, artificial lift strategy, and surface facility design that is compatible with accounting for long-term reservoir integrity and production optimization.

7.2. Nodal Analysis of Production Well Vertical (B-4H)

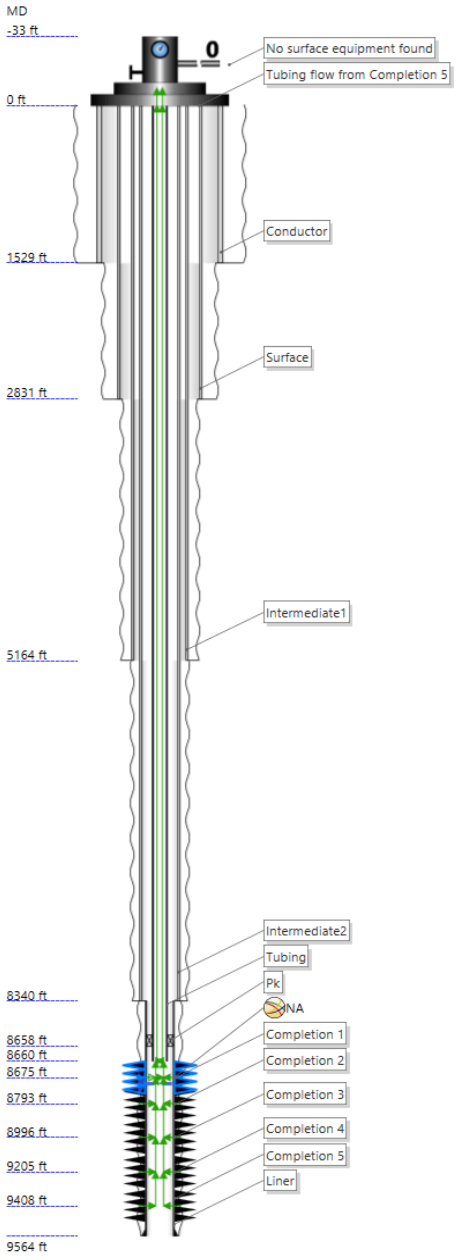

Figure 7.2.1. B-4H Vertical Well's Schematic.

	Section type	Name	From MD	To MD	ID	OD	Roughness
			ft	ft	in	in	in
1	Casing	Conductor	0	1528.871	28	30	0.001
2	Casing	Surface	0	2831.365	18.75	20	0.001
3	Casing	Intermediate1	0	5164.042	12.347	13.375	0.001
4	Casing	Intermediate2	0	8339.895	8.407	9.625	0.001
5	Liner	Liner	8339.895	9563.648	6.184	7	0.001

TUBINGS

	Name	To MD	ID	OD	Roughness
		ft	in	in	in
1	Tubing	8660	2.992	3.5	0.001

Figure 7.2.2. Casing and Tubing Design for B-4H.

Well integrity and efficient production are the main objectives in designing the B-4H well, which is equipped with a robust multi caging program and a liner. With the diameters decreasing from 28 in to 8.407 in, the conductor, surface, and intermediate casings supported the structural and zonal isolation. As a total measured depth of the well, it is completed with a liner up to 9563.65 ft, avoiding cost and providing reservoir access.

This is achieved by the use of a 3.5 in OD tubing having an inner diameter of 2.992 in (3.5 in OD tubing with an inner diameter of 2.714 in is available, but would be excessively costly and complex with comparatively little benefit to the flow rates and unrealistically increased frictional pressure losses). Also, all tubulars have a standard roughness of 0.001 in, or new steel surfaces for an accurate PIPESIM model.

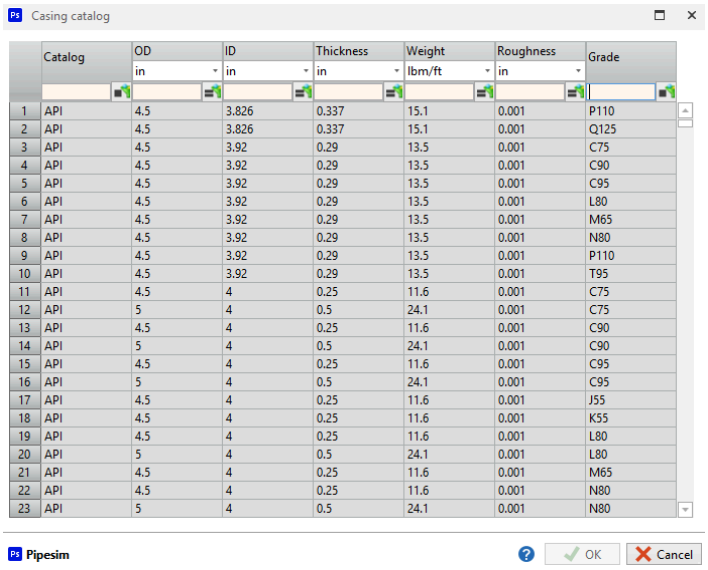

Figure 7.2.3. Casing and Tubing Catalog.

Next step was choosing the exact grades and other parameters from the casing catalog and implementing the information that was gained from the drilling and completion engineer we chose the most suitable models.

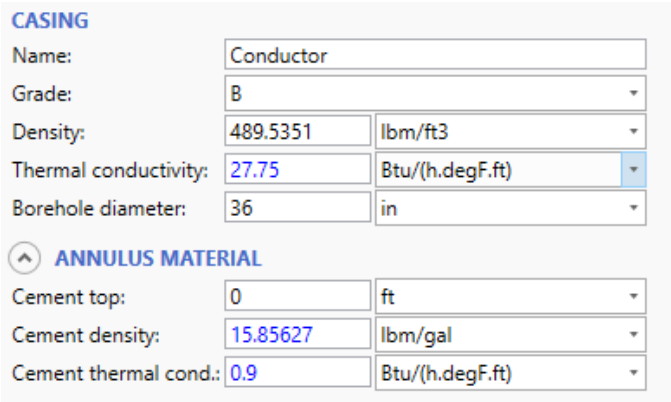

Figure 7.2.4. Example of casing parameters.

	Equipment	Name	Active	MD
				ft
1	Packer	Pk	☑	8658.458
2		NA	☑	8675

Figure 7.2.5. Packer Design for B-4H.

8658.46 ft above the tubing depth is the packer set at 8658.46 ft. It provides for this standard placement of the tubing, provides zonal isolation, provides protection of the casing, and directs flow through the tubing. This gives it further confirmation that it's sufficiently sealing the annulus for single zone production.

	Name	Geometry pro...	Fluid entry	Top MD	Middle MD	Bottom MD	Type	Active	IPR model
				ft	ft	ft			
1	Completion 1	Vertical	Single point		8675		Perforation	☑	Well PI
2	Completion 2	Vertical	Single point		8793.476		Perforation	☑	Well PI
3	Completion 3	Vertical	Single point		8995.919		Perforation	☑	Well PI
4	Completion 4	Vertical	Single point		9204.685		Perforation	☑	Well PI
5	Completion 5	Vertical	Single point		9407.802		Perforation	☑	Well PI

Figure 7.2.6.Completions for B-4H.

The well has five single point vertical perforations spaced between 8675 and 9407.8 ft into multiple reservoir intervals. Because all completions are active and have been modeled using the Well PI approach, inflow simulation can be achieved in a more simplified manner. It maximizes contact with productive zones and better drains reservoir across the lower well section.

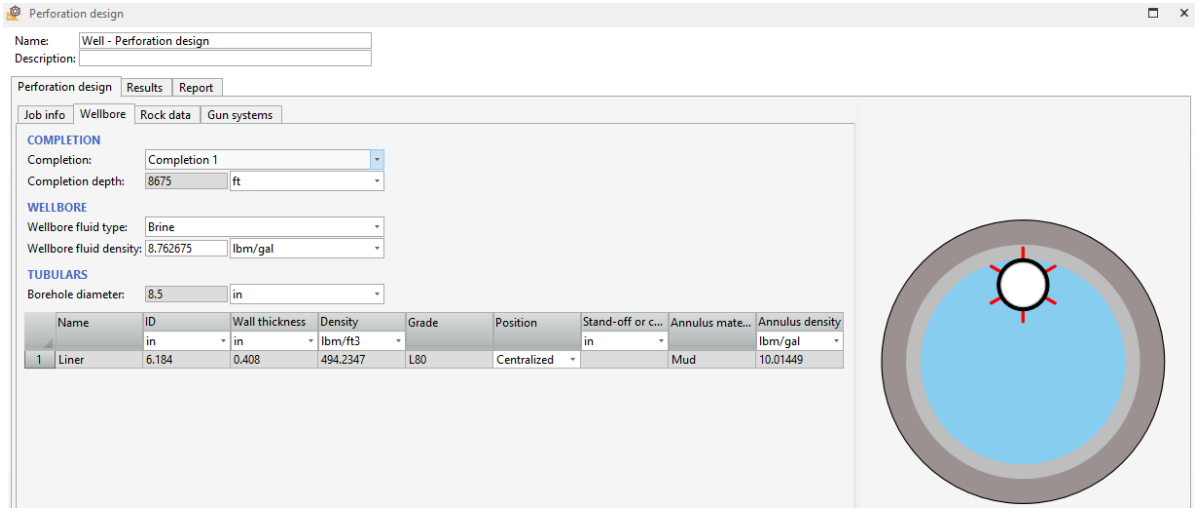

Figure 7.2.7. Perforation Design wellbore data.

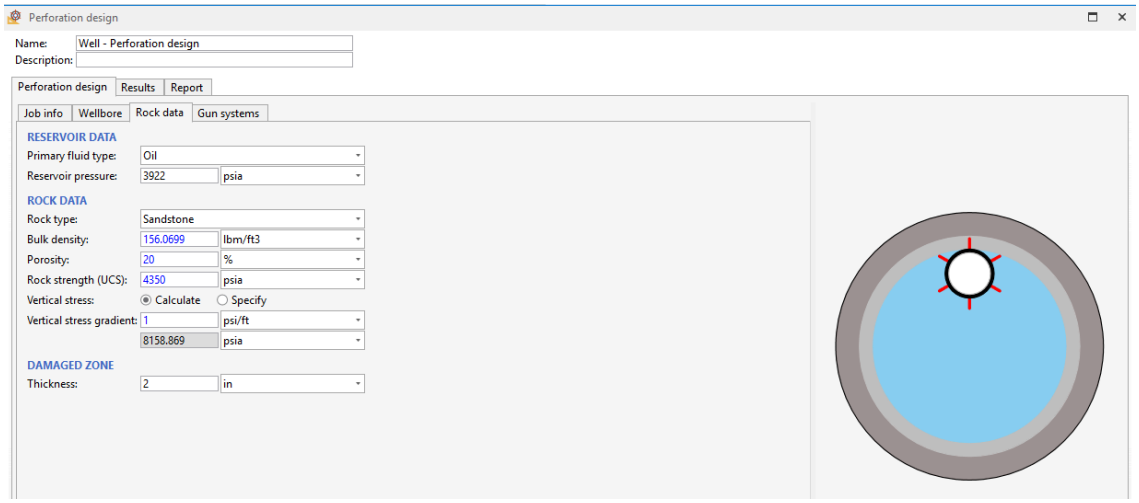

Figure 7.2.8. Perforation Design rock data.

Using a perforation design tool, just implementing the necessary parameters, design for perforation was done by the software.

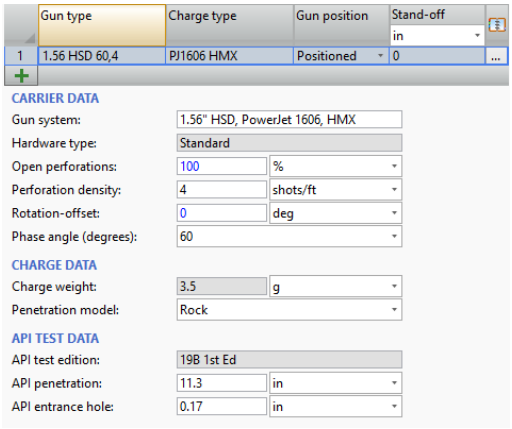

Figure 7.2.9. Gun type for Perforation.

For the final steps software choses the optimal gun type.

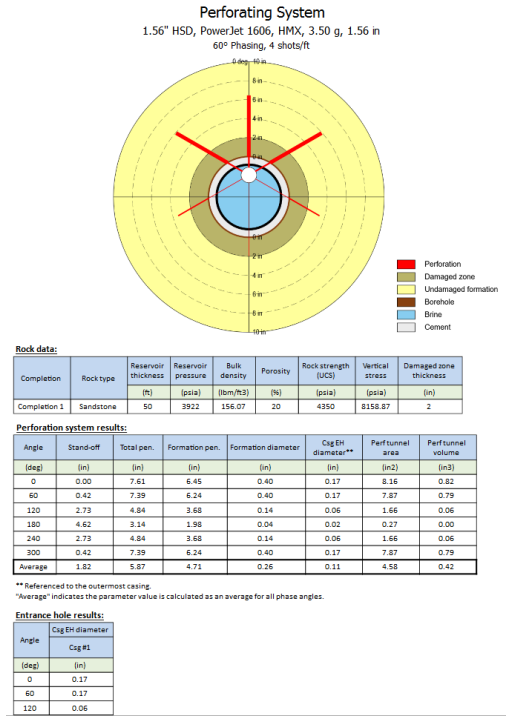

Figure 7.2.10. Final Perforation Design.

Finally, software designs the perforation design which you can install by clicking install button.

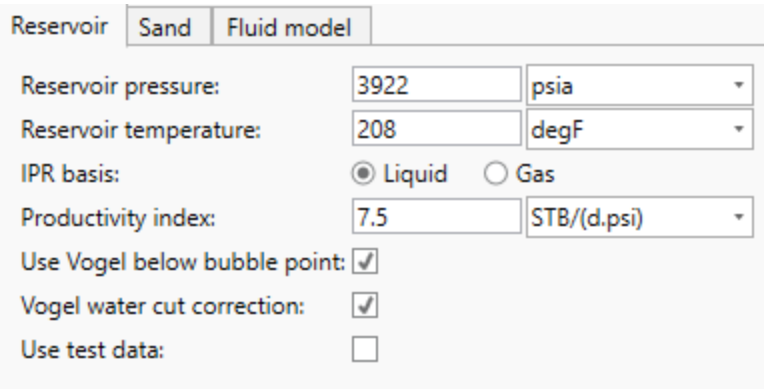

Figure 7.2.11. Reservoir Properties.

B-4H is an oil reservoir being liquid base operated at 3922 psia pressure and 208°F temperature. Productivity Index of 7.5 STB/d.psi makes the well moderate production potential. The fluid composition is corrected by water cut below bubble point and the Vogel model is applied below the bubble point. The model chosen is then a valid one for evaluation of the inflow performance under these conditions.

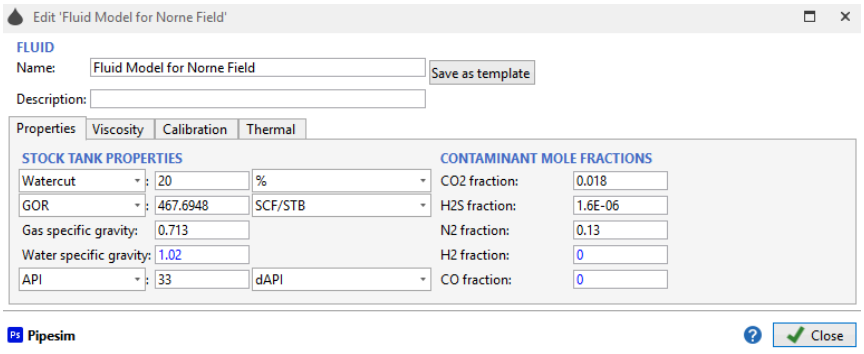

Figure 7.2.12. Fluid Properties.

For the Norne Field, the fluid model has a water cut of 20%, GOR of 467.69 SCF/STB, gas specific gravity of 0.713, and a water specific gravity of 1.02. The API gravity is 33 dAPI. Furthermore, the fluid contains 0.018 of CO_2, 0.13 of N_2, and a minimal H_2S fraction of 1.6E-06. Since they have these characteristics, a PIPESIM further downstream analysis is recommended in order to look at the oil and their related quantities and contaminants.

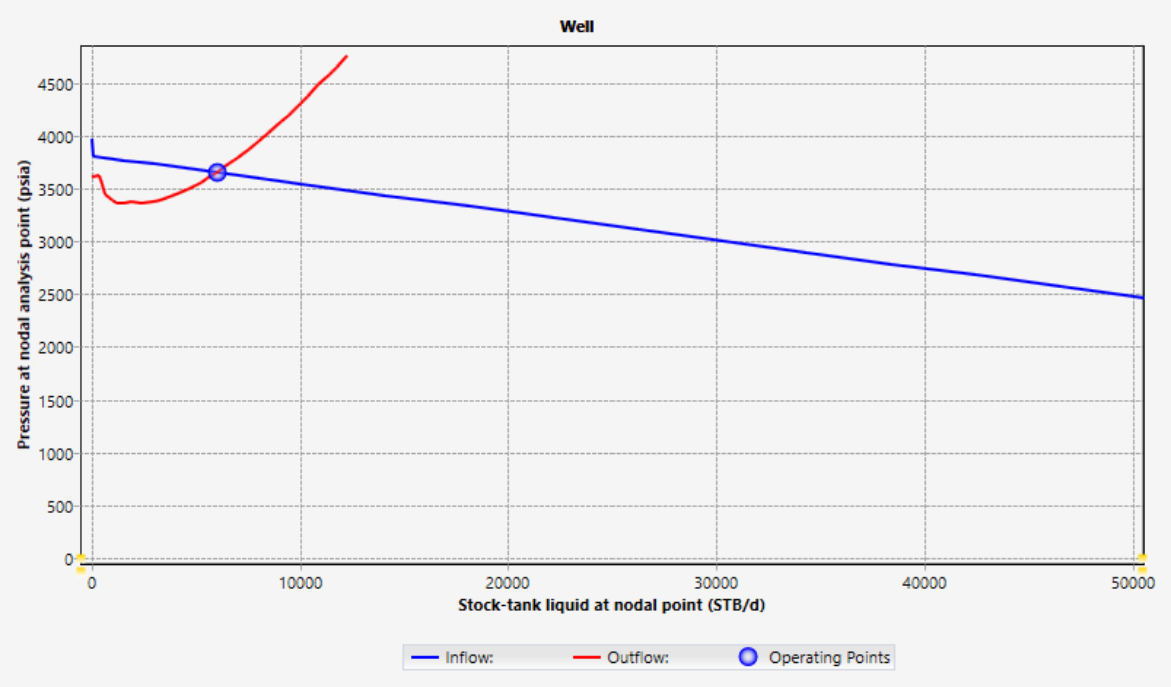

Figure 7.2.13. IPR/VLP curves for B-4H.

	Operating p...	ST Liq. at NA	P at NA
		STB/d	psia
1	Flowrate=60...	6020.545	3653.35

Figure 7.2.14. Operating Point.

The IPR curve (blue) and VLP curve (red) intersect at an operating point of 6020.545 STB/d flow rate and 3653.35 psia pressure. This point represents the optimal production rate and pressure under current well conditions.

$$\Delta P = \rho g h + f \frac{L}{D} \frac{\rho v^2}{2}$$

$$P_{th} = P_{bh} - \Delta P_{tubing}$$

Figure 7.2.15. Outlet Pressure Calculation Formula.

Using this formula and by nodal analysis that is provided below it was determined that the most optimal outlet pressure is 725 psia.

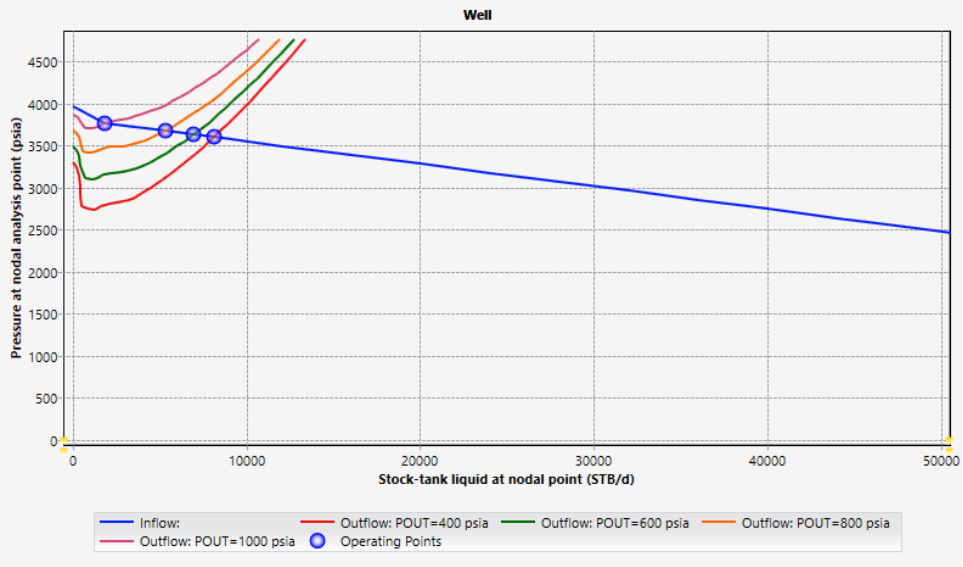

Figure 7.2.16. Sensitivity Analysis for Different Outflow Pressures.

	Operating p...	ST Liq. at NA	P at NA
		STB/d	psia
1	POUT=400...	8110.699	3597.601
2	POUT=600...	6974.199	3627.916
3	POUT=800...	5340.556	3671.483
4	POUT=1000...	1825.771	3765.164

Figure 7.2.19. Operating Points for different outflow pressures.

The figure depicts how the well's production rate diminishes with an increase in outflow pressure. The well produces 8110.699 STB/d at 400 psia with pressure of 3597.60 psia. At 600 psia outflow pressure, the production drops to 6974.199 STB/d at 3627.92 psia and additional down flow to 5340.556 STB/d at 800 psia. With a production rate of 1825.771 STB/d, production is reduced to only 1000 psia. This analysis illustrates that there is a significant loss of production when outflow pressure increases, highlighting the well

performance's sensitivity to the surface conditions. At the highest outflow pressure, the operating point is lowest and one can observe the need to manage backpressure in order to maintain maximum production rate.

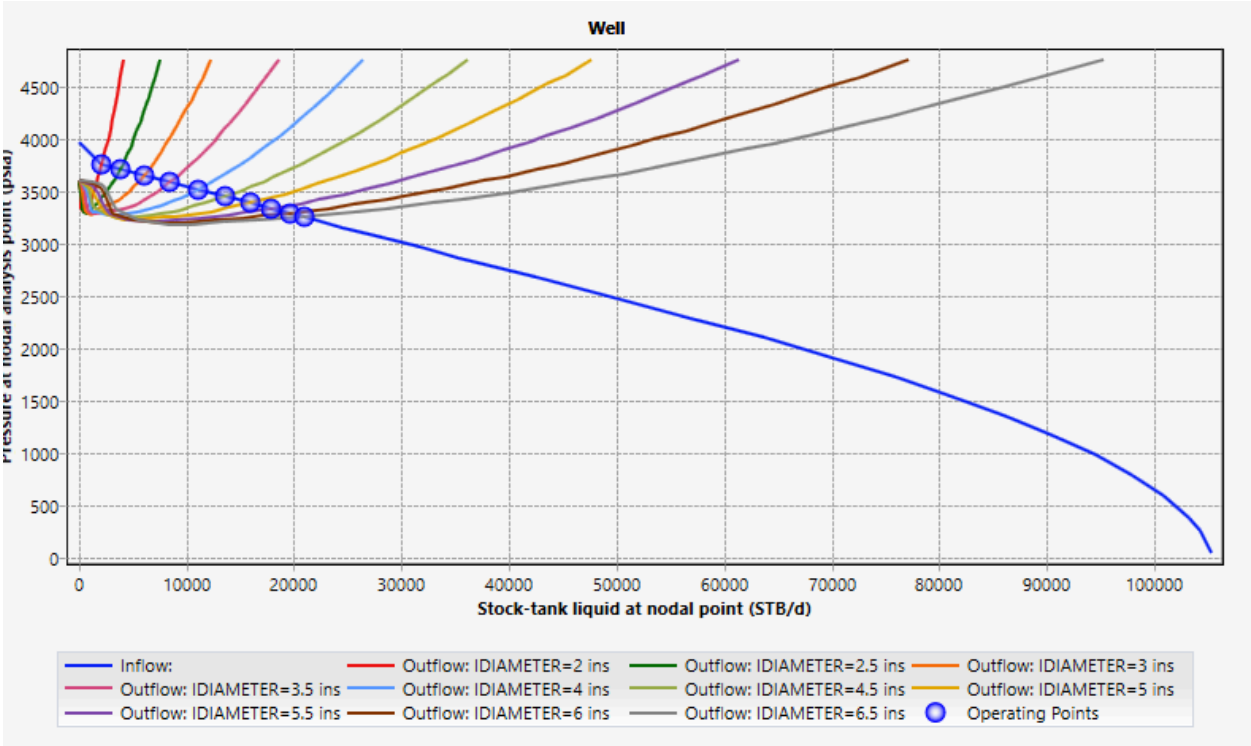

Figure 7.2.17. Sensitivity analysis for different tubing inner diameters.

	Operating point	ST Liq. at NA	P at NA
		STB/d	psia
1	IDIAMETER=2 ins Fl...	2151.523	3756.483
2	IDIAMETER=2.5 ins...	3905.187	3709.752
3	IDIAMETER=3 ins Fl...	6054.116	3652.454
4	IDIAMETER=3.5 ins...	8508.948	3586.976
5	IDIAMETER=4 ins Fl...	11079.98	3518.368
6	IDIAMETER=4.5 ins...	13612.56	3450.756
7	IDIAMETER=5 ins Fl...	15914.69	3389.27
8	IDIAMETER=5.5 ins...	17868.19	3337.076
9	IDIAMETER=6 ins Fl...	19650.8	3289.432
10	IDIAMETER=6.5 ins...	20997.17	3253.439

Figure 7.2.18. Operating Points for different tubing inner diameter.

The sensitivity analysis on various tubing inner diameters is presented and the production rate (STB/d) at the operating point increases greatly as the tubing diameter increases. The well is run at 2151.523 STB/d at 2 inches ID with a pressure of 3756.48 psia, and at 6.5 inches ID, the well runs at 20997.17 STB/d and at 3253.44 psia. In comparison the larger tubing diameters will reduce frictional pressure losses and thus also allow for higher flow rates at lower pressures, and exhibit that increased tubing diameter will improve well productivity but at the expense of greater equipment and higher initial costs.

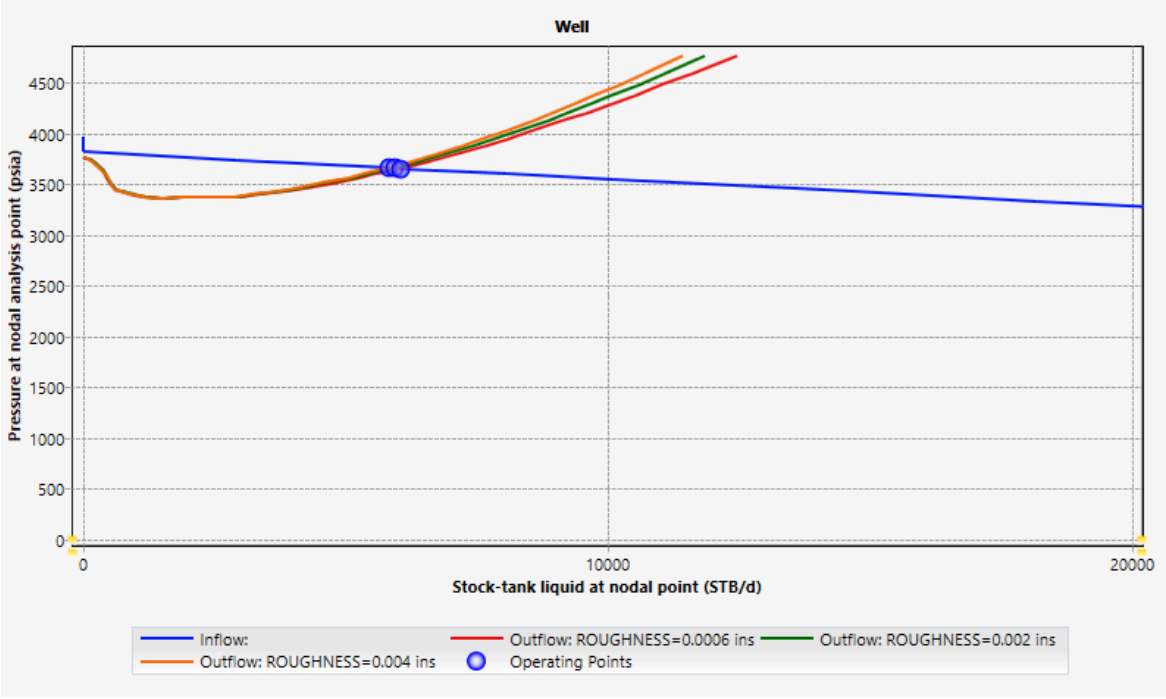

Figure 7.2.19. Sensitivity analysis for different tubing roughness.

	Operating point	ST Liq. at NA	P at NA
		STB/d	psia
1	ROUGHNESS=0.0006 ins...	6061.416	3652.26
2	ROUGHNESS=0.002 ins...	5933.378	3655.674
3	ROUGHNESS=0.004 ins...	5823.681	3658.599

Figure 7.2.20. Operating Points for different tubing roughness.

Therefore, different tubing roughness sensitivity analysis indicates that as the roughness increases, the well's production rate reduces. The operating point is 6061.416 STB/d at 3652.26 psia and is at a roughness of 0.0006 in. The production rate at 0.002 in roughness drops to 5933.378 STB/d at 3655.67 psia, and to 5823.681 STB/d at 3658.60 psia at 0.004 in roughness. This means that higher tubing roughness raises pressure losses and thus reduces the flow rate.

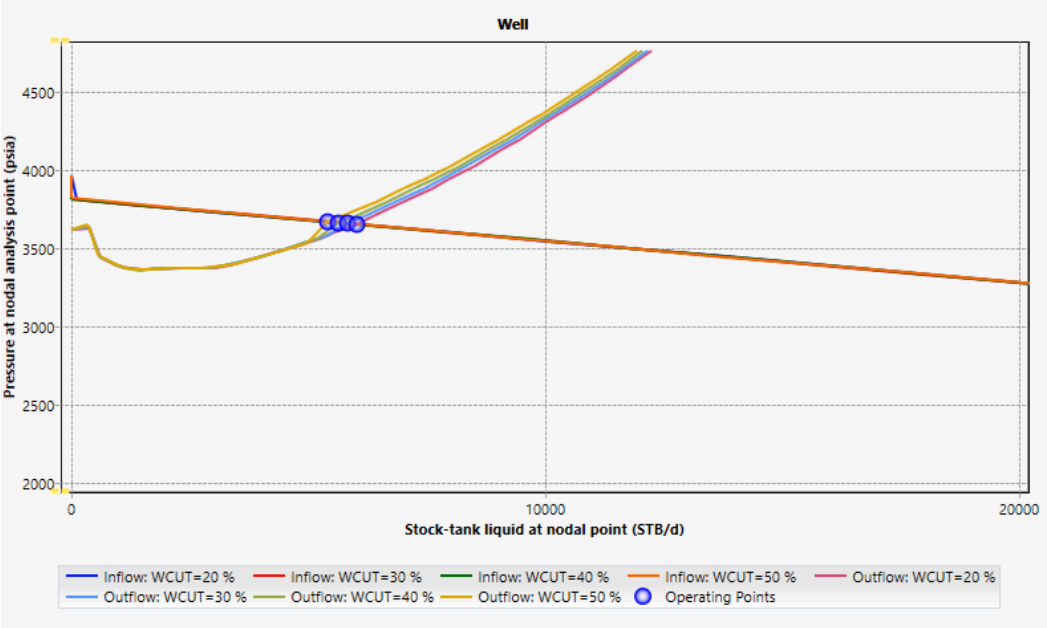

Figure 7.2.21. Sensitivity analysis for different water cuts.

	Operating p...	ST Liq. at NA	P at NA
		STB/d	psia
1	WCUT=20...	6020.545	3653.35
2	WCUT=30...	5845.397	3658.02
3	WCUT=40...	5635.457	3663.619
4	WCUT=50...	5402.936	3669.819

Figure 7.2.22. Operating Points for different water cuts.

Referring two graphs above it can be seen that water cut does not really affect the operating points. Which indicates good design.

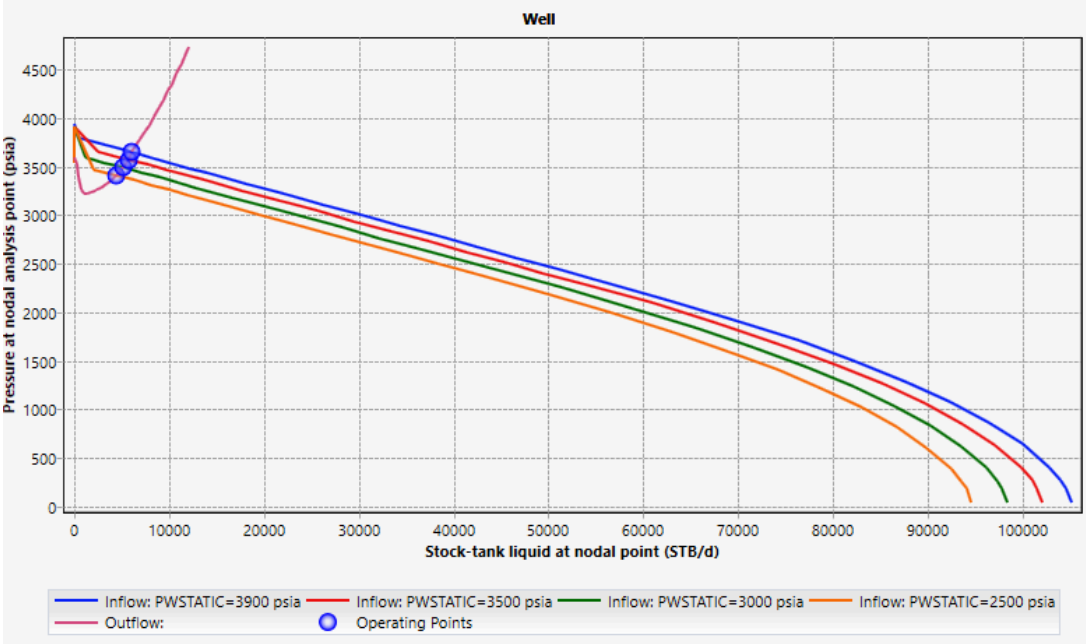

Figure 7.2.23. Sensitivity analysis for different reservoir pressure.

	Operating point	ST Liq. at NA	P at NA
		STB/d	psia
1	PWSTATIC=3900...	6011.224	3649.198
2	PWSTATIC=3500...	5803.24	3574.722
3	PWSTATIC=3000...	5140.452	3492.33
4	PWSTATIC=2500...	4438.2	3410.946

Figure 7.2.24. Operating Points for different reservoir pressures.

The operating point is 6011.224 STB/d at 3649.19 psia, which is an operating point at the highest reservoir pressure of 3900 psia. At the lowest pressure of 2500 psia, the production rate drops to 4438.2 STB/d at 3410.95 psia. Such a reduction in production is indicative of a decrease in reservoir pressure.

7.3 Design of Horizontal Well

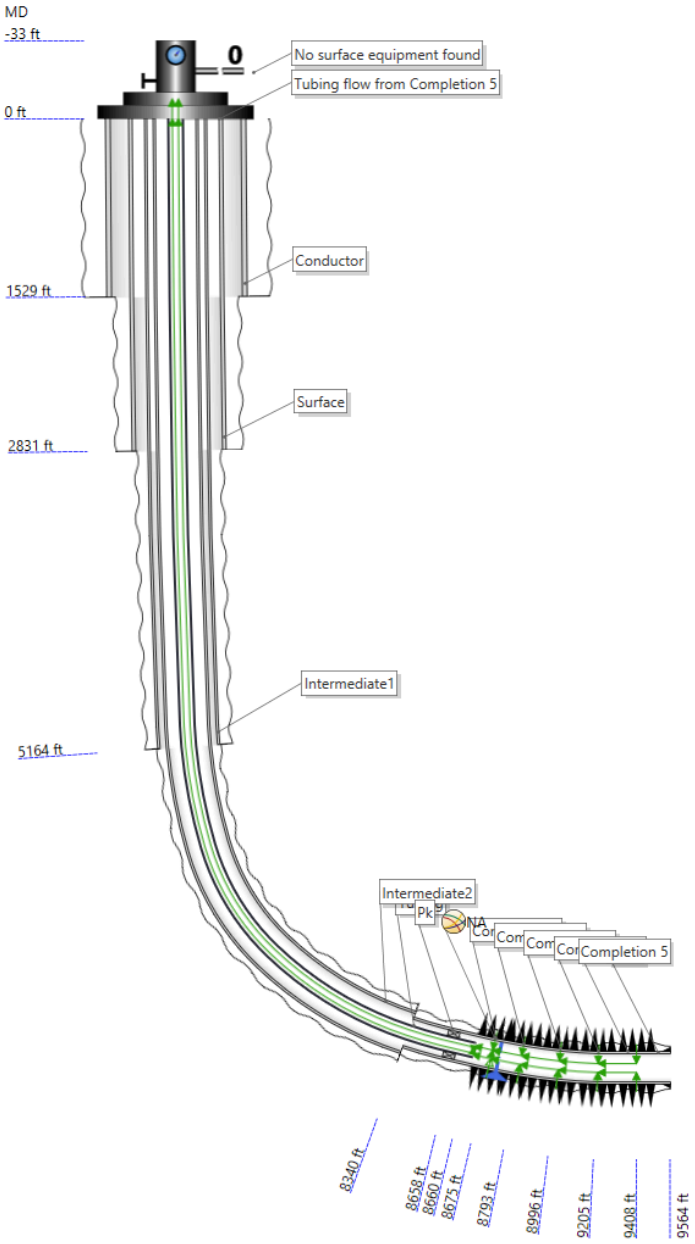

Figure 7.3.1. B-1H Horizontal Well's Schematic.

Both wells of B-1H horizontal well and B-4H vertical well have advantageous casing design, and equip comparable tubing and liner specification. The chief distinction is that the well,

B-1H, is horizontal to increase the reservoir contact area and increase the production potential as a result. Both wells are located close enough to each other so that the reservoir properties are almost the same. The comparison of these two wells is made mainly to study the difference in performance between vertical and horizontal completions under similar conditions and to decide which configuration leads to a better performance of production efficiency.

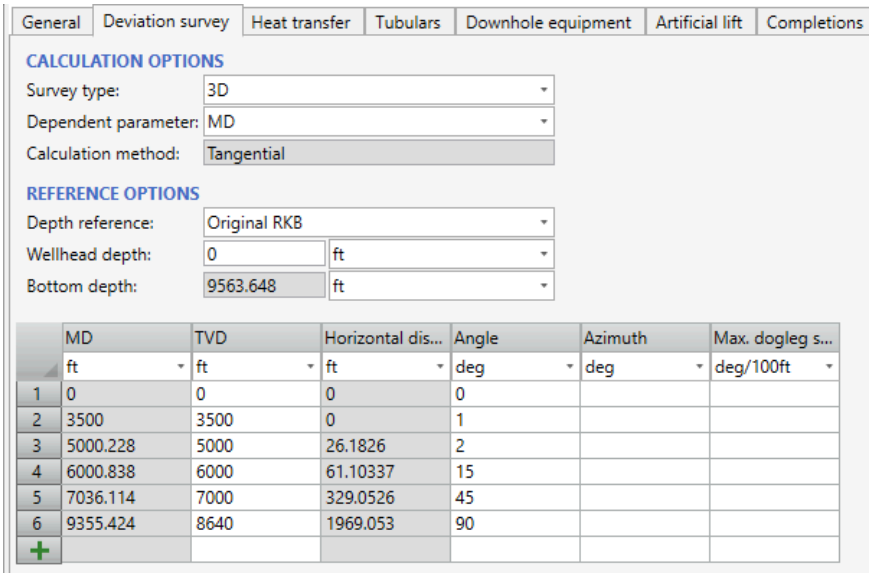

	MD	TVD	Horizontal dis...	Angle	Azimuth	Max. dogleg s...
	ft	ft	ft	deg	deg	deg/100ft
1	0	0	0	0		
2	3500	3500	0	1		
3	5000.228	5000	26.1826	2		
4	6000.838	6000	61.10337	15		
5	7036.114	7000	329.0526	45		
6	9355.424	8640	1969.053	90		

Figure 7.3.2. Deviation survey for Horizontal Well.

The B-1H horizontal well path from surface to 9563.648 ft. is shown in the deviation survey. The first step of the well is without horizontal displacement and gradually increases to 1969.053 ft at 9355.424 ft MD. At the target depth (7000 ft MD), the maximum dogleg severity is 45 degrees/100 ft, with an azimuth of 90°, at the well's depth of maximum deviation (dmd) of 7000 ft MD. As shown, this horizontal path improves contact with the reservoir for better production than vertical wells.

CASINGS/LINERS

	Section type	Name	From MD	To MD	ID	OD	Roughness
			ft	ft	in	in	in
1	Casing	Conductor	0	1528.871	28	30	0.001
2	Casing	Surface	0	2831.365	18.75	20	0.001
3	Casing	Intermediate1	0	5164.042	12.347	13.375	0.001
4	Casing	Intermediate2	0	8339.895	8.407	9.625	0.001
5	Liner	Liner	8339.895	9563.648	6.184	7	0.001

TUBINGS

	Name	To MD	ID	OD	Roughness
		ft	in	in	in
1	Tubing	8660	2.992	3.5	0.001

Figure 7.3.3. Casing and Tubing Design for B-1H.

	Equipment	Name	Active	MD
				ft
1	Packer	Pk	☑	8658.458
2		NA	☑	8675

Figure 7.3.4. Packer Design for B-1H.

COMPLETIONS

	Name	Geometry pro...	Fluid entry	Top MD	Middle MD	Bottom MD	Type	Active	IPR model
				ft	ft	ft			
1	Completion 1	Horizontal	Single point		8675		Perforation	☑	Joshi (Stea...
2	Completion 2	Horizontal	Single point		8793.476		Perforation	☑	Joshi (Stea...
3	Completion 3	Horizontal	Single point		8995.919		Perforation	☑	Joshi (Stea...
4	Completion 4	Horizontal	Single point		9204.685		Perforation	☑	Joshi (Stea...
5	Completion 5	Horizontal	Single point		9407.802		Perforation	☑	Joshi (Stea...

Figure 7.3.5. Horizontal Completions.

This shows the horizontal completions for the B-1H well with 8675 ft MD to 9407.802 ft MD based on five single point perforations in which the well passes through. The purpose is to complete these over the top of reservoir contact along the horizontal section of the well. All perforations are made active and are modeled using the Joshi (Steady State) IPR model, which is a typical model for evaluating horizontal wells under the steady state conditions. It

optimizes fluid entry from the reservoir into the wellbore and therefore it is very efficient in producing.

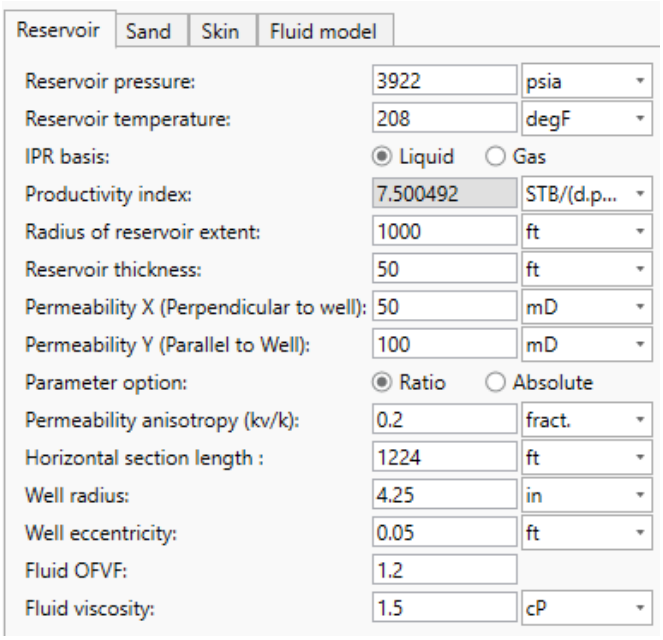

Figure 7.3.6. Reservoir Properties.

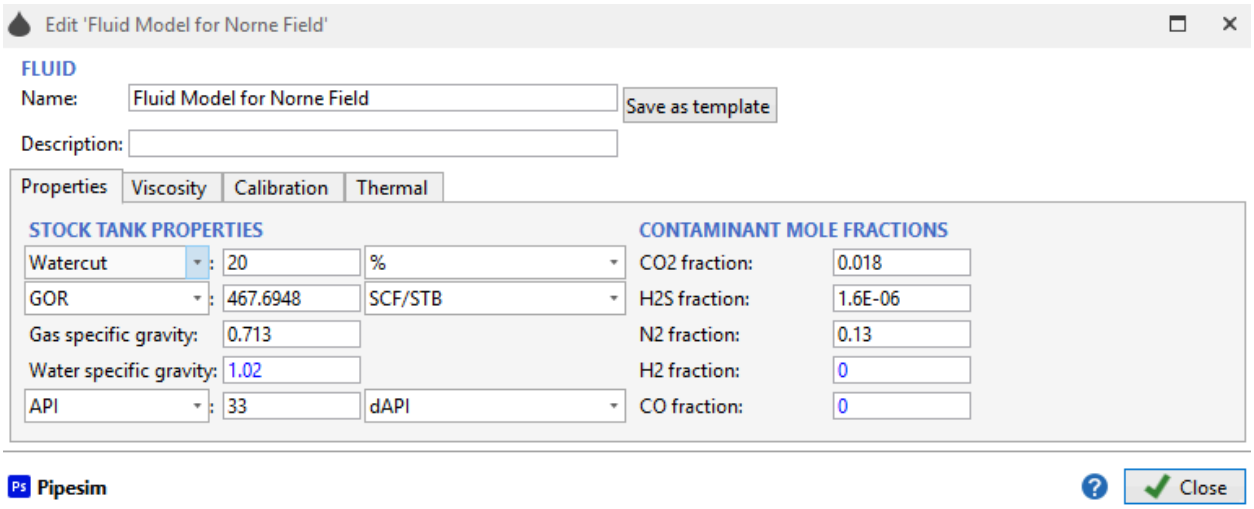

Figure 7.3.7. Fluid Properties.

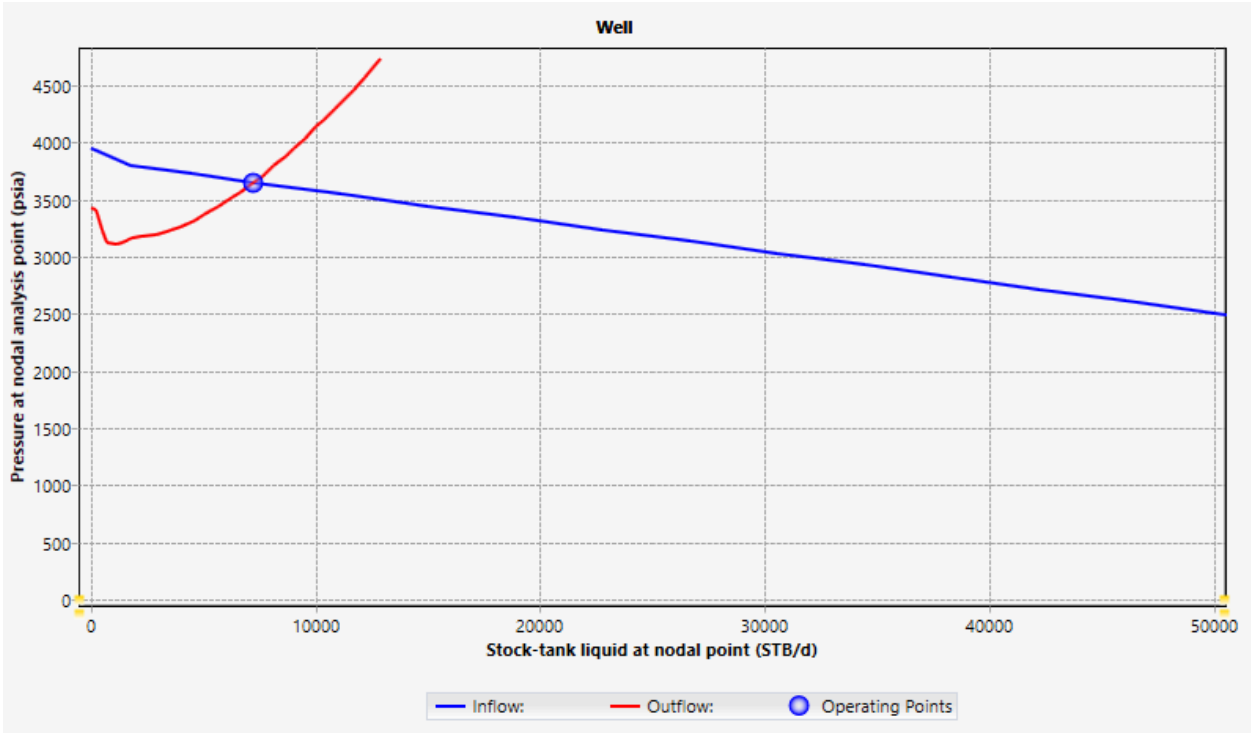

Figure 7.3.8. IPR/VLP curves for B-1H.

	Operating p...	ST Liq. at NA	P at NA
		STB/d	psia
1	Flowrate=72...	7259.787	3651.921

Figure 7.3.9. Operating Points for B-1H.

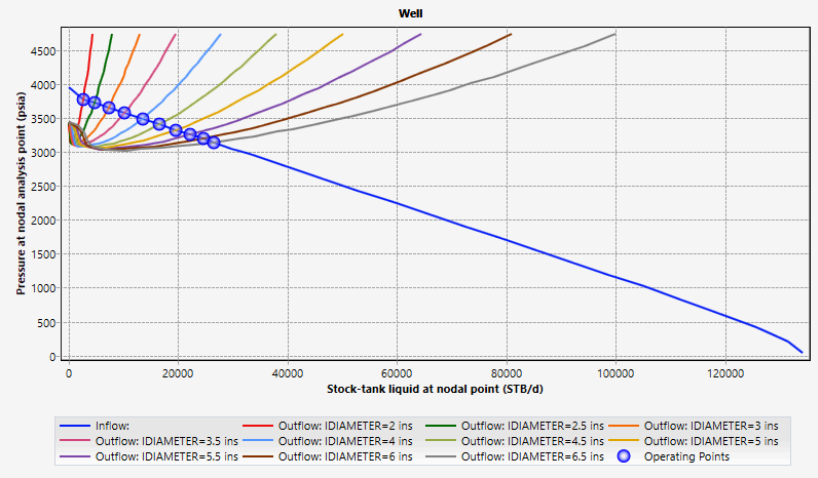

Figure 7.3.1. Sensitivity analysis for different tubing inner diameters.

	Operating point	ST Liq. at NA	P at NA
		STB/d	psia
1	IDIAMETER=2 ins...	2668.132	3774.386
2	IDIAMETER=2.5 in...	4720.596	3719.657
3	IDIAMETER=3 ins...	7298.574	3650.886
4	IDIAMETER=3.5 in...	10286.03	3571.15
5	IDIAMETER=4 ins...	13486.92	3485.668
6	IDIAMETER=4.5 in...	16645.02	3401.28
7	IDIAMETER=5 ins...	19649.31	3320.958
8	IDIAMETER=5.5 in...	22298.81	3250.087
9	IDIAMETER=6 ins...	24603	3188.427
10	IDIAMETER=6.5 in...	26484.49	3138.06

Figure 7.3.10. Operating Points for different tubing inner diameter.

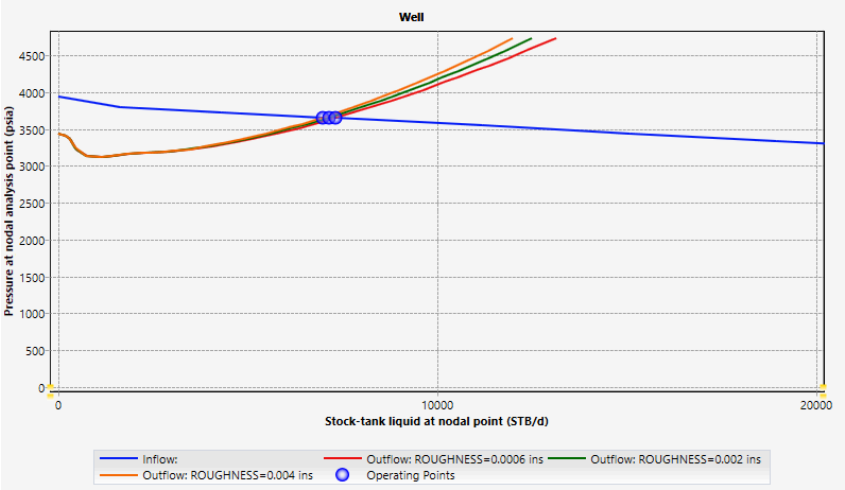

Figure 7.3.11. Sensitivity analysis for different tubing roughness.

	Operating point	ST Liq. at NA	P at NA
		STB/d	psia
1	ROUGHNESS=0.0006 ins...	7318.746	3650.348
2	ROUGHNESS=0.002 ins...	7143.437	3655.026
3	ROUGHNESS=0.004 ins...	6993.757	3659.019

Figure 7.3.12. Operating Points for different tubing roughness.

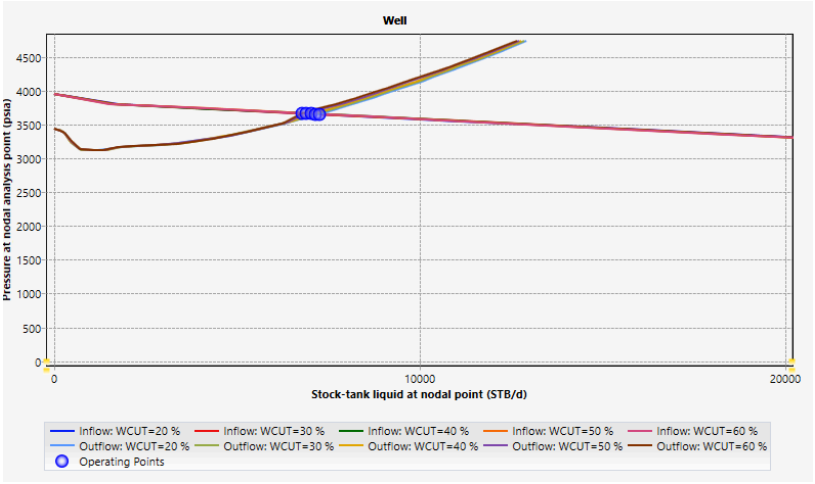

Figure 7.3.13. Sensitivity analysis for different water cuts.

	Operating p...	ST Liq. at NA	P at NA
		STB/d	psia
1	WCUT=20...	7259.787	3651.921
2	WCUT=30...	7150.393	3654.84
3	WCUT=40...	7034.256	3657.939
4	WCUT=50...	6910.067	3661.252
5	WCUT=60...	6777.008	3664.802

Figure 7.3.14. Operating Points for different water cuts.

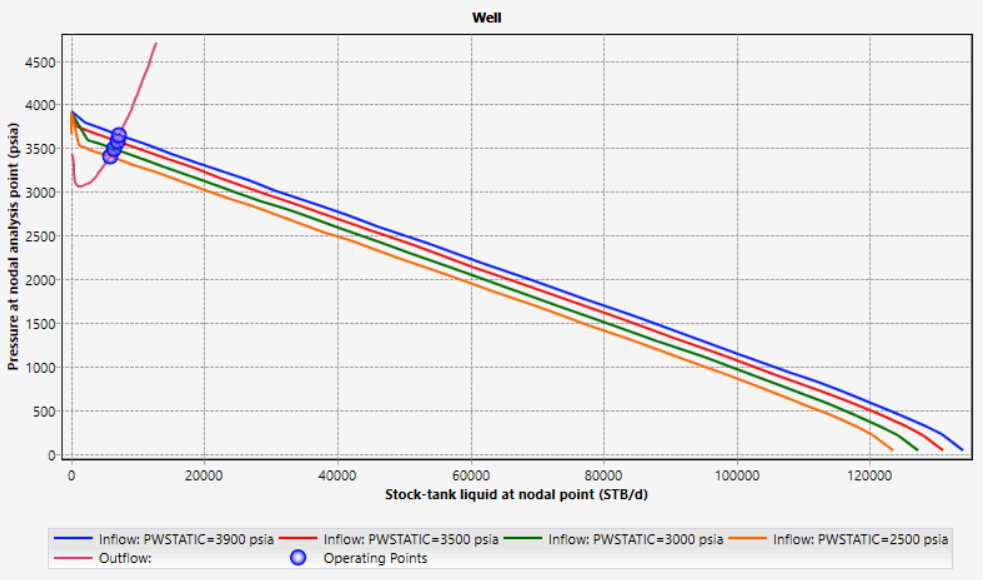

Figure 7.3.15. Sensitivity analysis for different reservoir pressure.

	Operating p...	ST Liq. at NA	P at NA
		STB/d	psia
1	PWSTATIC=...	7247.709	3647.84
2	PWSTATIC=...	6998.13	3574.425
3	PWSTATIC=...	6421.864	3489.664
4	PWSTATIC=...	5830.866	3405.247

Figure 7.3.16. Operating Points for different reservoir pressures.

The B-1H horizontal well has greater production potential than the B-4H vertical well, which have similar casing design but different orientations. Sensitivity analyses indicate that larger tubing diameters and smoother tubing surfaces lead to greater flow rates and less pressure at the outflow while increasing outflow pressure and water cut decrease production by wide margins. Both wells are shown to have a clear decline in production with reservoir pressure, which is imperative to maintaining reservoir pressure. However, horizontal well's enhanced reservoir contact area improves efficiency yet like well type, both must be managed with care for outflow pressure, tubing size, roughness and water cut either to avoid production failure.

Table 7.3.1. Comparison of two wells

Parameter	**B-1H Vertical Well**	**B-4H Horizontal Well**
Reservoir Pressure	3922 psia	3922 psia
Production Rate	6020.545 STB/d	7259.787 STB/d
Operating Pressure	3653.35 psia	3651.92 psia
Outflow Pressure Sensitivity	Significant drop with higher outflow pressure	Similar drop with higher outflow pressure
Tubing Diameter Sensitivity	Larger tubing slightly increases flow	Larger tubing moderately increases flow

Tubing Roughness Sensitivity	Smoother tubing slightly increases flow	Smoother tubing moderately increases flow
Water Cut Sensitivity	Higher water cut decreases flow	Higher water cut slightly decreases flow
Reservoir Pressure Sensitivity	Production declines with pressure drop	Similar trend as B-1H

7.4 Nodal Analysis of CO2 Injection Well (C-4H)

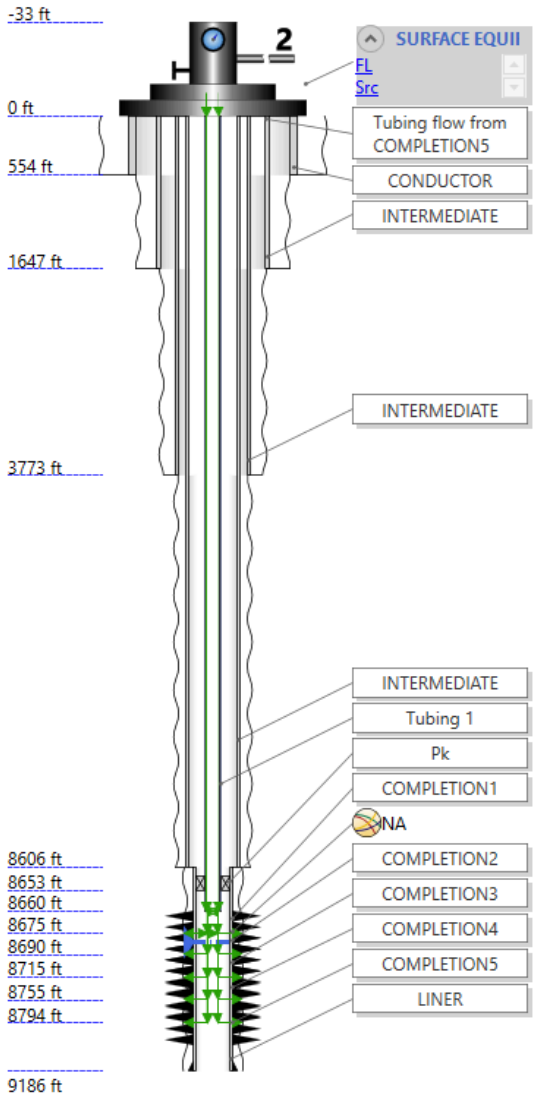

Figure 7.4.1. Schematic for Injection well (C-4H)

	Section type	Name	From MD	To MD	ID	OD	Roughness
			ft	ft	in	in	in
1	Casing	CONDUCTOR	0	554.4619	27.5	30	0.001
2	Casing	INTERMEDIATE	0	1646.982	18.73	20	0.001
3	Casing	INTERMEDIATE	0	3772.966	12.347	13.375	0.001
4	Casing	INTERMEDIATE	0	8605.643	8.435	9.625	0.001
5	Liner	LINER	8605.643	9186.352	6.004	7	0.001

TUBINGS

	Name	To MD	ID	OD	Roughness
		ft	in	in	in
1	Tubing 1	8660	2.195	2.875	0.001

Figure 7.4.2. Casing and tubing design for Injection well

General | Tubulars | Deviation survey | Downhole equipment | Art

	Equipment	Name	Active	MD
				ft
1	Packer	Pk	☑	8652.619
2		NA	☑	8675

Figure 7.4.3. Downhole Equipment

	Name	Geometry prof...	Fluid entry	Top MD	Middle MD	Bottom MD	Type	Active	IPR model
				ft	ft	ft			
1	COMPLETION1	Vertical	Single point		8675		Perforation	☑	Well PI
2	COMPLETION2	Vertical	Single point		8690		Perforation	☑	Well PI
3	COMPLETION3	Vertical	Single point		8715		Perforation	☑	Well PI
4	COMPLETION4	Vertical	Single point		8755		Perforation	☑	Well PI
5	COMPLETION5	Vertical	Single point		8794		Perforation	☑	Well PI

Figure 7.4.4. Completions

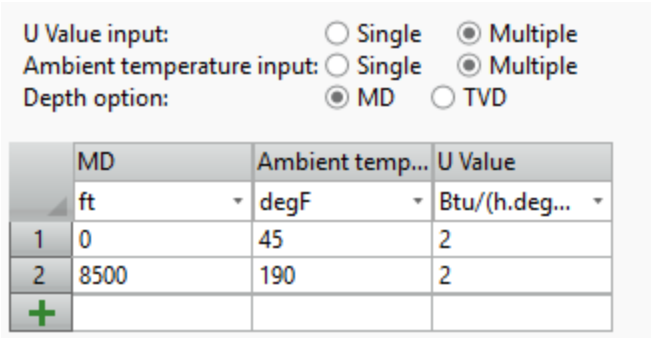

Figure 7.4.5. Heat Transfer Data

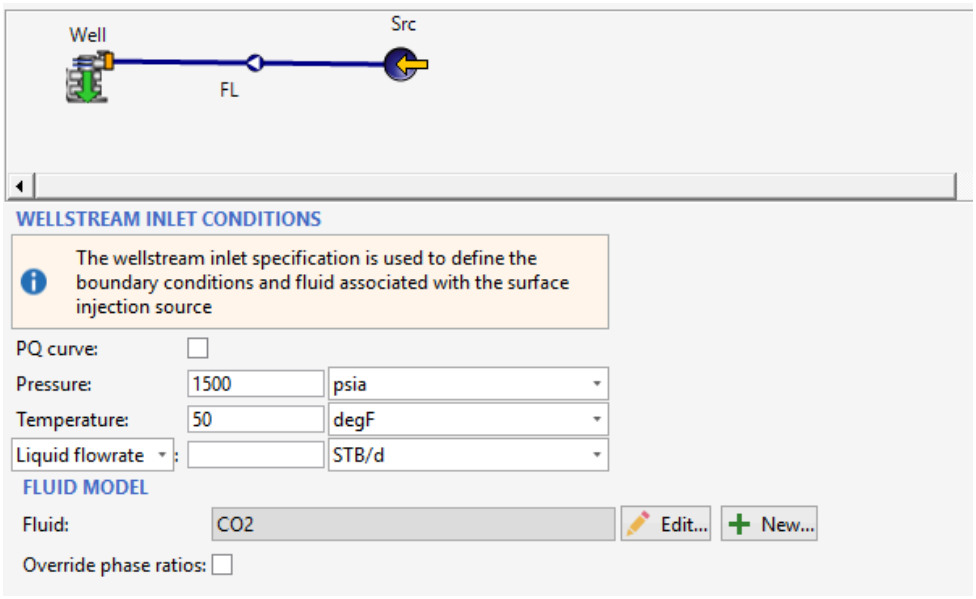

Figure 7.4.6. Surface Equipment

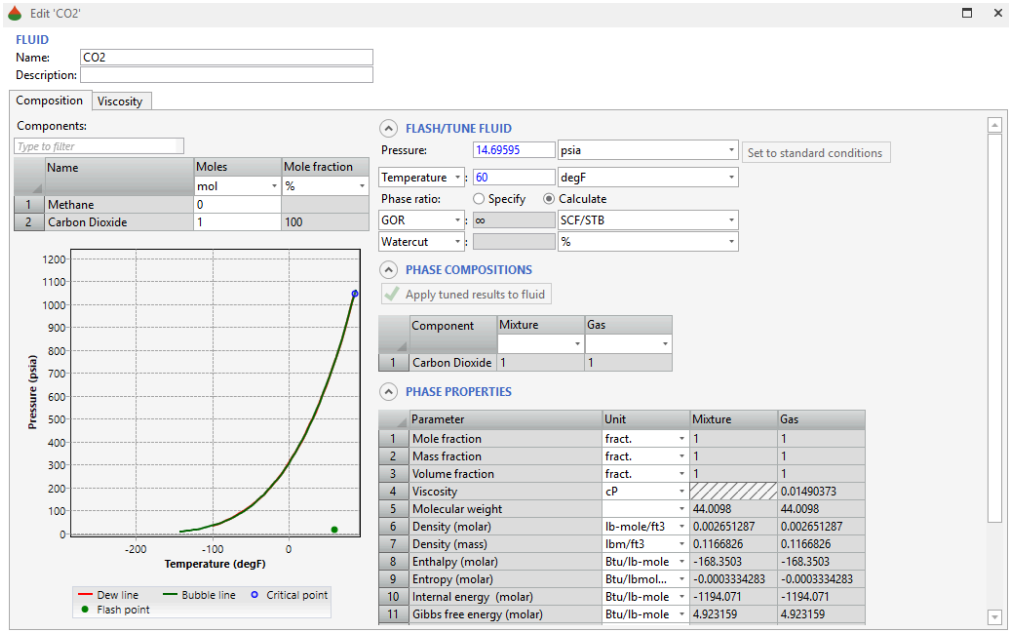

Figure 7.4.7. Compositional Fluid Manager (CO2)

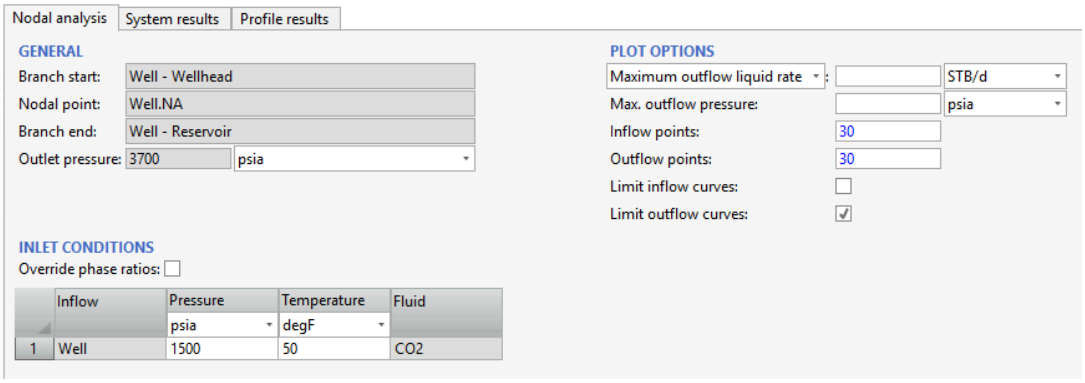

Figure 7.4.8. Inlet Conditions

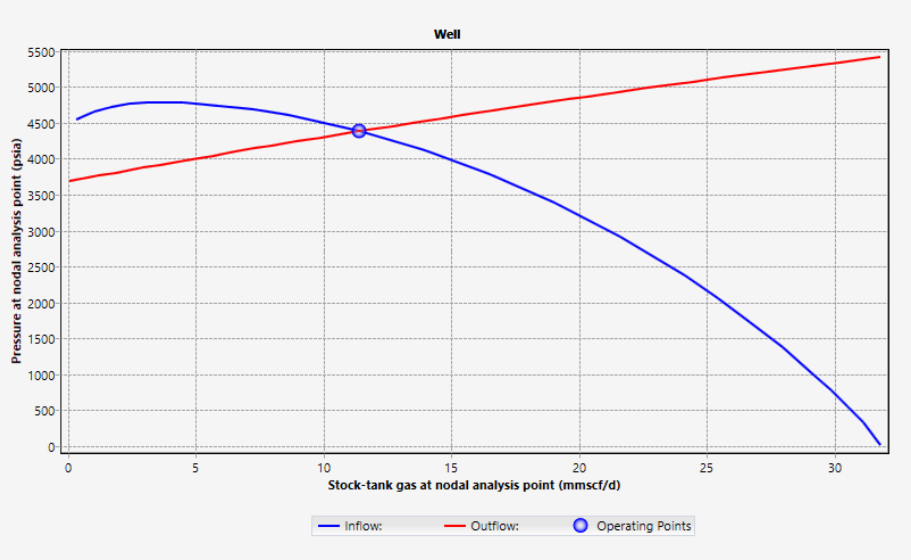

Figure 7.4.9. IPR and TPR curves

	Operating p...	P at NA	ST Gas at NA
		psia	mmscf/d
1	Flowrate=15...	4384.053	11.40587

Figure 7.4.10. Operating Point

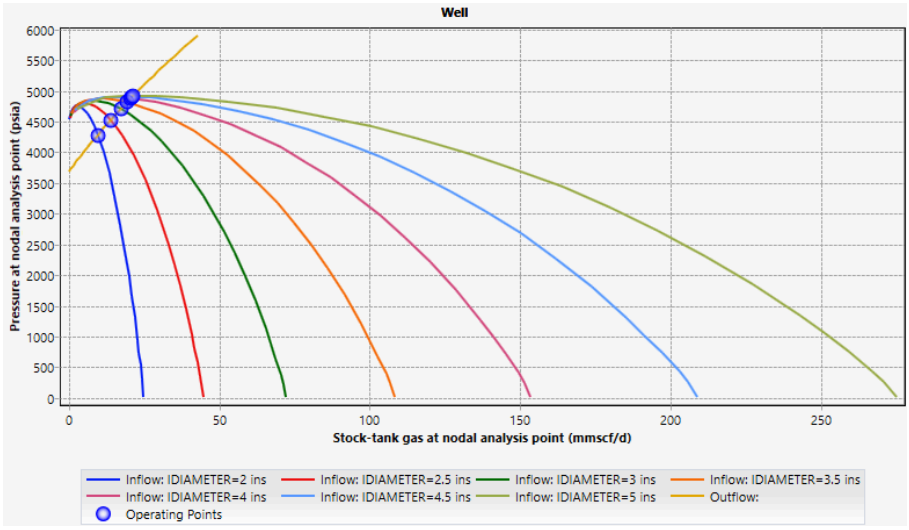

Figure 7.4.11. Sensitivity analysis for different tubing inner diameters.

	Operating point	P at NA	ST Gas at NA
		psia	mmscf/d
1	IDIAMETER=2...	4283.132	9.644122
2	IDIAMETER=2....	4527.175	13.97206
3	IDIAMETER=3...	4706.012	17.29289
4	IDIAMETER=3....	4815.3	19.38404
5	IDIAMETER=4...	4874.429	20.53535
6	IDIAMETER=4....	4904.075	21.11747
7	IDIAMETER=5...	4917.807	21.38661

Figure 7.4.12. Operating points for different tubing diameters.

The B-1H horizontal production well was designed and is implemented through utilization of the same casing and tubing as the C-4H injection well, but optimized for pressure maintenance. The well has five perforated feet at 8652.619 ft for zonal isolation and effective CO_2 injection into the target reservoir. It has an inner diameter of 2.195 inches for minimal roughness of 0.001 in reducing friction and increasing injection efficiency. Stable injection conditions are supported using an inlet pressure of 1500 psia and 50°F temperature at the surface with the fluid being 100% CO_2. Then the well's operating point at 15 mmscf/d CO_2 flow rate is 4384.053 psia. Results show that building injection performance through tubing diameter and roughness is important and IPR and TPR curves show that CO_2 injection supports reservoir pressure maintenance, thus enabling efficient field development.

7.5 Nodal Analysis of Water Injection Well (C-4H)

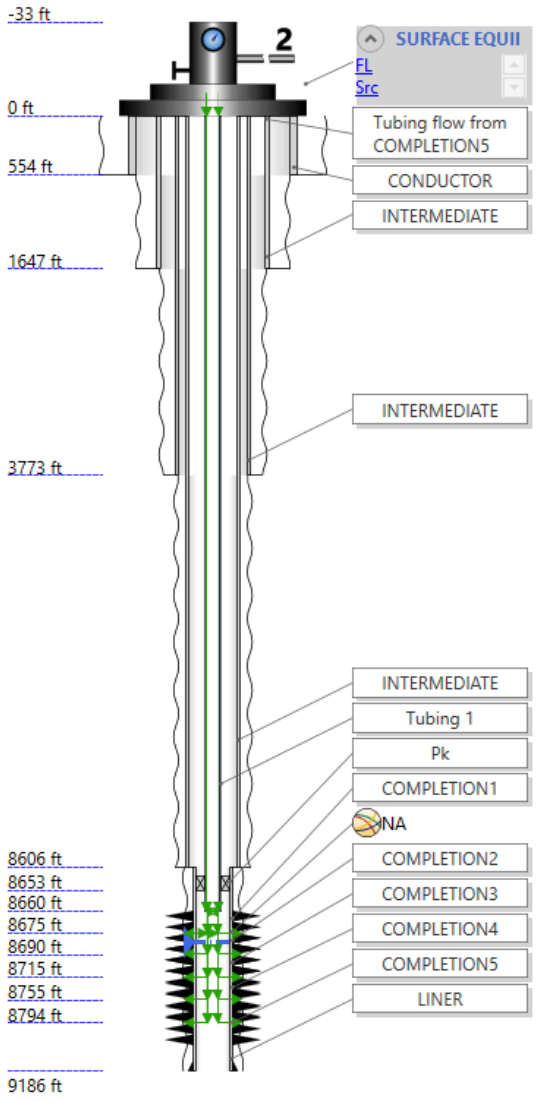

Figure 7.5.1. Schematic for new water injection well (C-4H)

	Section type	Name	From MD	To MD	ID	OD	Roughness
			ft	ft	in	in	in
1	Casing	Conductor	0	540	26	30	0.001
2	Casing	Surface	0	1650	18.5	20	0.001
3	Casing	Intermediate	0	3750	15	16	0.001
4	Casing	Intermediate	0	6500	12.4	13	0.001
5	Liner	Injection Liner	6500	7200	8.7	9.375	0.001

TUBINGS

	Name	To MD	ID	OD	Roughness
		ft	in	in	in
1	Tubing	7000	2.3	2.9	0.001

Figure 7.5.2. Casing and tubing design for new Injection well.

U Value input: ○ Single ◉ Multiple

Ambient temperature input: ○ Single ◉ Multiple

Depth option: ◉ MD ○ TVD

	MD	Ambient temp...	U Value
	ft	degF	Btu/(h.deg...
1	0	65	1.5
2	1650	100	1.8
3	3750	130	2
4	6500	170	2.5
5	7200	208	3

Figure 7.5.3. Heat Transfer Data.

	Name	Geometry prof...	Fluid entry	Top MD	Middle MD	Bottom MD	Type	Active	IPR model
				ft	ft	ft			
1	COMPLETION1	Vertical	Single point		8675		Perforation	☑	Well PI
2	COMPLETION2	Vertical	Single point		8690		Perforation	☑	Well PI
3	COMPLETION3	Vertical	Single point		8715		Perforation	☑	Well PI
4	COMPLETION4	Vertical	Single point		8755		Perforation	☑	Well PI
5	COMPLETION5	Vertical	Single point		8794		Perforation	☑	Well PI

Figure 7.5.4. Completions for new Injection well.

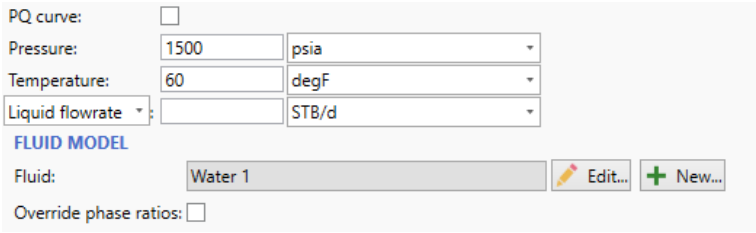

Figure 7.5.5. Wellstream inlet conditions

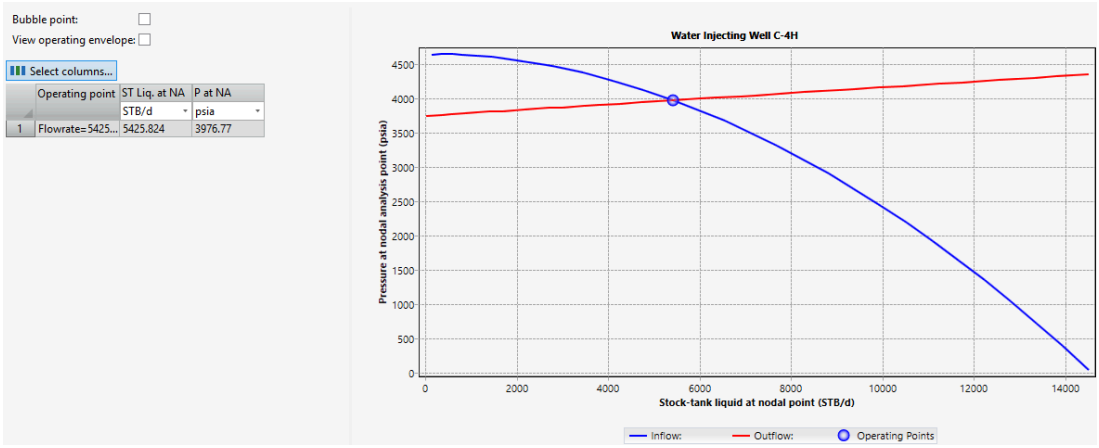

Figure 7.5.6. IPR and TPR curves with operating points.

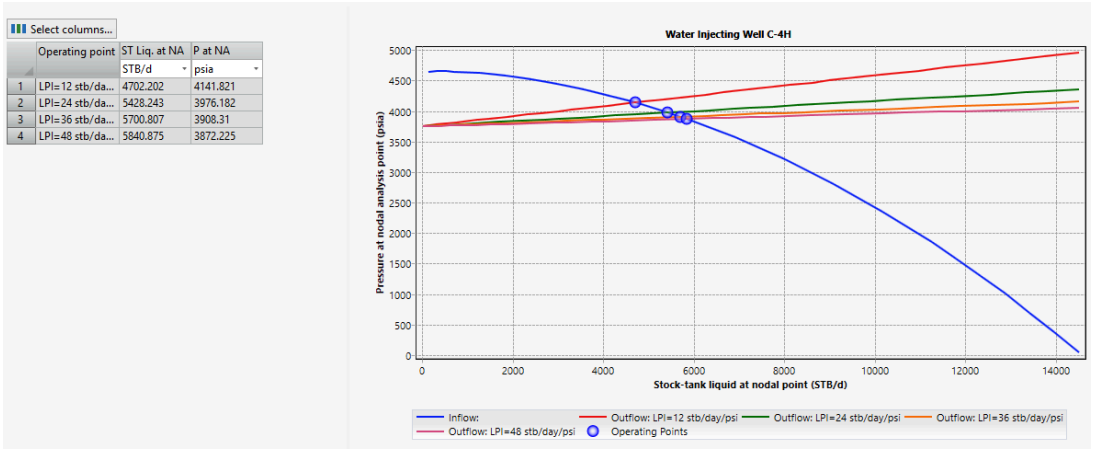

Figure 7.5.7. Sensitivity analysis for different injectivity index.

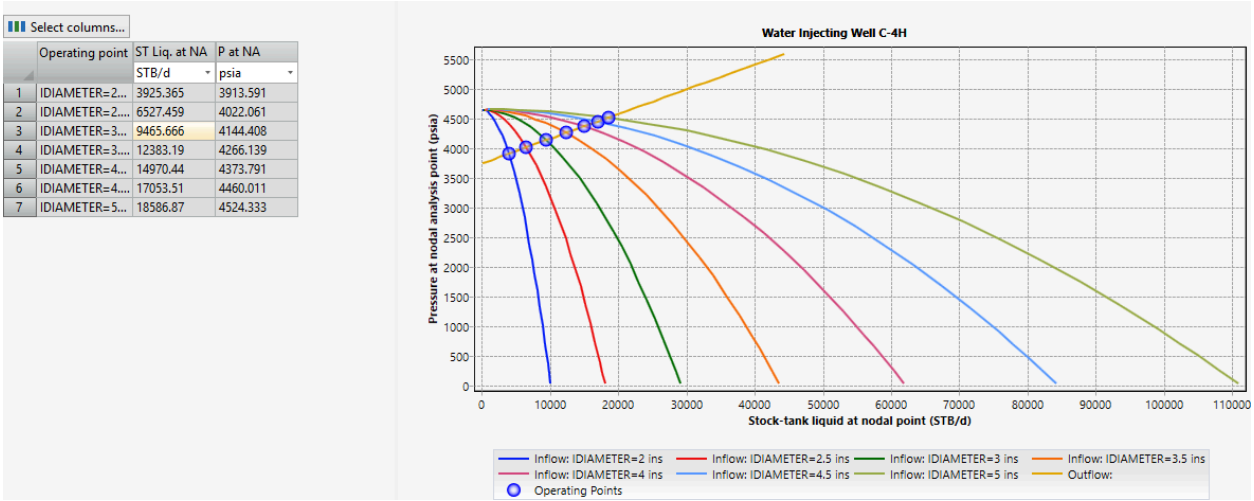

Figure 7.5.8. Sensitivity analysis for different tubing inner diameters.

The B-1H horizontal well and the C-4H water injection well are designed in basically the same way except for the latter being optimized for water injection. It has multiple perforations, optional packer at 8652.619 ft and zonal isolation. Minimal roughness of the tubing has an inner diameter of 2.3 inches, reducing friction to a great extent. The well is operated at 1500 psia and 60°F and produces 30 STB/d at the rate of flow. The injection rates are sensitive to larger tubing diameters and to higher injectivity. The well will also help to maintain reservoir pressure and improve sweep.

7.6 Artificial Lift

After 8 years of production, the reservoir pressure reduced to 2750 psia and the water cut increased to 40%, the well went non productive or so called “dead well”.

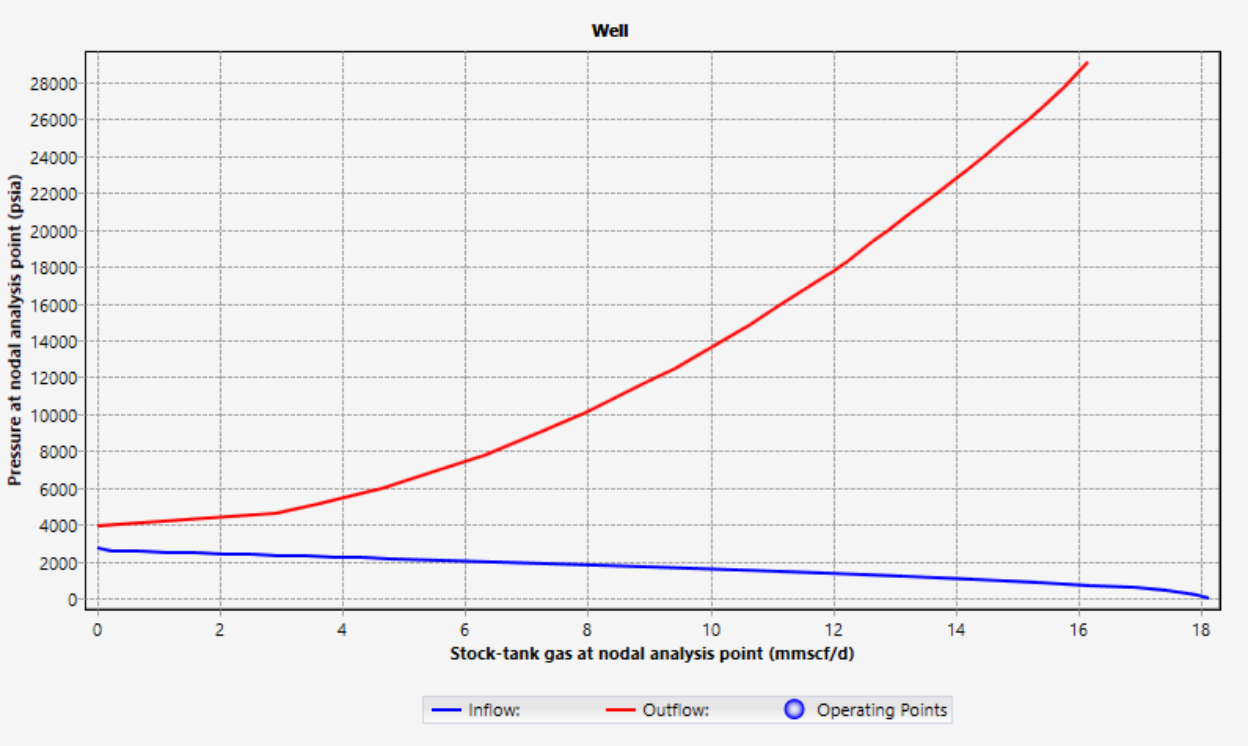

Figure.7.6.1. IPR/VLP curve after 8 years

Therefore artificial lift was needed and the first system of choice was the Electric Submersible Pump (ESP). Assuming that we are going to have high flow rate around 25000 stb/day

We chose this model and manufactures with parameters as follows:

7.6.1 ESP Design

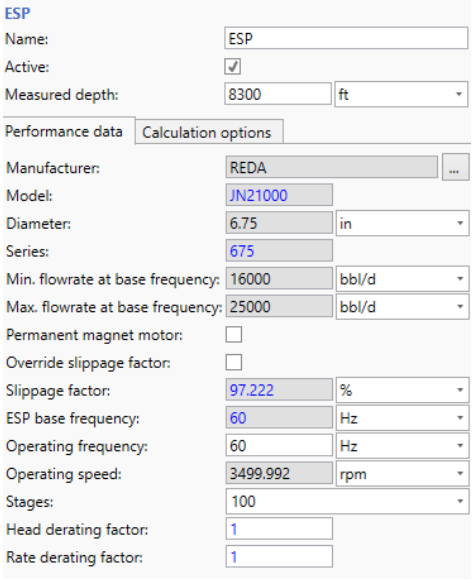

Figure 7.6.2. ESP design

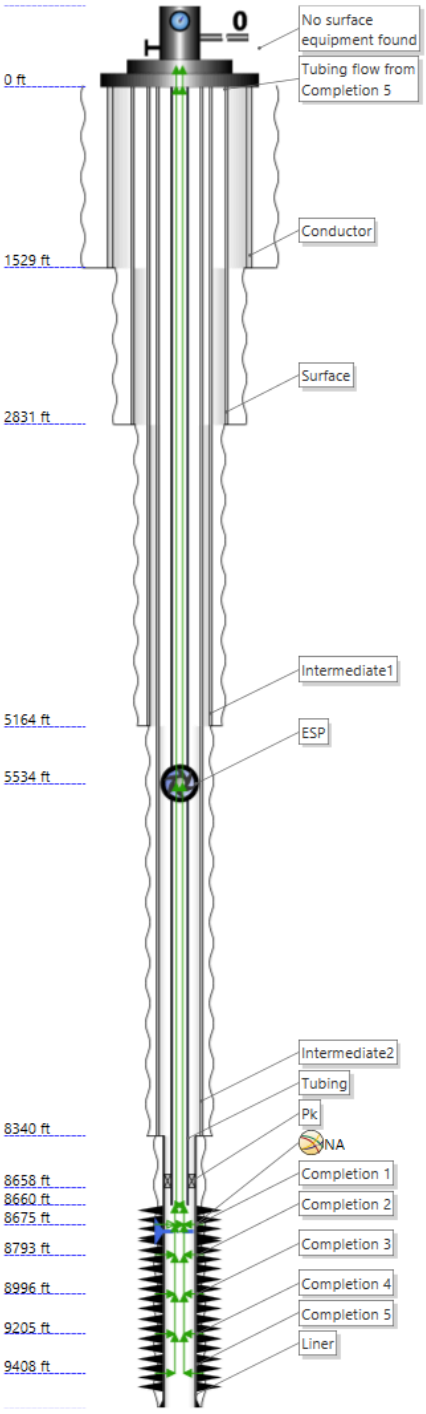

Figure 7.6.3. Schematic for Production well with ESP (B-4H)

Figure 7.6.4. IPR/VLP curve with ESP.

	Operating p...	ST Liq. at NA	P at NA
		STB/d	psia
1	Flowrate=11...	11016.8	2335.802

Figure 7.6.5. Operating points with installed ESP.

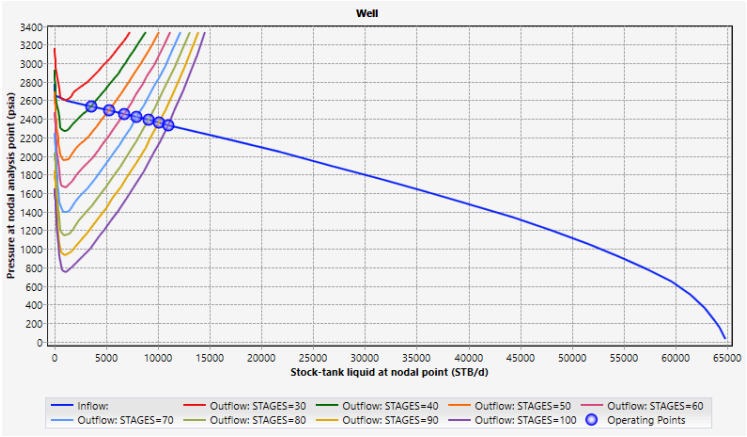

Figure 7.6.6. Sensitivity analysis at different stages of ESP.

	Operating point	ST Liq. at NA	P at NA
		STB/d	psia
1	UNCONVERGE...		
2	STAGES=40 FI...	3529.999	2535.366
3	STAGES=50 FI...	5251.396	2489.499
4	STAGES=60 FI...	6704.237	2450.775
5	STAGES=70 FI...	7957.514	2417.364
6	STAGES=80 FI...	9076.118	2387.546
7	STAGES=90 FI...	10090.29	2360.517
8	STAGES=100 F...	11016.46	2335.811

Figure 7.6.7. Operating point for different number of stages of ESP.

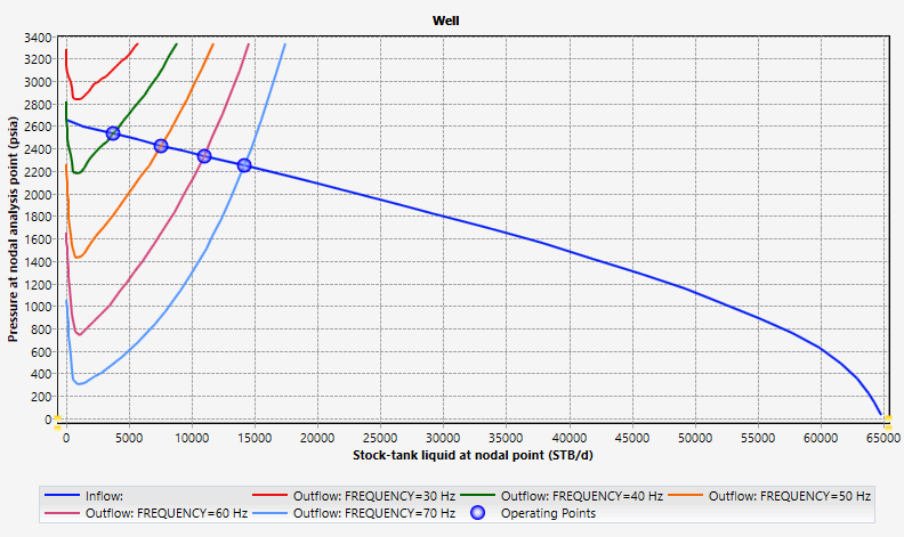

Figure 7.6.8. Sensitivity analysis at different operating frequencies of ESP.

	Operating point	P at NA	ST Liq. at NA
		psia	STB/d
1	UNCONVERGED FRE...		
2	FREQUENCY=40 Hz...	2529.592	3746.714
3	FREQUENCY=50 Hz...	2427.046	7594.376
4	FREQUENCY=60 Hz...	2335.803	11016.77
5	FREQUENCY=70 Hz...	2249.534	14216.85

Figure 7.6.9. Operating point for different operating frequencies of ESP

Sensitivity analysis of ESP (Electric Submersible Pump) system to various parameters and their effects over well performance have being carried out. ESP proves to be effective in restoring well productivity with ESP curve matched with appropriately modified IPR/VLP curve thus delivering elevated production to the operating point of 11016.8 STB/d at

2,335.80 psia. This leads to the analysis of the production based on the number of stages (30 stages, 50 stages and 100 stages) and to identify the maximum production at 100 stages. Like operating frequency sensitivity, flow rates and pressures are higher at higher frequencies (i.e. 70 Z) as compared with lower frequencies. This shows that the ESP system is capable of effectively restoring well production with the least number of stages and frequency settings and hence the best efficiency is offered.

7.6.2 Sucker Rod Pump

Next Artificial Lift that was designed is the Sucker Rod Pump. As cheap and most used artificial lift it was designed as follows:

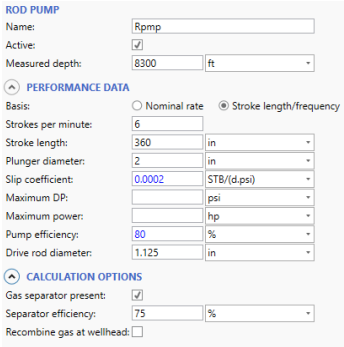

Figure 7.6.10. Parameters for Rod Pump

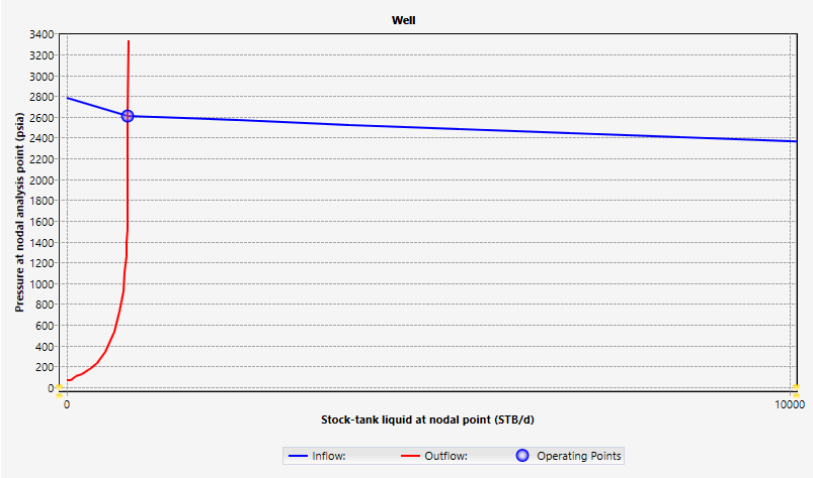

Figure 7.6.11. IPR/VLP curve after installation of Sucker Rod Pump.

	Operating point	ST Liq. at NA	P at NA
		STB/d	psia
1	Flowrate=.102e-...	848.2882	2606.782

Figure 7.6.12. Operating point for Sucker Rod Pump.

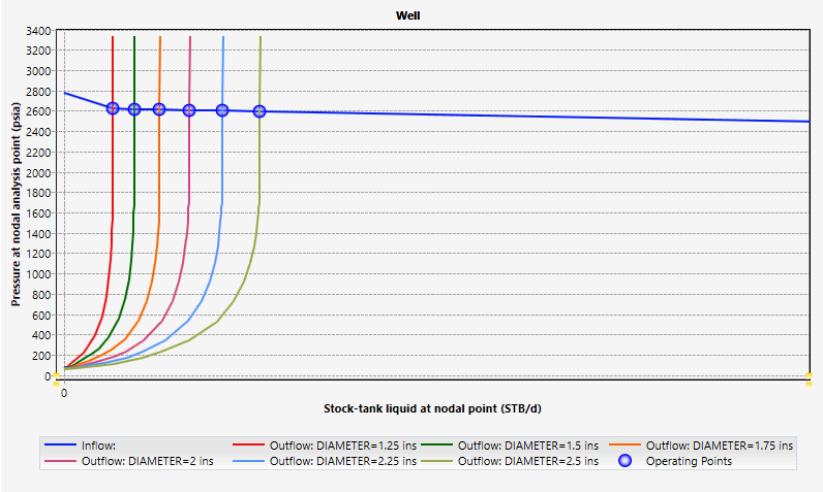

Figure 7.6.13. Sensitivity analysis for different plunger diameters.

	Operating point	ST Liq. at NA	P at NA
		STB/d	psia
1	DIAMETER=1.25 ins...	331.3788	2620.55
2	DIAMETER=1.5 ins F...	477.2048	2616.666
3	DIAMETER=1.75 ins...	649.5082	2612.077
4	DIAMETER=2 ins Flo...	848.2882	2606.782
5	DIAMETER=2.25 ins...	1073.53	2600.783
6	DIAMETER=2.5 ins F...	1325.247	2594.087

Figure 7.6.14. Operating points for different plunger diameters.

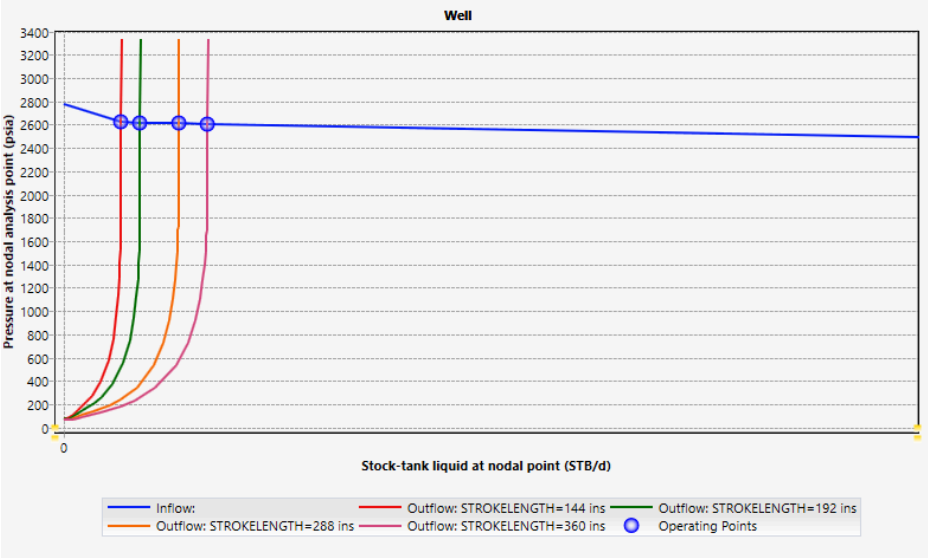

Figure 7.6.15. Sensitivity analysis for different stroke lengths.

	Operating point	ST Liq. at NA	P at NA
		STB/d	psia
1	STROKELENGTH=144 ins...	339.334	2620.339
2	STROKELENGTH=192 ins...	452.4619	2617.325
3	STROKELENGTH=288 ins...	678.6646	2611.3
4	STROKELENGTH=360 ins...	848.2881	2606.782

Figure 7.6.16. Operating points for different plunger diameters.

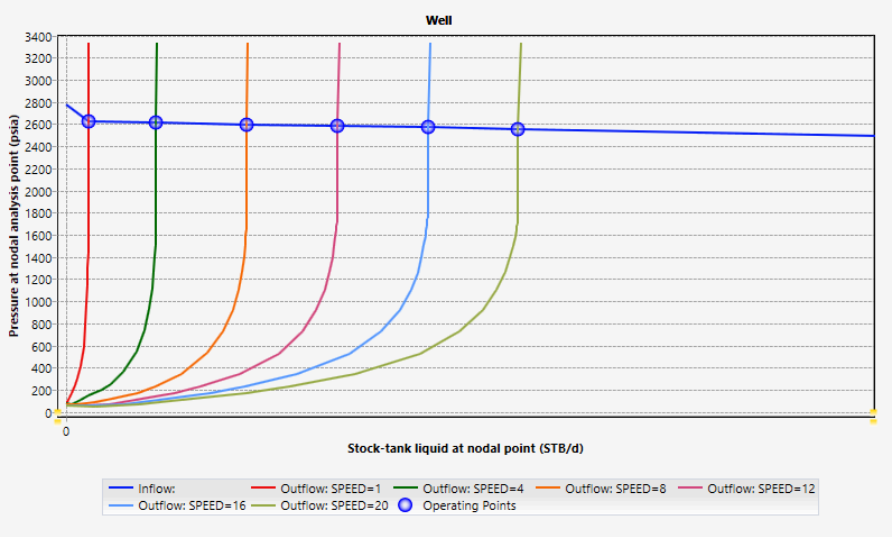

Figure 7.6.17. Sensitivity analysis for different strokes per minute.

	Operating p...	ST Liq. at NA	P at NA
		STB/d	psia
1	SPEED=1 Fl...	141.3291	2625.612
2	SPEED=4 Fl...	565.5689	2614.313
3	SPEED=8 Fl...	1130.937	2599.254
4	SPEED=12 Fl...	1696.101	2584.21
5	SPEED=16 Fl...	2260.991	2569.164
6	SPEED=20 Fl...	2825.651	2554.129

Figure 7.6.18. Operating points for different strokes per minute

SRP is a stroke of 360 inches, 6 stokes per minute, have a plunger of size 2 inches, and have 80% of mechanical efficiency. Once installed, the IPR, or the well produces at 848.29 STB/d at 2606.78 psia. Production can be increased by increasing plunger diameter, stroke length and strokes per minute according to sensitivity analysis. Increased stroke length as well as strokes per minute further increase flow rate, even to the largest plunger diameter (2.5 inches) resulting in the highest production rate of 1325.247 STB/d. Results of the analysis shows well production can be restored optimally using the SRP system on these parameters.

7.6.3 Gas Lift System

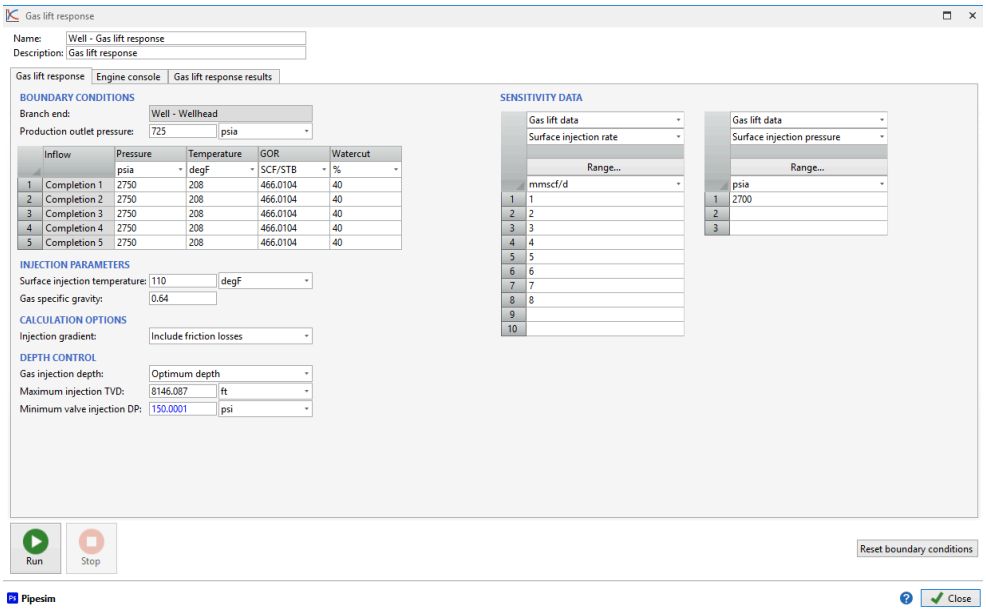

Figure 7.6.19. Parameters for Gas Lift Response.

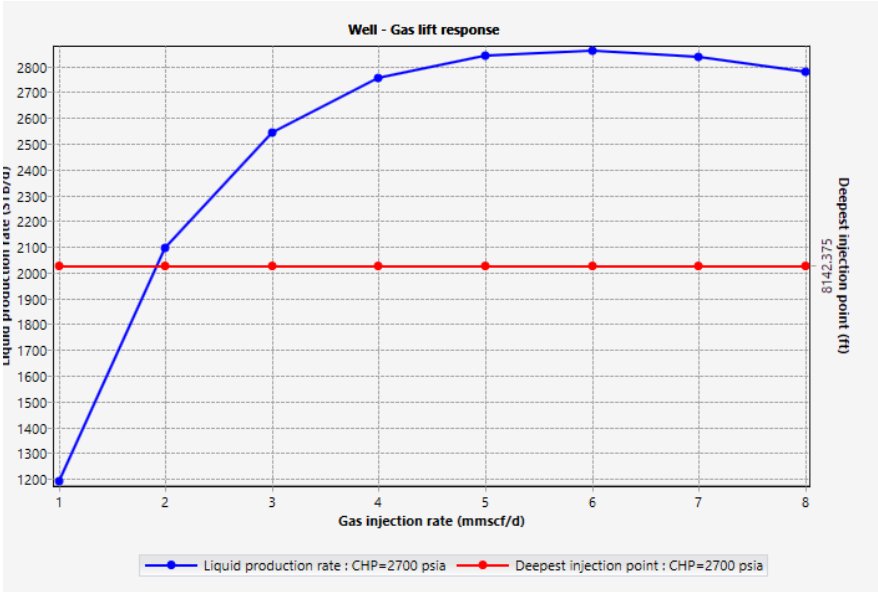

Figure 7.6.20. Results for Gas Lift Response.

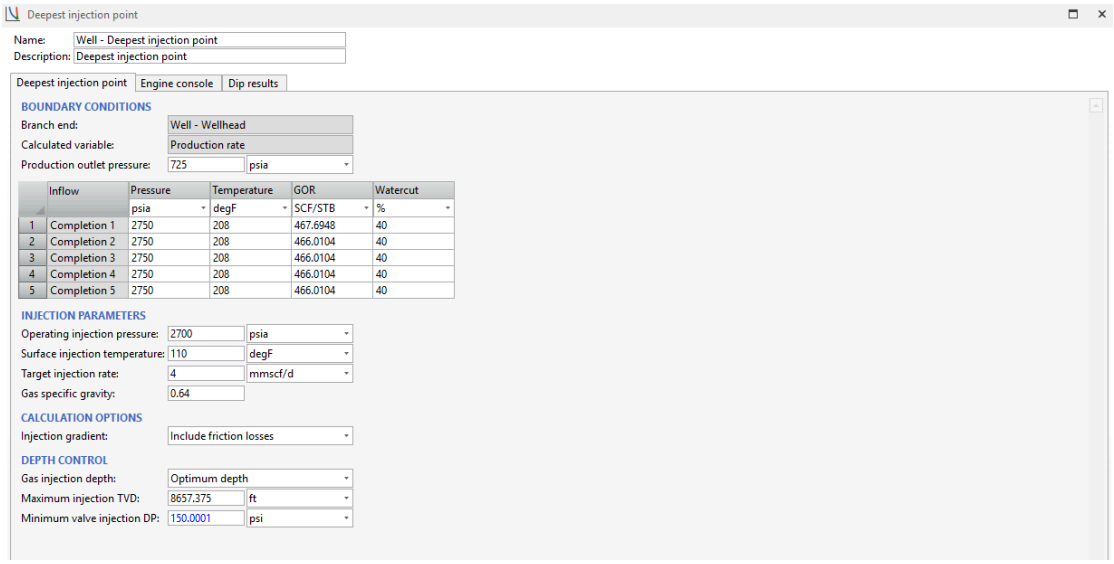

Figure 7.6.21. Parameters for Deepest Injection Point.

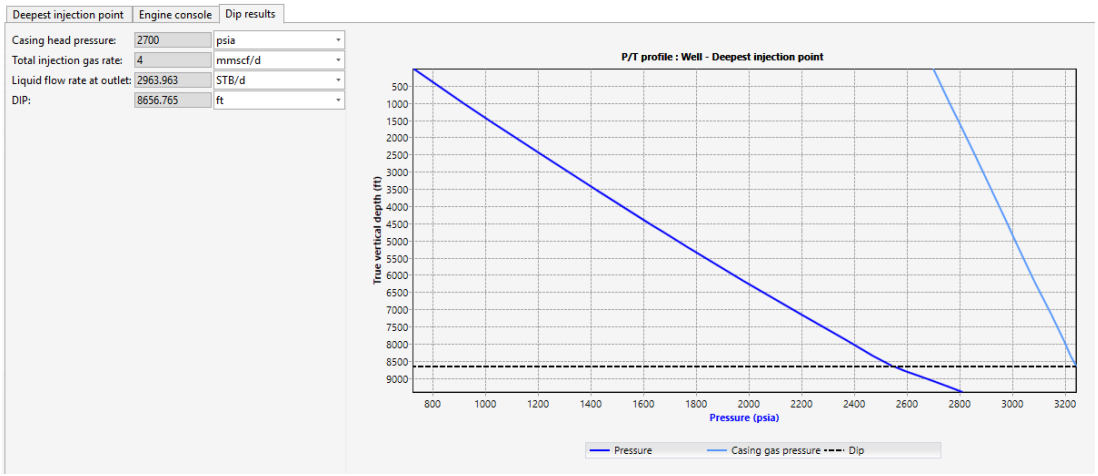

Figure 7.6.22. Results for Deepest Injection Point.

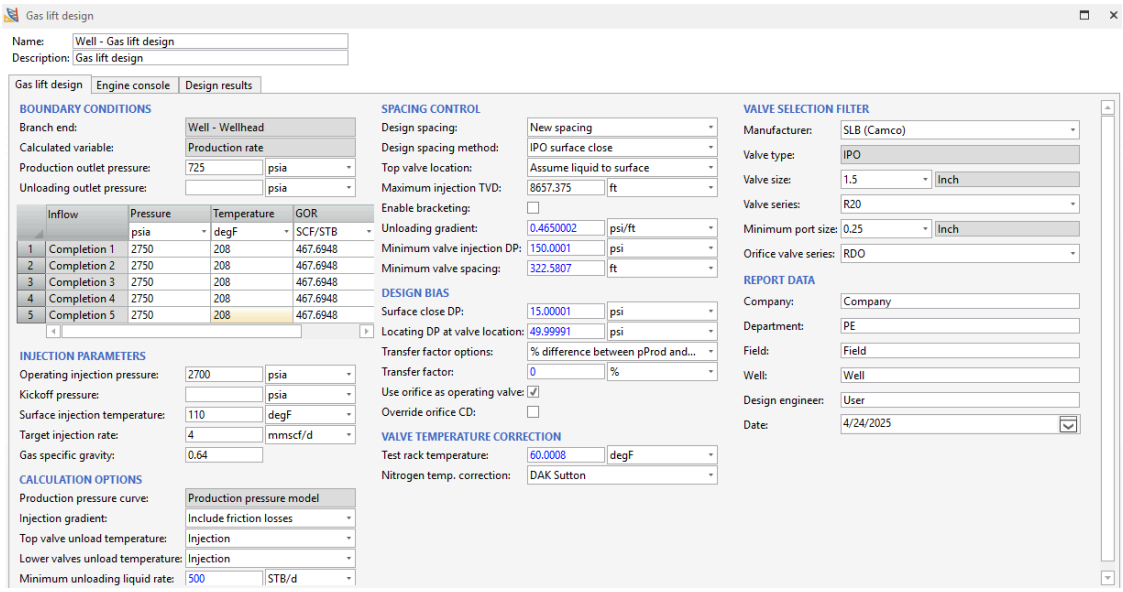

Figure 7.6.23. Parameters for Gas Lift Design.

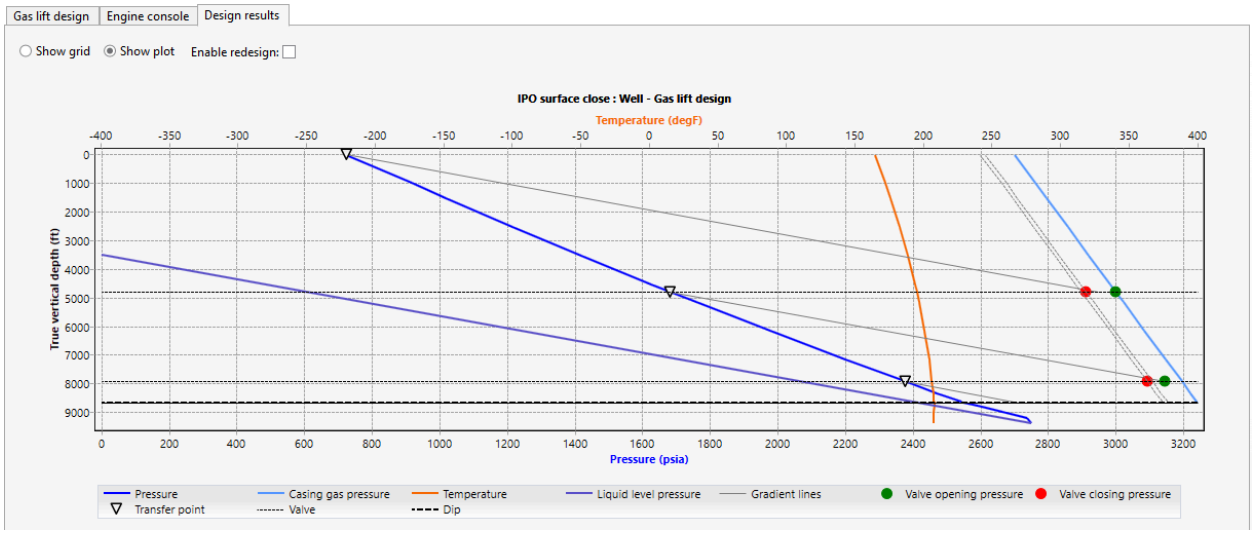

Figure 7.6.24. Gas Lift Design.

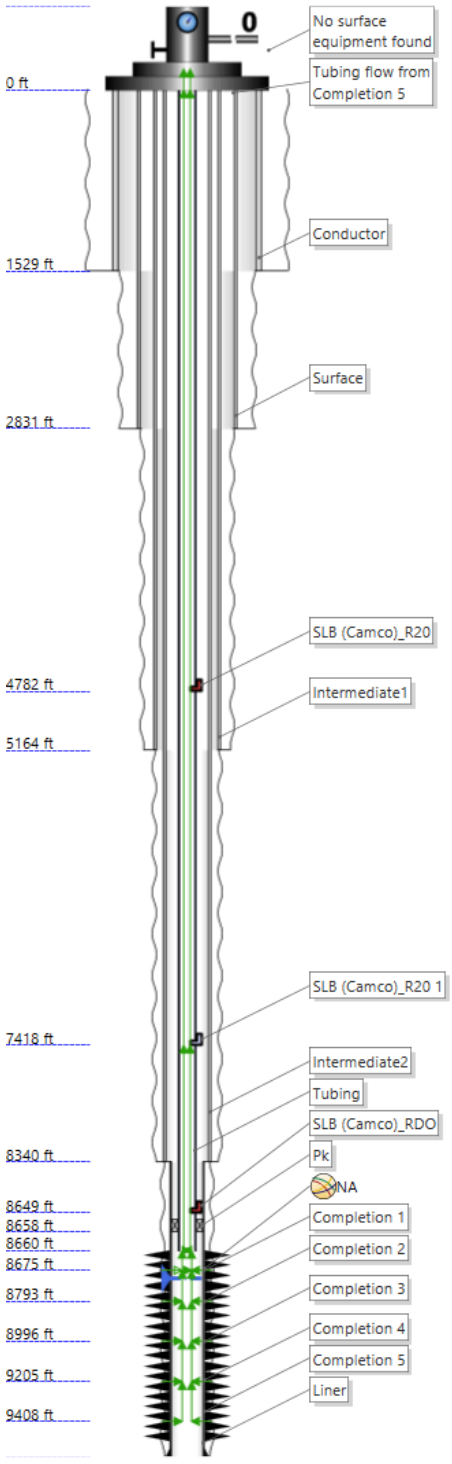

Figure 7.6.25 .Schematic of Well for Gas Lift.

	Gas lift	Active	MD	Manufacturer	Series	Valve type	Port size	Ptro	St	Discharge coe...	DP to fully open	
			ft				in	psia	psia		psi	
1	SLB (Camco)_...	☐	4782.41	SLB (Camco)	R20	IPO	0.25	2360.559		0.76	529	...
2	SLB (Camco)_...	☑	7418.351	SLB (Camco)	R20	IPO	0.25	2412.314		0.76	529	...
3	SLB (Camco)_...	☐	8649.059	SLB (Camco)	RDO	Orifice	0.3125			0.86		...

Figure 7.6.26. Gas Lift Design by PIPESIM

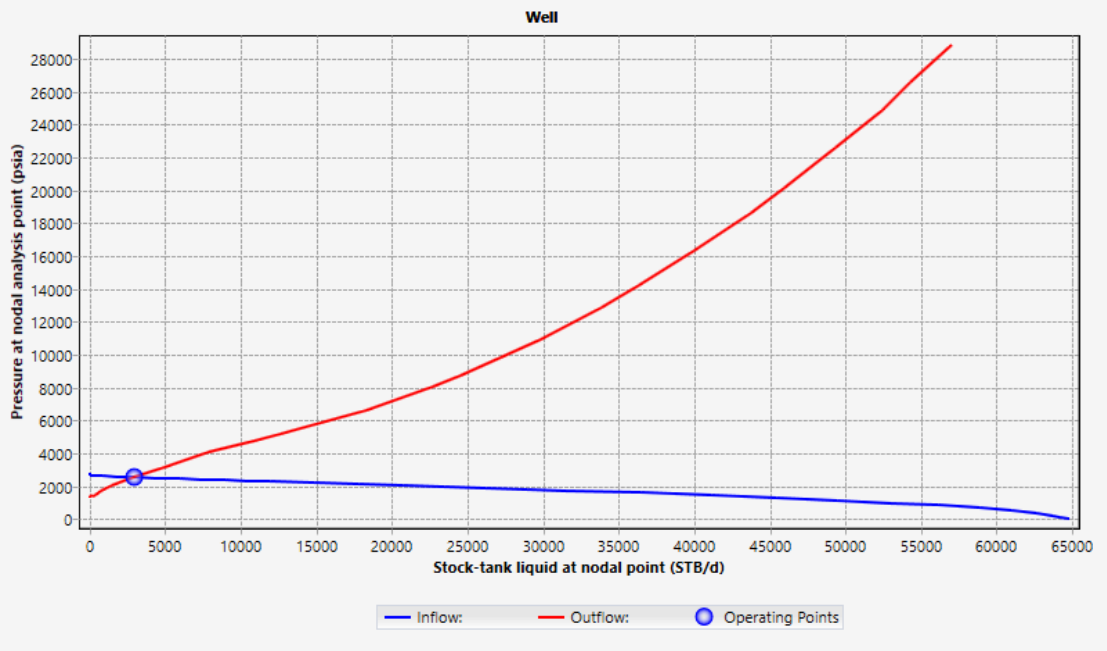

Figure 7.6.27. IPR/VLP curve after installation of Gas Lift System.

	Operating p...	ST Liq. at NA	P at NA
		STB/d	psia
1	Flowrate=29...	2962.749	2550.477

Figure 7.6.28. Operating Points after installation of Gas Lift System.

Optimal gas injection rate in the well is first determined to be used for the analysis of the gas lift system. As shown in the figure, the gas lift response curve indicates that the most adequate gas

injection rate is 4 mmscf/d, because it does not only minimize the dependence of production rate on gas injection rate more than and equal to this experimental value, but also minimizes the variation from the steady well condition, i.e., it does not propose any unstable condition in the wells.

The deep point of injection was then considered. The gas pressure and wellhead pressure are analyzed in the P/T profile of the deepest injection point. Maximum injection depth is optimized at 86566.765 ft, where the pressure gradient is to the best advantage to inject gas and at the same time supply enough pressure support to keep the well's injection capacity adequate.

The following analyses are further optimized by the designed gas lift design of the injection system. The software finds the best configuration of the valve and surface equipment that would guarantee stable operation of the system. For the final gas lift system, the correct injection rate and pressure are adjusted so that the gas injection flow is optimized and the resulting well performance is reached to 2962.749 STB/d and pressure of 2550.477 psia.

Overall, the optimized gas lift system increases well production by maintaining an optimal gas injection rate and well pressure, and provides the deepest gas injection point and gas lift design to obtain maximum flow and stability for any well's operations.

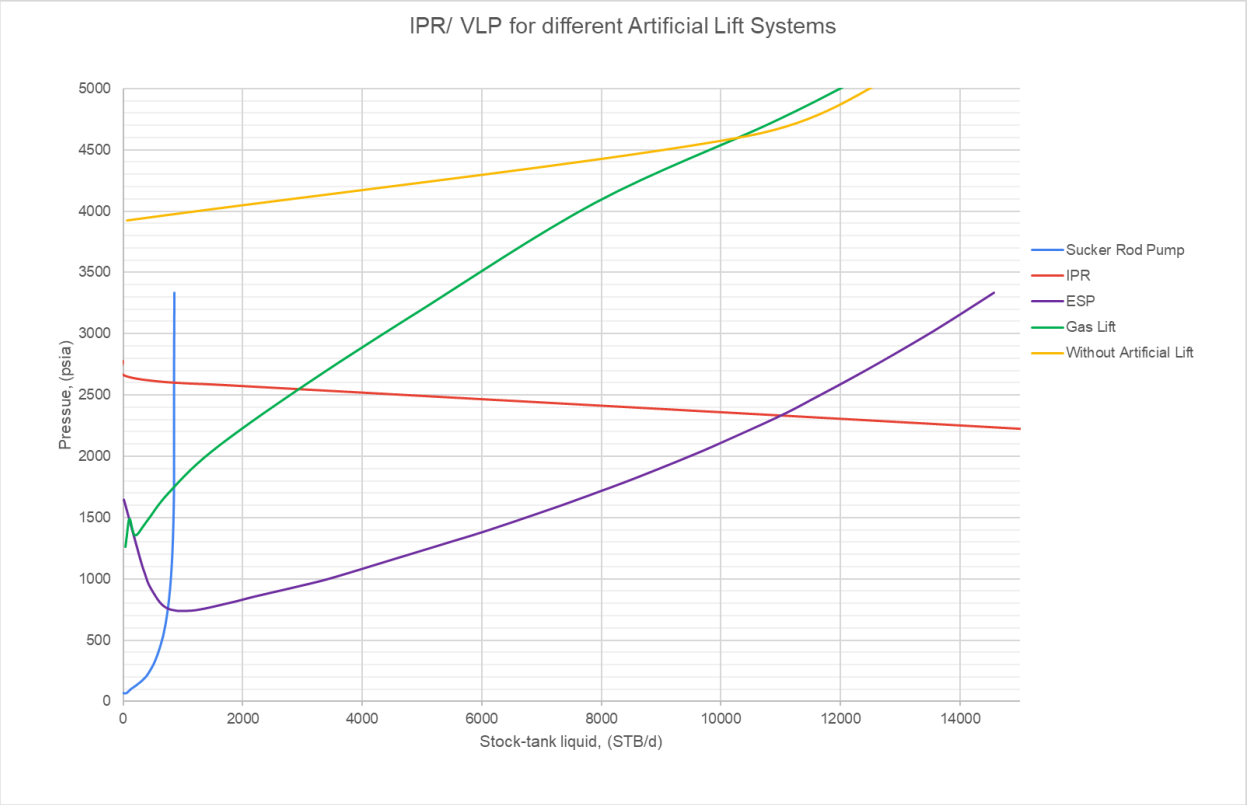

Figure 7.6.29. IPR/VLP curves for different artificial lifts

Comparison of IPR/VLP curve for different artificial lift systems is made and ESP (Electric Submersible Pump) gives the best production rate at relatively lower pressures as compare to other systems. The ESP curve is stable and high production rate across a wide range of stock-tank liquid (STB/d) production rates which is an indication of high efficiency in all ranges of production rate. At this point it operates at the least pressure drawdown, making it the one of the best at keeping the flow and maximizing production.

On the contrary, the poor performance of the Sucker Rod Pump (SRP) is shown through the steep initial decline in production for a rapidly increasing pressure, meaning that the SRP cannot sustain a stable production flow rate. The outflow pressure curve rises sharply under these conditions, i.e., higher depths or increasing pressures; the SRPs do not do so well. Therefore, it has less effect in those wells with depleted reservoir pressures.

Another poor result of the Gas Lift system indicate in the flattening of the production curve. Therefore it can only sustain flow at lower rates and cannot cope with high production demands. However, gas lift systems restricts its flow rate and requires higher gas injection rates for production enhancement, which can be inefficient in some of the wells.

The curve drops sharply to the dead well condition at very low production rates as expected because the well without artificial lift cannot maintain production. The poor production is clearly the result of no sustained flow in the face of low reservoir pressure and high water cut.

Finally, the ESP system is superior since it can be operated at lower pressures compared with other systems without suffering excessive pressure increases, or it does not increase production effectively in a meaningful way.

Chapter 8. Economics and Regulations

8.1. Economics and Financial Assessment

The economic analysis role is particularly critical to any field development project, particularly in the oil and gas industry. Offshore project – Norne Field has both advantages and disadvantages which need to be planned and assessed carefully in terms of costs and finance. In order to ensure that the development is financially viable the capital expenditures (CAPEX) as well as the operational expenditures (OPEX) needs to be evaluated. Together, these two elements make up the crux of the financial model and essentially dictate the way that the decision making process happens from the beginning of the investment phase and through the end in terms of dedicated and ongoing operations.

CAPEX is defined as the cost of drilling, installation of infrastructure and initial field development in oil and gas projects and OPEX is the ongoing expenses for maintaining in the field production, including maintenance, labor etc. The economic success of the Norne field depends heavily on controlling these costs while optimising production rate to ensure that revenue earned will be sufficient to carry the field through to life of field.

Field development is a risky business. One of their chief risk is fluctuations in oil prices. It is important to apply revenue generation potential with respect to pricing scenario in the economic model itself since prices have direct influence on this. An analysis of the field will be carried out in a structured manner, based on the changes of the oil price, amounts of production and costs, so to see if the project can deliver added value to investors.

The aim is to produce a picture of the financial viability of the Norne Field. We calculate NPV (Net Present Value) and IRR (Internal Rate of Return) in order to evaluate whether yields resulting from the field could justify initial and continuation expenditures. This will also assist in determining the potential sensitivities and risks to stakeholders who must make the critical decisions.

8.2. Drilling and Completion Costs

Drilling and completion phase constitutes a substantive part of the capital expenditure (CAPEX) of any oil and gas field. Each of the stages involved in drilling the well, casing, cementing and completion is referred to as critical for the drilling process for the Norne Field. The specific well design (vertical or horizontal) affects the overall cost structure also. Since they involve longer reach and more complicated operations, the horizontal wells tend to cost more than the vertical wells.

8.2.1. Drilling Costs

Drilling costs are the costs of utilizing rig, drilling fluids, labor, and logistics associated with drilling each well. Typically, the average daily rate of the offshore rigs utilised in the Norne Field is about 100,000 USD. The cost of rig utilization is as follows assuming average drilling duration of 60 days for vertical well and 90 days for horizontal well.

- Rig Costs (Vertical Well):

Rig Costs = 100,000 USD/day × 60 days = 6,000,000 USD

- Rig Costs (Horizontal Well):

Rig Costs = 100,000USD/day × 90days = 9,000,000 USD

Drilling budget includes these rig costs, particularly for horizontals, where extended wellbore length and other extended wellbore drilling challenges contribute to longer rig time.

Table 8.2.1. Casing and Tubing Costs

Casing Component	Diameter (inches)	Depth (m)	Material Cost (USD/foot)	Total Cost (USD)
Conductor Casing	30"	459 m	150	225,900
Surface Casing	20"	867 m	120	341,400
Intermediate Casing	13 3/8"	1520 m	100	498,700
Production Casing	9 5/8"	2561 m	90	756,180
Tubing	5.5"	2561 m	80	672,160

Casing and tubing are very critical components for a vertical as well as horizontal well, seeing to the fact that it's involves integrity and the ability of the well to produce oil or gas. Conductor casing, surface casing, intermediate casing, production tubing, are included in the casing program. All of these components have varying diameters, material cost, and the amount of installation complexity.For the vertical well (B-1H), the breakdown of casing and tubing costs is as follows:The total raw cost for casing and tubing of the B1H is about $2.49 million. Contingency and service costs add up to 15% on top of the final casing cost of 2.87 million USD.

Cementing and Perforation Costs

Casing strings need to be secured in place and different pressure zones in the reservoir need to be isolated with cementing. The cementing costs are usually calculated based on the well's depth and the size of the casing. For the cementing in the Norne Field it was estimated in terms of 150 USD per foot of casing cemented. For B-1H (cemented length total of 14,588 feet based casing), cement cost is calculated as follows:

Cementing Cost =14,588ft × 150USD/ft = 2,188,200 USD

In the vertical well, the perforating the well (required for creating communication between the reservoir and the wellbore) is estimated to cost 300,000 dollars.

Wellhead and Christmas Tree Installation

The cost for installing a wellhead and Christmas tree is also quite high for offshore fields. These are the components that control hydrocarbons flow and safety of the well during its life. Seemingly, 2.8 million usd per well is estimated for the total cost of a wellhead system plus a subsea Christmas tree installation.

Table 8.2.2. B-1H is Vertical Well, Total Drilling and Completion Cost.

Component	Cost (USD)
Rig Costs	6,000,000
Casing and Tubing	2,870,000
Cementing	2,188,200
Perforation	300,000
Wellhead and Christmas Tree	2,800,000
Total Cost	13,780,200

Therefore, the approximately 13.78 million USD cost for the vertical well (B-1H) is arrived at.

The complexity of the horizontal drilling and extended reach alsoadds to the cost of the well, that is, the horizontal well (B-4H). Horizontal well drilling and completion is estimated at:

Total Cost for B-4H = 13,780,200 × 1.4 = 19,292,280USD

Therefore, the costs to drill and complete B-4H will be about 19.29 million USD.

Table 8.2.3. Surface Facilities and Infrastructure Costs

Component	Quantity	Unit Cost (Million USD)	Total Cost (Million USD)
Subsea Manifold and Trees	1 unit	50	50
Subsea Flowlines and Risers	1 unit	30	30
FPSO (Floating Production Unit)	1 unit	45	45
Surface Processing Modules	1 unit	40	40
Total Surface Facilities			165

Total Surface Facility Cost = 165 million USD

Table 8.2.4. Operational Expenses (OPEX)10-Year

Expense Category	Annual Cost (Million USD)
Operation and Maintenance	35
Logistics (Vessels, Helicopters)	5
Well Interventions (e.g., ESP replacement)	2

Subsea/Surface Maintenance	6
Total Annual OPEX	48

OPEX = 480 million USD

Table 8.2.5 Total CAPEX with Artificial Lift Systems

Item	Estimated Cost (Million USD)
Drilling and Completion (B-1H)	13.78
Drilling and Completion (B-4H)	19.29
Surface Facilities and Infrastructure	165
Artificial Lift (ESP)	1.75
Artificial Lift (SRP)	0.8
Artificial Lift (Gas Lift)	1.8
Total CAPEX	202.62

8.3. Economic Analysis Scenarios

In this section, we evaluate the project's economic viability under three distinct oil price scenarios, reflecting market uncertainty and the need for robust planning.

Scenario 1: Low Oil Price Environment ($40/bbl)

This scenario assumes a conservative market outlook, with Brent crude prices stabilizing at $40 per barrel. The project's profit margins are narrower, but due to efficient cost management and low operating expenditure, the field remains profitable over the 10-year period. This case simulates a lower-risk, steady-return operation, highlighting resilience in a bearish market.

Scenario 2: Base Case Forecast ($60/bbl)

This is the central assumption of our model and reflects industry consensus forecasts for Brent crude over the next decade. It assumes a balanced market with stable investment climates and moderate demand growth. The economic indicators under this scenario are strong, supporting full recovery of capital expenditures and consistent profitability.

Scenario 3: High Oil Price Upside ($85/bbl)

This optimistic scenario explores the case of strong oil prices driven by geopolitical tension, supply limitations, or sharp demand increases. At $85 per barrel, this scenario projects significant returns and rapid payback, maximizing the value of high-efficiency horizontal well development and intelligent completions.

In all scenarios, the following inputs were consistent:

Table 8.3.1. Monte Carlo Scenarios

Scenario	Oil Price (USD/bbl)	Annual Revenue (USD)	Annual OPEX (USD)	Total Profit (1yr)
Low	40	$ 15,000,000	$ 1,500,000	$ 127,881,169
Base	60	$ 22,500,000	$ 1,500,000	$ 202,881,169

High	85	$ 30,000,000	$ 1,500,000	$ 277,881,169

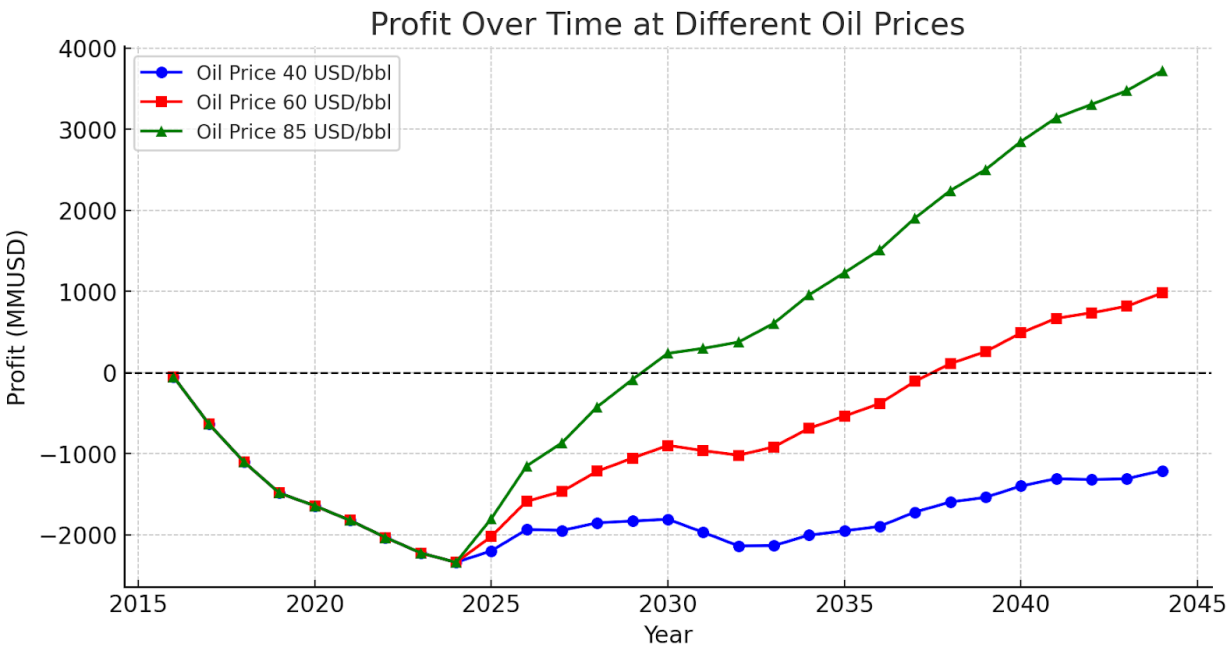

Figure 8.3.1 Profit Over Time at Different Oil Prices

8.4 HSE

8.4.1. Introduction to HSE in Petroleum Operations

On the one hand, the petroleum industry is the principal driver of global energy production and economic growth and, on the other hand, the petroleum industry is subject to large health, safety and environmental (further referred as HSE) risks. However, these are risks associated with the nature of oil and gas operations, which include a complex and high risk nature of operations related to their exploration, production, transportation, and processing. However, accidents, environmental degradation and health hazards are all potential, which make HSE management an important issue for companies engaged in petroleum operations.

These challenges are no exception in the case of the Norne Field development. It is a major offshore project, thus demands for an integrated approach in applying health, safety and environmental concerns. The HSE practices in the petroleum industry are not only related to taking care of the workers or surrounding communities but is also about ensuring that operations are environment friendly. Compliance with national and international regulations. Hence, it is necessary to adopt proactive safety measures, environmental safeguards and regulatory compliance to minimize human health and natural environmental impact of operations.

International frameworks to guide HSE management in the petroleum industry include ISO 14001 for environmental management, ISO 45001 for occupational health and safety management and OHSAS 18001 safety standards. The Norwegian Petroleum Safety Authority (PSA) regulates the safety of offshore installations in Norway where the Norne Field is situated and by carrying out stringent safety and environmental laws. In addition, the UN Sustainable Development Goals (SDGs) offer a broader layout for companies to ensure that their undertakings help human rights, fall in line with global sustainability targets, including accountable consumption, climate activity, and ecosystem conservation.

This section describes the overview of the HSE management practices at the Norne Field where the health, safety and environmental issues are integrated into every stage of the

project. Organizing goes on to describe the main regulations, standards and monitoring systems that ensure that the field's activities are safe, environmentally sound and sustainable.

8.4.2. Health and Safety Management Systems

Safety Standards and Regulations

To assure health and safety in offshore petroleum's operations, a sound safety management system (SMS) that meets international standards as well as national requirements, should be in use. The Norwegian Petroleum Safety Authority (PSA) and the norne field development require adherence to safety regulations and guidelines in order to avoid accidents and as such crime risk is considered minimized. Compliance with the Norwegian Offshore Safety Regulations (A-21), Safety and Emergency Response Plans are considered.

In offshore operations the facilities are designed, equipment operated and work procedures are defined to minimize the risks to human health. Drilling, production, maintenance, and transportation operations should be kept within safety standards. This includes such areas as risk assessment, incident reporting, hazard identification and activities aimed at elimination or reduction of the risks respectively. Reduction of health risks demands on implementation of the 'hierarchy of controls', i.e., elimination, substitution, administrative and engineering controls.

For the Norne Field, the planned operational design features safety aspects such as well control systems, BOPs, fire suppression systems, and hazardous materials handling procedures. Moreover, all personal are to use personal protective equipment (PPE) to protect against being exposed to harmful substances, or physical injury.

Emergency Response Planning

Inherently risk is associated with offshore petroleum operations, and emergencies such as blowout, fire, oil spill, and gas leakage must be foreseen and ready for. HSE management involves the planning, which includes the planning of emergency response, and this needs the

circumstance planning, which is to have some detailed contingency plans to face a number areas of the potential plan.

The Norne Field has drawn up comprehensive emergency response plans (ERPs) to face a wide spectrum of hazards from fire and explosion to gas release and chemical spills as well as from medical emergencies. These are evacuation and emergency rescue plan, communication and interaction with the respective authorities. In addition, the field has put in place safety drills and simulation exercises so all personnel are prepared in the case of an emergency.

Staff are trained and drilled regularly to familiarize them with emergency procedures. Emergency response teams (ERTs) are trained to go on alert to any incident so that the damage of human life, property, and the environment are minimized. Coordination with local emergency services is also assured in the field to facilitate quick responses in the event of serious incidents.

8.4.3. Environmental Protection and Sustainability

Environmental Impact and Mitigation

Offshore developments of petroleum fields, such as the Norne Field, imply a direct impact on the surrounding environment and the marine ecosystems. For this reason, measures should be taken in order to minimize environmental risks and to ensure that the operations are in line with local and international environmental regulations.

Offshore petroleum operations have primary environmental concerns of oil spills, gas flaring, emissions of greenhouse gases (GHGs), chemical dischargers and biodiversity disruption. To prevent and mitigate these risks, large efforts are made at the Norne Field. It includes implementation of the most advanced spill prevention systems, secondary containment as well as warning systems to prevent a hydrocarbon or other contamination to be accidental discharged into the marine environment.

Among the environmental protection strategy of the field, closed loop systems for handling the waste water and chemicals are pivotal. The field also has a zero discharge policy, which

takes the restraint of releasing any harmful waste into the ocean untreated. All produced water is treated by advanced separation technologies and will safely be disposed of or reinjected into the reservoir.

Periodically, environmental impact assessments (EIAs) are performed to monitor the possibility of field operations effects. In turn, these assessments produce results which then allow determining the focus areas of improvement and, in turn, suggest targeted mitigation measures. The aim is to have the minimum environmental footprint of operations while in compliance with Norwegian Oil and Gas Industry Environmental Regulations (OGER) and the EU Offshore Safety Directive.

Waste Management Systems

Environmental protection in offshore operation is an integral part of waste management. Sustainable waste management is taken by the Norne Field, aiming for minimizing waste generation, recycling and disposal of non-recyclable waste in a proper manner.

It produces a variety of waste, for example, hazardous waste (spent chemicals, drilling fluids), nonhazardous (paper, plastics, metal) and biodegradable (food scraps). Different kinds of specialized containers and methods of disposal are used for the management of hazardous waste to prevent its improper or undesirable handling and environmental compliance.

First sorting, and recycling where possible then non hazardous waste is disposed of responsibly. Composting biodegradable waste minimizes the amount of waste going into the landfill. The Norne Field also invested in waste-to-energy technologies to convert waste materials into usable energy, a reduction in overall waste volume, and an active part in supporting sustainability efforts.

Emissions Control and Reduction

Consequently, the oil and gas industry takes control and reduction of greenhouse gas (GHG) emissions, especially, CO_2 and CH_4 as a big concern. achieving the climate goals of Norway and as part of international efforts to mitigate global climate change, development of emission reduction strategies has been implemented at the Norne Field.

Flare gas recovery is one of the keys; flare gas recovery systems are used to capture and reprocess natural gas that is flared during production normally. It also saves on CO_2 emissions and methane leaks for the field and is thus a step in the right direction to cut down on its carbon footprint. In addition, the field makes full use of low emission technologies in their power generation and transport systems to minimize energy use and fuel consumption.

The field is in line with Norway's climate action targets, set to reduce emissions by 40 per cent by 2030 and reach zero emissions by 2050, and has two European Unions as its customers: Airlines operating to Norway (including SAS) and Scandinavian Airlines' own aviation division, within the My Ski Camp brand. In order to achieve those targets, the field remains under constant observation of air quality and emission levels and sticks to ISO 14001 standards for environmental management systems.

Spill Prevention and Response

Offshore operations have one of the greatest environmental risks—oil spills. With its Norne Field, the company has spent a great deal of money toward preventing spills, as well as on spill containment systems and various rapid response teams aimed at minimizing spills and limiting the environmental impact of spills.

The field employs double-hulled tankers, secondary containment systems for offshore storage, and real-time spill detection systems. In addition, all equipment used for the handling of oil and hazardous materials is designed to prevent leak and the wellheads and Blowout preventers (BOP) are monitored and maintained to ensure that they perform as intended in an emergency situation.

A spill response team equipped with specialized tools and resources is also in place on the Norne Field in the event of a spill. Drills are run constantly to test the field's spill response

plans and contingency plans are in place, including coordinated response plans with local authorities and environmental organizations for handling large spill incidents.

Biodiversity and Ecosystem Protection

Many people are interested in the environmental effects of offshore petroleum operations on local marine biodiversity. With Environmental Impact Assessments (EIAs) on the Norne Field, it has taken care of protecting the ecosystem around it by the potential risks of marine life and the overall ecosystem.

There are monitoring programs to monitor the health of local fish populations, as well as marine mammals and other species which might be influenced by field operations. Mitigation measures to limit noise pollution and minimize underwater disturbance and issues to sensitive marine habitats have been applied in the Norne Field. They include restricting seismic exploration activities during certain breeding seasons and, combining with reduced operations, minimizing the frequency and impact of operations on migratory patterns.

The field sticks to strict regulations regarding marine biodiversity and continuous monitoring and is able to simultaneously produce and minimally impact the environment in order to balance its production with environmental responsibility.

8.4.4 Regulatory Compliance and Risk Management

Local and International Regulations

A large amount of local and international regulations is applied to the safety, environmental protection and operational standards of the Norne Field. They include Norwegian Petroleum Safety Authority (PSA) regulations, EU Offshore Safety Directive, as well as ISO 14001 for environmental management. The field is also in accordance with the UN Sustainable Development Goals (SDGs) by adhering to responsible energy production, climate action and environmental protection.

Following these regulations helps to limit the operation of the field up to the limits of law and to keep the highest level of safety and environmental standards. All audits and inspections are regular, and if there is any discrepancy in results, they are addressed immediately in order to mitigate risks.

HSE Audits and Monitoring

The internal and external standards are regularly audited by HSE audits to see whether compliance is maintained. These audits focus on how low the health and safety management system, environmental protection measures and the risk management practice are. Real time data is obtained from the monitoring tools, namely emission monitoring systems and spill detection technologies, to monitor the field's environmental impact and safety performance.

Like any other offshore installation, the HSE work required at Norne field starts with HSE internal reviews and safety audits aimed at identifying potential hazards or non compliance issues. Measures are taken immediately to fix the field in order to fulfill regulatory and industry best practice.

HSE Performance Indicators

The field's HSE performance is measured via Key Performance Indicators (KPIs). Incident Frequency Rate (IFR), spill rates, emission levels and worker safety metrics are the type of KPI's these. Continuously tracking these indicators allows the field to know if there's a room for improvement, and what should be done so that the operations are sustainable and safe. HSE performance reviews are conducted on a regular basis to evaluate the effectiveness of the safety measures, and to identify the potential risks to take strategy for continuous improvement.

Risk Assessment and Mitigation Measures

Risks are regularly identified and evaluated by risk assessment with regard to the field operations and the risks concluded. These assessments include equipment failure, well blowouts, oil spills, gas leaks, and other scenarios. When risks show up, they are then put up

with mitigation strategies that involve the addition of equipment, improvement of training, or modification of operations. This proactive approach allows for potential risks to be managed effectively and secures the field and compliance.

Conclusion

The aim of the Norne Field Development Plan is specifically to address the problems of the complexity of the reservoirs and the deterioration of the efficiency of the production in a coordinated manner. The work which has emphasized the integration of enhanced geological, petrophysical and dynamic modeling techniques has helped the project to accurately delineate key reservoir features and form optimum field development plans. The use of polymer and gas injection as Enhanced Oil Recovery (EOR) techniques for recovery have also been considered, whilst limiting social and economic costs. Utilization of EIC completion designs, AI-driven completion designs and time-efficient dynamic multiphase flow simulations helps in accurate development and implementation of Cost-preserving measures and production strategies. Moreover, adherence to strict HSE policies reinforces the confidence of the idea being in line with Norwegian offshore practices.

Economic studies also provide an insight into the possible scenarios and encourage the notion of applying reconstruction and optimizing processes in order to satisfy all interested parties, while looking forward to the sustainable net profit. Because incorporating new technologies and a flexible system of control over production of the reservoirs, the life span of the Norne Field would be sufficiently increased, as if to draw analogies with the effective functioning of the global offshore oil and gas industry.

Overall, the Norne Field Development Plan is on target, because its purpose is to demonstrate best practice field development with regard to technical, commercial and environmental issues for a sustainable hydrocarbon recovery in the Norne field.

References

Abrahamsen, A. (2012). *Applying chemical EOR on the Norne Field C-segment* (Master's thesis). Norwegian University of Science and Technology, Department of Petroleum Engineering and Applied Geophysics.

Ahmed, T., & McKinney, P. (2011). *Reservoir engineering handbook* (4th ed.). Gulf Professional Publishing.

Akpan, A. A., Ekpo, E. U., & Ekpo, O. M. (2015). *Development of Norne Oil Field C-segment reservoir using Eclipse* [PDF]. *Journal of Multidisciplinary Engineering Science and Technology (JMEST)*, 2(3), 465-470. https://www.jmest.org/wp-content/uploads/JMESTN42350321.pdf

Akpan, S. E. (2012). *Well placement for maximum production in the Norwegian Sea: Case study of Norne C-segment oil field* (Master's thesis). Norwegian University of Science and Technology, Department of Petroleum Engineering and Applied Geophysics.

Amirbayov, T. (2014). *Simulation study of polymer flooding applied to the Norne Field E-segment* (Master's thesis). Norwegian University of Science and Technology, Department of Petroleum Engineering and Applied Geophysics.

Ammah, A. N. (2012). *Applying time-lapse seismic inversion in reservoir management: A case study of the Norne Field* (Master's thesis). Norwegian University of Science and Technology, Department of Petroleum Engineering and Applied Geophysics.

Archie, G. E. (1942). The electrical resistivity log as an aid in determining some reservoir characteristics. Transactions of the American Institute of Mining, Metallurgical, and Petroleum Engineers, 146, 54–62.

Arps, J. J. (1945). "Analysis of Decline Curves." Transactions of the American Institute of Mining and Metallurgical Engineers, 160(1), 228-247.

Bishop, C. M. (2006). Pattern recognition and machine learning. Springer.

Blasingame, T. (2022). Multiwell decline curve analysis using a type curve approach. *Proceedings of the 9th Unconventional Resources Technology Conference*. https://doi.org/10.15530/urtec-2022-3724101

Breiman, L. (2001). Random forests. *Machine Learning, 45*(1), 5–32. https://doi.org/10.1023/A:1010933404324

Chai, T., & Draxler, R. R. (2014). *Root mean square error (RMSE) or mean absolute error (MAE)? – Arguments against avoiding RMSE in the literature*. Geoscientific Model Development, 7(3), 1247-1250.

Cruz, D. C. (2015). *3D geological model of the Garn and Not formations in Norne Field, Mid-offshore Norway* [Master's thesis, Norwegian University of Science and Technology]. NTNU Open. https://ntnuopen.ntnu.no/ntnu-xmlui/handle/11250/2350369

Cuenca, J. (2017). *Enhanced oil recovery: An update*. Springer. https://doi.org/10.1007/978-3-319-51645-4

Draper, N. R., & Smith, H. (1998). *Applied Regression Analysis* (3rd ed.). John Wiley & Sons.

Economides, M. J., & Nolte, K. G. (2000). *Reservoir stimulation* (4th ed.). Wiley.

Falcon, G. E. G. (2021). Flowing Material Balance and Decline Curve Analysis: A Hybrid Approach for better EUR and Decline Profile Predictions for CSG Wells. *Proceedings of the 2021 Asia Pacific Unconventional Resources Technology Conference*. https://doi.org/10.15530/ap-urtec-2021-208381

Field, A. (2013). *Discovering Statistics Using IBM SPSS Statistics* (4th ed.). SAGE Publications.

Freedman, D. A. (2009). *Statistical models: Theory and practice* (2nd ed.). Cambridge University Press.

Ghalambor, A. (2011). "Production Optimization for Oil and Gas Reservoirs." *Gulf Professional Publishing*.

Gjerstad, H. M., Steffensen, I., & Skagen, J. I. (1995). The Norne field - Exploration history & reservoir development strategy. Offshore Technology Conference. https://doi.org/10.4043/7924-MS

Hyndman, R. J., & Koehler, A. B. (2006). *Another look at measures of forecast accuracy*. International Journal of Forecasting, 22(4), 679-688.

Islam, M. S., Kleppe, J., Abbassi, F., and M. F. Haque. "An Economic Feasibility Study of the Norne Field's E-Segment for Different Field Development Plans." Paper presented at the SPE Kingdom of Saudi Arabia Annual Technical Symposium and Exhibition, Dammam, Saudi Arabia, April 2018. doi: https://doi.org/10.2118/192434-MS

Jafarpour, B., et al. (2014). *Uncertainty quantification in reservoir modeling*. Journal of Petroleum Science and Engineering, 121, 1-16. https://doi.org/10.1016/j.petrol.2014.06.018

Khalil, M., et al. (2018). *Application of Monte Carlo simulation for reservoir performance prediction*. SPE Journal, 23(5), 1800-1813. https://doi.org/10.2118/190362-MS

Lake, L.W. (1989) Enhanced Oil Recovery. Prentice-Hall Inc., Englewood Cliffs, 550 p.

LeCun, Y., Bengio, Y., & Hinton, G. (2015). Deep learning. *Nature, 521*(7553), 436–444. https://doi.org/10.1038/nature14539

Liaw, A., & Wiener, M. (2002). Classification and regression by randomForest. *R News, 2*(3), 18–22.

Mbise, P. K. (2019). *Enhanced oil recovery for Norne Field E-segment using alkaline surfactant-polymer flooding* (Master's thesis). Norwegian University of Science and Technology, Faculty of Engineering, Department of Geoscience and Petroleum.

Norwegian Petroleum Directorate. (n.d.). *Field facts*. Norwegian Petroleum Directorate. Retrieved April 25, 2025, from https://www.norskpetroleum.no/en/facts/field

Osnes, M. O. (2018). *Geological constraints on hydrocarbon contacts in the greater Norne area*. Master's thesis, Basin and Reservoir Studies, Department of Earth Science, University of Bergen.

Pendaeli, K. M. (2019). *Enhanced oil recovery for Norne field E-segment using alkaline surfactant-polymer flooding* (Master's thesis). Norwegian University of Science and Technology.

Rwechungura, Richard & Suwartadi, Eka & Dadashpour, Mohsen & Kleppe, Jon & Foss, Bjarne. (2010). The Norne Field Case - A Unique Comparative Case Study. 10.2523/127538-MS.

Seber, G. A. F., & Lee, A. J. (2012). *Linear regression analysis* (2nd ed.). Wiley.

Singh, N. P. (2019). Permeability prediction from wireline logging and core data: A case study from Assam-Arakan basin. Journal of Petroleum Exploration and Production Technology, 9(1), 297–305. https://doi.org/10.1007/s13202-018-0459-y

Willmott, C. J., & Matsuura, K. (2005). *Advantages of the mean absolute error over the root mean square error in assessing average model performance*. Climate Research, 30(1), 79-82.